UNIVERSITÀ DI PISA

Scuola di Dottorato in Ingegneria "Leonardo da Vinci"

Corso di Dottorato di Ricerca in
SICUREZZA NUCLEARE ED INDUSTRIALE

Tesi di Dottorato di Ricerca

Realization of a Methodology for the assessment of "Best Estimate" codes for the analysis of nuclear systems and application to Cathare2 V2.5 code

Autore:

Dino Alfonso Araneo _____Firma_____

Relatori:

Prof. Francesco D'Auria _____Firma_____

Dr. Ing. Giorgio Maria Galassi __Firma_____

Anno 2008

SOMMARIO

Il presente lavoro riguarda la qualifica dei codici per la valutazione della sicurezza dei reattori nucleari.
La generazione attuale dei codici termoidraulici di sistema (come relap5, Cathare2, Trace,..), è basata sulla soluzione di sei equazioni di bilancio per il liquido e per il vapore, che sono integrate da un adeguato insieme di equazioni costitutive. Le equazioni di bilancio sono accoppiate con le equazioni di scambio termico e con le equazioni della cinetica neutronica (tipicamente la cinetica puntuale), per rappresentare le più importanti condizioni al contorno nelle simulazioni di un impianto nucleare durante condizioni normali e incidentali.

Un aspetto chiave nello sviluppo di tali codici è sia il processo di sviluppo stesso che il processo di qualifica indipendente. Il primo è collegato alla verifica del codice durante la realizzazione del codice stesso, mentre il secondo consiste nella validazione della capacità del codice di riprodurre i dati provenienti dagli esperimenti condotti in apparati sperimentali: "Integral Test Facility" (ITF) o "Separate Effect Test Facilities" (SETF). La qualifica indipendente è eseguita nella pratica comune da gruppi di utenti diversi dagli sviluppatori del codice. Un ruolo rilevante nella qualifica indipendente è rappresentato dalla procedura seguita dall'utilizzatore del codice, perché deve essere robusta e applicata in modo sistematico.

Negli studi per la sicurezza del comportamento degli impianti nucleari, possono essere identificati due differenti approcci (prevalentemente finalizzati all'ottenimento della licenza di esercizio):
Conservativo:

- Sovra/sotto stima di specifici parametri per coprire l'incertezza.
- Valori calcolati sono da considerarsi sovra/peggiori rispetto al valore reale.

Best estimate/realistico:

- Libero dal pessimismo deliberato.
- Comportamento reale dell'apparato sperimentale.
- Valutazione dell'incertezza.

La presente tesi è focalizzata sull'approccio "Best Estimate" (BE), vale a dire sulla revisione e razionalizzazione delle procedure sviluppate al Dipartimento di Ingegneria Meccanica Nucleare e della Produzione (DIMNP) dell'Università di Pisa (UNIPI), che tratta la qualifica dei risultati dei codici di BE.

Il codice di riferimento è il "Code for Analysis of Thermal-Hydraulics during an Accident of Reactor and safety Evaluation" (Cathare2).
Esso è stato sviluppato dal 1979 con la collaborazione del "Commissariat a l'Energy Atomique" (CEA), dell' "Institut de Protection et de Sûreté Nucleaire" (IPSN), dell' "Elecricitè De France" (EDF) e di Framatome.

Il presente lavoro ha come punto di partenza quello di individuare le necessità relative all'applicazione dei codici nelle analisi deterministiche per la sicurezza dei reattori nucleari. Il primo elemento analizzato è la qualifica della nodalizzazione.

Questa riguarda il livello di conoscenza di tutti gli elementi del sistema studiato (impianto nucleare o apparato sperimentale) che deve essere ben noto durante la realizzazione della nodalizzazione. Dopo aver realizzato la nodalizzazione, il processo di qualifica prevede due passaggi nei quali occorre dimostrare la corrispondenza geometrica tra il sistema studiato e la nodalizzazione e i maggiori parametri termoidraulici. Un ulteriore passaggio è rappresentato dalla qualifica della capacità della nodalizzazione di riprodurre gli stessi risultati provenienti dagli esperimenti, in modo da verificare se ci siano inadeguatezze nelle scelte dell'utilizzatore.

Un ruolo primario nel processo descritto è rappresentato dall' interazione codice-utente denominata "user-effect" e questo effetto viene analizzato in dettaglio mostrando alcuni esempi. Nel testo è stato evidenziato il ruolo primario dell'utilizzatore in tutte le fasi previste nell'applicazione del codice. Dopo aver analizzato il problema, sono state suggerite alcune contromisure da adottare per ridurre l'effetto dell'utilizzatore sul risultato finale. Per raggiungere tale scopo è stata utilizzata l'esperienza internazionale e le relative linee guide della "International Atomic Energy Agency" (IAEA) .

Un altro argomento rilevante, discusso nel presente lavoro, è l'effetto del computer e del compilatore sul risultato finale. A parte gli errori contenuti nel compilatore, sono state evidenziate alcuni pratiche scorrette durante la realizzazione del programma. Un ulteriore effetto del compilatore è connesso alla precisione (64 bits o 32 bits) della macchina utilizzata per il calcolo.

Sono descritti in dettaglio la disponibilità di strumenti computazionali per la qualifica dei risultati. In particolare è stato descritto il metodo basato sulla "Uncertainty Methodology based on Accuracy Extrapolation" (UMAE). Questo metodologia deriva l'incertezza dalla estrapolazione della accuratezza. Sono stati evidenziati usi differenti della UMAE e riguardano la qualifica dell'utilizzatore del codice, della nodalizzazione dell'apparato sperimentale e della nodalizzazione dell'impianto nucleare. Il metodo adottato nella UMAE non è solo usato per la qualifica dei calcoli, ma alcune procedure possono essere adottate per la dimostrazione della scalabilità dei dati sperimentali, per la dimostrazione della scalabilità (indipendenza dal fattore di scala), per la dimostrazione dell' accuratezza del codice, ecc.

E' stato proposto uno strumento addizionale capace di quantificare l'accuratezza di un dato calcolo di un codice: il "Fast Fourier Transform Based Method" (FFTBM).

Un risultato chiave discusso è la "Scaling Strategy" presa dal "Addressing the scaling issue", riguardante la valutazione dei codici a fronte dei dati sperimentali provenienti da apparati sperimentali integrali e/o apparati sperimentali ad effetto separato. Nella metodologia UMAE il problema della scala ha un ruolo rilevante, perchè l'incertezza collegata alla previsione del codice per l'impianto nucleare è estrapolata dal database costruito considerando l'accuratezza dei calcoli nelle simulazioni dei dati sperimentali provenienti dagli apparati sperimentali integrali ITF. Questo aspetto rappresenta il collegamento tra il problema della scala e la valutazione dell'incertezza, un passo necessario all'interno dell'approccio BE

nell'applicazione del codice. L'approccio al problema della scala proposta da UNIPI è sostanzialmente l'uso dei dati sperimentali e dei risultati delle analisi di supporto.

Nell'ottica del miglioramento della metodologia per la qualifica indipendente, sono stati illustrati i risultati dell'uso di un codice di Fluido Dinamica Computazionale (CFD), come strumento di supporto durante la realizzazione della nodalizzazione per un calcolo più accurato della distribuzione dei coefficienti di perdita di carico in alcune parti scelte del sistema studiato.

Nella stessa ottica, è state illustrata una ulteriore attività che riguarda l'analisi della accuratezza nella valutazione dei coefficienti di perdita di pressione concentrate K per mezzo di un codice di CFD. Lo scopo è stato quello di evidenziare quali parametri geometrici e termoidraulici hanno effetto sul valore di K.

Infine, un breve sommario illustra i maggiori risultati ottenuti dall'applicazione del codice Catharte2 nello sviluppo e nella qualifica delle procedure di "Accident Management" (AM) per gli impianti nucleari VVER1000, sulla base dei dati sperimentali provenienti dall'apparato sperimentale PSB-VVER (Russia). Inoltre è stato descritta la qualifica del codice per i fenomeni di trasporto di boro con i dati provenienti dall'apparato sperimentale PKL III operante in Germania, che simula un impianto nucleare PWR. In entrambe le applicazioni è stata utilizzata la metodologia sviluppata al DIMNP e il codice Cathare2 ha dimostrato di adempiere a tutti i requisiti previsti nella metodologia.

ABSTRACT

The present work deals with the assessment of thermal hydraulic system codes to be applied in the safety evaluation of nuclear reactors.
The actual generation of system thermal-hydraulic codes (e.g Relap5, Cathare2, Trace, …), is based upon the solution of six balance equations for liquid and steam that are supplemented by a suitable set of constitutive equations. The balance equations are coupled with conduction heat transfer equations and with neutron kinetics equations (typically point kinetics), to represent the main boundary conditions in the simulation of a Nuclear Power Plant (NPP) during normal and accident conditions.

A key aspect in the development of such kind of codes is the process of their development and independent assessment. The first one is related to the code verification process during the set up of the code, while the second one consists in the validation of the capability of the code to reproduce the data coming from experimental facilities: Integral Test Facilities (ITF) or Separate Effect Test Facilities (SETF). The independent assessment process is performed in the common practice by groups of users different from the code developers. A relevant role in the independent assessment process is represented by the procedure followed by the code user, because it has to be robust and systematically applied.

Two different approaches can be identified in the safety studies of the NPP behaviour (mainly devoted to the licensing of the NPP):
Conservative:
- Over/under-estimation of specific parameters to cover uncertainties.
- Calculated value(s) is expected to be over/worse the real value.

Best estimate/realistic:
- Free of deliberate pessimism.
- Real behaviour of the facility.
- Evaluation of uncertainty.

The present thesis is focused on the Best Estimate (BE) approach, namely on the review and the rationalization of the procedures developed at the Department of Mechanical Nuclear and Production Engineering (DIMNP) of the University of Pisa (UNIPI) dealing with the qualification of the results of the BE codes.

The reference code is the Code for Analysis of Thermal-Hydraulics during an Accident of Reactor and safety Evaluation (Cathare2) code.
It has been developed from 1979, in joint effort by Commissariat A l'Energy Atomique (CEA), Institut de Protection et de Sûreté Nucleaire (IPSN), Elecricitè De France (EDF) and Framatome.

The starting point of the work is the overview of the needs in the application of the code to deterministic analyses in nuclear reactor safety. The first element analyzed is the nodalization qualification. It concerns the level of knowledge of all the elements of the studied system (NPP or experimental facility) that have to be well known during the realization of a nodalization. Once the nodalization is realized, the qualification process foreseen two steps in which the geometrical

correspondence between the analyzed system and the nodalization and the main thermalhydraulic parameters is demonstrated. Another step is constituted by the qualification of the capability of the nodalization to reproduce the same results coming from selected experiments, in order to check if there are any user choice inadequacies.

A primary role in the process described is the code-user interaction named “user effect”. This effect is analyzed in detail and some evidences have been provided. In the text has been highlighted the primary role of the user in all the steps foreseen in the application of the code. Once the problems have been analyzed, some countermeasures to be adopted in order to reduce the user effect on the final result are suggested. The international experience and the related International Atomic Energy Agency (IAEA) guidelines are taken into account in regard to this.

Another sensitive argument discussed in the present work is the effect of the computer and compiler on the final results. Apart the error contained in the compiler program, some bad practices have been highlighted during the realization of the software. A further effect of the compiler is connected to the precision (64 bits or 32 bits) of the machine where the calculation is performed.

The available computational tools for the qualification of the results are described in detail. More in particular the Uncertainty Methodology based on Accuracy Extrapolation (UMAE) based method is described. This methodology derives the uncertainty by the extrapolation of the accuracy. Different uses of the UMAE are highlighted concerning the assessment of the code user, the qualification of the facility nodalization and of the NPP nodalization. The method adopted in UMAE is not only used for the calculation qualification, but some procedures can be adopted for demonstration of the scalability of experimental data sets, demonstration of scalability (independence from scaling) of code accuracy, etc.

An additional tool able to quantify the accuracy of a given code calculation is proposed: the Fast Fourier Based Method (FFTBM).

A key finding discussed is the “Scaling strategy” taken from the “Addressing the scaling issue”, regarding the validation of codes against the experimental data coming from ITF and/or SETF. In the UMAE methodology the scaling issue has a relevant role because the uncertainty related to the NPP code prediction is extrapolated from the database built considering the calculation accuracy in the simulation of experimental data obtained in ITF. This aspect represents the connection between the scaling issue and the code uncertainty evaluation, a needed step within the BE approach in code application. The scaling approach proposed by UNIPI is substantiated by the use of experimental data and by the results of supporting analyses.

With the aim to improve the above independent assessment methodology, the results of the use of the a Computational Fluid Dynamics (CFD) code, as support tool during the nodalization set up for the calculation of a more accurate pressure drop coefficient distribution in selected parts of the analyzed system, have been shown.

In the same framework a further activity deal with the investigation of the accuracy in the evaluation of the concentrate pressure drop coefficient K by mean of a CFD code has been shown. The aim has been the investigation of the geometrical and thermal hydraulic parameters that affect the calculated value of K.

Finally, a short summary is presented of the main results achieved from the application of the Cathare2 code to the development and assessment of the Accident Management (AM) procedures suitable for VVER1000 NPP, on the basis of experimental data coming from PSB-VVER facility (Russia). Moreover the assessment of the code model against the Boron transport phenomena with data measured in PKL III experimental facility operating in Germany and simulating a PWR NPP has been described. In both applications the methodology developed at DIMNP has been applied and the Cathare2 code has demonstrated to fulfil all the requirements of the methodology.

INDICE

LISTA SIMBOLI

AFE = Accuracy Finalized to Extrapolation
AFWP = Auxiliary Feed-Water Pump
AM = Accident Management
AMP = AM Procedure or Programme
ASM = Analytical Simulation Model
ATWS = Anticipated Transient Without Scram
BE = Best Estimate
BIC = Boundary and Initial Conditions
BL = Broken Loop
BRU-A,-K,-D,-TK = Safety Valves in the steam line
CCVM = CSNI Code Validation Matrix
CIAU = Code with capability of Internal Assessment of Uncertainty
CMFR = Core Mass Flow Rate
CO = Confinement (this includes RC, ALS and RB)
CPS = Control Protection System
CSF = Critical Safety Function
CSNI = Committee on the Safety of Nuclear Installations
DB = Data Base
DBA = Design Basis Accident
DC = Down-Comer
DIMNP = Dipartimento di Ingegneria Meccanica Nucleare e della Produzione
DP= Differential Pressure
EC= European Commission (also adopted for the identification of references)
ECCS = Emergency Core Cooling Systems
EFW = Emergency Feed-Water
EOP = Emergency Operating Procedures
EREC = Electrogorsk Research and Engineering Center
ESF = Engineered Safety Features
EU = European Union
FA = Flow Area or Fuel Assembly
FFTBM = Fast Fourier Transform Based Method
FRS = Fuel Rod Simulator
HA = Hydro-accumualtor
HPIS = High Pressure Injection System
HTA = Heat Transfer Area
IAEA = International Atomic Energy Agency
ITF = Integral Test Facility
ITM = Ideal Test Matrix
LOCA = Loss of Coolant Accident
LOFW = Loss of Feed Water
LPIS = Low Pressure Injection System
LWR = Light Water Reactor
MCP = Main Coolant Pump
MSIV = Main Steam Isolation Valve
MSLB = Main Steam Line Break
NC = Natural Circulation
NCFI = Natural Circulation Flow Interruption

NCFM = Natural Circulation Flow Maximum
NEA = Nuclear Energy Agency
NPP = Nuclear Power Plant
NRC = Nuclear Regulatory Commission
OD = Outside Diameter
OECD = Organisation for Economic Cooperation and Development
OTSG = Once-Through Steam Generator
PDE = Primary side Depressurization
PIRT = Process and Identification Ranking Table
PORV = Power Operative Relief Valve
PRISE = Primary to Secondary System Leak
PRZ = Pressurizer
PS = Primary System
PSA = Probabilistic Safety Assessment
PTS = Pressurized Thermal Shock
PWR = Pressurized Water Reactor
QA = Quality Assurance
QAM = Quantity Accuracy Matrix
QUM = Quantity Uncertainty Matrix
RHR = Residual Heat Removal
RPV = Reactor Pressure Vessel
SBLOCA = Small Break LOCA
SBO = Station BlackOut
SCRAM = Safety cut rope axe man
SET = Separate Effect Test
SETF = Separate Effect Test Facility
SG = Steam Generator
SGTR = Steam Generator Tube Rupture
SL = Steam Line
SS = Secondary Side
SUNCOP = (Training on) Scaling, Uncertainty and 3D COuPled Code Calculation
TACIS = Technical Assistance for the Commonwealth of the Independent States
TAV = Time Accuracy Vector
TH = Thermal-Hydraulics
UBEP = Uncertainty Bands Extrapolation Process
UMAE = Uncertainty Method based on Accuracy Extrapolation
UNIPI = University of Pisa (also adopted for the identification of references)
UP = Upper Plenum
UPI = Upper Plenum Injection
UPTF = Upper Plenum Test Facility
VVER = Water-cooled Water-moderated Energy Reactor
BETHSY = Boucle Etudes Thermo-Hydraulic System, CEA, France
LOBI = Loop for Off-Normal Behaviour Investigation, EC-JRC Ispra, Italy
PKL = Primär Kreisläufe (Primary Coolant Loops), Framatome-ANP Erlangen, Germany
PSB-VVER = Russian Test facility, EREC, Russia

INTRODUCTION

The safety technology of the NPP is based upon two main approaches: deterministic analysis and probabilistic analysis:

- Deterministic safety analysis predicts the response of a NPP in specific predetermined operational states to postulated initiating events. This type of safety analysis applies a specific set of rules and specific acceptance criteria. Deterministic analysis is typically focused on neutronic, thermal-hydraulic, radiological and structural aspects, which are often analyzed with different computational tools [1].
- Probabilistic safety analysis starts with the establishment of a hierarchy of transients can be achieved by using suitable probabilistic approaches. The importance of a transient is usually established on the basis of the probability of occurrence and the consequences of the accident in terms of radioactive releases. Probabilistic analyses have also been used in individual plant examinations and risk assessments to identify the specific accident conditions to be used for best estimate analysis of Beyond Design Basis (BDBA) [1].

The sector of interest for the present thesis is the first one (deterministic analysis). In particular, among the deterministic analysis several different activities can be identified but in this work the attention is focused on the analysis of the accidents in the Nuclear Power Plant (NPP). The tools able to perform these kind of analyses are the system thermal-hydraulic codes like: Relap 5, Cathare 2, Trace.
The Cathare2 code developed at Commissariat a l'Energie Atomique (CEA), Institut de Protection et de Sûreté Nucléaire (IPSN), Electricité De France (EDF) and Framatome has been taken into consideration and the methodology developed at DIMNP of the UNIPI concerning the assessment of the results of the system thermal hydraulic codes has been applied.

Because the results of the codes are affected by unavoidable errors, the use of such codes in the nuclear technology is allowed (by IAEA and National Regulatory Body) only after the previous demonstration of the qualification level of codes and model used, nodalization, Boundary and Initial Conditions (BIC), User, quality of data coming from the experiments.

A large effort has been spent by scientific community in the years for the evaluation/quantification of the uncertainty connected with the application of TH-system codes in predicting the behavior of a NPP.

Recent advancements in the development of best estimate code and in the introduction of new uncertainty evaluation methods are coming to gradually replace the conventional conservative Evaluation Methods (EM) of US NRC Appendix K.

Some critics can be made to the conservative approach:

- No information about real behavior and safety margin.
- Due to complex interactions applying conservative data does not necessarily leads to conservative results.

- Mixture of unphysical (but conservative) parameters.
- Possibility of missing some phenomena overwhelmed by conservativism.

Some benefits can be identified for a Best-estimate approach:

- More detailed and complex evaluation of plant safety.
- Possibility to benefit from the safety margin reduction.

The BE approach can be applied for the following applications:

- Plants up rate.
- New designs with economically improved performances.

At present these codes are considered suitable for practical needs and some applications of the Best Estimate Plus Uncertainty (BEPU) have been proposed.

The BEPU approach is proposed in contrast with the “classical”, adopted conservative approach. The use of the BE robust and very well tested codes in several years as Cathare2, Relap5, Athlet, Cathena, Apros, connected with an uncertainty methods as CSAU, GRS-method and CIAU suitable of technological applications in the Licensing of a NPP is one of the main objective of the Nuclear Technology, but this has to be accepted, in the framework of the licensing process, by the regulatory bodies.

The objective of the present work is the a systematic review of all the procedure developed and adopted at DIMNP for the qualification of the BE codes results. A systematic reorganization of all the procedures comes from the need of a clear identification of the input and output data and of the connections of each step to the others inside the followed path of the methodology.

The system thermal hydraulic code is the first element taken in consideration. The code contains several empirical models and thousand of code lines. The use of such tool in the analysis have to be carefully adopted after a suitable assessment program able to check the presence of programming errors, improperly implemented models etc.

The nodalization is strictly connected with the code because it represents the collection of the input data for the code. The code output depends from the input data. The nodalization is the “translation” in the code language of the geometrical and thermalhydraulic data of the studied system. It is relevant from this point of view to have correct input data and after their implementation a check for the correspondence between the system model (nodalization) and the real system from the geometrical and thermal hydraulic point of view.

The code-user is another key element. All the choices during the code application phase, the realization of the nodalization, the control of the quality of the data in input are in charge to the user. In particular during the nodalization realization several choices in the modeling of the system can affect the code result. The realization of the nodalization implies the translation of a three dimensional real system in a one-dimensional model. In this process the users has a primary role.

One of the main effect on the code result is the computer and compiler effect. The same code can give different results depends on the compiler used (and the option adopted during the compilation phase) and the computer where the calculation is performed.

The reorganization of the procedures developed at DIMNP object of the present thesis, has to be considered in the optic of the establishment of a QA program for the evaluation of the results of the BE codes. The standard, systematic and rigorous application of the methodology for the qualification of the codes results or for the others objectives for which the methodology has been designed (qualification of the user, of the facility and NPP nodalization etc.) is the final objective of the present work. Furthermore the quality of the results of the application of the methodology depends on how the methodology is applied.

Nowadays, beside the system thermal hydraulic codes, the Computational Fluid Dynamic (CFD) codes have registered a very fast development.

The adoption of such codes as additional tools among the once already available in the methodology, represents a new achievement in the present work. The use of such codes in the Nuclear technology requires some preliminary and necessary steps for the acceptability of their results that have been highlighted.

A second objective of the present thesis is the assessment of the Cathare2 code. The development of AM procedures for the Eastern VVER1000 NPP by mean the use of the Cathare2 code for the post-test analysis of the experiments conduct in the PSB-VVER facility, constitutes the framework in which the Cathare2 code has been applied following the procedures foreseen in the methodology developed at DIMNP. A second activity has been the application of the Cathare2 code for the post-test analyses of the experiments conduct in the PKL III facility for addressing the Boron transport phenomena relevant for the PWR NPP safety.

1. NEEDS IN NUCLEAR REACTOR SAFETY DETERMINISTIC ANALYSIS

System thermal-hydraulic codes have been developed within the framework of accident analysis in water cooled reactors since the 60's. The sketch in *Fig. 1* gives an idea of the process pursued for the development, the qualification and the application of these codes.

The system thermal-hydraulic codes are based upon the solution of six balance equations for liquid and steam that are supplemented by a suitable set of constitutive equations. The balance equations are coupled with conduction heat transfer equations and with neutron kinetics equations (typically point kinetics).

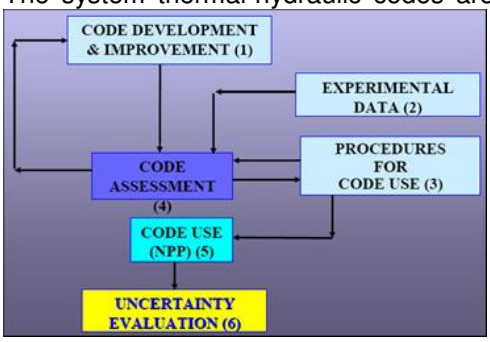

Fig. 1 Process for the development, the assessment and the application of thermal-hydraulic system codes

The code development and improvement process, block 1 in the *Fig. 1*, is carried out by 'code developers' who make extensive use of assessment, block 4 in the *Fig. 1*, typically performed by independent users of the code (i.e. groups of experts independent from those who developed the code). The consistent code assessment process implies the availability of experimental data and of robust procedures for the use of the codes, blocks 2 and 3 in the *Fig. 1*.

Once the process identified by blocks 1 and 4 is completed, a qualified code is available to the technical community, ready to be used for NPP applications, block 5 in the *Fig. 1*. The NPP application, still requires 'consistent' procedures for code user, block 3 in the *Fig. 1*. The results from the calculations are, whatever the qualification level achieved by the code, affected by errors that must be quantified; this is known as uncertainty evaluation, block 6 in the *Fig. 1*.

The specific routes pursued to demonstrate that a code or a nodalization is qualified are discussed in the following: namely, the demonstration of code qualification implies the availability of qualified nodalizations (and qualified users). Criteria and thresholds of acceptability for calculation results at steady-state and at 'on-transient' level are introduced.

The code user has a crucial role within the entire process. The characterization of the role of the code user passes through the identification of the (huge) user effect, the proposition of means to prevent or minimize user errors and the identification of the essential role of user training.

A 'transversal' and continuously questioned topic occurring within the framework of the qualification process for computational tools is constituted by the scaling issue. The problem is originated by the fact that the quality of computational tools can be

demonstrated at conditions (primarily geometric, but also for combinations of relevant thermal-hydraulic parameters) that are not the same and in some cases are far from the values applicable for real (NPP) situations [1].

1.1. Nodalization qualification needs

In order to analyze the NPP behavior during transient scenario it is necessary to develop a nodalization that reproduces all the aspects of the plant and of the transient/accident considered. The nodalization development is a process involving many different aspects:

- ✓ Code capabilities: what in the nodalization is related with the code analysis capabilities and input capabilities, generally described in the code user manual.
- ✓ Plant data: the information about the plant must be available and complete to be implemented in the nodalization for a correct analysis.
- ✓ Transient/accident conditions: the data about the boundary and initial conditions to be implemented in the nodalization are selected and translated in the input deck to correctly reproduce the plant and accident conditions in the analysis.
- ✓ Schematization of the relevant zones of the plant: in this phase the relevant zones and systems for the considered accident or transient are selected. The user selects the general strategy for the representation of the plant and related system in the analysis. It is relevant to note that this activity is partially independent from the selected code. However some systems or zones schematization are affected by the code nodalization capabilities (e.g. the 1D or 3D capability of the code).
- ✓ Nodalization: this phase is strongly connected with the selected code. The number of nodes (hydraulic, thermal, etc) the dimension, the connections, the disposition are selected by the user, taking into account the code capabilities. This phase includes the implementation in the input deck of all the plant systems and their intervention logic; the possibility of nodalization of the code strongly affects the simulation of these components of the nodalization. Another aspect to be considered in the nodalization is constituted by the calculation time: different acceptable nodalization solutions are generally different from the time consuming point of view.
- ✓ It must be noted that in the nodalization typically are neglected or simulated by boundary conditions the systems or zones of the plant not relevant for the analysis object of the calculation.
- ✓ Qualification of the nodalization capability. In this check the nodalization to be used as model of the plant for the selected analysis is proved capable.

It is easily recognizable the user role in many of the above items. Assumed a qualified code and a qualified user, it is necessary to define a qualification procedure for the nodalization. It is necessary to put in evidence that the fundamental concepts are the same, but from the operative point of view some difference are evidenced in the qualification process of a NPP or of a facility.

A major issue in the use of a mathematical model is constituted by the model capability to reproduce the plant or facility behavior under steady state and transient conditions. These aspects constitute two main checks that must be passed in the qualification process. The first of them is related to the realization of a schematization of the reference plant; the second one is related to the capability to reproduce the transient analysis to derive the needed information.

The checks about the nodalization are necessary to take into account the effect of many different sources of approximations:

a) Data of the reference plant available to the user are typically non exhaustive to reproduce a perfect schematization of the reference plant.
b) The user derives from the available data an approximated schematization of the plant reducing the detail level of the plant representation.
c) The code capability to reproduce the hardware, the plant systems and actuation logic of the systems again reduces the schematization detail level.

The reasons for the checks about the capability to perform the transient analysis derive from the following statements:

1. The code options must be adequate.
2. The schematization solutions must be adequate.
3. Some systems simulations can be tested only in the simulation of the transient (e.g. ECCS that are not involved in the normal operation).
4. The system code-nodalization capability to reproduce relevant TH phenomena expected in the transient must be tested.

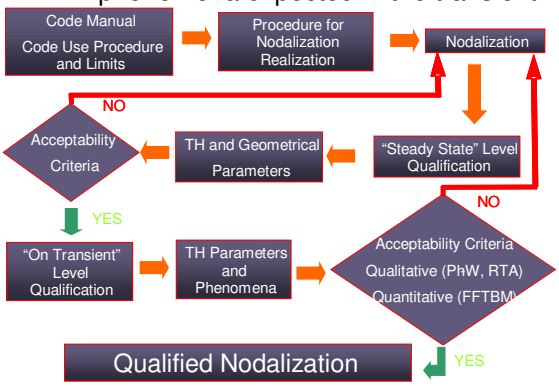

Fig. 2 Flow sheet of nodalization qualification procedure

A procedure is prepared including the necessary checks for these different aspects and the criteria adopted to produce a judgment about acceptability of the code analysis results

Hereafter the qualification procedure for nodalization is presented. A Simplified scheme of the nodalization qualification procedure is also reported in the *Fig. 2*.

In the following it has been assumed that the code has fulfilled the validation and qualification process and a "frozen" version of the code has been made available to the final user. It means that the user does not have any possibility to modify or change the physical and numerical models of the code (only the options described in the user manual are available to the user).The nodalization procedure is described step by step with reference to the *Fig. 2*.

From a generic point of view the following attentions should be adopted:

- ✓ Homogeneous nodalizations.
- ✓ Strict observation of the user guidelines.
- ✓ Standard use of the code options.

Step “b”: user experience and developers recommendations are useful to set up particular procedures to be applied for a better nodalization. These special procedures are related to the specific code adopted for the analysis. An example is constituted by the slice nodalization adopted with the Relap code to improve the capability of the code in the simulations involving the natural circulation phenomenon.

Step “c”: the nodalization realization depends on several aspects: available data, user capability and experience, code capability. From a generic point of view the following recommendations can be done:

- ✓ data must be qualified. This means data derived from:
  - ❖ qualified facility (if the analysis is performed for a facility);
  - ❖ qualified test design;
  - ❖ qualified test.
- ✓ The data base for the realization of the nodalization should be derived from official documents and traceability of each reference should be maintained. However three different type of data can be identified:
  - ❖ qualified data, from official sources;
  - ❖ data deriving from non-official sources; these type of data can be derived from similar plant data, or other qualified nodalization for the same type of plant; the use of these data can introduce potential errors and the effect on the calculation results must be carefully evaluated.
  - ❖ data assumed by the user; these data constitute assumptions of the user (on the base of the experience or by similitude with other similar plants). The use of this type of data should be avoided. Any special assumptions adopted by the user or special solutions in the nodalization must be recorded and documented.

The nodalization must reproduce all the relevant parts of the reference plant; this includes geometrical and materials fidelity and reproduction of systems and related logics.

Step “d”: the “steady state” qualification level step includes different checks: one is related to the evaluation of the geometrical data and of numerical values implemented in the nodalization; the other one is related to the capability of the nodalization to reproduce the steady state qualified conditions. The first check should be performed by a user different from the user who has carried out the nodalization. In the second check a “steady state” calculation is performed. This activity depends on the different code peculiarities. As an example, for the Relap, the steady state calculation is constituted by a “null transient” calculation (“null transient” means that the “transient” option is selected in a calculation without any variation of the relevant parameters).

Step “e”: the relevant geometrical values and the relevant thermal-hydraulic parameters of the steady state conditions are identified. The selected geometrical values and the selected relevant parameters are derived from nodalization and from steady state calculation respectively for a comparison with the hardware values and the experimental parameters.

A minimal list of the geometrical values and thermal-hydraulic parameters to be checked is reported in the *Tab. 1*. Other parameters can be added if needed.

Items from 1 to 11 are related to geometrical values and are checked in the nodalization. Items from 12 to 25 are obtained from the steady state calculation.

Step “f”: this is the step where acceptability criteria are applied to the comparison between experimental and calculated geometrical values and the steady state parameters. Tab. 1 shows the geometrical values and TH parameters list together the acceptability errors. Some comments can be added:

- The experimental data are typically available with an error band, which must be considered in the comparison with the calculated values and parameters.
- The steadiness of the steady state calculation must be checked.

	QUANTITY
1	Primary circuit volume
2	Secondary circuit volume
3	Non-active structures heat transfer area (overall)
4	Active structures heat transfer area (overall)
5	Non-active structures heat transfer volume (overall)
6	Active structures heat transfer volume (overall)
7	Volume vs. height curve (i.e. “local” primary and secondary circuit volume)
8	Component relative elevation
9	Axial and radial power distribution (°°)
10	Flow area of components like valves, pumps orifices
11	Generic flow area
(*)	
12	Primary circuit power balance
13	Secondary circuit power balance
14	Absolute pressure (PRZ, SG, ACC)
15	Fluid temperature
16	Rod surface temperature
17	Pump velocity
18	Heat losses
19	Local pressure drops
20	Mass inventory in primary circuit
21	Mass inventory in secondary circuit
22	Flow rates (primary and secondary circuit)
23	Bypass mass flow rates
24	Pressurizer level (collapsed)
25	Secondary side or downcomer level

Tab. 1 Geometrical values and thermal-hydraulic parameters considered for the nodalization “steady state” qualification

Step “g”: if one or more than one of the checks in the step “f” are not fulfilled a review of the nodalization (step “c”) must be performed. This process can request more detailed data, improvement in the solution of the schematization, different user choices. The path “g” must be activated up to all the checks in the *Tab. 2* are passed.

Step “h” this step constitutes the “On Transient” level qualification. This activity is necessary to demonstrate the capability of the nodalization to reproduce the relevant thermal-hydraulic phenomena expected in the transient. This step also permits to verify the correctness of the simulation of some systems that are taken into operation only during transient events.

	QUANTITY	ACCEPTABLE ERROR (°)
1	Primary circuit volume	1 %
2	Secondary circuit volume	2 %
3	Non-active structures heat transfer area (overall)	10 %
4	Active structures heat transfer area (overall)	0.1 %
5	Non-active structures heat transfer volume (overall)	14 %
6	Active structures heat transfer volume (overall)	0.2 %
7	Volume vs. height curve (i.e. "local" primary and secondary circuit volume)	10 %
8	Component relative elevation	0.01 m
9	Axial and radial power distribution (°°)	1 %
10	Flow area of components like valves, pumps orifices	1 %
11	Generic flow area	10 %
(*)		
12	Primary circuit power balance	2 %
13	Secondary circuit power balance	2 %
14	Absolute pressure (PRZ, SG, ACC)	0.1 %
15	Fluid temperature	0.5 % (**)
16	Rod surface temperature	10 K
17	Pump velocity	1 %
18	Heat losses	10 %
19	Local pressure drops	10 % (^)
20	Mass inventory in primary circuit	2 % (^^)
21	Mass inventory in secondary circuit	5 % (^^)
22	Flow rates (primary and secondary circuit)	2 %
23	Bypass mass flow rates	10 %
24	Pressurizer level (collapsed)	0.05 m
25	Secondary side or downcomer level	0.1 m (^^)

(°) The % error is defined as the ratio $\frac{|\text{reference or measured value} - \text{calculated value}|}{|\text{reference or measured value}|}$ The "dimensional error" is the numerator of the above expression

(°°) Additional consideration needed
(*) With reference to each of the quantities below, following a "transient-steady-state" calculation, the solution must be stable with an inherent drift < 1% / 100 s.
(**) And consistent with power error
(^) Of the difference between maximum and minimum pressure in the loop.
(^^) And consistent with other errors.

Tab. 2 Acceptable errors for the nodalization "Steady State" qualification level

Two different aspects can be identified:

1. The nodalization is constituted by the schematization of a facility. In this case the code calculation is used for Code Assessment. It is necessary to prove the capability of the code during a transient analysis. In this check are included the code options selected by the user, the schematization solutions, the logic of some systems (i.e. ECCS). Typically many experimental results are available from the facility; a test similar to that object of the analysis can be adopted as test for the "On Transient" level qualification.
2. The objective of the code calculation is constituted by the analysis of a transient in a NPP. In this case is necessary to check nodalization capability to reproduce the expected thermal-hydraulic phenomena occurring in the transient, the selected code options, the user adopted solution for the plant schematization, the logic of the system not involved in the steady state calculation, but called into operation during the transient. Typically no data exist for transients or tests performed in the NPP. So data from experiments performed in facilities can be used. What is performed is the "Kv-scaled" calculation. The Kv-scaled calculation consists by applying the realized nodalization for the calculation of the same transient (chosen among the transients similar to the one selected for the investigation) performed in a facility. The

NPP nodalization is prepared for a Kv-scaled calculation by properly scaling the BI (boundary and initial) conditions adopted in the facility. It generally means that power, mass flow rates and ECCS capacity are scaled adopting as scaling factor the ratio between the volume of the facility and the volume in the schematized NPP. The capability of the nodalization to reproduce the same transient evolution and the TH relevant phenomena is the needed request for the "On Transient" qualification level.

Some criteria are established to express the acceptability of an "On Transient" qualification calculation, both qualitative and quantitative.

Step "i" in this step the relevant thermal hydraulic phenomena and parameters are selected to perform the comparison between the calculated and experimental data. The selection of the phenomena derives from the following sources:

- ✓ Experimental data analysis (engineering judgment request).
- ✓ CSNI phenomena identification.
- ✓ Use of RTA (engineering judgment request).

Step "j": in this step the checks are performed to evaluate the acceptability of the calculation. The checks are performed from the qualitative and from the quantitative point of view.

For the qualitative evaluation the following aspects are involved:

- ✓ Visual observation. It means that a visual comparison is performed between experimental and calculated relevant parameters time trends.
- ✓ Sequence of the resulting events. It means that the list of the calculated timing of the events is compared with the timing of experimental events.
- ✓ Use of the CSNI phenomena. The relevant phenomena suitable for code assessment, the relevance in the selected facility and the phenomena that are well defined in the selected test can be derived. A judgment can be express taking into account the characteristics of the facility, the test peculiarities and the code results.
- ✓ Use of the RTA (Relevant thermal-hydraulic aspects). RTA are typically identified inside the phenomenological windows (time windows including relevant phenomena of the transient) and are constituted by special parameters (these parameters can be time values, single values like mass, pressure, etc., integral values, gradient values and non-dimensional values) introduced to better characterize the phenomena.

For the quantitative checks, the FFTBM is adopted. This special tool performs the comparison between experimental and calculated parameters in the frequency domain. A list of parameters is selected for the involved transient. The FFTBM performs the comparison and produces the judgment about the comparison between the two (corresponding) parameters by a numerical value (no engineering judgment is involved in this evaluation). This tool also makes possible to obtain a numerical judgment of the overall results of the calculation in comparison with the

experimental results. Criteria had been selected to accept the results for the parameter of the primary side pressure and the overall results.

Step “k”: this path is actuated if any of the checks (qualitative and quantitative) are not fulfilled. The nodalization is improved by changing some schematization solution, some code options or increasing the detail level eventually with new data. Every time the nodalization is modified, a new process is performed through the loop “c-d-e-f-h-i-j”.

Step “l”: this is the last step of the procedure. The obtained nodalization can be used for the selected transient and the selected facility or plant. However the nodalization can be used for other transients. The eventuality of a modification of the nodalization (i.e. necessary to better reproduce the experimental results) requests a new qualification process both “steady state” and “on transient level”[1].

1.1.1 Nodalization development

This first step includes these main aspects:

- ✓ Identification of the plant data necessary to derive a suitable model of the plant. The knowledge of the plant is necessary to derive:
  - ❖ the geometrical quantities characterizing the circuits;
  - ❖ the thermal hydraulic parameters and all the other parameters necessary to identify the status of the plant;
  - ❖ the systems hardware, how they are actuated, what are the working parameters (e.g. thermal-hydraulic parameters) and what is their availability. The knowledge of the plant is also relevant to evaluate if a conditions occurring in the calculation is realistic or not possible.
  - ❖ Collection of needed data; qualification of sources and data. Selected the data necessary for a suitable identification of all the aspects of the plant, these data are searched and collected. The data about the plant are not always easily available or sometime different sources report different data; additional problems can be originated by the existence of different version of the same plant. The qualification level of the sources and of the data must be evaluated; particularly the congruence of the data must be checked.
  - ❖ Schematization of the plant. In this phase the user choices about how to include in the plant model what is necessary for a correct analysis. Essentially in this phase the peculiarities of the plant and relevant for the analysis are identified and the simplifications necessary for their implementation in the calculation are decided. As an example, it can be considered the core active structure schematization. A short list of related issues is given in the following:
    - o How many group of fuel rods. Relevance or not to realize different core zones (e.g. in asymmetrical accidents).
    - o How to group the fuel rods. Criteria for grouping can be different (power, location, etc.).
    - o Hot rod simulation or homogeneous power distribution.
    - o How many fuel rods in the same hydraulic channel and how many hydraulic channels.

- The core power supplied to the structure as a table or considering the neutron kinetics.
- Neutron kinetics 0D or 3D (choice affecting also the hydraulic schematization).

Preparation of the nodalization. This phase is the operative writing of the input deck. In this phase the specific code solutions for the selected schematization are performed. Of course the user manual indications and recommendations are to be considered and applied. Continuing the previous example of the core active structure nodalization, after selected the schematization options, the user has to decide how many vertical nodes, how many radial nodes are suitable for the analysis, what material property to use (embedded in the code or from external sources, which special code options are to be actuated, which additional paths in the hydraulic nodalization have to be implemented to simulate special effects (e.g. transversal junctions between parallel channels for the coupling with 3D neutron kinetics). Some other attentions could improve the code response, as slice nodalization to realize the same dimension in nodes of different zones of the nodalization simulating zones of the plant at the same elevation to improve the natural circulation performance in the code. Other special attentions are to be paid for the nodalization of some zones to avoid an increase of the time necessary to complete the calculation These aspects affects the number of nodes and the dimensions of near nodes in the nodalization.

1.1.2 Steady state

The Steady State level qualification is demonstrated in two different steps:

- ✓ Relevant geometrical parameters.
- ✓ Significant system parameters (e.g. thermal-hydraulic parameters).

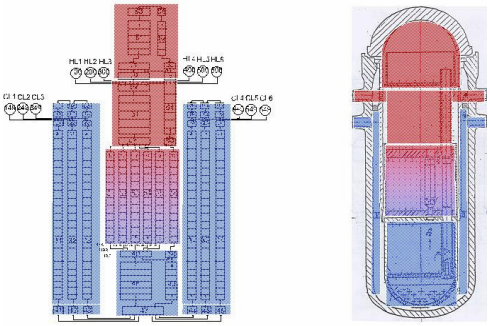

Fig. 3 Nodalization qualification at "Steady State" level - Example of nodalization of the hardware (e.g. VVER vessel).

Relevant geometrical parameters of the plant are constituted by volumes, heat transfer areas, elevations, etc. They are compared with the input data in the nodalization and the differences must be acceptably (*Fig. 3* and *Tab. 1*). The adopted acceptability criteria are reported in the first part of the *Tab. 2*; of course the uncertainties related to each parameter must be taken into account. Some additional details must be added about the item 7 of *Tab. 2*.

This parameter must be reproduced by two curves: the volume (primary and secondary side) versus height for the primary and the secondary side. The experimental and calculated curves must be prepared. An example of these curves is given in the *Fig. 4* and *Fig. 5*.

No	QUANTITY	DESIGN	RELAP5	NOTES
1	RPV DC	24.2	24.2	Including extended DC region inside LP (hydraulic DC).
2	RPV LP	20.7	20.64	
3	RPV LP inside BCAGT	2.5	3.39	Design value assumed.
4	RPV core active	–	7.7129	Included between BAF and TAF.
5	RPV core bypass	–	0.63715	Included between BOHC and TOHC.
6	Region BOHC–BAF (active)	–	1.06883	
7	Region TAF–TOHC (active)	–	1.08123	
8	UP outside BCAGT	22.2	22.2	
9	UP region inside BCAGT	3.0	3.0	
10	UH	15.7	15.7	UH boundaries defined in Tab. 2.
11	RPV total	98.84	99.68	
12	HL up to SG inlet collector.	2.762	2.762	Each individual loop.
13	CL from SG outlet collector to RPV, without MCP	3.246	3.574	Each individual loop.
14	MCP	0.63	0.301	Part of MCP included in CL in the Relap5 input.
15	SG inlet/outlet collector	1.796	1.796	Per each collector
16	PRZ SU LI	1.723	1.723	Both of these
17	PRZ	38.	38.	
18	H–tubes	6.833	6.835	
19	No of H–tubes (–)	5536	5536	

Tab. 3 Nodalization qualification at "Steady State" level - Example of the comparison between elevation in the hardware and nodalization corresponding zones.

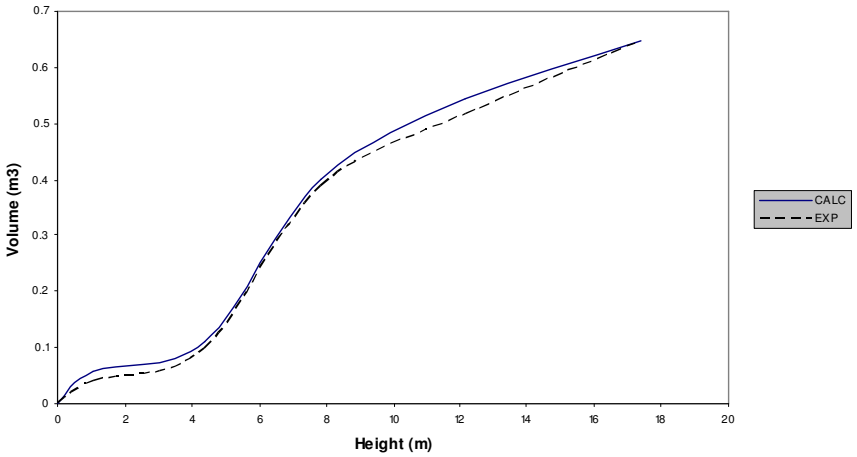

Fig. 4 Nodalization qualification at "Steady State" level - Example of the curve of the primary side volume vs. height.

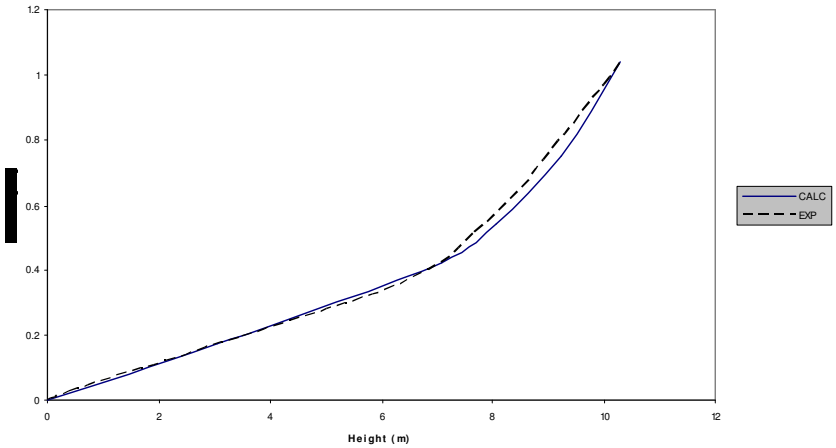

Fig. 5 Nodalization qualification at "Steady State" level - Example of the curve of the secondary side volume vs height.

All the significant thermal-hydraulic parameters necessary to identify the plant status are selected and evaluated. The steady state conditions are related to the plant conditions before the accident or transient occurrence and generally correspond to the nominal conditions of the plant. A list of relevant parameters to evaluate the steady state is reported in the *Tab. 2* An example of the steady state parameters values evaluation is reported in *Tab. 4* and *Fig. 6*. Criteria for acceptability are reported in the second half of the *Tab. 2* Item 19 of this Table is about pressure distribution versus loop length: both the experimental and calculated curves must be prepared. An example of these curves is given in the *Fig. 7*.

QUANTITY	UNIT	EXP	CALC CATHARE* UNIPI	CALC CATHARE CEA
Core power	kW	2817 ± 14	2861	2864
Pressurizer pressure	MPa	15.44 ± 0.07	15.68	15.48
Pressurizer level	m	7.27 ± 0.04	7.27	7.26
Downcomer mass flow rate	kg/s	15	14.5	13.59
DC-UH bypass flow rate	kg/s	-	0.042	0.102
Core bypass flow rate	kg/s	-	0.023	0.001
Core inlet temperature	°C	286. ± 2	288	286
Core outlet temperature	°C	-	323	322
Core ΔT	°C	35. ± 2	35	36
Upper head temperature	°C	325	328	320
Primary mass	kg	1954	1868	1952
Acc. liquid temperature	°C	17.5± 2	17	17
Secondary pressure SG	MPa	6.93 ± 0.03	6.87	6.87
SG downcomer level	m	13.66 ± 0.04 13.48 ± 0.04 13.50 ± 0.04	13.51 12.12 12.81	13.56 13.56 13.56
Feedwater temperature	°C	214 ± 2	214	214
Feedwater flow rate	kg/s	0.54	0.52	0.51
Total primary side heat losses	kW	(*)	(*)	(*)
Secondary side heat losses	kW	(*)	(*)	(*)
UP Pressure	MPa	-	15.75	15.55
SS total fluid mass	kg	-	2207	2370
Pump seal inlet flow rate	kg/s	0.025	0.0243	0.0243
Pump seal exit flow rate	kg/s	-	0.0243	0.0243

Tab. 4 Nodalization qualification at "Steady State" level - Example of the comparison between steady state conditions in the plant and nodalization results.

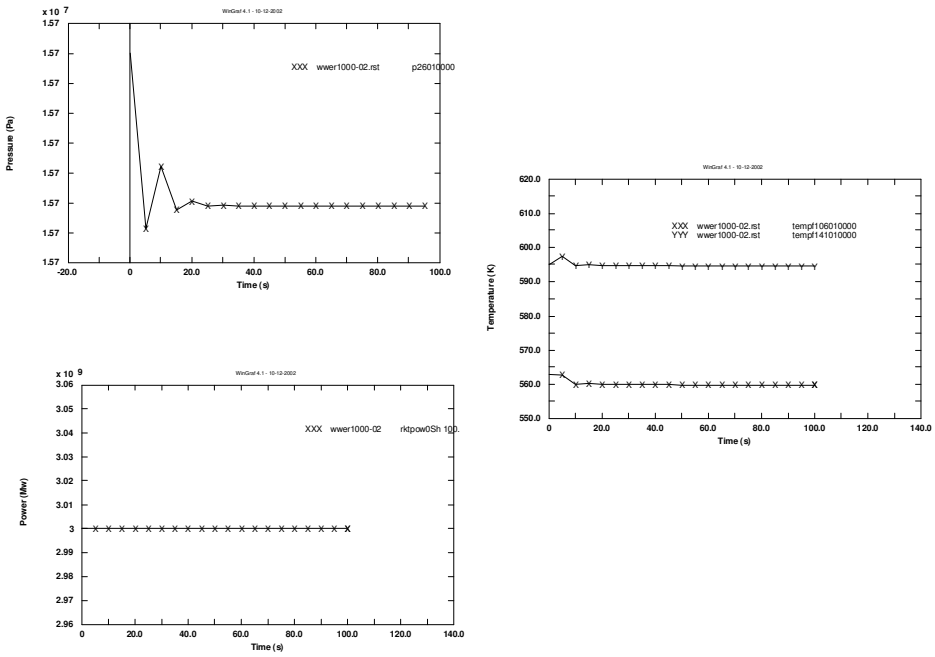

Fig. 6 Nodalization qualification at "Steady State" level - Example of the time trends of calculated steady state conditions.

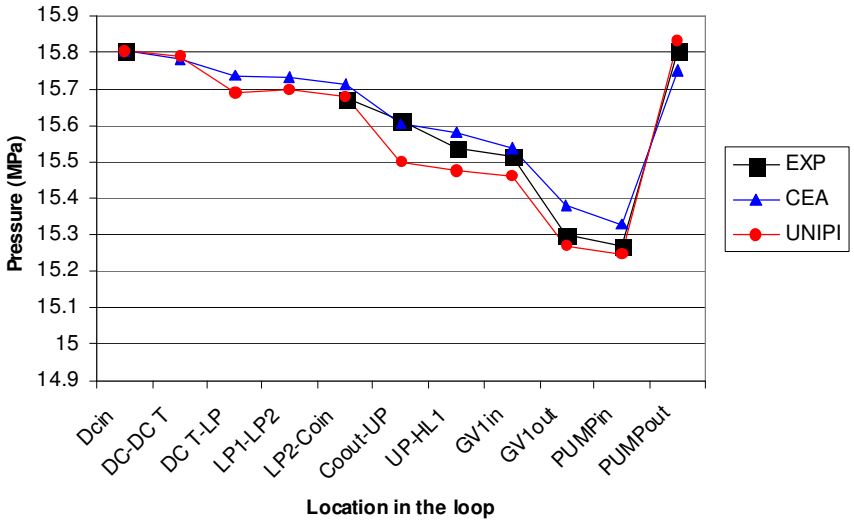

Fig. 7 Nodalization qualification at "Steady State" level - Example of the curve of the primary side pressure vs. loop length.

Any significant change in the nodalization requests that a new qualification process at steady state level is fulfilled

1.1.3 On transient

The “On Transient” qualification level is performed by comparison between calculated data and experimental data. This check is performed before adopting the nodalization for any kind of calculation, to detect nodalization and user choice inadequacies. Correction of errors or deficiencies leads to an “on transient” qualified nodalization ready to be used for other purposes.

If a facility nodalization must be checked a comparison with experimental data obtained in the facility for another analysis can be used. The qualitative evaluation of the results adopting comparison between corresponding parameters in the experiment and in the calculation results and judgments of the RTA is performed. If this step is fulfilled, the quantitative accuracy is evaluated by application of the FFTBM.

The on transient qualification is performed in a different way is a NPP nodalization has to be qualified. The difference is due to the lack of experimental data from NPP. However, at least one among the following activities must be performed:

- ✓ “Kv scaled” calculation: comparison between the nodalization performance and experimental data in another facility In this frame, adopting proper scaling criteria (time preventing, volume/power scale factor) a comparison can be made between predicted and experimental data performed in a facility (proper scaling factors must be adopted to fix initial and boundary conditions).
- ✓ Compare results of the nodalization with experimental data obtained by reference plant (these can be operational transient data in the case of a Nuclear Power Plant).
- ✓ Compare the results of the nodalization with calculation data coming from a previously qualified nodalizations.

Again the qualitative evaluation of the results compared whit the experimental results is performed to check that all the relevant thermal-hydraulic phenomena are reproduced. The application of FFTBM in this case is not mandatory because differences are generally found between calculation and experimental results due to unavoidable differences between the NPP and the facility hardware.

An example of the Kv-scaled parameters is reported in the *Tab. 5*. In *Tab. 6* and *Fig. 8* some results from a Kv-scaled calculations are reported.

Tab. 7 reports an example of qualitative evaluation of the code results. Each RTA is identified by some parameters. For each parameter the comparison with the experimental value is judged: E means excellent and a good agreement exists between code and experimental results; R is for reasonable and means that the phenomenon is reproduced by the code, but some minor discrepancies exist; M is for minimal and means that a relevant discrepancy is present between the code results and the experiment, but reason for the difference is identified and it is not

caused by a nodalization deficiency; U is for unqualified and means that a relevant discrepancy exists but reasons for the difference are intrinsic to the code and nodalization capability. If a U result is obtained in the qualitative evaluation the process of qualification is stopped and the nodalization is considered as not suitable for analysis.

Systems	Boundary and initial conditions	Scaling Factor	Notes
Accumulators	Start on PRZ pressure < 3.46 MPa Stop on water volume inside ACC < 31.45 m^3	V_{NPP}/V_{LOBI}	Only one ACC connected to loop 1 simulating the Intact Loop ACC of the LOBI
LPIS	Start on clad temperature > 792K	V_{NPP}/V_{LOBI}	Connected to the loops 1 2 3 4 5.
Break	Start at time = 0 s Break area = 0.01573 m^2	$A_{rupture}/V$	In loop 6 (loop connected to PRZ)
Electric core rods	Core power 1943 MWTh	V_{NPP}/V_{LOBI}	
RCP run down	Scram signal	–	

Tab. 5 Nodalization qualification at "On Transient" level - Example of scale parameters for a Kv-scaled calculation.

N.	Event	BL44	Calculation Results	Notes
		Time (s)		
1	Break opening	0.	0.	
2	Scram power curve enabled	1.4	1.8	
3	Start of MCPs run down	1.2	3	
4	MSIV closure	–	3	
5	FW closure	1.3	3	
6	UP in saturation condition	10	20	
7	PRZ empty	25	39	
8	First DryOut	189	–	Does not occur in calculation
9	Minimum mass inventory occurrence	427(first) 2071 (second)	398 (first) 2003 (second)	
10	Second DryOut	372	–	Does not occur in calculation
11	Accumulators injection start	428	367	PRZ pressure < 3.46 MPa
12	Accumulator injection stop	964	1129	Residual mass in Acc. < 32.45 m^3
13	Final (third) DryOut	1711	1658	
14	Final (third) rewetting	2137	2029	
15	LPIS start	2066	2010	Clad temp. > 792 K
16	End of calculation	2350	2900	

Tab. 6 Nodalization qualification at "On Transient" level - Example of resulting events for a Kv-scaled calculation.

Tab. 8 reports an example of FFTBM application. The AA for the primary pressure and the AA for the total calculation must be inside the acceptability range of 0.1 and 0.4 respectively. Larger values for the two parameters are considered as unqualified results for the calculation [3].

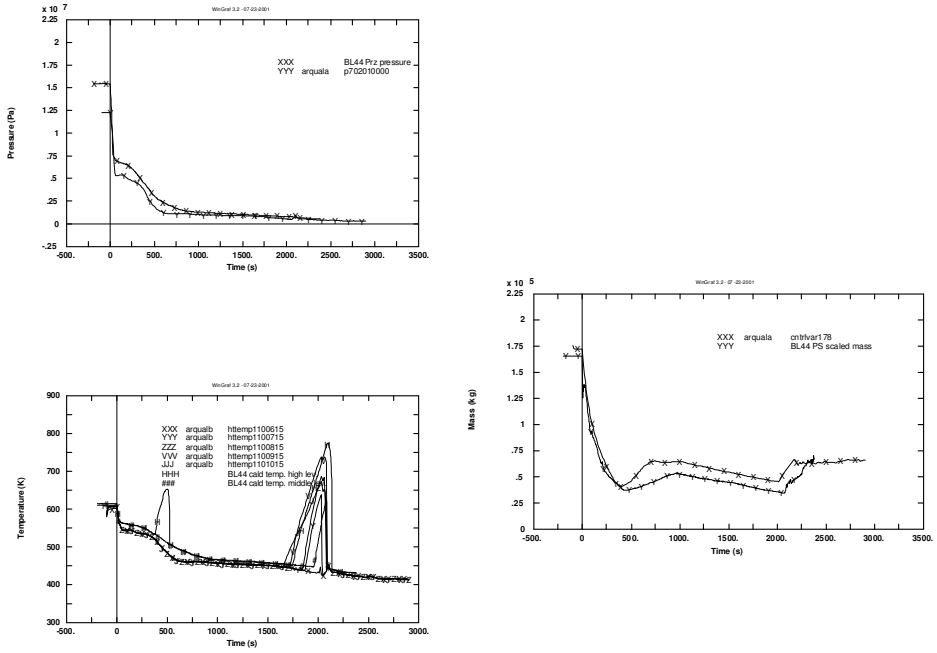

Fig. 8 Nodalization qualification at "On Transient" level - Example of time trends a for a Kv-scaled calculation.

		UNIT	EXP	UNPI 91BN10LPSI	CEA c2m4_1cea	Judgment UNIPI/CEA
RTA: Pressurizer emptying						
TSE	emptying time*	s	131	46	-	R/-
	scram time	s	41	38	41	R/E
RTA: Steam generators secondary side behavior						
TSE	main feed water off, turbine bypass	s	59	55	42	E/R
	difference between PS and SG1 SS pressure at 100 s	MPa	0.42	0.33	0.37	R/R
SVP	SG1 mass	Kg/(s)				
	• at the end of subcooled blowdown		774/(82)	781/(75)	761/(82)	E/E
	• when PS pressure equals SG1 SS pressure		869/(618)	938/(408)	847/(463)	R/E
	• when ACC starts		804/(2955)	802/(3019)	788/(3075)	E/R
	• when LPIS starts		938/(5176)	1126/(6529)	956/(5474)	R/R
SVP	SG1 pressure	MPa				
	• at the end of subcooled blowdown		7.15	7.10	7.05	E/E
	• when PS pressure equals SS pressure		6.95	7.04	7.03	R/R
	• when ACC starts		4.11	3.95	4.00	R/E
	• when LPIS starts		0.88	0.83	0.83	E/E
RTA: Subcooled blowdown						
TSE	upper plenum in sat. conditions	s	83	100	110	R/R
IPA	break flow up to 100 s	kg	152	161	162	R/R
RTA: First dryout occurrence						
TSE	time of dry out	s	2237	2299	2444	E/R
	range of dry out occurrence at various core levels	s	2237÷2471	2299÷2518	2444÷2625	R/R

Tab. 7 Nodalization qualification at "On Transient" level - Example of qualitative evaluation of code results by identification of the RTA.

PARAMETER	CATHARE v 8.1		R5/M3	
	AA	WF	AA	WF
PRZ pressure	0.08	0.093	0.05	0.027
SG pressure - secondary side	0.01	0.149	0.27	0.035
ACC pressure	0.09	0.048	0.06	0.033
Core inlet fluid temperature	0.04	0.050	0.04	0.013
Core outlet fluid temperature	0.04	0.076	0.06	0.04
Upper head fluid temperature	0.33	0.026	0.39	0.033
Integral break flow rate	0.09	0.052	0.10	0.061
Break flow rate	0.76	0.135	0.76	0.113
ECCS integral flow rate	0.11	0.050	0.11	0.048
Heater rod temp. (bottom level)	0.05	0.076	0.05	0.030
Heater rod temp. (middle level)	0.56	0.056	0.73	0.026
Heater rod temp. (high level)	0.52	0.039	0.62	0.023
Primary side total mass	0.33	0.082	0.34	0.064
Core level	0.47	0.102	0.45	0.039
DP inlet-outlet SG (IL)	0.61	0.086	1.18	0.066
Core power	0.22	0.143	0.45	0.034
DP loop seal BL - ascending side	0.86	0.099	1.42	0.020
DP loop seal BL - descending side	1.04	0.093	1.19	0.019
PRZ level	0.31	0.119	0.18	0.037
DP SG inlet plenum U tubes top IL	0.26	0.085	*	*
TOTAL	**0.29**	**0.072**	**0.29**	**0.034**

Tab. 8 Nodalization qualification at "On Transient" level - Example of results of application of the FFTBM.

1.2 Role and relevance of the code-user

The application of a selected code must be proven to be adequate to the performed analysis. Many aspects from facility and experimental data necessary to create the input deck, to the selection of the nodding solutions and eventually the code itself are under the user responsibility.

As can be easily derived the role of the code user is extremely relevant: experience with large number of ISPs has shown the dominant influence of the code user on the final results and the goal of reduction of user effects has not been achieved.

Before finalizing the main outcomes in relation to the user effect, the following can be emphasized:

- ✓ the user gives a contribution to the overall uncertainty that unavoidably characterizes system code calculation results;
- ✓ in the majority of cases, it is impossible to distinguish among uncertainty sources like 'user effect', 'nodalization inadequacy', 'physical model deficiencies', 'uncertainty in boundary or initial conditions', 'computer/compiler effect';
- ✓ 'reducing the user effect' or 'finding the optimum nodalization' should not be regarded as a process that removes the need to assess the uncertainty;

- ✓ generally, it is misleading to prepare guidelines that focus code predictions into a narrow part of the uncertainty.

In addition, wide range activities have been recently completed in the system thermal-hydraulic area. Problems have been addressed whose solution has been at least partly agreed at an international level; these include the need for best-estimate system codes, the general code qualification process, the proposal for nodalization qualification, and the attempts aiming at the qualitative and quantitative accuracy evaluations.

The demonstration of sufficient quality in performing an adequate code analysis involves two main aspects:

Code adequacy. Thermal-hydraulic system code assessment and adequacy demonstration are the responsibility of the code developers. When a particular code is used in new situations for which assessment has not been performed by the code developers or by other user groups (e.g. new plant designs), a complete adequacy demonstration must be performed by the user. There are three essential elements of code assessment:

- ✓ a complete and accurate understanding of the facility and the test to be analyzed;
- ✓ accurate knowledge of facility boundary and initial conditions;
- ✓ understanding of the code architecture, the numeric, and the governing equations and physical models.

The adequacy demonstration process must be undertaken by a code user when a code is used outside its assessment range, when changes are made to the code, and when a code is used for new applications where different phenomena are expected. The impact of these changes must be analyzed and the analyses must be thoroughly reviewed to ensure that the code models are still adequate to represent the phenomena that are being observed.

The process to demonstrate code adequacy for a specific application involves the following key activities:

- ✓ The relative importance of systems, components, processes, and phenomena are identified, with particular emphasis on those that are most important.
- ✓ A phenomena identification table lists the phenomena occurring in a specific plant during a specific accident scenario. The process considers the thermal-hydraulic phenomena, processes and conditions that affect the plant response.

The above process is used to guide user's evaluation of whether the code contains the essential capabilities for modelling phenomena important for the plant and the scenario being analyzed. Additionally, the information is central in the decision as to whether specific models that are deemed to be inadequate must be corrected

before the code can be considered adequate and applied with confidence for plant analysis.

Quality of results. The results of code predictions, specifically when compared with experimental data gathered from properly scaled test facilities, have revealed inadequacies that raised concerns about the reliability of the code and its practical usefulness. Discrepancies between measured and calculated values were attributed to model deficiencies, approximation in the numeric solutions computer and compiler effects, nodalization inadequacies, imperfect knowledge of boundary and initial conditions, un-revealed mistakes in the input deck, and to "user effect". In several ISPs sponsored by CSNI, several users modelled the same experiment using the same code, and the code-calculated results varied widely, regardless of the code used. Some of the discrepancies can be attributed to the code user approach as well as to a general lack of understanding of both the facility and the test.

The two items are main aspects related to the code user. The first aspect is included in the framework of the qualification issue of the code and of the nodalization. Special procedures are established to address this issue. The second aspect is directly related to the user choices generally referred as User Effect.

1.2.1 User effect

The definition of user effect may be subjective; however, for the purpose of this section, the user effect will be defined as follows: user effects are any differences in calculations that use the same code version and the same specifications (e.g., initial and boundary conditions) for a given plant or facility [9].

The following are some of the reasons for the user effects:

- ✓ Code use guidelines are not fully detailed or comprehensive.
- ✓ Based on the current state of the art, the actual 3-dimensional plant geometries are usually modelled using several 1-dimensional zones; these complex 3-dimensional geometries are suitable for different modelling alternatives; as a consequence an assigned reactor vessel part is modelled differently by different users of the same code. Beside the major 1-dimensional code modules, a number of empirical models for system components, such as pumps, valves, separators are specified by the users, sometimes based on extrapolation from scaled devices, thereby introducing additional inaccuracies.
- ✓ Experienced users may overcome known code limitations by adding engineering knowledge to the input deck.
- ✓ Problems inherent to a given code or a particular facility have been dealt with over the years by the consideration and modelling of local pressure drop coefficients, critical flow rate multipliers, or other bias to obtain improved solutions. This has been traditionally done to compensate for code limitations (e.g., application of steady state qualified models to transient conditions, and lack of validity of the fully developed flow concept in typical nuclear reactor conditions). Furthermore specific effects such as

small bypass flows or distribution of heat losses might exacerbate the user effect.

- ✓ An increasing number of users have access to system codes and they are able to perform calculations; however, they may not correctly interpret results due to lack of understanding of the code capabilities and limitations. This item includes the failure to obtain a stable steady state by the user prior to the initiation of the transient.
- ✓ A non-negligible effect on code results comes from the compiler and the computer used to run an assigned code selected by the user; this has been found to be true also for very recent code versions.
- ✓ The available information could be not exhaustive to interpret the facility set-up and the experimental data used as the bases of the comparison are to be interpreted; the user in the large majority of cases “reinterprets” data.
- ✓ Error bands and the values of initial and boundary conditions which are needed as code inputs are not well defined; this could permit the user to slightly vary or adjust the initial and boundary conditions or to justify some results as very close to the reference considering an assumed uncertainty band of the experimental results.
- ✓ Analysts lack complete information about the facility before developing input decks and hence filling the gaps with unqualified data.
- ✓ Although the number of user options is thought to be reduced in the advanced codes, for some codes there are several models and correlations for the user can chose. The user is also required to specify some uncertain parameters such as pressure loss coefficients, manometric characteristics, efficiencies and correlation factors.
- ✓ Most codes have algorithms to adjust the time step control (e.g. Courant limit) to maximum efficiency and minimize run time. However, users are allowed to change the time step to overcome code difficulties and impose smaller time steps for a given period of the transient. If the particular code uses an explicit numerical scheme, the result will vary significantly with the time step size.
- ✓ Quality assurance guidelines should be followed to check the correctness of the values introduced in the input decks despite the automatic consistency checks provided by the code.

Typical examples of user and other related effects on code calculations of selected experiments are presented in several CSNI reports (e. g. ISP-25, ACHILLES reflooding test; LOBI natural circulation test; ISP-22 on SPES loss-of-feedwater test; ISP-26 on LSTF 5% cold-leg-break LOCA; ISP-27 on BETHSY 2" cold-leg LOCA without HPSI).

Due to the lack of common agreement about code capabilities, code developers may also exacerbate the user effect problem through feedback from the code's validation and verification process.

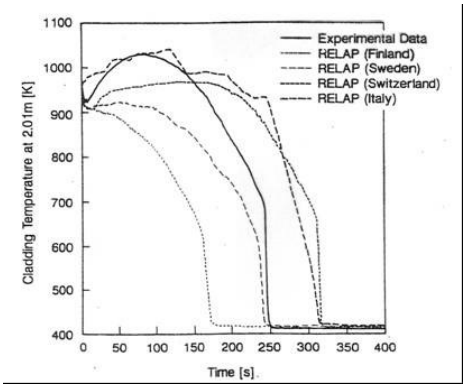

Fig. 9 User effect: Different results for the cladding temperature in the ISP25 test from different users adopting the same code and BIC.

They may change the technique of nodalization taking into account those systems, components, processes and phenomena that have the most influence on the predicted course of an accident without assessing the implication on a wider application of the code. This problem can be minimized by requiring that code models necessary for accurately simulating the most important systems, components, phenomena and processes fully satisfy appropriate adequacy standards and guidance be given to the users about the nodalization schemes to be used for plant calculations.

With the current capabilities, a system code (e.g. Relap5, Cathare, Trac or Athlet) can be put into operation in a few days. In the same time results can be achieved, provided the availability of a nodalization after the check of "grammatical" errors. It is possible to set up an unqualified input deck related to a complex system (e.g. the nuclear power plant) in a few weeks using the available code manuals, considering the robustness of the code capable to running input decks also including not physical conditions. Of course this practice should be discouraged.

It is necessary to say that code user effects on the predicted system behaviour cannot be completely avoided. However different organizations (CSNI, CNRA and European Nuclear Regulators) have defined some general principles in order to reduce the user effects.

1.2.2 Measures to reduce the user effect

Three different aspects can be identified:

A. User training and qualification.
B. Adoption of a suitable Quality Assurance Program.
C. Code improvements.

About the three items above mentioned it is possible to summarize the main principles to solve the user effect issue

In general terms, the following activities are suggested. The user guidelines are not complete for many of the accident analysis codes and need to be improved. Systematic quality assurance procedures need to be used to qualify new sets of input data and to certify the use of previously developed sets for new applications. Code improvements also need to continue to address these concerns through the elimination of unnecessary input options, improved user interfaces and expanded checking of input errors. More extensive user instruction and training needs to be

provided. Software users need to participate in software user groups and other technical exchange programmes associated with the validation and application of the software.

a) Improved user guidelines. Although not a substitute for experience, improved user guidelines are necessary for new users. The detailed guidelines need to be code specific and also to reflect the possibilities of the organization in terms of hardware, software and personnel. In addition, these guidelines help to provide a mechanism to transfer knowledge from experienced users and code developers to new users.
b) Continued improvement in codes. Improved checking for input errors and development of more advanced graphics–user interfaces will continue to reduce potential user errors.
c) Independent validation of safety studies by each organization. It is essential for the training of the code user that independent validation of each specific code is performed by each organization. This validation can be based on a reasonably limited number of experiments taken from the whole validation matrix available and properly selected from three categories of experimental data:
    (i) Partial experiments related to the specific phenomena or a specific component.
    (ii) Integral experiments performed on a dedicated experimental facility.
    (iii) Real plant transient data. The selection of experimental data needs to reflect the characteristics of the particular reactor design.
d) Independent checking and/or peer review of input decks. This is a powerful way of finding user errors. Critical calculations need to be performed by two individuals (or teams) acting independently. Independent checks using a different computer code on the same problem can also be effective. This can include duplicate calculations by the same organizations or, if the plants and conditions are similar, can include a review of similar calculations made by other organizations.
e) Systematic user training. Responsibility is assigned to the code user to provide an adequate representation of the facility, to have adequate knowledge of important phenomena, and to be knowledgeable about the strengths and limitations of the individual codes. Although international standard problem exercises serve as training material for new users through exposure to relevant experiments and to more experienced users, systematic training and possibly user certification programmes for many of the codes need to be supported. This will be increasingly important as remaining experimental programmes are completed. In the past, many thermohydraulic systems analysts gained experience on codes through the analysis of large scale integral experiments such as the Loss of Fluid Test Facility in the USA. This experience was invaluable when these same codes were applied to the analysis of commercial power plants.
f) Participation in software user groups and other technical exchange programmes. Participation in groups with other users not only ensures that a group of users is better informed about best available practices but also promotes improvement in those practices on a wider basis. Technical

exchanges between experimentalists, model developers and other researchers involved in resolving important technical issues relating to a user's analytical work are effective ways of obtaining a greater breadth of experience and training. In particular, for severe accident analysis, for which active experimental and other research programmes are still in progress, such technical exchanges may be the only effective way of learning about important phenomena and methods of analysis [5].

1.2.2.1 User qualification and training

User effects on the quality of the results of analysis can be reduced by systematic training. Even more important is the use of systematic training to ensure that software users are qualified to perform safety related analyses. Although the training necessarily depends to some extent on the type and end use of the results of the analysis, certain minimum conditions need to be satisfied to ensure that users can be effective analysts.

1. Firstly, analysts performing safety related analyses need to have at least a basic understanding of the important phenomena and of methods of analysis, in particular reactor physics, thermohydraulics and fuel behaviour.
2. Secondly, analysts need to have a basic understanding of the plant and its performance. The depth of understanding necessary on the part of the analyst in both cases depends strongly on the type of analysis being performed, the extent of supervision by more experienced staff and the overall knowledge of staff members available to support analytical activities. In general terms, strong supervision, teamwork, careful review and a good overall quality assurance programme (with associated standard practices and guidelines) can partially compensate for the limitations of individual analysts.

A prime factor contributing to efficient training and to achieving reliable results from a safety study is that the user belongs to a safety analysis group in charge of the methods and related applications for safety studies. In this framework, newer users can perform sensitivity calculations, whereas more experienced users can check the list of the key physical phenomena for an accident. Additionally, training of analysts can be performed as part of an overall formal training programme established by the organization responsible for the analysis. Such a training programme needs to include formal training plans with objectives and milestones, success criteria and written records of training activities. The training itself may consist of lectures prepared by more experienced analysts, reading assignments, participation in external courses and workshops, performance of relevant calculations and, most importantly, apprenticeships with more experienced analysts.

Although there are many different ways of classifying the specific training necessary for effective analysis, four fundamental types of training are suggested:

(a) University studies or other comparable courses in the phenomena important for analysis,
(b) Practical training on the design and operation of plants,
(c) Training specific to the software for the analysis,

(d) Application specific training.

Training on the phenomena is the most basic level of training and is, in many cases, provided at university level. University courses in thermohydraulics, heat transfer, structural analysis and/or reactor physics form the basis for design analysis or the analysis of normal plant operation and DBAs. Unfortunately, university courses on severe accident phenomenology and methods are much less widely available. As a result, training for severe accident analysis may be much more difficult to obtain. An effective severe accident analyst may need additional training in:

(1) Behaviour of fuel and other core materials, including the metallurgy of reactor core materials, material interactions and other chemical interactions, and the release of fission products;
(2) Combustion phenomena;
(3) Aerosol physics;
(4) More specialized thermohydraulics such as that for steam explosions.

In addition, severe accident analysis may necessitate some knowledge of probability theory and other methods used in PSA. Practical training in the design and operation of the plant is also important for the effective analysis of DBAs and BDBAs. *Tab. 9* gives an example of the relationship between the type of activity and the respective level of experience required. In *Tab. 9*, activities identified as research and training denote the analysis of experimental facilities, the validation of individual code models through code to data and sensitivity studies on the basis of existing results of analysis. Analysis of plant accidents denotes the use of analytical software for plant calculations using preexisting plant models. Development of plant models denotes the development of the plant system input models for the software. It should be noted that cumulative experience may be built up through the total knowledge of the analysis group, embodying individual staff experience, rigorous documentation and the development of analytical procedures and guidelines (methods). This enables a reliable safety analysis to be performed by the group, while minimizing the influence of the actual number of years of experience of individual staff members. The cumulative experience may also come from outside the group through the use of consultants with suitable experience, in combination with rigorous training and the development of procedures and guidelines for use by group members. Specific training in the use of the analysis software is usually provided by the software developer or certified trainer or optionally by other experienced users within the analysis group. Such training is important for an analyst to be able to use individual software packages effectively. The type of training necessary depends on the specific software being used but would cover, as a minimum, a review of the modelling concepts used in the software, validation of the software and application of the software to problems comparable with those the analyst is expected to encounter. In the case of software for analysis of severe accidents, a review of the important severe accident phenomena and the experimental data is probably appropriate because of the wide diversity of possible accident phenomena and the relative lack of other training specific to severe accidents. Application specific training will typically be provided by the analyst's organization, although it is possible that some training can be provided by software developers or external bodies for generic classes of applications. Training in this area is most effective within the framework of a strong group of experienced analysts in combination with careful supervision and review.

In the absence of a strong support group, participation in external software user groups and other technology exchange groups to discuss experience and problems is essential. In addition, such participation is important for the group as a whole to maintain an awareness of good practices in other organizations. Analysts need to be encouraged during training at all levels to use independent tools and to make 'hand' calculations and other types of engineering calculations to check their analysis, whenever possible. Examples include the use of steady state mass and energy balances and the review of similar calculations. Integrated graphics–user interfaces which animate the results of analyses are also valuable tools which can be used to identify discontinuities, inconsistencies and in some cases numerical instabilities. Where possible, relevant experimental results could be used to benchmark the results of the analysis.

Activity	**Experience**
Research/analyst training	<3 years (phenomenological training assumed)
Analysis of plant accidents	3–5 years
Development of plant models	5–10 years

Tab. 9 Examples of activities and experience required of analysts

Formal qualification of analysts or of analyst training programmes is a more controversial goal, although it would be valuable in promoting a higher level of effectiveness on the part of the analyst and in helping to ensure the continued improvement of training methods. Unfortunately, because of the diversity of applications, development of a set of standards that could be used on a national or international basis would seem to be unlikely.

1.2.2.2 Adoption of a suitable quality assurance program

Quality assurance. Input decks should only be produced according to a quality assurance strategy that includes review, checking and feedback. When input decks are shared and used to produce a new version, the process should follow the same quality assurance standard. It can be pointed out that quality assurance requirements for the analyses are being set up through regulatory guides in several countries (Finland, The Netherlands, Hungary, and the USA).

Quality assurance is essential at each step of the study. The procedures should cover the following:

- ✓ Quality assurance for code calculation. Quality assurance for code calculation requires that an identified and frozen code version be used after appropriate installation and implementation tests; this ensures that no unjustified modifications of the constitutive models will alter the study results. The code must be able to correctly simulate all the transient dominant phenomena. Quality assurance must demonstrate code assessment and qualification; justifying documents must be provided.
- ✓ Quality assurance for the methodology. The methodology - frozen and described within specific documents - reduces the user's effect because it

imposes a common and precise formalism to all users. This formalism requires the user to:

- Describe the type of accident studied:
  - Initiators,
  - study rules,
  - criteria to respect.
  - Describe the accident transient, using the physical knowledge acquired during physical analysis. For this step, comparison with studies performed previously with an equivalent calculation code (and the experience of other users) can be useful.
- Justify the code capability to simulate all the physical phenomena of the transient. For this task, the user relies on:
  - code descriptive documentation,
  - code qualification documentation,
  - (eventually) complementary validation tests.
- Describe and justify the chosen nodalization.
- Describe the chosen methodology:
  - chosen scenario,
  - main assumptions (according to plant operation, for example) - uncertainties in the initial conditions,
  - uncertainties in the calculation code and in the dominant phenomena - treatment of uncertainties, introduced conservatism.

Organizational requirements. Well-structured and effective organisations are regarded as necessary to reduce the faults introduced into a system. Proper documentation of input decisions is needed to minimize the risk of incorrect safety system behaviour. This applies to any code. Evidence should be provided that the safety aspects are adequately monitored.

Delineation of responsibility. Clear delineation of responsibility should eliminate unsafe decisions due to a lack of attention. The responsibilities of, and relationships between, all staff and organizations involved shall be documented

Improved user guidelines. Detailed user guidelines are recommended to reduce mistakes; however, they cannot be a substitute for training and experience.

User discipline. Sensitivity studies are a good way to understand code capabilities and deficiencies. However, tuning of the results through unrealistic values for physical parameters only adds to the confusion and leads to getting the right answer for the wrong reasons, the errors compensating each other.

Safety culture. Safety culture is a key issue, emphasizing safety within the organisation and promoting practices to keep organizations aware of the risk linked to potential consequences of incorrect operations. The staff must be aware of the risks posed by the plant. Safety culture should reduce - unfortunately it cannot eliminate - inattention to details and slipshod procedures that could adversely affect

the outcomes of an analysis. A written safety policy shall be available demonstrating a commitment to a safety culture

Staff competencies. If the staff does not have the appropriate level of training and experience, errors will be introduced and not be detected. Suitable evidence of staff's appropriate level of training and experience shall be available for inspection. It shall be demonstrated that the levels of staffing are adequate. There shall be an appropriate balance between the numbers of hired staff and full-time employees.

Project pressure. Both financial and temporal project pressures might lead to inadequate safety provisions.

Procedures. There is generally a need for internal procedures to minimise errors and explain the code guidelines. The documentation should aim at passing information about the corporate knowledge base. The verification process is usually done by an independent analyst or a senior expert, and approved by the group leader. Adequate procedures should be in place for controlling the documentation and the specifications.

1.2.2.3 Code improvements

Code improvement. In the long term, the best way to reduce the user effect is through improvement of the code physical modelling and numerical techniques as by using of numerical methods for automatic mesh refinement and multi-dimensional capabilities for important subsystems. It would be an advantage if the code developer has experience in carrying plant analysis and appreciates the difficulties that the user might have in performing real plant nodalizations. The codes should be designed so that an analyst who is quite familiar with the phenomena can use the codes reliably. The choice of the time step should be checked through sensitivity studies, focused on convergence. If numeric instabilities cannot be avoided, the code is not appropriate to the application.

Graphical user interfaces. Graphical user interfaces (GUIs) would reduce user effect by allowing the code users more time to check the input deck, interpret the data, and run time control. One of the main advantages of such tools is the development of input decks by eliminating inconsistent choices. A GUI would also isolate the code users from the computational engine, automatically preventing the user from selecting an inconsistent option.

Pre-processor. There is an agreement to recommend the use of a pre-processor, the development of which should follow the same quality assurance process as the code itself. It is even generally requested, although it was stated that one cannot depend on it. The benefits of using such a pre-processor are:

- ✓ reducing the user errors through controls of the input deck (noding and meshing rules, main guidelines, elevations, wall area and mass, etc.) and of various balances and integrated quantities,
- ✓ increasing the efficiency of handling the large amount of data required to build up a model,

- ✓ improving the visualization of the models (checking the geometry, friction coefficients, etc.),
- ✓ improving the understanding of all the logical signals,
- ✓ allowing the use of a high level language that reduces the need for the code syntax knowledge.

1.3 Process for user qualification

Best estimate codes are used by Designer/Vendors of Nuclear Plants, by Utilities, by Licensing Authorities, by Research Organisms including Universities, by Nuclear Fuel Companies and by other Organizations supporting in various manners the above bodies. The purposes in the use of the code may be quite different, including the optimization of the design of a component or system, the improvement of EOP, the confirmation of overall plant safety, the investigation of a physical phenomenon, the qualification or the training of plant operators or just the understanding of the transient behavior of a complex system.

Clearly, the requirements for code user may be very different also depending upon the objectives of the calculation and the subsequent use of the results.

The user training activity proposed hereafter is connected with the most important use of the code, dealing with situations that imply consequences owing to the obtained results for the design of the nuclear plant, for the normal and off-normal operating procedures or in terms of safety.

Two main levels for code user qualification are distinguished in the following:

- ✓ code user, level "A" (LA);
- ✓ responsible of the calculation results, level "B" (LB).

A Senior grade level should be considered for the LB code user (LBS). Requisites are detailed hereafter for the LA grade only; these must be intended as a necessary step (in the future) to achieve the LB and the LBS grades.

The main difference between LA and LB lies in the documented experience with the use of a system code; for the LB and the LBS grades, this can be fixed in 5 and 10 years, respectively, after achieving the LA grade.

In such a context, any calculation having an impact in the sense previously defined must be approved by a LB (or LBS) code user and performed by a different LA or LB (or LBS) code user.

The starting condition for LA code user is a scientist with generic knowledge of nuclear power plants and reactor thermal-hydraulics (e.g. in possession of the master degree in US, of the 'Laurea Magistrale' in Italy, etc.).

The requisites for the LA grade code user are in the following areas:

A. Generic code development and assessment processes.

a. Sub-area A1): Conservation (or balance) equations in thermal-hydraulics including definitions like HEM/EVET, UVUT(UP), Drift Flux, 1D, 3-D, 1-field, Multi-field, Conduction and radiation heat transfer. Neutron Transport Theory and Neutron Kinetics approximation. Constitutive (closure) equations including convection heat transfer. Special Components (e.g. pump, separator). Material properties. Simulation of nuclear plant and BoP related control systems. Numerical methods. General structure of a system code.
b. Sub-area A2): Developmental Assessment. Independent Assessment including SET Code Validation Matrix, and Integral Test Code Validation Matrix. Examples of specific Code validation Matrices.

B. Specific code structure.
   a. Sub-area B1): Structure of the system code selected by the LA code user: thermal-hydraulics, neutronics, control system, special components, material properties, numerical solution.
   b. Sub-area B2): Structure of the input deck; examples of user choices.

C. Code use - Fundamental Problems (FP).
   a. Sub-area C1): Definition of Fundamental Problems (FP): simple problems for which analytical solution may be available or less. Examples of code results from applications to FP; different areas of the code must be concerned (e.g. neutronics, thermal-hydraulics, and numerics).
   b. Sub-area C2): The LA code user must deeply analyze at least three specified FPs, searching for and characterizing the effects of nodalization details, time step selection and other code-specific features.

D. Code use - Basic Experiments (BETF).
   a. Sub-area D1): Definition of Basic test facilities and related experiments (BETF): researches aiming at the characterization of an individual phenomenon or of an individual quantity appearing in the code implemented equations, not necessarily connected with the NPP. Examples of code results from applications to BETF.
   b. Sub-area D2): The LA code user must deeply analyze at least two selected BETF, searching for and characterizing the effects of nodalization details, time step selection, error in boundary and initial conditions, and other code-specific features.

E. Code use - Separate Effect Test Facilities (SETF)
   a. Sub-area E1): Definition of Separate Effect Test Facility (SETF): test facility where a component (or an ensemble of components) or a phenomenon (or an ensemble of phenomena) of the reference NPP is simulated. Details about scaling laws and design criteria. Examples of code results from applications to SETF.
   b. Sub-area E2): The LA code user must deeply analyze at least one specified SETF experiment, searching for and characterizing the

effects of nodalization details, time step selection, errors in boundary and initial conditions and other code-specific features.

F. Code use - Integral Test Facilities (ITF).
    a. Sub-area Fl): Definition of Integral Test Facility (ITF): test facility where the transient behavior of the entire NPP is addressed. Details about scaling laws and design criteria. Details about existing (or dismantled) ITF and related experimental programs. ISPs activity. Examples of code results from applications to ITF.
    b. Sub-area F2): The LA code user must deeply analyze at least two specified ITF experiments, searching for and characterizing the effects of nodalization details, time step selection, errors in boundary and initial conditions and other code-specific features.

G. Code use - Nuclear Power Plant transient Data.
    a. Sub-area G1): Description of the concerned NPP and of the relevant (to the concerned NPP and calculation) BoP and ECC systems. Examples of code results from applications to NPP.
    b. Sub-area G2): The LA code user must deeply analyze at least two specified NPP transients, searching for and characterizing the effects of nodalization details, time step selection, errors in boundary and initial conditions and other code-specific features.

H. Uncertainty Methods including concepts like nodalization, accuracy quantification, user effects. Description of the available uncertainty methodologies. The LA code user must be aware of the state of the art in this field.

“Deeply analyze” indicated above means:

- ✓ to develop a nodalization starting from a supplied data base or problem specifications;
- ✓ to run a reference test case;
- ✓ to compare the results of the reference test case with data (experimental data, results of other codes, analytical solution), if available;
- ✓ to run sensitivity calculations;
- ✓ to produce a comprehensive calculation report (having an assigned format).

A qualified user at the LB grade must be in possession of the same expertise as the LA grade and:

I. he must have a documented experience in the use of system codes of at least 5 additional years;

J. he must know the fundamentals of Reactor Safety and Operation and Design having generic expertise in the area of application of the concerned calculation;

K. he must be aware of the use and of the consequences of the calculation results; this may imply the knowledge of the licensing process.

A qualified user at the LBS grade must be in possession of the same expertise as the LB grade and:

L. he must have an additional documented experience in the use of system codes of at least 5 additional years.

Two years training and "Home Work" with modalities defined below, are necessary to achieve the LA grade, following an examination. An examination is needed for achieving the LB Code User grade (5 years after the LA grade). The LBS code use grade can be obtained (5 years after achieving the LB grade) following the demonstration of performed activity in the 5 years period [1].

Tab. 10 to *Tab. 12* report the modalities for the achievements of the LA, LB and LBS Code User grades.

Weeks	**Lectures**	**Specific. for home works**	**Home works**	**On site test**
1-2	A1 A2^ B1 B2^ C1 D1			
3		C2 D2		
4-25			A B C2* D2*	
26				A1 B1 C D C2+ D2+
27	A2 E1	E2		
28-50			E2*	
51				A2 E E2+
52	B2 F1	F2		
53-76			F2*	
77				B2 F F2+
78	H G1	G2		
79-102			G2*	
103				G H G2+

Tab. 10 Subjects and time schedule necessary for the LA Code User grade

Weeks	Lectures	Specific. for home works	Home works	On site test
1				I* J K K+

Tab. 11 Subjects and time schedule necessary for the LB Code User grade

Weeks	Lectures	Specific. for home works	Home works	On site test
1				L*

Tab. 12 Subjects and time schedule necessary for the LBS Code User grade

1.4 Training

The computer code user represents a source of uncertainty that can influence the results of system code calculations. This influence is commonly known as the 'user effect' and stems from the limitations embedded in the codes as well as from the limited capability of the analysts to use the codes. Code user training and qualification is an effective means for reducing the variation of results caused by the application of the codes by different users. A systematic approach to training code users who, upon completion of the training, should be able to perform calculations making the best possible use of the capabilities of best estimate codes, is a need of the scientific community. In other words, the aim of the training program is a contributing towards solving the problem of user effect.
It is from 2004 that UNIPI organizes as follow-up of the proposal to IAEA for a permanent training course for system code users, in collaboration with other Universities, a semina named 3D S.UN.COP (Scaling, Uncertainty and 3D COuPled code calculations). Five seminars have been held at University of Pisa (2003, 2004), at The Pennsylvania State University (2004), at University of Zagreb (2005) and at the School of Industrial Engineering of Barcelona (2006). It was recognized that such courses represented both a source of continuing education for current code users and a mean for current code users to enter the formal training structure of a proposed 'permanent' stepwise approach to user training.
The main feature of the seminar course may be identified in the following:

- The idea of practical use of the code: a course without practical code application has (much) lower validity.
- The idea to mix different codes*:* the use of different code is worthwhile also to establish a common basis for code assessment and for the acceptability of code results.
- The need of exam: exams were in the past courses (very) well accepted by code users. The exam gave them the possibility to show their expertise and to demonstrate the effort done during the course.
- The practical use of procedures for nodalisation qualification that can be directly applied in the participants institutions.
- The practical use of procedures for accuracy quantification that are demonstrated at the qualitative and the quantitative level.
- The "joining" between BE codes and uncertainty evaluation that shows the full application of uncertainty methodologies and the worth of these within a licensing process.
- The establishment, promotion and use of international guidance through large participation of very well known international experts

1.5 The computer and the compiler effect

The computer dependence is generally caused by:

1. programming errors;
2. bad programming practices;
3. different precision.

The first item is related to many different aspects, mainly related to real compiler errors or incorrect programming.

- ✓ Initialization of variables: some variables are connected to values deriving from previous calculations and a unwanted initialization value is used.
- ✓ Reuse of some variables used in subroutines: in some case the variables value can be maintained or deleted.
- ✓ Type and length of parameters: the portability requests that the same variable in subroutines are the same of the calling routines.
- ✓ Use of some special not standard commands and instructions.
- ✓ Arithmetic relational expressions: these expressions are sensible to the precision of the floating point numbers.
- ✓ Use of different precisions data: inaccuracies arises when single and double precision data are used to derive high accuracy results.

The above mentioned aspects may lead to different code results as a consequence of the change of the kind of computer independent of the compiler optimization.

A typically situation indicated in the item 2 occurs during the writing of formulas; it can causes some problems if singularity points exist in the formula; generally a different way to write the formula can avoid the singularity points and any connected problems.

The item 3 is related to the effect of the different precision options assumed; precision can vary from single precision to quadruple precision (64 bits). Even if the word length is equal, the storage of the floating point numbers can be different. Effects are evidenced especially in these kinds of aspects:

- ✓ bifurcation or cliff edge effects especially related to actuation set point or to the transition between different models when the transition is discontinue;
- ✓ iteration process during calculation have to be adapted to the precision of the computer used to assure the portability of the code.

Other relevant aspects are related to the qualification level of the compilers especially if the compiler is a new version.

From a general point of view, the quality of the software must be assessed. The different aspects of a compiler/code, must be evaluated considering the following attributes:

- ✓ Functionality,
- ✓ Reliability,
- ✓ Usability,
- ✓ Efficiency,
- ✓ Maintainability,
- ✓ Portability.

Some analyses have been performed by University of Pisa to check the effect of a different computer configuration on the results. Two calculations using exactly the

same input, but run on different computer results are compared; the experimental results are also added. The calculation labeled “psb_test7c1gg” has been run using a P-IV, 32 bits, 2800 MHz processor and Windows 32 bits as operative system; the calculation labeled as “psb_testtc1ggAMD” has been run adopting a AMD Athlon, 64 bits 3200+ 2200 MHz as processor and Windows 32 bites as operative system. Both the calculations reproduce the Test 7 of the test matrix (see paragraph 4) in the list of the experiment performed in the PSB-VVER1000 facility for this project.

Some obtained results are shown in *Fig. 10, Fig. 11* and *Fig. 12* reporting the primary side pressure during the PORV cycling period, the secondary side pressure and the core rods superficial temperature in the upper level.

The comparison between calculated results puts in evidence some differences in the two calculations results. The differences are particularly notable in the trend of primary and secondary side pressure; a slight (but not important) effect is also notable in the core rods superficial temperature.

As a conclusions it is possible to say that the error generated by computer and/or compiler is acceptable if it is smaller than the uncertainty related to the code models, so a validation code method must be adopted; the dependency of code results from machine precision and compiler optimization can be minimized by a correct and structured programming strategy.

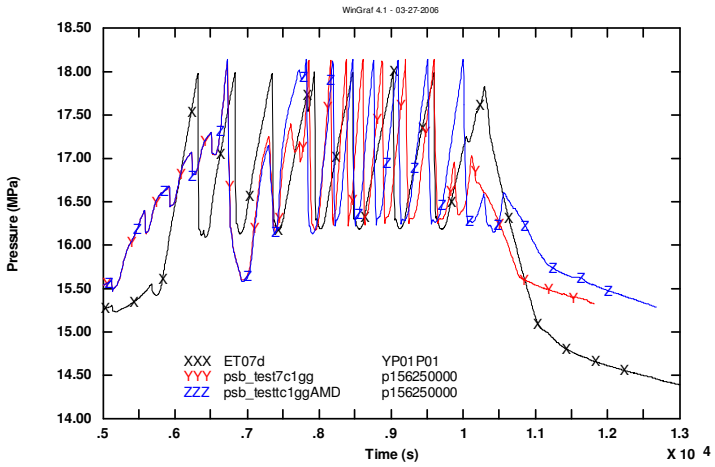

Fig. 10 Computer/compiler effect. Test 7, primary side pressure in the period of the PORV cycling

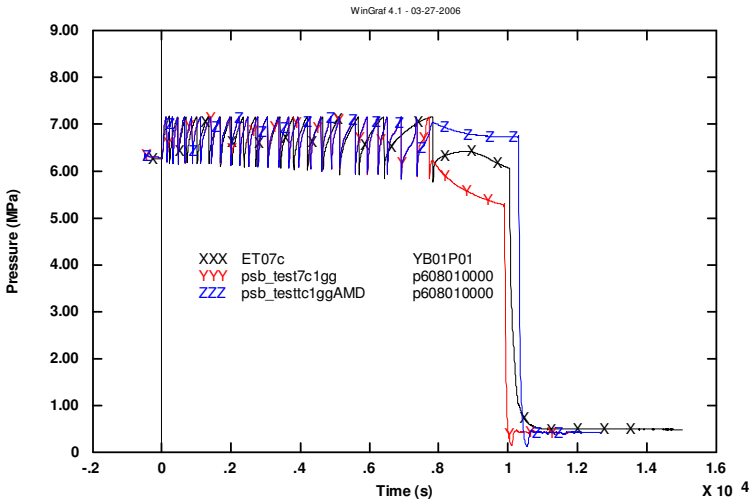

Fig. 11 Computer/compiler effect. Test 7, secondary side pressure

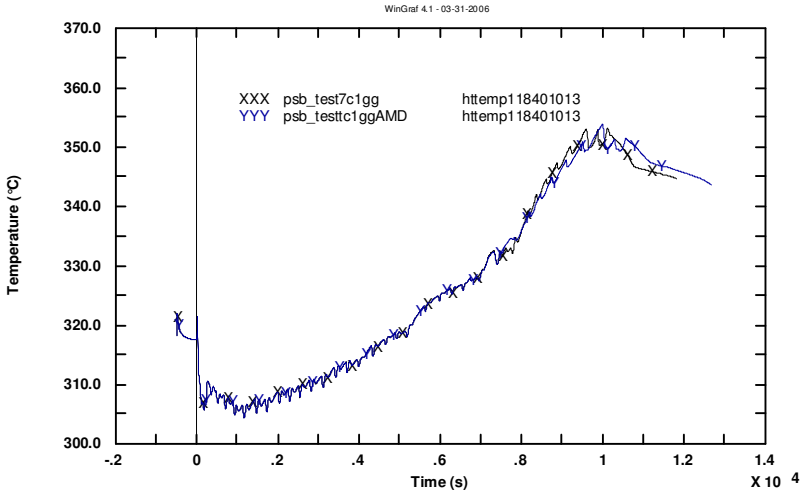

Fig. 12 Computer/compiler effect. Test 7, core rods surface temperature in the upper level (only calculated results)

2. COMPUTATIONAL TOOLS FOR QUALIFICATION

2.1 The UMAE based Method

The UMAE (Uncertainty Methodology based on Accuracy Extrapolation) is a methodology developed to derive the uncertainty related to the code application. The peculiarity of UMAE is constituted by deriving the uncertainty by the extrapolation of the accuracy. In the UMAE the code application to obtain the accuracy and to perform the reference calculation for uncertainty application constitute absolutely relevant steps. The code application involves the input data, the codes, the user and the evaluation of the results. As a consequence a method to qualify the code application and all the related aspects had been developed and included in the UMAE. From the UMAE qualification procedure a general method for qualification process has been derived without relevant changes. Notwithstanding the origin, the method is not only used for calculation qualification, but it can be adopted for different scope. Some procedures connected with UMAE are listed in the following:

1. Demonstration of scalability (independence from scaling) of experimental data sets.
2. Nodalisation development criteria.
3. Nodalisation qualification criteria.
    a. 'Steady-state' level.
    b. 'On-transient' level.
    c. 'Kv-scaled' calculation.
4. Demonstration of scalability (independence from scaling) of code accuracy.
5. Criteria for code accuracy evaluation.
6. Qualitative level evaluation.
7. Quantitative level evaluation (FFTBM tool).
8. 'Intrinsic' & independent demonstration of code-user quality.

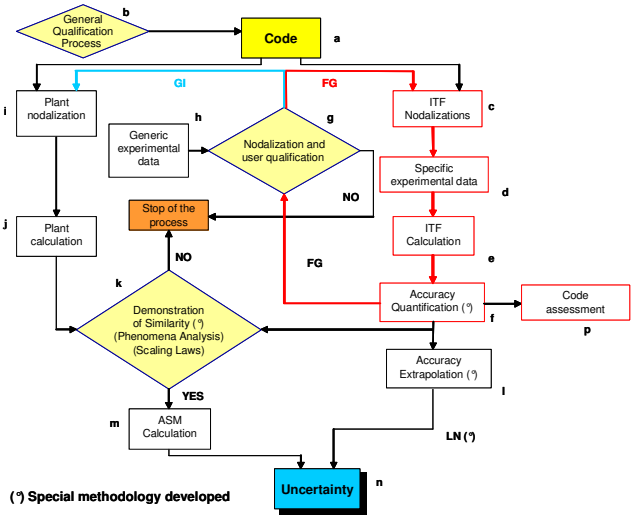

Fig. 13 Simplified flow chart of the UMAE

Points 3 and 5 are suitable for different steps of the of the code assessment process.

The main scheme of the UMAE is reported in the *Fig. 13*. A description of each step of the UMAE is reported hereafter.

Lower letters identify main steps and the relevant connections are indicated by capital letters. The following logical steps or conditions to be verified are part of the methodology

1. Frozen code (block “a”): an internationally recognized code version must be available; the consequences of the installation of the code on the computer must be checked.
2. Reactor and accident scenario: a PWR or a BWR can be selected; the choice of the reactor system and of the accident scenario should be restricted to those for which valuable assessment activity has been carried out.
3. Relevant experimental data: experimental data include hardware data of facilities, suitable boundary and initial conditions and time trends of important quantities measured during the experiments of interest.
4. Code and user capabilities (block "b"): the code must be the object of a wide international use; no special deficiencies should have been detected in predicting the phenomena to be considered. The code user or group of users taking part in this activity should be properly qualified.
5. Suitability of integral facilities design: the scaling and design factors of the involved test facilities must comply with the actual state of the art in the field. This includes unavoidable scaling distortions like the heat release from structures that must be carefully evaluated.
6. Suitability of test design: a scaling analysis must be performed to fix boundary and initial conditions especially in the case of counterpart tests; reactor conditions should be taken as reference in each case.
7. Suitability of test data: instrumentation, data acquisition system and assumptions made to derive complex quantities like total mass in primary system, heat losses to environment, etc., should be checked.
8. Development of nodalization (blocks "c" and "i"): a qualified user (or group of users), in the sense defined in the previous paragraph, must build up the input data decks of the involved facilities and plant.
9. Generic and specific experimental data (blocks "d" and "h"): 'generic' and 'specific' experimental data are derived from the involved facilities; the former set of data is not necessary in the accuracy extrapolation process and must be used for the independent qualification of the nodalization; the latter must include all the key phenomena expected to occur during the considered transient.
10. Nodalization qualification (block "g"): the developed nodalization must be qualified considering the comparison with hardware data, boundary and initial conditions and time trends of relevant quantities. A procedure has been developed and applied in which a 'steady state' and a 'transient' level of qualification are distinguished; criteria for the selection of relevant quantities are discussed below.
11. Plant nodalization qualification (block "i"): plant nodalization must be developed using the same criteria utilized for nodalizing facilities: again it must be qualified following the same procedure defined in the discussion of block "g". Plant start-up data or operational transients must be used in this connection.
12. Evaluation of the specific data base: the specific data base is constituted by the signals recorded during the considered experiments and by the results of the code calculations. Each test scenario (measured or calculated) should be divided into 'Phenomenological Windows' (Ph.W). In each Ph.W. 'Key Phenomena' (K.Ph) and 'Relevant Thermal-hydraulic

Aspects' (RTA) must be identified. K.Ph characterize the different classes (e.g. small break LOCA, large break LOCA, etc.) of transients and RTA are specific of the assigned one; K.Ph and RTA qualitatively identify the assigned transient; in order to get quantitative information, each RTA must be characterized by 'Single Valued Parameters' (SVP, e.g. minimum level in the core), 'Non-Dimensional Parameters' (NDP, e.g. Froude number in hot leg at the beginning of reflux condensation), 'Time Sequence of Events' (TSE, e.g. time when dryout occurs) and Integral Parameters (IPA, e.g. integral or average value of break flowrate during subcooled blowdown).

13. Similarity of experimental data (path "FG"): RTA, SVP, NDP, IPA and TSE are used in each Ph. W to demonstrate the similarity among the available experimental data. If this is not achieved, UMAE cannot be used.
14. Acceptability of calculation results (block "e"): RTA, SVP, NDP, IPA and TSE are used in each Ph.W to demonstrate the qualitative accuracy of the calculation, (again path "FG"). If this is not achieved UMAE cannot be used.
15. Accuracy quantification (block "f"): if the above two steps are acceptable, the accuracy of code calculations can be quantified utilizing the already mentioned special procedure. This produces a single value in the frequency domain from each comparison between calculated and measured parameters in transient scenario: the so-called 'Average Accuracy' must be smaller than an assigned value.
16. Feedback on the plant nodalization (path "GI"): the result of block "g" is a qualified nodalization that predicts satisfactorily the assigned transient or the related K.Ph if counterpart tests are not available. The relevant experience gained in this process must be transferred for setting up the plant nodalization.
17. Plant calculation (block "j"): two plant calculations must be carried out: a) the 'facility Kv scaled' and, b) the 'realistic conditions' calculation. In the former case boundary and initial conditions utilized as input should be derived from those in the experimental facilities following the counterpart test scaling criteria. In the latter case nominal conditions should be used.
18. Acceptability of plant calculation (block "k"): RTA, SVP, NDP, IPA and TSE are used in each Ph.W to demonstrate the similarity of the plant predicted scenarios in the 'facility Kv scaled' case with measured and calculated scenarios in the facilities. Furthermore, Ph.W, and K.Ph must be the same in the cases a) and b) of the previous step. If these conditions are not fulfilled, UMAE cannot be used.
19. Analytical simulation model, ASM (block "m"): this essentially consists of a 'qualified' plant nodalization running on a 'qualified' code by a 'qualified' user. The ASM can be used to predict plant scenarios characterized by the same Ph. W and K.Ph as the assigned transient.
20. Accuracy extrapolation (block "l"): summing up, if the following conditions are fulfilled, accuracy in predicting SVP, NDP, IPA and TSE can be extrapolated:
    - ✓ the design scaling factors of the involved facilities are suitable;
    - ✓ the test design scaling factors of the involved experiments are suitable;
    - ✓ the experimental data base is qualified;

- ✓ the nodalizations and the related users are qualified;
- ✓ RTA are the same in the considered experiments if counterpart or similar tests are involved; otherwise, the same RTA can be identified in different experiments;
- ✓ RTA are well predicted by the code at a qualitative and a quantitative level;
- ✓ RTA are the same in the plant calculation 'facility Kv scaled' and in the experiments;
- ✓ parameters ranges (SVP, NDP, TSE and IPA), properly scaled, are also the same. This must be interpreted in different ways depending upon the availability of counterpart tests;
- ✓ in the plant calculation 'realistic conditions' Ph.W and K.Ph are the same as in the considered experiments; SVP, NDP, TSE and IPA may be different: reasons for this are understood.

The extrapolation of accuracy is achieved with reference to the above mentioned parameters through the use of the statistics. The ratios of measured and ca1culated values of SVP, NDP, TSE and IPA are assumed randomly distributed around the unit value. This is also justified by the huge number of variables affecting the considered ratios. In this way 'mean accuracy' and '95th percentile accuracy' are derived that are applicable to the plant calculation. In this procedure the measurement errors, the unavoidable scaling distortions and the dimensions of the facility are direct1y considered.

21. Uncertainty calculation (block "n"): the extrapolated accuracy can be superimposed direct1y to the results of the ASM calculation. Nevertheless, some additional analytical elaboration is necessary to transform the point values into continuous error bars that envelope the reference ASM calculation. In particular, 'timing', 'spatial' and 'mean integral' uncertainty have been defined, taking as reference TSE, SVP, NDP and IPA values, respectively.
22. Code assessment (block “p”): the determination of the accuracy results are also useful in uncertainty evaluation by application of the CIAU methodology.

Some aspects especially involving qualification activities of the method are to be noted:

- ✓ “b” block: this step is constituted by the qualification process of the code and represents the qualification activity performed by the development team of the code.
- ✓ “h” block: qualification of the data derived by the experiment is checked.
- ✓ “i” block: qualification of the data and of the sources of the data is checked.
- ✓ “g” block: this step is about the qualification of the nodalization and user.
- ✓ “k” block: the quality level of the NPP model (nodalization) is evaluated.
- ✓ “p” block: the code response is evaluated to judge the code capabilities.

It is necessary to note that the activity of the user in the blocks “b”, “h” and “i” is simply constituted by the check of the quality of the data. In the blocks “g”, ”k” and “p” the user has an operative role, performing the necessary activity to derive and to evaluate the quality level of nodalization and/or codes.

The different uses of the procedure for qualification of the UMAE are summarized in the *Fig. 14 to Fig. 15*.

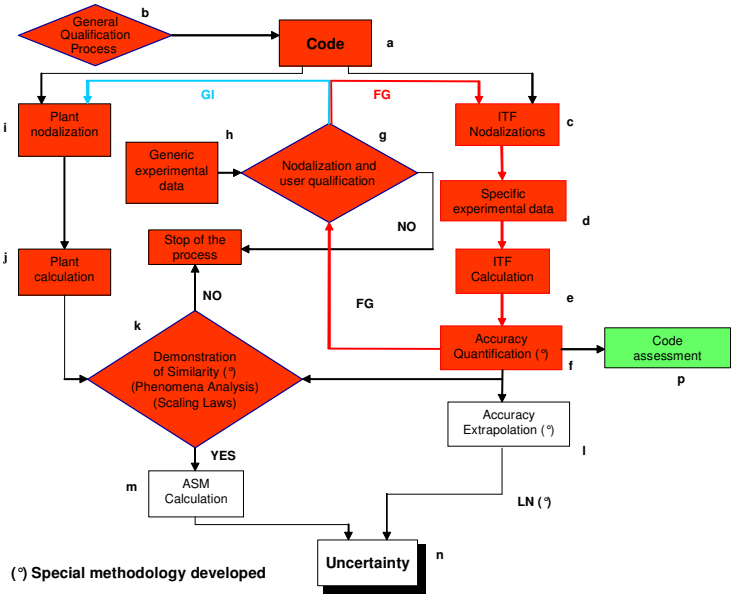

Fig. 14 Use of the qualification procedure of UMAE for code assessment and code-user qualification

Fig. 14 shows the main steps necessary to asses the code capabilities. The Code is generally qualified by the development team (blocks “a” and “b”); this phase constituted the internal validation of the code. The independent validation is performed by preparing a qualified nodalization to reproduce experimental tests (sequence “c”, “d”, “e”, “f” and “g”), to evaluate the code accuracy (block “f”) and by preparing a qualified nodalization of NPP (sequence “i”, “f”) to demonstrate the capability of the code at different scale (block “k”). The output of the procedure is constituted by the green block in the figure: a judgement about code capabilities is derived (block “p”).

Fig. 15.outlines the main steps to be performed to qualify the nodalization of a facility. The qualification of the nodalization of a facility is an activity typically involved in the code assessment procedure, in the accuracy evaluation of a code (again for code assessment or for use in the error data base for uncertainty evaluation) or in the code-user qualification. In this procedure the code is assumed as qualified and frozen. The sequence “c”, “d”, “e”, “f” and “g” is performed eventually in an iterative way to fulfil the criteria of acceptability (block “g”) for the accuracy related to the nodalization (block “f”). The output of the process is represented by the green block in the figure (block “g”): at the end of the process, a qualified nodalization is obtained

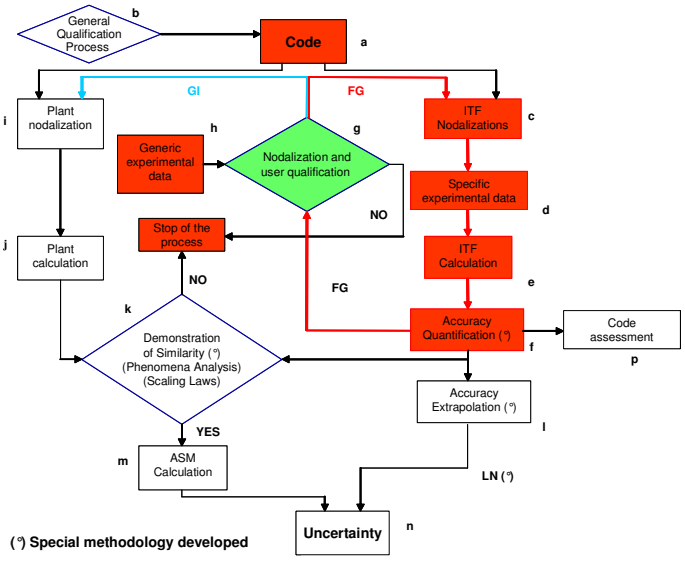

Fig. 15 Use of the qualification procedure of UMAE for facility nodalization qualification

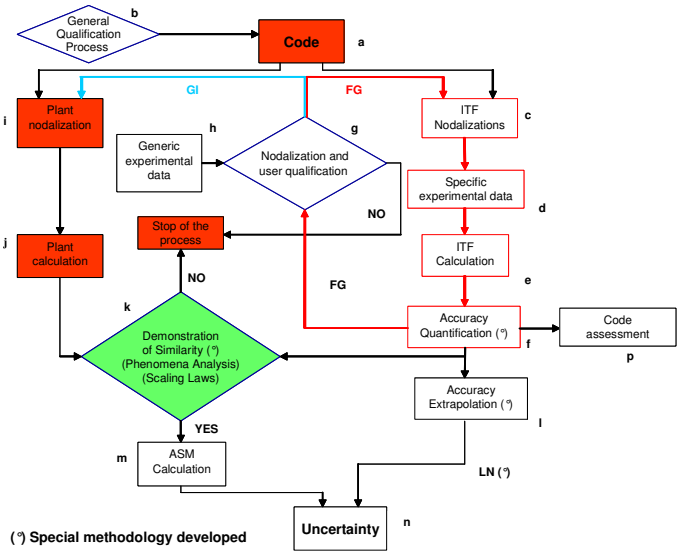

Fig. 16 Use of the qualification procedure of UMAE for NPP nodalization qualification

Fig. 16 describes the main steps related to the qualification of the NPP nodalization. Differences exist with the above described procedure for the qualification of the facility nodalization, because in the case of NPP generally no

suitable or only few data are available for nodalization qualification. In the procedure the code is considered as qualified and frozen (block “a”).The NPP nodalization is prepared (block “i”) and similarity analysis is performed (blocks “j” and “k”). The similarity analysis is generally based on the Kv-scaled calculation that uses as references data the experimental results obtained in an integral test facility. The capability of the code at the NPP scale is evaluated by application of qualitative criteria. A qualified NPP nodalization is obtained if the acceptability criteria are fulfilled (green block “k”) [3].

2.2 The FFTBM

Several approaches have been proposed to quantify the accuracy of a given code calculation. Even though these methods were able to give some information about the accuracy, they were not considered satisfactory because they involved some empiricism and were lacking of a precise mathematical meaning. Besides, engineering subjective judgment at various levels is deeply inside in proposed methods. Generally, the starting point of each method is an error function, by means of which the accuracy is evaluated. Some requirements were fixed which an objective error function should satisfy:

1. at any time of the transient this function should remember the previous history;
2. engineering judgment should be avoided or reduced;
3. the mathematical formulation should be simple;
4. the function should be non-dimensional;
5. it should be independent upon the transient duration;
6. compensating errors should be taken into account (or pointed out);
7. its values should be normalized.

The simplest formulation about the accuracy of a given code calculation, with reference to the experimental measured trend, is obtained by the difference function

$$\Delta F(t) = F_{calc}(t) - F_{exp}(t) \quad (1)$$

The information contained in this time dependent function, continuously varying, should be condensed to give a limited number of values which could be taken as indexes for quantifying accuracy. This is allowed because the complete set of instantaneous values of $\Delta F(t)$ is not necessary to draw an overall judgment about accuracy.

Integral approaches satisfy this requirement, since they produce a single value on the basis of the instantaneous trend of a given function of time. On the other hand, searching for functions expressing all the information through a single value, some interesting details could be lost. Therefore, it would be preferable to define methodologies leading to more than one value in order to characterize the code calculation accuracy.

Information that comes from the time trend of a certain parameter, be it a physical or a derivated one, may be not sufficient for a deep comprehension of a concerned phenomenon; in such a case, it may be useful to study the same phenomenon from other points of view, free of its time dependence. In this context, the complete behaviour of a system in periodic regime conditions (periodic conditions due to instability phenomena are explicitly excluded), can be shown by the harmonic response function that describes it in the frequency domain. Furthermore, the harmonic analysis of a phenomenon can point out the presence of perturbations otherwise hidden in the time domain.

It is well known that the Fourier transform is essentially a powerful problem solving technique. Its importance is based on the fundamental property that one can

analyze any relationship from a completely different viewpoint, with no lack of information with respect to the original one. The Fourier transform can translate a given time function g(t), in a corresponding complex function defined, in the frequency domain, by the relationship:

$$\tilde{g}(f) = \int_{-\infty}^{+\infty} g(t) e^{-j2\pi ft} dt \qquad (2)$$

Afterwards, it is assumed that the experimental and calculated trends to which the Fourier transform is applied verify the analytical conditions required by its application theory; i.e., it is assumed that they are continuous (or generally continuous) (1) in the considered time intervals with their first derivatives, and absolutely integrable in the interval (- ∞ + ∞ (2)), [7]. This last requirement can be easily satisfied in our case, since the addressed functions assume values different from zero only in the interval (0, T).

Therefore:

$$\tilde{g}(f) = \int_{0}^{T} g(t) e^{-j2\pi ft} dt \qquad (3)$$

The Fourier integral (equation 3) is not suitable for machine computation, because an infinity of samples of g(t) is required. Thus, it is necessary to truncate the sampled function g(t) so that only a finite number of points are considered, or in other words, the discrete Fourier transform is evaluated. Truncation introduces a modification of the original Fourier transform (the Fourier transform of the truncated g(t) has a rippling); this effect can be reduced choosing the length of the truncation function as long as possible. When using functions sampled in digital form, the FFT can be used. The FFT is an algorithm that can compute more rapidly the discrete Fourier transform. To apply the FFT algorithm, functions must be identified in digital form by a number of values which is a power of 2. Thus, if the number of points defining the function in the time domain is N = 2m+1

$$N = 2^{m+1} \qquad (4)$$

The algorithm gives the transformed function defined in the frequency domain by 2m+1 values corresponding to the frequencies (n = 0, 1, .., 2m)

$$f_n = \frac{n}{T} (n = 0, 1, .., 2^m) \qquad (5)$$

in which T is the time duration of the sampled signal.

Taking into account the fact that the adopted subroutine packages evaluate the FFT normalized to the time duration T, from equations. (3) and (5) it can be seen that $|g,\tilde{}(0)|$ represents the mean value of the function g(t) in the interval (0,T), while $|g,\tilde{}(f_i)|$ represents the amplitude of the i-th term of the Fourier polynomial expansion for the function g(t).
Generally, the Fourier transform is a complex quantity described by the following relationship:

$$g,\tilde{}(f) = Re(f) + jIm(f) = |g,\tilde{}(f)|\, e^{j\theta(f)} \quad (6)$$

where Re(f) is the real component of the Fourier transform, Im(f) is the imaginary component of the Fourier transform, $|g,\tilde{}(f)|$ is the amplitude or Fourier spectrum of g(t) and θ (f) is the phase angle or phase spectrum of Fourier transform.

It is well known that:

$$|g,\tilde{}(f)| = \sqrt{(Re(f))2+(Im(f))2} \quad * \theta(f) = tg^{-1}\frac{Im(f)}{Re(f)} \quad (7)$$

The method developed to quantify the accuracy of code calculations is based on the amplitude of the FFT of the experimental signal and of the difference between this one and the calculated trend. In particular, with reference to the error function $\Delta\tilde{}F(t)$, defined by the eq. (1), the method defines two values characterizing each calculation:

a dimensionless average amplitude

$$AA = \frac{\sum_{n=0}^{2^m} \left|\tilde{\Delta}F(f_n)\right|}{\sum_{n=0}^{2^m} \left|\tilde{F}_{exp}(f_n)\right|} \quad (8)$$

a weighted frequency

$$WF = \frac{\sum_{n=0}^{2^m} \left|\tilde{\Delta}F(f_n)\right| \cdot f_n}{\sum_{n=0}^{2^m} \left|\tilde{\Delta}F(f_n)\right|} \quad (9)$$

The AA factor can be considered a sort of "average fractional error" of the addressed calculation; the weighted frequency WF gives an idea of the frequencies related with the inaccuracy.

The accuracy of a code calculation can be evaluated through these values, by representing the discrepancies of the addressed calculation with respect to the experimental data with a point in the WF-AA plane. The most significant information is given by AA, which represents the relative magnitude of these discrepancies; WF supplies different information allowing to better identify the character of accuracy. In fact, depending on the transient and on the parameter considered, low frequency errors can be more important than high frequency ones, or vice versa.

Trying to give an overall picture of the accuracy of a given calculation, it is required to combine the information obtained for the single parameters into average indexes of performance.

This is obtained by defining the following quantities:

$$(AA)_{tot} = \sum_{i=1}^{N_{var}} (AA)_i (w_f)_i \quad (WF)_{tot} = \sum_{i=1}^{N_{var}} (WF)_i (w_f)_i \quad (10)$$

with $\sum_{i=1}^{N_{var}} (w_f)_i = 1$ (11)

where N_{var} is the number of parameters selected (to which the method has been applied), (wf)i are weighting factors introduced for each parameter to take into account their importance from the viewpoint of safety analyses. This introduces some degree of engineering judgment that has been fixed by a proper and unique definition of the weighting factors, necessary to account for the different relevance, from the point of view of safety and reliability of the measurement, of the various addressed quantities.

In the following, the FFT method application will be dealt with from an operative point of view. To apply the methodology described in the previous section, after selecting the parameters to be analyzed, it is necessary to choose the following parameters:

- ✓ number of points,
- ✓ sampling frequency,
- ✓ cut frequency.

All these items are related each other; nevertheless they will be treated in separate sub-sections, in order to allow a better comprehension of their requirements.

In order to evaluate the discrete Fourier transform, it is necessary, first of all, the sampling of signals to be analyzed. The choice of the sampling frequency depends on transient, kind of parameter trend to be investigated (i.e. pressure, flow rate, clad temperature, etc.); obviously, the fulfilment of the sampling theorem (4) is required to avoid distortion of sampled signals due to aliasing occurrence (5). Aliasing occurs until the frequency sampling is increased to

$$T = \frac{1}{2f_c} \quad (12)$$

where f_c is the highest frequency component of Fourier transform characterizing the spectrum of the continuous function g(t).

Therefore, experimental data acquisition should be characterized by sampling frequency greater than 2fc; similar frequencies of acquisition should have the corresponding calculated trends. Of course, compared analysis of these data requires that the lowest value of fc (between the experimental and calculated one) should be taken as limiting value. A typical value of fc related to parameters of interest in thermal-hydraulic transients is 1 Hz; specifically, break flow rates or pressure drops measurements can include higher values.

Since the FFT algorithm requires that functions are identified by a number of values, equally spaced, which is a power of 2, an interpolation is necessary to satisfy this requirement. On the other hand, the comparison of experimental and calculated signals, and the evaluation of their difference function $\Delta F(t)$, imposes that they have the same time scale.

Furthermore, after selecting the number of points N (see eq. (4)), the maximum frequency of transformed functions by the FFT, is given by

$$f_{max} = \frac{2^m}{T_d} = \frac{f_c}{2} \quad (13)$$

where Td is the transient time duration and f_c is the sampling frequency.

Then, the number of points is strictly associated with the adopted sampling frequencies; it is meaningless to choose a number of points corresponding to a frequency greater than the f_{max} achievable using a certain fc. On the other hand, during the interpolation step, some information could be lost choosing a too low number of points. Last, it is worthwhile to remember that the increase of the number of points involves the growth of the array dimensions utilized by the program package set up for the full method application.

Besides, the interpolation introduces an additional effect on signals, i.e. each interpolation, using a linear method, adds a slope. It has been verified that this effect is negligible, because it causes the addition of some spurious frequencies in the original signal spectrum, having values greater than the typical frequencies of thermal-hydraulic parameters. On the other hand, most thermal-hydraulic quantities are characterized by low frequencies, then high frequency errors (therefore, these spurious contributions too) can be totally avoided considering proper filtering techniques. To filter any spurious contribution, a cut frequency has been introduced. This cut frequency characterizes the frequency upper value which has to be considered in evaluating the AA and WF factors, as defined by (8) and (9). Typical thermal-hydraulic parameter trends (for different kinds of transients) have been analyzed [8], aiming at defining an unique suitable value of cut frequency, in such a way to avoid partial loss of information.

A cut frequency value of 1 Hz is generally suitable to analyze trends of thermal-hydraulic parameters; only flow rates and densities require cut frequency values up to 2 Hz, as a consequence of their higher frequencies, to avoid loss of information in accuracy evaluation. In order to give an overall picture of the accuracy of the addressed calculation, the FFT method accounts for the accuracy evaluated for each parameter, and defining some weighting factors (wf)i, global indexes of code performance are evaluated (see (10) and (16)). The need of (wf)i definition derives from the fact that the addressed parameters are characterized among other things by different importance and reliability of measurement.

Thus, each $(wf)_i$ takes into account of:

- ✓ "experimental accuracy": experimental measures of thermal-hydraulic parameters are characterized by a more or less sensible uncertainty due to:
  - o intrinsic characteristics of the instrumentation
  - o assumptions formulated in getting the measurement
  - o un-avoidable discrepancies existing between experimental measures and the code calculated ones (mean values evaluated in cross-sections, volume centers, or across junctions, etc.);

- ✓ "safety relevance": particular importance is given to the accuracy quantification of calculations concerned with those parameters (e.g. clad temperature, from which PCT values are derived) which are relevant for safety and design.

Last, a further contribution is included in the weighting factors definition; this is a component aiming at accounting for the physical correlations governing most of the thermal-hydraulic quantities. Taking as reference parameter the primary pressure (its measurement can be considered highly reliable), a normalization of the AA values calculated for other parameters with respect to the AA value calculated for the primary side pressure is carried out. In other words, the following factor has been defined (for the generic j-th parameter):

$$\left(W_{norm}\right)_j = \frac{\left(AA\right)_{pr}}{\left(AA\right)_j} \tag{14}$$

where (AA)pr is the average amplitude calculated for the primary side pressure and (AA)j is the average amplitude calculated for the j-th parameter.

So doing, the weighting factor for the generic j-th parameter, is defined as:

$$\left(w_f\right)_j = \frac{\left(W_{exp}\right)_j * \left(W_{saf}\right)_j * \left(W_{norm}\right)_j}{\sum_{j=1}^{N_{var}} \left(W_{exp}\right)_j * \left(W_{saf}\right)_j * \left(W_{norm}\right)_j} \tag{15}$$

and $$\sum_{j=1}^{N_{var}} \left(w_f\right)_j = 1 \tag{16}$$

where N_{var} is the number of parameters to which the method is applied, (Wexp)j is the contribution related to the experimental accuracy and (Wsaf)j is the contribution expressing the safety relevance of the parameter. (Wexp)j and (Wsaf)j values have to be assigned using engineering judgment, starting from measuring and safety related considerations. Such an evaluation of a suitable set of weights (see *Tab. 13*) to be utilized for typical thermal-hydraulic quantities has been performed, [8]. Some criticism could be raised because engineering judgment is required in weights assignment, but actually, this appears the only practicable way to define the relative importance of the parameters selected to evaluate the accuracy of a code calculation. These weights must remain the same for any comparison between code results and experimental data concerning a same class of transient. Once chosen a set of weights with the above described criteria, any variation of some weight involves a homogeneous change of all the calculations analyzed, above all if a sufficiently high number of parameters has been selected for the accuracy evaluation. Obviously, this affects only global accuracy evaluation of a code calculation; no concern is related to the single parameters accuracy.

The FFT package suitable for the personal computers is available; the version has been built compiling the source program utilizing the Microsoft FORTRAN Compiler 6.1; in particular, the option "Windows executable" program was chosen, in such a way to utilize the Windows extended memory, along with the same powerful Windows environment. Furthermore, obviously, this allowed a significant reduction

of the fees related to the program running, being also optional the use of a workstation to perform these analyses.

As above mentioned, some new features have been introduced in the program, increasing its flexibility and applicability. The program capabilities can be summarized as follows:

- ✓ research and extraction of the addressed variable from data files, allowing various data format;
- ✓ conversion of current data units in SI units, or more generally possibility of manipulate data (optional);
- ✓ analysis of several time windows in a same execution, where each time window can identify whatever phase in the transient;
- ✓ time shifting of data trends to analyze separately the effects of delayed or anticipated code predictions concerning some particular phenomena or systems interventions (optional);
- ✓ interpolation of data points to a power of 2 number of points, coherent with sampling frequency and minimum analysis frequency;
- ✓ FFT evaluation of the signals to be processed;
- ✓ evaluation of the AA and WF quantities (see (8) and (9));
- ✓ output files generation, including information to be processed by standard software in order to trace any desired graphic concerning data curves, error curves, interpolated curves, FFT signals transforms, FFT data spectra, AA-WF data (optional).

After the application of the method to the selected variables, global code accuracy for the analyzed code calculations is carried out by a second program, also running in Windows environment, characterized by "user friendly" characteristics, automatically determining AAtot and WFtot values in all the previously considered time windows. Obviously, this last step must be performed after the analysis of all the variables; then it is not automatically executed after the FFT analysis. Nevertheless, it is easy to build a shell of commands automatically launching the program for the selected variables and finally calculating the global values.

Parameter	W_{exp}	W_{saf}	W_{norm}
Primary pressure	1.0	1.0	1.0
Secondary pressure	1.0	0.6	1.1
Pressure drops	0.7	0.7	0.5
Mass inventories	0.8	0.9	0.9
Flow rates	0.5	0.8	0.5
Fluid temperatures	0.8	0.8	2.4
Clad temperatures	0.9	1.0	1.2
Collapsed levels	0.8	0.9	0.6
Core power	0.8	0.8	0.5

Tab. 13 Selected weighting factor components for typical thermal-hydraulic parameters,[8], [11].

3. KEY FINDINGS

3.1 Addressing the scaling issue

A NPP is characterized by high power (up to thousands of MW), high pressure (tens of MPa) and large geometry (hundreds of m3). The prediction of the transient performance of a so complex system is the main topic of a safety analysis. It is well understandable the impossibility to perform an experiment preserving all these three quantities; so the use of TH codes appears unavoidable. Any TH code should be validated against experimental data that can be collected quasi exclusively in ITF and/or SETF.

The term scaling is in general understood in a broad sense covering all differences existing between a real full size plant and a corresponding experimental facility. An experimental rig may be characterized by geometrical dimensions and shapes, arrangements and availability of components, or by the mode of operation (e.g. nuclear vs. electrical heating). All these differences have the potential to distort an experimental observation precluding its direct application for the design or safety analysis of the reference plant. Distortion is defined as a partial or total suppression of physical phenomena caused by only changing the size (geometric dimension) or the shape (arrangement of components) of the test rigs.

Three main objectives can be associated to the scaling analysis:

- ✓ The design of a test facility.
- ✓ The code validation, i.e. the demonstration that the code accuracy is scale independent.
- ✓ The extrapolation of experimental data (obtained into an ITF) to predict the NPP behaviour.

For the test facility design three types of scaling principles can be adopted:

a) Time–reducing scaling: rigorous reduction of any linear dimension of the test rig would result in a direct proportional reduction in time scaling. This is considered to be of advantage only for cases where body forces due to gravity acceleration are negligible compared to the local pressure differentials.
b) Time preserving scale: based on a scale reduction of the volume of the loop system combined with a direct proportional scaling of energy sources and sinks (keeping constant the core power to system volume ratio).
c) Idealised time preserving modelling procedures: based on the equivalency of the mathematical representation of the full size plant and of the test rig. It is deduced from a separated treatment of the conservation equations for all involved volume nodes and flow paths assuming homogeneous fluid.

Integral Test Facilities are normally designed to preserve geometrical similarity with the reference reactor system. Generally all main components (e.g. rector pressure vessel, downcomer, rod bundle, loop piping, etc.) and the engineered safety

system (HPIS, LPIS, accumulators, auxiliary feed water, etc.) are represented. ITF are used to investigate, by direct simulation, the behaviour of a NPP in case of off-normal or accident conditions. The geometrical similarity of the hardware of the loop systems has been abandoned in favour of a preservation of geometric elevations, which are decisive parameters for gravity dominated scenarios (e.g. in case of natural circulation processes). Thus the reduction of the primary system volume is largely achieved by an equivalent reduction in vertical flow cross sections.

The historical ways to address the issue

In order to address the scaling issue different approaches have been followed:

- ✓ Fluid balance equations, deriving non-dimensional parameters adopting the Buckingham theorem.
- ✓ Semi-empirical mechanistic equations, deriving non-dimensional parameters.
- ✓ To perform experiments at different scales (very expensive way and could not be totally exhaustive).
- ✓ To develop, to qualify and to apply codes showing their capabilities at different scales.

The first bullet recall a typical approach based on a theorem (applied also to solve heat transfer problems) that permits to determine the number of independent non dimensional groups needed to describe a phenomenon. It states that a physical relationship among n variables, which can be expressed in a minimum of m dimensions, can be rearranged into a relationship among (n-m) independent dimensionless groups of the original variables. Buckingham called the dimensionless groups pi-groups and identified them as Π1, Π2, Π3,..,Πn-m. Thus a dimensional functional equation reduces to a dimensionless functional equation of the form: Π1 = f (Π2, Π3,..,Πn-m).

The second bullet implies the definition of non-dimensional parameters derived from relationships that link in an empirical way some dependency, e.g. from consideration of experimental evidence. Again dimensionless groups are defined similar to the pi-groups. It should be reminded that the relationship defined in this approach are valid for a restricted range; thus also the dimensionless parameter are affected by this limitation.

Performing experiment at different scale (third bullet) might be a way to solve the scaling problem, but firstly a lot of experiments should be conducted to cope with the wide range of the scaling factor, secondly the experimental results are affected by peculiarity related to the typical dimension of a test rig at a certain scale.

The last proposal to solve the scaling problem (fourth bullet) is to accept all the limitation remarked above, to develop a system code, to qualify it against experimental data, to prove that its accuracy is scale-independent and to apply such code to predict the same relevant phenomena that are expected in a same experiment (or transient) performed at different scales.

A scaling study can be conducted at different levels:

- ✓ Macroscale.
- ✓ Component scale.
- ✓ Microscale.

The target of the macro scale is to evaluate the global system performance as a whole (e. g the prediction of the pressure behaviour in case of blow-down following a LOCA); in the component scale it has been taken into account the single component (e. g. downcomer-cold leg mixing in case of ECCS injection). It must be noted that at this level in ITF some components adopt the most desirable scaling factor: 1:1, this occurs for the active length, for the fuel rod diameter, diameter and length of the SG tubes, etc. Finally when the investigation is pushed at the microscale the interest is concentrate to the local evolution of thermal hydraulic phenomena, such as Critical Heat Flux occurrence in fuel rods, two phases critical flow in a break, etc.

At whatever level the investigation is conducted a compromise to obtain a solution of the scaling problem should be accepted, especially when complex systems are considered.

The scaling strategy

The scaling strategy followed at University of Pisa

i. Selection of a scaling approach at the system level (macroscale): the full pressure / full height / time preserving scaling (this requires “full” bundle active length and preserving linear power, not all ITF & SETF are suitable for scaling studies).
ii. Considering the rod surface temperature at the hot spot as the reference thermal-hydraulic phenomenon at the microscale level: this assumption is guided by finalizing of the scaling analysis to the NPP safety.
iii. Identification and creation of a hierarchy of thermal-hydraulic phenomena: it is strictly recommended the adherence to the CSNI lists for SETF and ITF for the identification of each phenomenon and an individual scaling analysis related to each selected phenomenon.
iv. (checking of the) design of ITF.
v. (checking of the) design of “counterpart experiments”.
vi. Analysis of CT experimental data: identification and explanation of detected discrepancies among corresponding values.
vii. Application of Best Estimate codes: to demonstrate that discrepancies between measured and calculated trends only depend upon BIC values (within the assigned variation ranges), calculation accuracy is not affected by the scale of concerned ITF, performing Kv-scaled calculation and explanation of discrepancies (if any) between NPP calculated and ITF measured trends considering BIC values and hardware differences.

viii. Connection of the uncertainty evaluation to the scaling issue: extrapolation of the error of the code in NPP prediction based on error in ITF prediction (ref. 14, ref. 15 and ref. 16]).

It could happen that some local events are not predicted because they are driven by parameters that does not appear in balance equations but, thanks to the correct selection of the parameters, it is possible to demonstrate that these phenomena are effectively local, they have a little duration if compared to the entire transient and cannot affect the overall behaviour of the main thermal hydraulic selected parameters chosen to describe the transient.

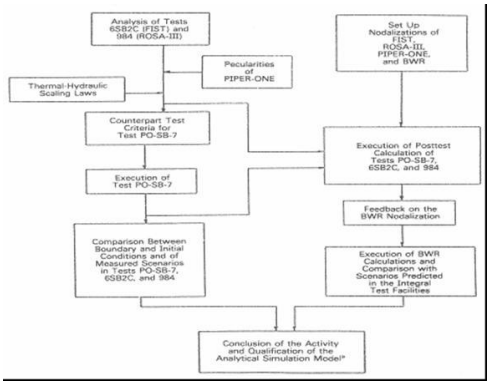

Fig. 17 Flow chart for the interaction between experimental data and code application in the scaling analysis

In the uncertainty method UMAE in the flow chart of *Fig. 17* (referred to the Piper-one CT design and execution), two main paths can be recognized on the diagram: one for the experimental part, in which the CT preparation and execution, the use of the experimental data considering the scaling implication and the comparison with BIC of other tests are included; a second one where analytical tools (i.e. TH code and nodalisations) are developed and applied which benefits of the experimental data consideration. The conclusion of the activity common for both paths is the setting up of an analytical simulation model able to predict the transient behaviour in a NPP with a suitable accuracy.

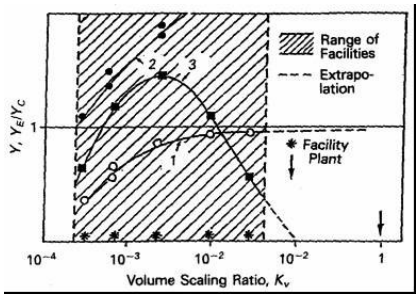

Fig. 18 The extrapolation framework: possible trend resulting from scaling analysis

The UMAE method foresees the extrapolation of the code accuracy. Such extrapolation can be performed because, as already stressed, there is not any systematic dependence between a parameter and the scaling factor; thus it is impossible to direct extrapolate experimental results to predict plant behaviour. In addition the relevant phenomena (that characterize a transient) experienced in different facilities are the same and hence they are not affected by the scaling. *Fig. 18* reflects the situation already illustrated, selecting a parameter and plotting it as a function of Kv the trend is depicted by the curve No 3, i.e. no convergence towards a desirable value is obtained as might be represented by the curve No 1. On the other hand in the range of the test facilities there is not any 'unpleasant' trend as highlighted by the curve No 2.

Support to the UMAE method are given by experimental evidence coping with all the three scaling levels listed above. *Fig. 19* represents the performance of ten natural circulation experiments at different core power conducted in six test rigs.

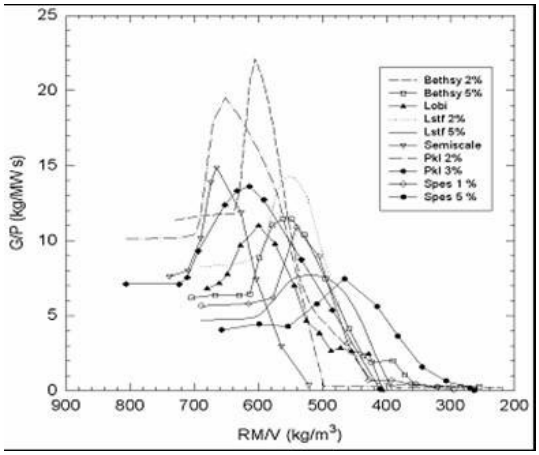

Fig. 19 Experimental support to the UMAE method: similar behaviour at macroscale level

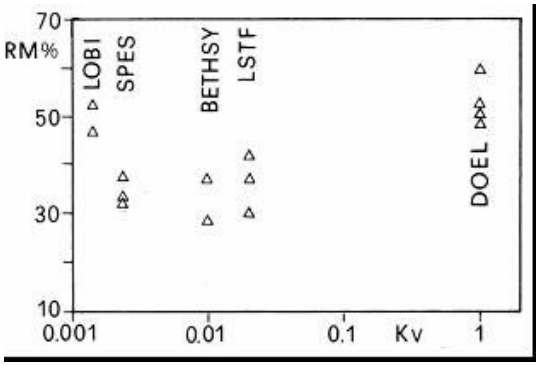

Fig. 20 Experimental support to the UMAE method: scaling independency at the microscale level, dryout occurrence in the phase space residual mass vs. Kv, [20]

The similar behaviour of the plotted quantity (core mass flow rate over core power vs. the residual mass over volume) is put in evidence confirming that relevant phenomena are scale independent.

Fig. 20 reports the experimental data of dryout occurrence in the phase space residual mass in percentage vs. the Kv. No relevant monotonous effect of the volume scaling factor on the residual mass at dryout appears from the experimental data utilized. In addition the uncertainty in the measurement of the residual mass is negligible compared to the differences shown below. At the microscale level there is not any scaling relationship (or similarity) to pursue, the dryout occurrence (hence its prediction) is selected because of its relevance from the safety point of view.

Concerning the component scale level let us consider *Fig. 21* in which the spread of experimental (a) and of code (b) results for the data related to the two databases (experimental and calculated) containing SBLOCA and LBLOCA CT performed in PWR and BWR simulators is reported. Again the similarity of the two sets of data is highlighted.

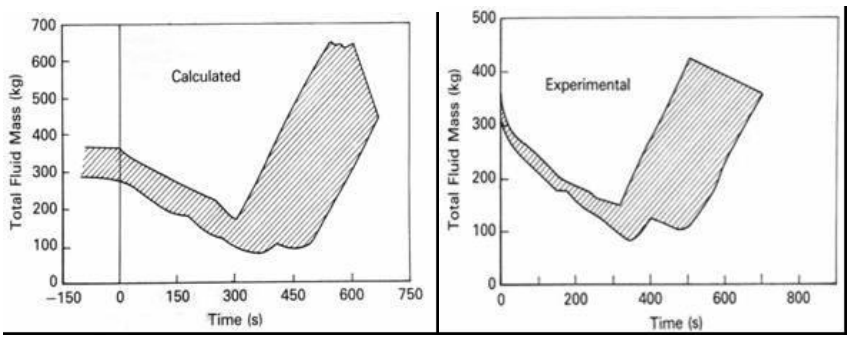

Fig. 21 Experimental (a) and calculation (b) support to the UMAE: similarity at component scale level, spread value for SBLOCA and LBLOCA CT in PWR and BWR facilities

From the paragraphs above it has been demonstrated the scale independence of the main phenomena occurring in the test facilities for a selected transient. The same conclusion can be done when the code prediction is accounted for, as highlighted in *Fig. 22*. Such figure reports the calculation accuracy of SBLOCA transients as well as PWR natural circulation tests, in which it can be seen that the code accuracy prediction is not affected by the scaling factor.

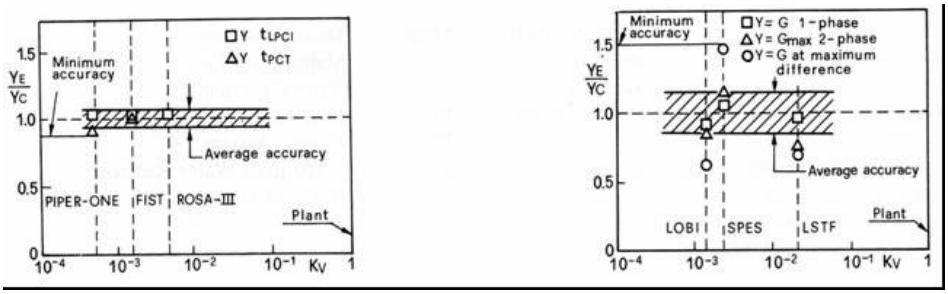

Fig. 22 Calculation support to the UMAE: code accuracy independency as resulting from the SBLOCA CT in BWR facilities and from the PWR natural circulation analysis, [22]

The philosophy at the basis of the UMAE method is to set up a database which contains the accuracy of the ITF code predictions. NPP calculation cannot be checked against experimental data; so a direct code accuracy evaluation is not possible. Nevertheless the uncertainty related to the NPP code prediction is extrapolated from the database built considering ITF calculations accuracy. This aspect represents the connection between the scaling issue and the code uncertainty evaluation, a needed step within the BE approach.

The scaling approach proposed by University of Pisa is substantiated by the use of experimental data and by the results of supporting analyses. The approach does not constitute an alternative to established classical 'approaches' available in the literature like the 'Ishii-approach' or the 'power-to-volume-time-preserving'. Rather, the proposed one is a procedure, or a strategy, where the classical approaches are (or can be) embedded [21][25].

3.2 Use of CFD code in the nodalization realization

The quality of the results obtained from the best estimate code, but in general for every code, is strictly connected to the quality of the data provided as input and to the maturity of the code itself, the experience of the user etc. Several article have been written with the aim to address the effect of the various terms involved in the in these kind of analysis to the final results.
The possibility to have an Analytical Simulator Model (ANS) of the studied system (NPP or ITF) is one important requirement in the safety analysis study. During the input deck preparation, it's not difficult to find in the common practice, inaccurate or missing data in the experimental dataset. Errors in the measurement of the experimentalist, difficulty of the measures are the main reasons that create the need of some alternative method able to provide to the analyst a valid tool to reconstruct the missing data, or to have a good comparative term in case of uncertain experimental data.

The aim of this paragraph is to describe the activity concerning the use of a CFD code (ANSYS-CFX) for the calculation of a more accurate distribution of the pressure drop coefficients to be used in the nodalization realization. In order to observe the effect of the introduction of the new calculated pressure drop coefficients, an already qualified PSB-VVER Cathare2 nodalization developed, qualified and used for the calculation of several transients in the framework of the TACIS contract (see paragraph 4) has been used.

It is important to note that the already implemented coefficient in the qualified nodalization, are taken form the experimental PSB-VVER data set for the pressure drop along the circuit. As can be observed from *Fig. 23* in which the positions of the measurement points along Loop #1 of the PSB-VVER facility are reported, between one measurement point and another, there are straight parts, elbows, bends, so that, the measured value is a "medium value". The use of a CFD code could give a more detailed pressure drop distribution along the circuit.

In the following, the qualification process has been applied to the nodalization with the new coefficients implemented and the results, labeled "CFX", are compared with the already qualified ones, labeled "Base" and with the experimental data labeled "Exp" in the figures. The FFBM has been applied to the new calculated data set and the results have been summarized in the *Tab. 14.*

The Cathare2 nodalization of the PSB-VVER facility used in the TACIS project (see in paragraph 4) for a detailed description of the qualification process and of the main results obtained. For the purposes of this activity, it is important to know that the nodalization is qualified following the criteria of the methodology developed at UNIPI discussed in the previous paragraphs.
The CFD code can simulate in principle the whole facility, but the huge amount of mesh elements needed (hundred millions of cells) requires an extremely powerful computer and very long calculation time. This exercise can be considered as a first attempt and just few geometrical parts of the facility have been modeled in order to observe if some there are some improvement in the results. time for modeling the various parts and calculation time

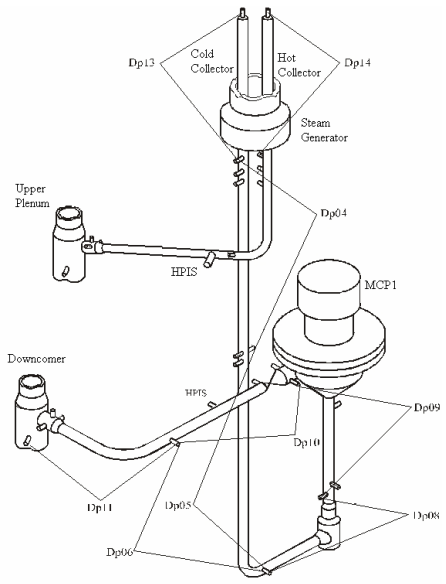

Fig. 23 Cold Leg #1 Pressure Drop measurement points

The four Cold Legs of the PSB-VVER facility model and the mesh have been realized with ICEM-CFX code. This is a powerful tool able to reproduce complex geometry and to create different kind of mesh element shape (hexahedral, tetrahedral *Fig. 24*). shows the spatial configuration of the Cold Leg #1. The others three Cold Legs differ from the Cold Leg #1 just for few centimeters of length.
The shape of the Cold leg is very simple, it's just a long tube of about 15 meters with fix diameter and some bends and elbows as shown in *Fig. 23*. The only part not simulated is the MPC (Main Coolant Pump)
, because it's shape is very difficult to simulate and it's out of the purpose of the present work. The inlet part of the Steam Generator and part of the Downcomer have been simulated in order to have a better estimation of the pressure at the beginning and at the end of the Cold leg. Just a quarter of the downcomer region has been simulated and a symmetry condition has been imposed on the face for taking into account the effect of contemporary injection of the 4 Cold legs

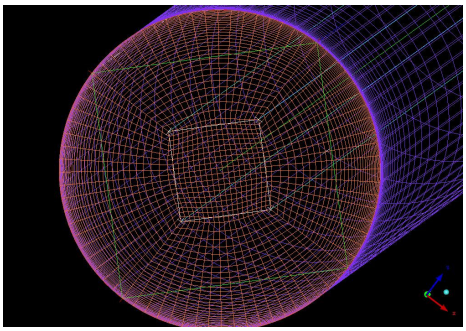

Fig. 24 Particular of the mesh

The mesh has been realized with hexahedral element (*Fig. 24*) with a growing factor in two directions, along the radius in order to increase the number of the element close to the wall, and along length of the long tube in order to have small mesh element the size at the end close to the discontinuity. This adopted criteria is necessary for saving calculation resources. The number of the element used to simulate the whole Cold Leg is about 2500000 for the so called "Base" calculation. The mesh has been imported with the ANSYS-CFX code, and the BIC of the transient has been implemented
The transient chosen is the Test 11 of the PSB-VVER test matrix. It is a SBLOCA with break area 0.7% of the CL area. The break is located in CL of loop #4 between MCP and DC. All HPIS are assumed to fail. Following the AM procedures, the HPIS train, connected with the affected loop is recovered and the cool-down procedure of the secondary side occurs.
The BIC and the imposed sequence of main events are summarized in *Tab. 14* and *Tab. 15*. The operator actions for the AM measures are:

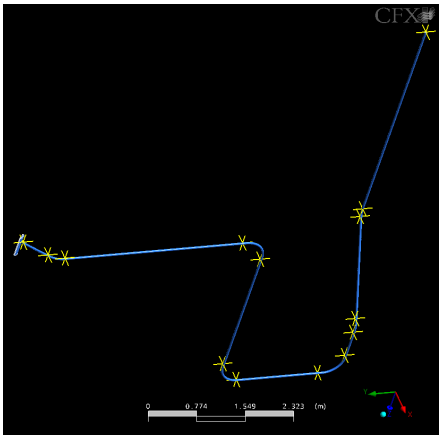

Fig. 25 Ansys-CFX model of CL 1# with the measurement points of the pressure

- ✓ at 1800 seconds activation of 30 K/h cooldown rate of PS by SS;
- ✓ activation of one train of HPIS in the broken loop when cladding temperature reaches 350 ℃, but not earlier that 1800 seconds;

No	PARAMETER	MEASUREMENT	UNIT	VALUE	ERROR
	Primary System				
1	UP pressure	YC01P17	MPa	15.7	±0.05
2	UP outlet fluid temperature	YA01T03 YA02T03 YA03T03 YA04T03	℃	310. 309. 307. 310.	±3 ±3 ±3 ±3
3	DC inlet fluid temperature	YA01T02 YA02T02 YA03T02 YA04T02	℃	277. 278. 276. 276.	±3 ±3 ±3 ±3
4	Core power	YC01N01	kW	1512.	±15
5	Core by-pass power	YC01N02	kW	15.0	±0.4
6	PRZ level	YP01L02	m	6.63*	±0.3
7	Level: ACC-1 ACC-2 ACC-3 ACC-4	TH01L01 TH02L01 TH03L01 TH04L01	m	4.86* 4.85* 4.85* 4.88*	±0.07 ±0.07 ±0.07 ±0.07
8	Pressure: ACC-1 ACC-2 ACC-3 ACC-4	TH01P01 TH02P01 TH03P01 TH04P01	MPa	5.9 5.9 5.9 5.9	±0.03 ±0.03 ±0.03 ±0.03
	Secondary System				
9	Pressare: SG 1 SG 2 SG 3 SG 4	YB01P01 YB02P01 YB03P01 YB04P01	MPa	6.26 6.26 6.31 6.25	±0.05 ±0.05 ±0.05 ±0.05
10	Level: SG 1 SG 2 SG 3 SG 4	YB01L01 YB02L01 YB03L01 YB04L01	m	1.69* 1.69* 1.68* 1.66*	±0.08 ±0.08 ±0.08 ±0.08
11	FW: SG 1 SG 2 SG 3 SG 4	RL01T02 RL02T02 RL03T02 RL04T02	℃	220. 220. 220. 220.	±3 ±3 ±3 ±3
12	AFW: SG 1 SG 2 SG 3 SG 4	RL01T02 RL02T02 RL03T02 RL04T02	℃	150. 150. 150. 150.	±3 ±3 ±3 ±3

Tab. 14 PSB-VVER experimental data base, Test 11: boundary and initial conditions

No	EVENT	SET POINT			
		QUANTITY	UNIT	VALUE	DELAY
1	Leak opening	operator action	s	0.	-
2	SCRAM signal	UP pressure	MPa	< 13.7	+ 2.
3	PRZ heaters switched off	PRZ level	m	4.18	-
4	Turbine valve simulation closure begins	UP pressure	MPa	< 13.7	+ 11.
5	Transition to the AFW	UP pressure	MPa	13.7	+ 15.
6	MCP coast-down onset	difference between saturation temperature (UP pressure) and HL temperature	℃	< 10.	+ 15.0
7	ACC #1 operation	UP pressure	MPa	< 5.9	+ 1.
8	ACC #2 operation	UP pressure	MPa	< 5.9	- 5 .
9	ACC #3 operation	UP pressure	MPa	< 5.9	- 3.
10	ACC #4 operation	UP pressure	MPa	< 5.9	- 7.
11	PS cooldown procedure	operator action	s	1800.	+ 1.
12	HPIS system injection starts	core cladding temperature	℃	338.	-
13	LPIS system injection starts	UP pressure	MPa	2.45	-

Tab. 15 PSB-VVER experimental data base, Test 11: imposed sequence of main events.[3]

For the CFD calculation the turbulence model chosen is the classical K-epsilon. The wall are considered without roughness and the pressure drops have been calculated during the steady state of the selected transient.
The calculation has been executed on 1 node of the a IBM 8 node cluster with 16 AMD Opteron processors (1 node is has two AMD Opteron 2.5 GHz with 2 Gb of RAM) with Linux RedHat Enterprise edition. The duration of the calculation is about 30 minutes.

From the post processing of the ANSYS-CFX code, the value of the pressure has been taken in 13 points along the Cold Leg at the beginning and at the end of every bend or elbow (see *Fig. 25*). In the experimental data set, just seven points have been considered for the pressure drop measurements.

The values of the pressure calculated with CFX in the 13 selected points have been implemented in the excel file in order to calculate the pressure drop coefficient to be implemented in the Cathare2 input deck. The classical Darcy-Weisbach formulas for the pressure drop estimation in the singularity or along a tube has been used:

$$\Delta p_{\sin g} = \mathrm{K}\frac{1}{2}\rho w_{z,m}^2 \tag{17}$$

and for the distributed pressure drop along a conduct:

$$\Delta p_f = f\frac{L}{D}\frac{1}{2}\rho w_{z,m}^2 \tag{18}$$

Once the pressure drop coefficients have been obtained and substituted in the Cathare2 nodalization, the first run have been performed.
The introduction of the new pressure drop coefficients has required a new set up of the initialization values in the nodalization for the obtainment of a steady state in the error band as foreseen by the methodology. All the main parameters: primary and secondary pressure and temperature are stable and fixed on the nominal

value of the transient. In the *Fig. 26* and *Fig. 27*, the first 500 seconds refers to the steady state.
The figures *Fig. 26* and *Fig. 27* show the comparison between the same time trend in the Base case, the calculation performed with the qualified nodalization, the experimental and the new calculation with the pressure drop coefficient modified with the calculated value from CFX code.
As can be observed, the time trends of the main variables calculated with the modified nodalization with the new pressure drop coefficients along the 4 Cold Legs calculated with CFX code are in better agreement with the experimental ones.

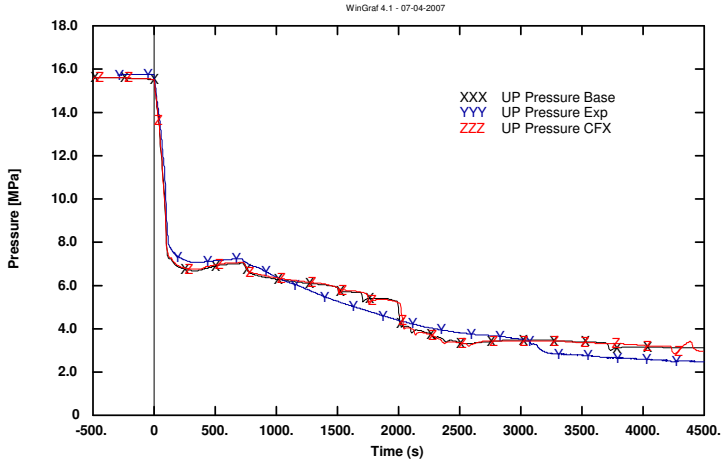

Fig. 26 UP Pressure

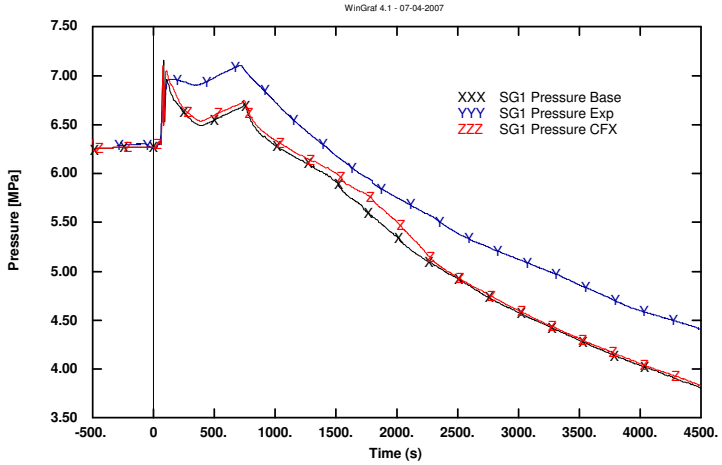

Fig. 27 SG #1 Pressure

Fig. 26 shows the comparison between the time trend of Upper Plenum pressure (UP) for the original qualified nodalization, with the one with the coefficient calculated with CFX and the experimental data. The introduction of the new coefficients moves the calculated time trend close to the experimental one.
The same effect can be observed in the pressure trend of the secondary side (SS) of the SG #1. The reason for the improvement of the agreement between calculation and experimental data is due to an improvement of the fluid flow conditions along the primary circuit that has effect even on the SS. Because of the primary pressure has a primary relevant in the safety of the NPP, in the FFTMB the limits associated for the acceptance of the results is lower (AA = 1.0) than for the other variable.

No	PARAMETER	CATHARE2 (0-4700)		CATHARE2 + CFD (0-4700)		FFTBM weighting factor*		
		AA	WF	AA	WF	W_{exp}	W_{saf}	W_{norm}
1	YC01P17 - UP pressure	0.1006	0.0220	0.0869	0.031	1.0	1.0	1.0
2	YB01P01 - SG 1 pressure	0.2028	0.0240	0.1981	0.043	1.0	0.6	1.1
3	YB04P01 - SG 4 pressure	0.2082	0.0210	0.2029	0.043	1.0	0.6	1.1
4	TH01P01- ACC 1 Pressure	0.1784	0.0330	0.1816	0.047	1.0	0.6	1.1
5	TH01L01 - ACC 1 level	0.2077	0.0410	0.2831	0.056	0.8	0.9	0.6
6	YB01L01 - SG 1 level	0.2921	0.0210	0.3562	0.051	0.8	0.9	0.6
7	YB04L01 - SG 4 level	0.2253	0.0470	0.2093	0.042	0.8	0.9	0.6
8	YP01L02 - PRZ level	0.1941	0.0780	0.0974	0.010	0.8	0.9	0.6
9	Lrm - RPV level	--	--	--	--	0.8	0.9	0.6
10	YC01DP11+12+13+14+15 - DPup	--	--	--	--	0.7	0.7	0.5
11	YC01DP07+08+09+10 - DPcore	0.9271	0.0740	0.6644	0.069	0.7	0.7	0.5
12	YA01DP04+05 - DP loop seal #1 descending side	1.0501	0.0502	0.6438	0.042	0.7	0.7	0.5
13	YA02DP04+05 - DP loop seal #2 descending side	1.1934	0.0450	0.5996	0.034	0.7	0.7	0.5
14	YA04DP04+05 - DP loop seal #4 descending side	1.2731	0.0460	0.6720	0.036	0.7	0.7	0.5
15	YA01DP13 - DP SG 1 inlet and top	0.2058	0.0300	0.2894	0.021	0.7	0.7	0.5
16	YA01DP14 - DP SG 1 top and outlet	0.3067	0.0510	0.2894	0.021	0.7	0.7	0.5
17	YC01T20 - Heater temperature top level	0.4743	0.0450	0.6178	0.031	0.9	1.0	1.2
18	YC01T120 - Cladding temperature lower level	0.3196	0.0710	0.1266	0.046	0.9	1.0	1.2
19	YC01T85 - Cladding temperature middle level	0.1672	0.0470	0.1130	0.045	0.9	1.0	1.2
20	YC01T04b - Core outlet fluid temperature	0.2240	0.0430	0.4042	0.050	0.8	0.8	2.4
21	YC01T06- Core inlet fluid temperature	0.5530	0.0740	0.0924	0.013	0.8	0.8	2.4
22	YC01T05 - UH coolant temperature	0.7063	0.0520	0.1650	0.016	0.8	0.8	2.4
23	XL01F01 - Break mass flow rate	--	--	--	--	0.5	0.8	0.5
24	*Mass1 - Primary side total mass	0.5156	0.0730	0.2209	0.082	0.8	0.9	0.9
25	*MassBr - Integral break flow rate	0.3180	0.1500	0.2482	0.151	0.8	0.9	0.9
26	YC01N01 - Core power	--	--	--	--	0.8	0.8	0.5
27	Integral ECCS (active)	0.6976	0.0690	--	--	0.8	0.9	0.9
Total		0.3957	0.0562	0.285	0.0409	--	--	--

* These weights are used by the FFTBM to derive the Total values from the single parameter values

Tab. 16 FFTBM results for the comparison EXP Calc

The reason for this is related to the fact that the value of the primary pressure is an index of the energy stored in the primary circuit and this fact is extremely relevant from the safety point of view.
As can be observed in the *Tab. 16* the application of the new pressure drop coefficients calculated with CFX decreases the total value of the FFTBM.
Looking at this first application of the CFD code in the framework of the nodalization realization, it is possible to conclude that an improvement in the accuracy between experimental and calculated results has been observed, but, for a more accurate and systematic conclusion about the effect of the introduction of the CFD code as support tool, additional analysis with different facilities and comparison with different experimental data have to be performed.
After the qualitative analysis, following the rules of the UMAE methodology, the FFTBM have to be applied in order to quantify the agreement between the experimental and the calculated time trends.
The *Tab. 16* summarizes the results of the application of the FFTBM.

As can be observed from the table above, the introduction of the new pressure drop coefficients improves the results of the application of the FFTBM.
At the end of this activity, it is possible to state that for the CFD code can constitute a valid tool for the system thermal hydraulic code user as support for the realization of the nodalization. Even if this work is just a first attempt in the employment of the CFD code for the pressure drop calculation, more deep analyses can be performed in order to check the dependence of the pressure drop from the geometric and thermal hydraulic parameters.

3.3 Characterization of pressure drop coefficient by mean a CFD code

The aim of this chapter is to investigate by mean a CFD code the influence of the geometrical and thermal-hydraulic parameters on the concentrate pressure drop coefficient K. In order to highlight these dependences a simple configuration geometry has been chosen and several sensitivities calculations have been performed. The values of K obtained for each sensitivity calculation have been reported as function of the Reynolds number.

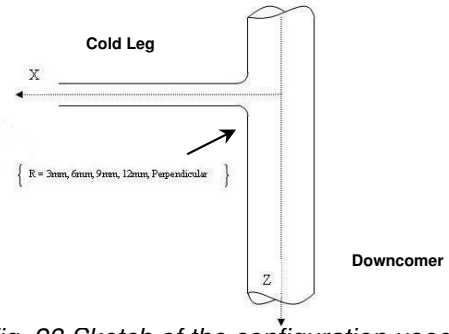

Fig. 28 Sketch of the configuration used for the calculations

The geometry chosen for this analysis is the connection between the Downcomer (DC) and Cold Leg (CL) of the Lobi facility because it is very well known in the scientific literature. In this exercise the core barrel is missing and the value of the tube fitting radius at the intersection region between the CL and DC is varied with the values: perpendicular (tube fitting radius = 0), 3mm, 6mm, 9mm, 12mm. The length of the CL and the DC are calculated with a factor L/D = 70 in order to have a fully developed fluid flow at the end of the tube length. In *Fig. 28*, a sketch of the fluid model simulated is shown, the value of the roughness on the surface has been applied as boundary condition in the preprocessing of the Ansys-CFX code.

Before to start with the description of the performed activity, it is important to note that for a proper and standard use of the CFD code inside the Nuclear Reactor Safety, a group of experts coming from members of NEA OECD-CSNI associations have started to define some documents indicated as Best Practice Guidelines for the establishment and for giving to the CFD users a proper and systematic approach in the application of the CFD code in the nuclear safety technology see in the Ref.[32] [33].

In this work, the reference documents have been taken into account and some of the recommendations have been followed, regarding the check on the geometry, the check on the quality of the mesh concerning the shape and ratio between the dimension of the mesh elements etc., but for a deep and exhaustive agreement of the directive contained in the cited documents, several additional analyses have to be performed for addressing the effect of the convergence of the results with the mesh size and all the other parameters on the final result. This further analysis are out of the scope of the present thesis in which the methodology developed at UNIPI is analyzed and some improvements are suggested. A deep investigation of the pressure drop coefficient, can constitute an interesting follow up of this thesis.

The geometry showed in *Fig. 28* has been modeled for each chosen tube fitting radius with the CAD software Ansys-Workbench. Each model has been imported in the Ansys-ICEM code and have been meshed with tetraedric elements, refined in the CL-DC intersection region. In agreement with the Ref.[32] [33], some checks

have been done in order to avoid error in the geometry and in the mesh. For each model the number of element is about 300.000. The realized mesh files have been imported with the pre-processor of Ansys-CFX code for the implementation of the boundary conditions chosen. The studied case with 3mm fitting radius, 5 m/s velocity (at CL inlet), turbulence model K-epsilon, is considered the reference case and indicated hereafter "Base" case.

One interesting aspect of this work has been the evaluation of the concentrate pressure drop coefficient for both fluid directions. All the calculations have been subdivided in two main classes, "forward" and "reverse". In the forward case, the inlet condition is applied to the CL, while in the reverse case the inlet condition is applied to the lower opening of the DC. In both classes of calculations to the upper opening the "Wall" boundary condition of Ansys-CFX is applied because no fluid flow is foreseen from this part of the model. All the velocities summarized in *Tab. 17* have been applied at the CL inlet for the forward case. The calculations have been performed at the nominal pressure of the Lobi facility 15.5 MPa with water temperature of 281 °C. Roughness of $10e^{-3}$ mm has been considered in the tube surfaces.

Tube Fitting Radius (mm)	**Fluid Velocity (m/s)**							**Turbulence model**	**Roughness (mm)**	**Mesh**
Perpendicular, **3**, 6, 9, 12	1	2	**5**	10	20	50	100	K-epsilon	10-3	300000
3			**5**					K-epsilon	no	300000
3			**5**					SST	10-3	300000
3			**5**					K-epsilon	10-3	**Refined** 600000

Tab. 17 Cases studied and sensitivities in Forward and Reverse

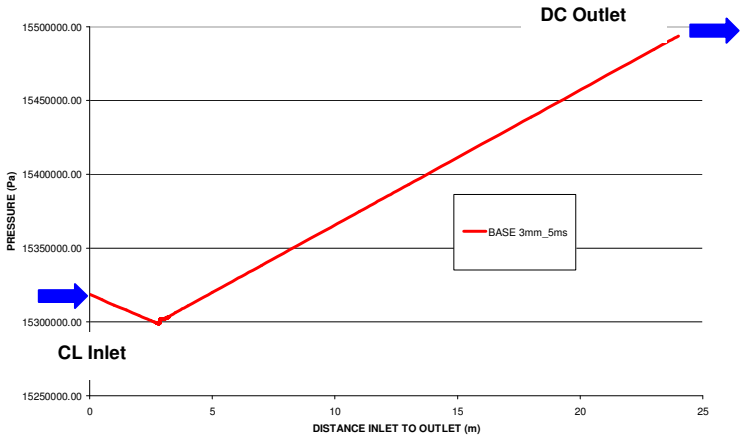

Fig. 29 Absolute Pressure along the CL and DC in the forward case

The model realized has been imported with the tool ICEM-CFD and has been meshed with tetraedric elements, refined in the intersection region for better observing the tube fitting radius region.

The Ansys-CFX "Absolute Pressure" output trend along the center path CL-DC is reported in

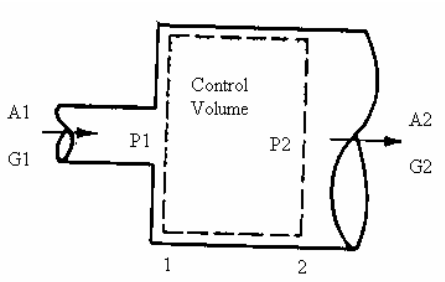

Fig. 30 Expansion reference case

Fig. 29 for the "Base" case. As can be observed in the figure, the pressure in the CL is dominate by the pressure drop proportional to the fluid velocity and decreases going from the entrance to the intersection region. In the DC the effect of the hydrostatic head (ρgh) is predominant and the pressure at the DC exit is higher than at the entrance.

Since Ansys-CFX code cannot give in the output the value of the concentrate pressure drop coefficient K, his value has been calculates by mean the analytical expression of the irreversible pressure drop combined with the Bernoulli theorem. Hereafter the reference formulas are reported together with the final expression of the K as function of the calculate pressures upstream and downstream the discontinuity.

$$\Delta P_{Tot} = \Delta P_{\mathrm{Re}v} - \Delta P_{Irr} \tag{18}$$

$$\Delta P_{Irr} = k\left(\tfrac{1}{2}\rho\, v^2\right) \tag{19}$$

The selected geometrical configuration CL and DC, can be studied as the case of a tube injecting in another one with an abrupt increase of the area as in the *Fig. 30*. The CL area is 0.001662 m^2, the DC area is 0.075477 m^2, about 45 times bigger. The value of the concentrate pressure drop (K), the Bernoulli's theorem has been applied and K has been expressed as function of the geometrical (CL and DC areas) and thermal hydraulic fluid conditions: density, velocity. The equation can be written:

$$K = (1-\sigma^2) - \frac{(\Delta P_{tot} 2\rho)}{\Gamma^2} \tag{20}$$

A1 = CL area
A2 = DC area
G = mass flow rate
ρ = fluid density

Where $\sigma = \dfrac{A_1}{A_2}$; $\Gamma = \dfrac{G}{A_1}$

The ΔP_{tot} term has been calculate as the difference between two calculated pressures one upstream and the other downstream the intersection zone. In this exercise the pressure are measured on the center of the CL and DC in the section just before the intersection and just after. In order to quantify the error connected to the measurement point, for the "Base" case, an error band has been added to the figure, taking another value of the pressure at a length of 1Diameter from the discontinuity upstream and 1Diameter downstream.

From this error band is possible to observe that the other values measured are inside the band.

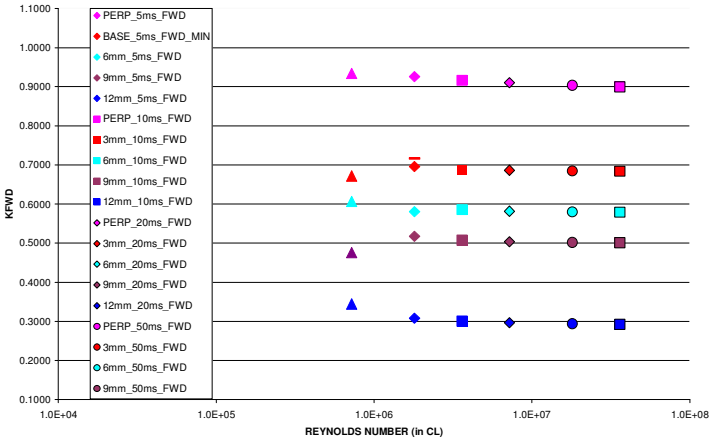

Fig. 31 K forward as function of Re

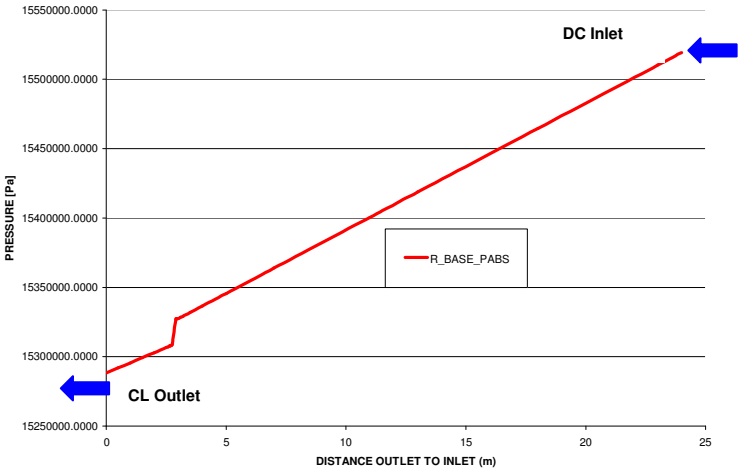

Fig. 33 Absolute Pressure along the CL and DC in the forward case

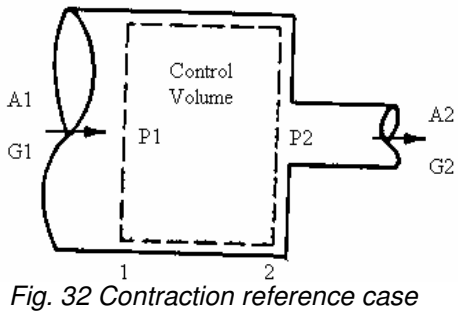

Fig. 32 Contraction reference case

This means that the variation observed are due to approximations made by the code and that the other cases calculated are out from the Base case range.

In *Fig. 33*, the pressure along the circuit is reported for the reverse case, where the fluid inlet is from the Downcomer and the exit from the Cold Leg. The pressure trend is dominate by the hydraulic head in the DC while in the CL because of the higher velocity the leaning of the curve is due to the pressure drop proportional to the square of the velocity.

The reference case for the reverse fluid flow condition is shown in *Fig. 32*. All the results of the calculated cases have been reported as function of Reynolds number (*Fig. 34*). The results show the effect on the concentrate pressure drop coefficient of the Re and the tube fitting radius. The first macroscopic effect is the growth of the K coefficient going from the 12 mm (blue points) case to the perpendicular one (pink points). Looking at one single set of points, the effect of the Reynolds number is small and should be investigated with more

care because in this kind of calculation, the effect of the mesh size, the chosen wall roughness and the other boundary conditions on the results, can be of the same order of magnitude of the measured variable. For the reverse case, the equation used for the calculation of K are reported hereafter. The situation for this configuration is the abrupt expansion of the area.

$$K = \frac{(1-\sigma^2)}{\sigma^2} - \frac{(\Delta P_{tot} 2\rho)}{\Gamma^2 \sigma^2} \qquad (21)$$

A1 = CL area
A2 = DC area
G = mass flow rate
ρ = fluid density

Where $\sigma = \frac{A_1}{A_2}$; $\Gamma = \frac{G}{A_1}$

All the calculations have been repeated inverting the direction of the fluid flow and also for this calculations the uncertainty band for the Base calculation has been introduced, in order to observe the effect on the calculated K of the measurement point. The values of K are calculate with the same method used for the forward cases, an analytical expression of the K as function of the geometrical and hydraulic parameter has been derived combining the Bernoulli theorem and the expression of the irreversible pressure drop.

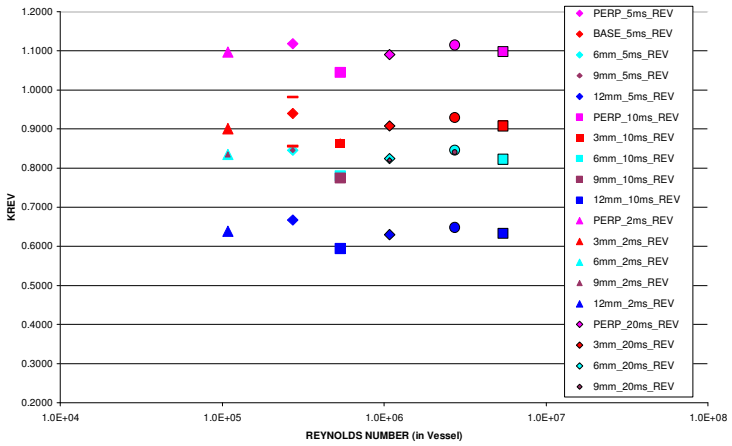

Fig. 34 K reverse as function of Re

As observed in the forward case, the tube fitting radius has the biggest effect on the K values. The highest value of K are related to the perpendicular set of values because the edge creates an high turbulence region with high dissipation of energy, while passing to cases with smooth tube fitting radius, the expansion (or the contraction) is gradual and the turbulence region is smaller.

Sensitivities

All the calculations showed in the figures above have been performed with the K-epsilon turbulence model, with a value of the wall roughness of 10^{-3}mm and with

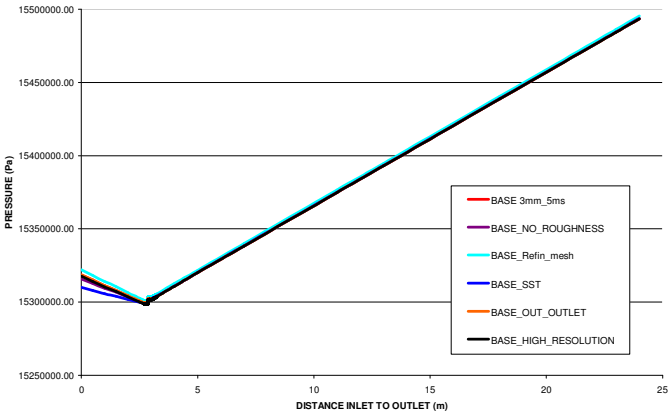

Fig. 35 Sensitivities calculations

the same boundary conditions (pressure, fluid velocity, etc) adopted by the Ansys-CFX code. The aim of this paragraph is to observe with few additional calculations starting from the "Base" case, the effect of the use of different fluid dynamic model, the roughness and some main boundary condition foreseen in the Ansys-CFX code. In *Fig. 35* the comparison among the sensitivities performed for the Base case in forward conditions is reported. In the DC region, all the model and the modifications introduced have no influence in the value of the pressure. Small differences can be observed in the CL, where the fluid velocity is high. The use of the SST model foreseen a value of the pressure lower respect to the case with the k-epsilon model.
In the DC all the cases reported have the same trend, because the effect of the hydraulic head (ρgh) on the pressure is predominant on the term due to the pressure drop.
In order to better understand the sensitivity performed, a short description of the turbulence models used (K-epsilon and SST) is reported hereafter.

The k-ε Model is one of the most prominent turbulence models, the k-ε (k-epsilon) model, has been implemented in most general purpose CFD codes and is considered the industry standard model. It has proven to be stable and numerically robust and has a well established regime of predictive capability. For general purpose simulations, the k-ε model offers a good compromise in terms of accuracy and robustness. Within ANSYS CFX, the k-ε turbulence model uses the scalable wall-function approach to improve robustness and accuracy when the near-wall mesh is very fine. The scalable wall functions allow solution on arbitrarily fine near wall grids, which is a significant improvement over standard wall functions. While standard two-equation models, such as the k-ε model, provide good predictions for many flows of engineering interest, there are applications for which these models may not be suitable. Among these are: Flows with boundary layer separation. Flows with sudden changes in the mean strain rate. Flows in rotating fluids. Flows over curved surfaces [34].

SST has been developed because one of the main problems in turbulence modeling is the accurate prediction of flow separation from a smooth surface. Standard two-equation turbulence models often fail to predict the onset and the amount of flow separation under adverse pressure gradient conditions. This is an important phenomenon in many technical applications, particularly for airplane

aerodynamics since the stall characteristics of a plane are controlled by the flow separation from the wing. For this reason, the aerodynamic community has developed a number of advanced turbulence models for this application. In general, turbulence models based on the ε-equation predict the onset of separation too late and under-predict the amount of separation later on. This is problematic, as this behaviour gives an overly optimistic performance characteristic for an airfoil. The prediction is therefore not on the conservative side from an engineering stand-point. The models developed to solve this problem have shown a significantly more accurate prediction of separation in a number of test cases and in industrial applications. Separation prediction is important in many technical applications both for internal and external flows. The SST model is recommended for high accuracy boundary layer simulations. To benefit from this model, a resolution of the boundary layer of more than 10 points is required. For free shear flows, the SST model is identical to the k-ε model. The SST model was developed to overcome deficiencies in the k-ω and BSL k-ω models [34].

At the end of the description, it is possible to conclude that the work described in this paragraph constitute a first starting point for a more systematic assessment of all the parameters affecting the concentrate pressure drop coefficient. One of the problem to be addressed is the convergence of the results with the mesh size. This is of extremely relevance in the CFD applications and require the execution of several sensitivities analysis with different mesh sizes. But this is can constitute a follow up activity of this thesis. The scope of this paragraph is a first attempt to investigate which are the main parameters affecting the concentrate pressure drop coefficient by mean a CFD code in a simple geometry. In addition another interesting follow up activity can be the simulation of the concentrate and distribute pressure drop coefficients with additional comparison with experimental data.

4 CATHARE2 V2.5 QUALIFICATION

This paragraph summarizes the results of two relevant activities developed in the Nuclear field from the 2004 till 2006 at DIMNP, dealing with the assessment of the Cathare2 code. The first one is devoted to the development of the AM procedures in the Eastern VVER1000 NPP with Cathare2 code. For this purpose, an intense experimental activity has been performed the Russian PSB-VVER facility and the results of the experiments have been used for the assessment. The second activity deals with the assessment of the Cathare2 code against the boron transport phenomena in PWR NPP. Even in this case the results of the experiments coming from the PKL III facility (4 loops PWR NPP simulator) has been used.
In the following the main results achieved are shown.

4.1 Development of AM procedures for VVER1000 NPP [3]

For the assessment of the Cathare2 code in the development of the AM procedures in the Eastern VVER1000 NPP, the UMAE methodology and the FFTBM tools have been intensively used. All the steps of the methodology described in the previous paragraphs have been applied. The main subdivision of the activities during the execution of the contract have been:

1. Identification of the Test Matrix with 12 transients of interest of the VVER1000;
2. Execution of the 12 experiments in the PSB-VVER facility;
3. Realization of the Cathare2 nodalization for the PSB-VVER facility and execution of the pretest and post test analysis of the 12 transients;
4. Realization of the VVER-1000 Cathare2 nodalization;
5. Execution of the 12 tests of the Test Matrix with the Cathare2 VVER-1000 nodalization.

The nodalization realized for the facility and the NPP are qualified following the directive of the UMAE methodology and the FFTBM has been used for the quantification of the accuracy between the experimental and the calculated data.
Here after some results related to the application of the UMAE will be showed with the aim to show the application of the methodology and the capability of the Cathare2 code to reproduce the main phenomena observed during the experiments executed in the PSB-VVER facility, the Kv scale calculations and the capability of the NPP nodalization to reproduce the relevant phenomena observed in the facility.

Within the scope, support activities are performed including proving the quality of computational tools suitable for accident analysis, performing accident analysis, understanding and documenting the current state of the art for in the area of accident management.

The objective 1 is “To help the Russian Federation to address all the safety issues related to the operation of VVER-1000 nuclear power plants, in such a way it does not appear anymore as a subject of concern notably for international nuclear organizations such as the IAEA.”.

The objective 2 is “To ensure the safety and effectiveness of the reactor confinement, the margins on operational parameters during normal operation and the adequacy of safety systems for the prevention of accidents and the mitigation of their consequences have to be analyzed and evaluated with best-estimate computer codes.”.

The analysis of the individual tasks and sub-tasks of the Project, including the availability of complementary resources by the Project Partners, brought to the following list of detailed objectives for the technical conduct of the activities:

- ✓ To propose a unified nomenclature suitable in the area of AM for PWR and VVER-1000, but applicable to a wider area within the deterministic accident analysis for NPP.
- ✓ To establish a connection between AM technology in Western PWR and in Russian VVER-1000.
- ✓ To identify research needs in the area of the operation and planning of experiments for Integral Test Facilities simulating VVER-1000 and PWR types.
- ✓ To establish a database of integral experiments suitable for the qualification of any system thermal-hydraulic code.
- ✓ To address the scaling issue when designing experiments and performing code calculations related to both the PSB-VVER and the VVER-1000 NPP.
- ✓ To further characterize concepts like accuracy, uncertainty and code user-effect based on the application of the concerned codes to the analysis of the PSB-VVER experiments. The outcome is to gather in a single document (the present one) the technology of thermal-hydraulic system code application that is at the basis of a qualified calculation.
- ✓ Based on the outcomes from the last three items, to judge the qualification level, the capability and the suitability of the concerned system-thermal hydraulics codes and other computational tools adopted within the Project.
- ✓ To establish and to agree among Project Partners, as far as possible, principles for the optimization of AM strategies (considering the distinction between AM procedures and strategies) applicable to the overall class of water cooled reactors.
- ✓ To determine an AM strategy suitable for implementation in existing VVER-1000 NPP. The financial investment for the application of the related procedure should be negligible compared with the daily operational cost of the NPP and a substantial risk reduction should be achieved, even though none of the last two issues (i.e. cost of the implementation of the procedure and PSA evaluation of risk reduction) are part of the Project activities.
- ✓ To identify in a systematic way the connection between the areas of AM and neighboring areas including (licensing) best-estimate calculations and related uncertainty prediction, three-dimensional neutron kinetics, Emergency Operating Procedures (EOP), NPP operator training and PSA.
- ✓ To propose a suitable training for researchers, technologists and NPP operators working or interested to the area of AM (not only focusing on VVER-1000).

The third bullet implied the consideration of experiments (order of magnitude equal to one-thousand) carried out all over the world during the last 30 years in a dozen ITF and of the needs in system thermal-hydraulics with main reference to the ATWS area. Connections with EC, IAEA and OECD/NEA Projects were established even in this context to design PSB-VVER experiments and to identify future needs.

The scaling issue (fifth bullet above) constitutes a central problem in system thermal-hydraulics. Within the present context, three key steps of the overall issue have been addressed: a) comparison between experimental scenarios measured in PSB-VVER and in other ITF simulating PWR and characterized by a volume & power scaling ration different from the value of PSB-VVER; b) comparison between experimental data measured in PSB-VVER and of data recorded in 'similar' transients occurred in VVER-1000 NPP; c) comparison between PSB-VVER experimental scenarios and scenarios calculated for the same events in VVER-1000. The first and the second steps deal with the counterpart and the similar test analysis and the third step also includes the 'Kv-scaled' calculations.

VVER1000

The VVER-1000/V-320 is a PWR with a thermal power of 3000 MW and electrical output of 1000 MW. The unit under consideration in this analysis is a typical V-320 model with four circulation loops, each including a main circulation pump and a horizontal steam generator. The steam generators are fed by three different feedwater systems: main, auxiliary and emergency feedwater.

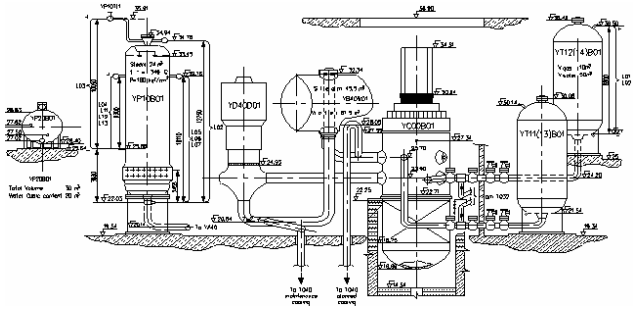

Fig. 36 The VVER-1000 V320 main equipments

Each system consists of turbine-driven or electrical pumps and piping connecting the feedwater line at four different locations in each steam generator. All elements of the primary side are situated in a steel-lined, cylindrical, concrete containment building. Configuration schemes with geometric dimensions and elevations are shown in *Fig. 36.* In the VVER-1000 primary system, coolant enters into the reactor vessel through four inlet nozzles associated with the four primary loops. The flow then passes into the downcomer between the reactor vessel and the inner vessel. The flow enters the lower plenum of the reactor vessel and passes through orifices in the inner vessel and then enters slots in the fuel support structures that lead directly to the fuel assemblies.

The flow passes through the open bundles of the core. The fuel assemblies are in the configuration of a hexagon with each containing 312 fuel rods. There are 163 fuel assemblies of which 61 have control rods. After exiting the reactor core the coolant flows into the upper plenum, which contains the shielding block, and then out to the hot legs of each of the four primary loops in the system.

The Primary System

The primary coolant system consists of the reactor pressure vessel and its four attached four primary loops (loops 10, 20, 30 & 40). Each loop has a horizontal SG (YB) and a shaft-sealed reactor coolant pump (YD). A pressurizer (YP10B01) is attached to loop 40. A spray line is attached to the cold leg of loop 20. Nominal primary system pressure is 15.7 Mpa. The hot leg nozzles are located above the cold leg nozzles on the reactor vessel. There is a water seal in the pressurizer surge line. Low pressurizer level is about at the elevation of the hot legs, and the surge line nozzle into the pressurizer is at about the elevation of the top of the core. The total primary side water volume is 336.9 m3 (including the water in the pressurizer). The entire primary geometric volume is 360.9 m3. There is a loop seal in the cold leg at the suction of the RCP. The reactor coolant pumps are controlled leakage pumps with a four-stage seal. Seal injection is provided between seal number one and seal number two of each pump by the charging system (TK). One part of the seal injection flow enters the primary system and the rest returns to the TK system through a seal return line.

The pressure boundary

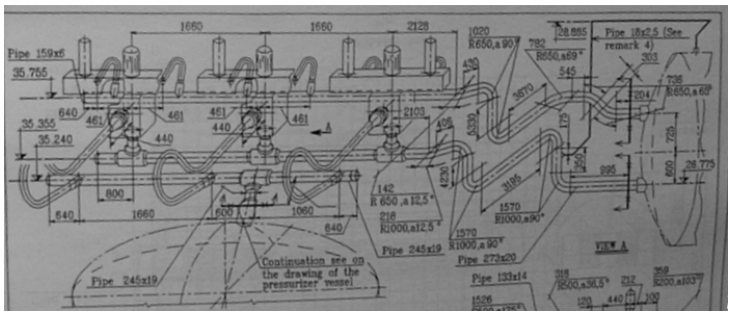

Fig. 37 Pressurizer PORV.

The pressurizer (*Fig. 37*) is the only location within a pressurized water reactor that has a steam/liquid interface during normal operation. The interface reduces the risk from water hammer and provides a compressible steam (gas) space, which is used to set the absolute pressure of the reactor vessel.

The bottom of the volume is connected to one of the hot legs by a piping system called the surge line while the top of the pressurizer has sprays with piping connected to a cold leg and the makeup system. This configuration for the spray injection inherently allows the higher pressure in the cold leg to inject into the pressurizer, but other systems are available to inject water to condense and reduce the steam in the system. Since the function of the pressurizer is so crucial to the pressure prediction, the system will be described below.

The system consists of the following components:

- ✓ Pressurizer;
- ✓ Condense tank with a breaking membrane to the containment volume;
- ✓ Spray subsystem with spray valves and “fine spray” valves;
- ✓ Safety relief valves (Sempel type);
- ✓ Electromagnetic relief valve which actuates and closes, the regulating relief valve;

- ✓ Electromagnetic relief valves, which actuates all Sempel type valves at specified set points.

A general view of the pressurizer is given in *Fig. 38*.

No	Parameter	Unit	Balakovo	Comment
1	CL axis	[m]	23.90	
2	SG tubes top	[m]	30.10	SG bottom (27.91) plus height to upper edge of tube system (2.19, p 30)
3	Loop seal Axis	[m]	20.64	
4	HL axis	[m]	25.70	
5	RPV bottom	[m]	16.85	
6	RPV top	[m]	28.71	(p 217)
7	PRZ bottom	[m]	22.34	(p.237)
8	PRZ top	[m]	34.60	(p.237)
9	PRZ Volume	[m3]	79.00	
10	SG top	[m]	31.91	axis (29.91) plus 2.0m
11	SG bottom	[m]	27.91	axis (29.91) minus 2.0m
12	Steam header axis	[m]	34.70	
13	SIT 1 top	[m]	29.40	bottom (19.34) plus height 10.06) p224 plus p262
14	SIT 1 bottom	[m]	21.26	bottom (19.34) plus total height (10.06) minus vessel height (8.14)
15	SIT 3 top	[m]	35.76	bottom (25.7) plus height 10.06) p224 plus p262
16	SIT 3 bottom	[m]	27.62	bottom (25.7) plus total height (10.06) minus vessel height (8.14)
17	HL length	[m]	9.83	length as reported on p.27 (9.16) plus (0.67, derived quantity) for the SG-inlet header part up to the first U-tubes
18	CL length	[m]	27.97	length as reported on p.27 (9.16) plus (0.67, derived quantity) for the SG-outlet header part up to the first U-tubes
19	CL internal diameter	[m]	0.85	
20	HL internal diameter	[m]	0.85	
21	PRZ diameter	[m]	3.00	

Tab. 18 NPP system elevations and main dimensions. Pages referenced in the comment column refer to [36].

The VVER-1000 typical main coolant pumps are run by electrical motors 6kV AC. The GCN-195M pump is a vertical, single stage, centrifugal pump. The nominal flow of the MCP at 50 HZ is 5.88 m3/s. The nominal head is 0.66 MPa. The actual pump capacity for 3 pumps in operation is 3x6.76 m3/s, for 2 pumps in operation – 2x7.33 m3/s, for 1 pump – 7.50 m3/s. For the normal operation of the MCPs the following supporting systems are required:

- ✓ Oil lubrication system
- ✓ Intermediate circuit water system
- ✓ Sealing water system
- ✓ Service water system

✓ Independent cooling circuit

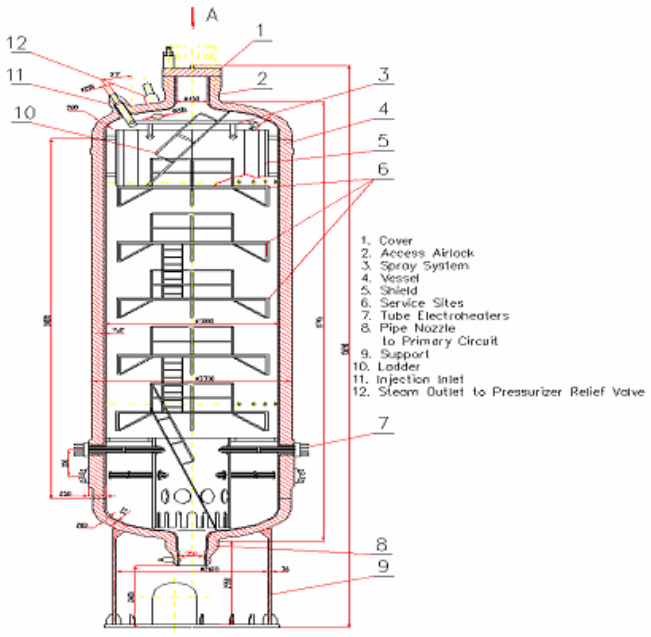

Fig. 38 A general view of the VVER-1000 pressurizer

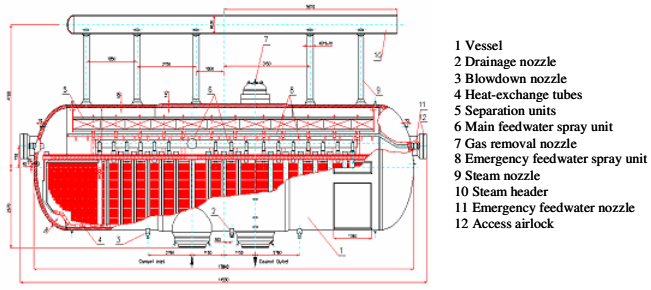

Fig. 39 The VVER-1000 steam generator

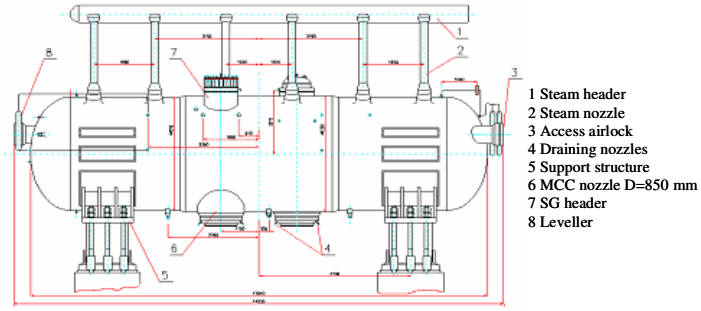

Fig. 40 The VVER-1000 steam generator – assembled view

In case of loss of service water or intermediate circuit water the operation of MCPs is available up to 180s. In case of loss of sealing water – the operation of MCPs is available up to 7200 s. In case of primary saturation (loosing of subcooling margin) or containment overpressure protection signals, 15 s after the closure of the isolation valves the MCPs are stopped by self-protection on low oil pressure. The pump coast down time in case of loss of power supply is 232 s.

The steam generators of VVER-1000 type reactors are of horizontal, U-tube, natural circulation type. The horizontal steam generator represents an important difference between VVER designs and Western reactor designs. The transients response of horizontal steam generators can be very different than that of Western type vertical steam generators due to the larger water mass in horizontal steam generators.

This larger water mass can affect the reactor transient

response particularly during secondary side occurrences.

The steam generators include horizontal U-shaped heat exchanger tubes and provide natural separation on the secondary side without the use of coarse separators.

The main components of the steam generators are:

- ✓ steam generator vessel;
- ✓ heat transfer tubes and primary coolant heads;
- ✓ feedwater nozzle facility;
- ✓ emergency feedwater nozzle facility;
- ✓ a perforated plate;
- ✓ moisture separator;

No	Parameter	Unit	Balakovo
1	Total tubes length	[m]	122100
2	Tube number	#	11000
3	Tube ID	[mm]	13.0
4	Tube OD	[mm]	16.0
5	SG collector volume	[m3]	2.4
6	SG collector height	[m]	5.0
7	PS total volume	[m3]	23.4
8	PS tubes volume	[m3]	16.2

Tab. 19 SG elevations and main dimensions. Pages referenced in the comment column refer to [15].

Feedwater flows into the steam generator through a pipe 426x24 mm, then through 16 collectors of 80 mm inside diameter which couple to the distribution pipes, see *Fig. 40*. Each of these distribution pipes has 38 perforated pipes. Some are at the upper steam tubing elevation while another portion is over the perforated sheet in order to balance the nonuniform steam generation. This is achieved by partial condensation of the voids in high steam areas.

The reactor pressure vessel is the pressure boundary of the reactor core and high-pressure coolant. The detailed geometry of the vessel is presented in *Fig. 41*.

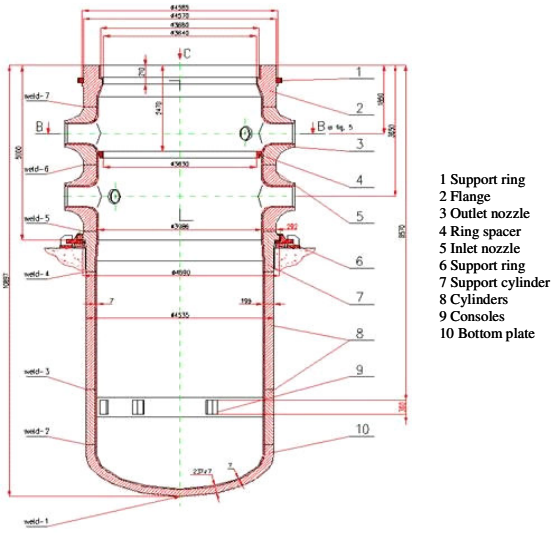

Fig. 41 The reactor pressure vessel

No	Parameter	Unit	Balakovo
1	Total internal height	[m]	11.76
2	RPV top	[m]	28.71
3	RPV bottom	[m]	16.85
4	Bottom of hydraulic core	[m]	18.29
5	Bottom of active core	[m]	18.48
6	Top of active core	[m]	22.03
7	Top of hydraulic core	[m]	22.36
8	CL axis	[m]	23.90
9	Top of DC	[m]	24.95
10	HL axis	[m]	25.70
11	UP top	[m]	26.75
12	UH top	[m]	28.71

Tab. 20 RPV - main parameters. Pages referenced in the comment column refer to [15].

The Core

The reactor core of VVER-1000/V320 consists of 163 fuel assemblies, 61 fuel assemblies have control rods The fuel assemblies of the VVER-1000 are hexagonal in shape and without a shroud. The fuel pins are arranged on a triangular pitch. Within the control assemblies, each cluster of control rods includes 18 absorber rods moving within stainless steel guide tubes.

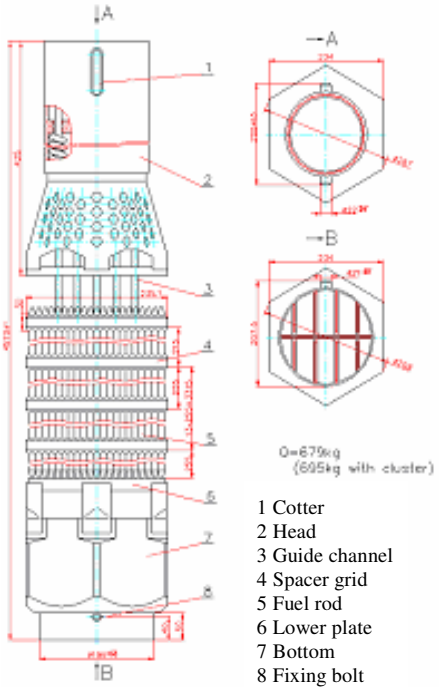

Fig. 42 Fuel assembly

The upper part of the fuel assembly ends with a perforated head. The orifices are 23 in a row with diameter about 15 mm. There are six rows with a chess layout. The *Fig. 42* shows a schematic of the fuel assembly. The lower part of the assembly contains a flow nozzle that fits into the upper portion of the support column. An aligning pin on the shank fits into a recess in the support column to orient the fuel assembly in the support column.

No	Parameter	Unit	Balakovo
1	Active length	[m]	3.55
2	Bottom of active fuel	[m]	0
3	Top of active fuel	[m]	0
4	Number of Active rods	#	50856
5	Fuel Assemblies	#	163
6	Rods/Assembly	#	312
7	Fuel assemblies with control rod	#	61
8	Fuel assembly flow area		n.a.
9	Total core flow area	[m2]	4.17
10	Bypass flow area	[m2]	0.13
11	Pellet diameter	[mm]	7.53
12	Center void diameter of the fuel pellet	[mm]	1.40
13	Clad internal diameter	[mm]	7.72
14	Clad external diameter	[mm]	9.10

Tab. 21 Reactor core main dimensions. Pages referenced in the comments refer to [15].

The Balance of Plant

The feedwater system supplies water from the condensate storage tank back into the steam generators through the high pressure heaters (or bypassing them) which controls the steam generator water level during plant operation. The system consists of two turbine driven feedwater pumps (FWP) two auxiliary electrically driven feedwater pumps (AFWP) and ten control valves..

The main steam lines: the steam produced in the steam generators is transported to the turbine by the main steam lines (*Fig. 39* and *Fig. 40*). It is also used for in-house supply of steam to the turbo-pumps. The main steam lines system includes the following components:

- ✓ 8 SG relief valves;
- ✓ 4 steam dump to atmosphere facilities BRU-A;
- ✓ 4 steam isolation valves;
- ✓ 4 check valves;
- ✓ 4 main steam intercept valves (MSIV);

The Containment System

The containment system comprises not only the leak-tight pressure resistant containment, but also the turbine hall and the reactor building.

The pressure resistant building

The main element of the VVER-1000/V320 containment containing the reactor pressure vessel and the primary side consist of a cylinder (height 38 m, diameter45 m) with a dome on top. The building material is pre-stressed concrete with a thin steel liner (8 mm) on the inside. The concrete wall thickness is about 1.2 m for the cylinder and 1.1 m for the dome. The containment design overpressure is 0.41 MPa, covering the pressure peak after double-ended guillotine rupture of the main primary loop of 0.85 m diameter.

The typical feature of the containment is, that the containment shell is a part of reactor building with square ground plan with the side length 66 m, *Fig. 43*. It is separated from the non-leaktight lower parts of the building by a 3 m reinforced concrete plate, but connected to one rectangular leaktight room in the lower part of the building housing the main ECC recirculation sump. The bottom of the containment is at +13.7 m above the ground, the bottom of the ECC sump at +7.4 m. The ECC pumps and different supporting equipment are located in the lower part of the reactor building. The square building extends also above the containment shell base plate, up to about +40 m protecting large part of the containment shell with the reactor against external impact and improving the primary system shielding. There is a narrow gap between the cylindrical shell and the cylindrical inner shaft in the square building.

Other feature, visible at the first sight on the top “collar”, is the pre-stressing system separation for the cylindrical and the ellipsoidal looking (in reality bi-spherical) dome parts. The pre-stressing ducts and tendons location is depicted in *Fig. 43*, we can see two helical directions in the cylindrical part and a network in the dome part. In reality, there is no sharp change in the direction of ducts and pre-stressing wires in the lower part as depicted in *Fig. 43*. The wires are not anchored here, but only in the top “collar”. This means that each wire is in two helical directions. The ducts are made from polyethylene, the pre-stressing wires from steel.

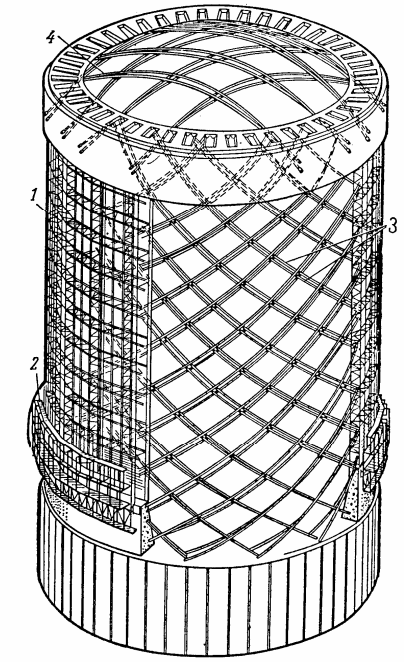

Fig. 43 The containment prestressing

The non-leaktight rooms directly from concrete panels, the cylindrical part of the containment from large blocks including inner liner, reinforcing and the ducts for pre-stressing. After their welding to other blocks, concrete is poured into them, using sliding or “walking” form. Blocks are joined also by extending reinforcing to be covered by concrete of other blocks. Most of the construction is made from a usual (sometimes called heavy) concrete of about 2300 kg/m3 density. Shielding walls are made of heavy concrete over 2500 kg/m3, shielding walls extended to higher temperature (which is the case of part of the reactor cavity) from serpentine (formula 3MgO.2SiO2.2H2O or Mg6.Si4O10.(OH)8) concrete. Individual units may differ in the gravel type, which is used as coarse aggregate in the concrete. The containment is equipped with 3 (200 % backup) active spray systems to reduce pressure after steam leak from the primary or secondary circuit. Their distributors are rings with spray jets at the top of the dome. They are connected by vertical lines with the pumps and containment heat removal exchangers located below the containment which take water from the main recirculation sump. The sump is common for all three systems and is shared together with the heat exchangers of the containment heat removal system with the active ECC systems.

Originally, V-320 containments were not equipped with a filtered venting system for severe accident conditions. There are only recirculation and air exchange ventilation systems designed for normal operation regimes. The recirculation systems are equipped with water coolers and one of them with aerosol and iodine filters, but their capacity is (most probably) insufficient for severe accident conditions.

The turbine hall

In serial V-320, the typical arrangement is attaching the turbine hall of each unit to the reactor building, with equipment room between, housing mainly secondary safety and relief valves. There may be small differences among units, but the good safety practice, where the turbine axis is almost radial to the reactor midpoint, is observed in all.

The ESF and the Emergency Systems

The plant safety system concept is, with some exceptions, a 3×100% redundancy design with three nominally identical trains of equipment for each system. The high pressure injection (HPI), low pressure injection (LPI), and containment spray (CS) systems take suction from a common containment sump, which is contained in an extension of the containment below the cavity basement.

The HPI system is designed to supply up to 133 m3/h at a primary pressure of 8.83 MPa. Maximum flow rate amounts to 255 m3/h, and the maximum PS pressure which still allows injection is 10.88 MPa. The HPI pumps are also used in what is termed "feed and bleed" cooling, in which the operators depressurise the primary system to a pressure below the HPI injection capability by opening the PORV, and injecting coolant with the HPI pumps. The fluid discharged from the PORV results in the barbotage tank including a rupture disk discharging the coolant into the containment sump. As the coolant is drawn from the sump by the HPI pumps, it is cooled by the residual heat removal (RHR) heat exchangers before being injected back into the primary coolant system. Feed and bleed cooling is used upon loss of secondary heat removal capability (loss of all feed water).

The low pressure injection system (LPI) provide emergency coolant makeup in the event of a large pipe break. The system also can be operated in the RHR mode to remove decay heat from the reactor coolant system after shutdown. The LPIS can inject up to a PS pressure of 2.5 MPa, and the maximum flow rate amounts to 763 m3/h. Residual heat removal (RHR) is a mode of operating the LPI system to take the primary system to, and maintain it in, cold shutdown. Initiation of RHR cooling is a series of operator manual actions taken from the main or emergency control room.

There are four accumulators pressurized by nitrogen which automatically inject borated water into the reactor coolant system (RCS) at a pressure of 5.9 MPa. Two accumulators inject into the upper plenum and two into the down comer of the reactor pressure vessel. Each accumulator has a capacity of 50 m3of water. Following injection, fast acting electric powered isolation valves close on low level in the accumulators to prevent injection of nitrogen gas into the primary system. The accumulators are located in two pairs on elevation level 27.0m and 36.0m in the containment.

The makeup system is part of the chemical and volume control system, which performs a variety of functions supportive of normal operation. From the standpoint of accident analysis the makeup pumps are important as regards steam generator

tube rupture (SGTR) sequences and also in their role in providing reactor coolant pump (RCP) seal support functions to maintain RCP seal integrity. The system can be connected to the TB10 system which is made up of 2 tanks of 200 m3, each containing 40 g/kg (4 wt% or 7000 ppm) boric acid. With all three TB10 system pumps operating, the system can achieve a maximum flow of 100 m3/h. The high pressure boron injection system or high high pressure injection system (HHPIS) is capable of injecting up to 19.6 MPa at a flow rate of 6.2 m3/h. It takes suction from three tanks with highly borated water, with a volume of 15m3 each.

The VVER-1000 nominal operating conditions are 3000 (+/-60) MW, the nominal flow rate is 84800 (+4000 /-4800) m3/h, the primary side pressure is 15.7 MPa, the temperature at the reactor inlet 289 °C, the temperature at the reactor outlet is 320 °C

No	Parameter	Unit	Balakovo
1	Power	[Mw]	3000
2	Core inlet temperature	[deg C]	290
3	Core temperature	[deg C]	30
4	Core outlet temperature	[deg C]	320
5	Coolant pressure outlet core	[Mpa]	15.70
6	One loop flow rate	[m3/h]	21200
7	Core flow rate	[m3/h]	84800
8	Pump rotation speed	[rev/min]	995
9	PRZ pressure	[Mpa]	15.70
10	PRZ temperature	[deg C]	346
11	Pump flow rate	[m3/h]	20000
12	SG exchanged power	[Mw]	750
13	SG steam production	[kg/s]	408
14	SG pressure	[Mpa]	6.27
15	SG steam temperature	[deg C]	279
16	FW temperature	[deg C]	220

Tab. 22 Nominal operational parameters. Pages referenced in the column 'comment' refer to [15].

Overview on the VVER-1000 operation in the world

The following description can be found in [37]. The VVER-1000 reactors constitute the latest generation of soviet-designed pressurized water reactors (PWRs). NPPs with VVER-1000 reactors, which are in operation at present, have been developed in four different models. Main characteristics of different models are described based mainly on the book [38].

The designs of earlier models 187, 302 and 338 were started in 1972 and were completed in 1979. The standard used for their design was the Russian regulatory document OPB-73. These early models have historically been called the small series because only five units of these models have been constructed.

Originally the design of VVER-1000 small series differs significantly between each other and VVER-1000 V-320 design. The design of VVER-1000 small series model 187 was developed in the early seventies in accordance with standards of that time, including such issues as insufficient environmental qualification of equipment belonging to instrumentation and control and electric power supply, as well as separation between control and safety functions.

In addition, the overall system layout provided sometimes an insufficiency in protection against environmental impact. For example, all emergency feedwater pumps were installed in the turbine hall without real separation. V320 model has been designed and built according to the requirements set out in the new OPB-82 safety regulations, which attempted at complying with international practices and safety standards. The concept of defense in depth was realized by general design criteria including the use of redundancy, diversity, independence and single failure criterion for safety systems.

For standard VVER-1000/V320 units the design differences are not so significant, with exception for Temelin NPP at which a lot of upgrading measures have been implemented during the construction phase. Several generic design features for all VVER-1000 reactors remained unchanged for all models, and they are very similar to Western PWRs with few exceptions as follows:

- ✓ Reactor pressure vessel has relatively small diameter, with inlet and outlet nozzles located at different elevations;
- ✓ Hexagonal fuel assemblies, with triangular fuel rods array;
- ✓ Fuel rods with relatively small diameter, with Zr+Nb used as a cladding material;
- ✓ Four loops in the primary circuit, with the horizontal steam generators as a characteristic design feature;

As compared with initial (small series) VVER 1000 designs, evolutionary steps towards V-320 model in addition to already mentioned improved safety features included mainly:

- ✓ Reduced number of control rods;
- ✓ Utilization of the 3-year fuel campaign;
- ✓ Fuel assemblies without shroud tubes;
- ✓ Main circulation loops without isolation valves;
- ✓ Improved seismic resistance;
- ✓ Possibility for residual heat removal during maintenance of a circulation loop;
- ✓ Possibility for operation of the reactor at reduced power.

There is a number of new designs derived from the basic V320 model, mainly upgraded towards better resistance to severe accidents; these are however not considered further in the present project.

No	COUNTRY	PLANT	UNIT/MODEL	START OF OPERATION (grid connection)
1	Bulgaria	Kozloduy	5/320	1987
			6/320	1991
2	India	Kudankulam	1/412	Under construction
			2/412	Under construction
3	Iran	Bushehr	1/446	Under construction
4	China	Tianwan	1/428	Under construction
			2/428	Under construction
5	Czech Republic	Temelin	1/320	2000
			2/320	2002
6	Russia	Balakovo	1/320	1985
			2/320	1987
			3/320	1988
			4/320	1993
			5/392	Under construction
		Kalinin	1/338	1984
			2/338	1986
			3/320	2010 (expected)
		Novovoronezh	5/187	1980
			6/392	Construction licensed
		Volgodonsk	1/320	2001
			2/320	2008 (expected)
7	Ukraine	Khmelnitsky	1/320	1987
			2/320	2004
		Rovno	3/320	1986
			4/320	2004
		South Ukraine	1/302	1982
			2/338	1985
			3/320	1989
		Zaporozhye	1/320	1984
			2/320	1985
			3/320	1986
			4/320	1987
			5/320	1989
			6/320	1995

Tab. 23 Overview of VVER-1000 reactors in operation and under construction (taken from [16] and updated).

PSB-VVER Facility

The availability of a suitable Integral Test Facility (ITF) constitutes the second prerequisite for performing the Project activities. In this case, the acronym ITF identify the PSB-VVER experimental rig available at the Electrogorsk Research establishment near Moscow (Ru).

The role of ITF in accident analysis within the nuclear reactor safety technology, as already mentioned, is primarily to confirm the capabilities of system thermal-hydraulics codes and to trigger the process of code improvement in the case when such capabilities cannot be demonstrated.

The PSB-VVER ITF is part of the series of ITF build-up within the nuclear reactor safety technology that includes, among the others, LOFT, Semiscale, LOBI, Bethsy, Spes, LSTF, PKL and PMK. All those facilities are characterized by the 'time-preserving', 'full-pressure', 'full-height', 'full-linear-heat-generation-rate' and 'power-to-volume' scaling laws

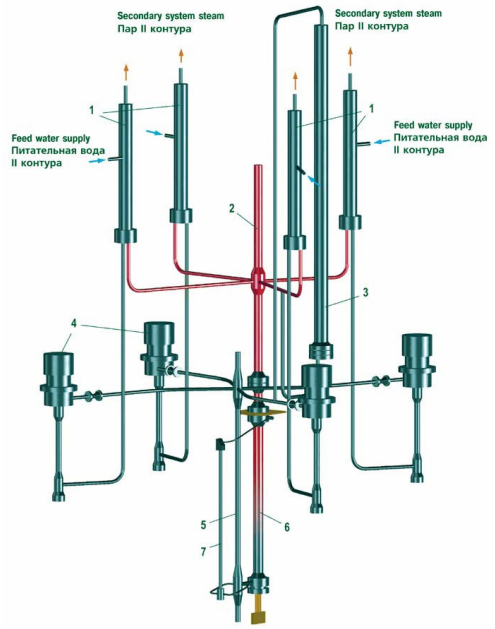

Fig. 44 PSB-VVER general view of the facility

The PSB-VVER facility (shown in *Fig. 44*) models the entire primary system and most of the secondary system (except turbine and condenser) of a VVER1000 (V-320 design) NPP. This facility has been designed and constructed with the purpose to:

- ✓ obtain experimental data for studying phenomena and processes specified in the verification matrices developed for VVER NPPs;
- ✓ assess the efficiency of the existing safety systems and verify engineering approaches proposed in new VVER NPP designs;
- ✓ check and evaluate the existing accident management recommendations and procedures;
- ✓ fill the experimental database used for thermal-hydraulic code validation.

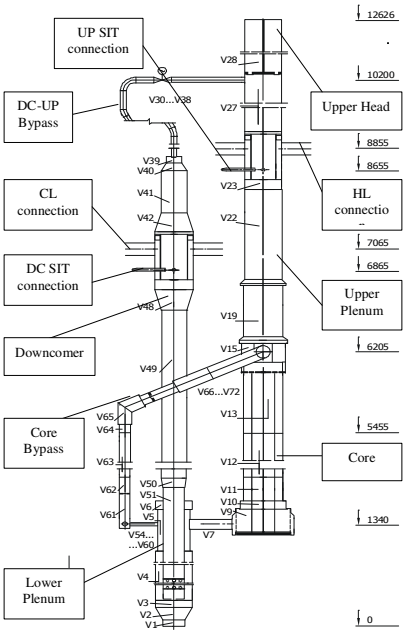

Fig. 45 Reactor model

The scaling concepts of the facility are based on the objective to simulate overall thermal hydraulic behavior of the full-scale power plant. The following features can be highlighted:

- ✓ facility elements scaled in elevation 1:1;
- ✓ power, volume, and cross-sectional area scaling factor of 1:300;
- ✓ full pressure of the primary and secondary systems;
- ✓ simulation of all four loops;
- ✓ core and SG have full-scale rod and horizontal tubes length.

The facility models the VVER1000 vessel with separate pipes: one for the down-comer, one for the core and upper plenum, and one for the core bypass. A horizontal pipe connects the lower plenum to the lower part of the core model, another bypass links the down-comer to the upper plenum, see *Fig. 45*.

The reactor core model is placed in a hexagon channel below the upper plenum (*Fig. 46*). The two zones are separated by a plate 31mm high with 330 holes. The length of

the heated section of the core is the same as in the reactor-prototype (3.53m). There are 15 steel spacer grids welded to the central tube (not heated) of the Fuel Rod Simulator Bundle (FRSB).

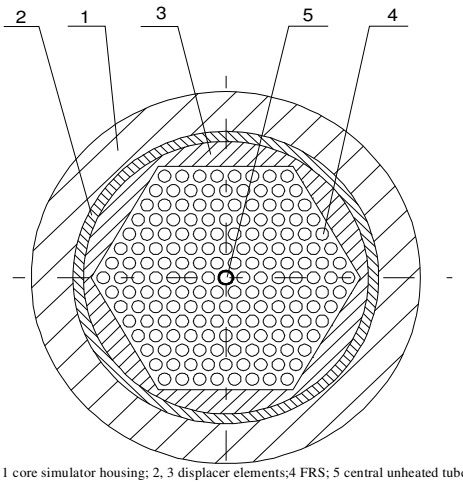

1 core simulator housing; 2, 3 displacer elements;4 FRS; 5 central unheated tube

Fig. 46 Cross-sectional view of the Fuel Rod Simulator bundle

The bundle consists of 168 FRS heated indirectly (D=9.1 mm) and a central non-heated tube (D=10.2 mm) grouped along a triangular lattice with 12.75 mm pitch.

The materials adopted for the FRS are: stainless steel for the external cladding; nichrome for the heaters and Periclase (MgO) as insulator, see *Fig. 47*. There are 29 instrumented FRS (with thermocouples) in the bundle and placed at different height (*Fig. 47*). The maximum assembly power is 1.5 MW that is 15 % from the prototype reactor. A new full-power core (10 MW) is scheduled to be installed in 2007.

The core bypass section is heated over the same elevation range of the core to simulate the heating that water receives in the reference plant.

The facility has four separate loops, see *Fig. 44*. They can be divided in hot leg, steam generator primary side, loop seal, Main Coolant Pump (MCP), and cold leg.

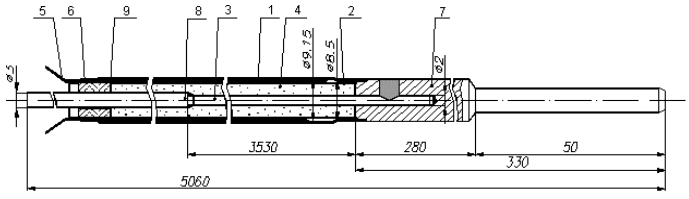

1 – external cladding 9.1x0.8 ? 18? 10?; 2 – internal cladding 7.5?0.25 ? 18? 10?; 3 – heater ? 20? 80?; 4 – periclase; 5 – cable thermocouple KTMS ChAL; 6 – ceramic or fluoroplastic bushing; 7 – upper current lead ? 18? 10?; 8 – lower current lead ? 1; 9 - sealant

Fig. 47 Instrumented fuel rod simulator

The MCP are designed to provide forced circulation in primary circuit, and present vertical hermetic installations, that include the hydraulic part and asynchronous motor embedded in the housing. The flow part of the pump is a centrifugal stage with console position of rotor. Primary coolant is drawn off by branch pipe tangentially positioned and supplied from below by axial branch pipe

The primary pressurization system includes the pressurizer, surge lines with fittings, injection pipelines with fittings, and relief valve. By means of the surge and injection lines the pressurizer may be connected to broken loop (loop #4) or to one of the intact loops (loop #2) of the test facility. For primary pressure suppression of the test facility, steam blanket is used. Pressurizer is a vertical pressure vessel. Its height, volume and nominal level position are fullsize. Electric heater with power up to 80 kW is built in the lower part of the pressurizer housing.

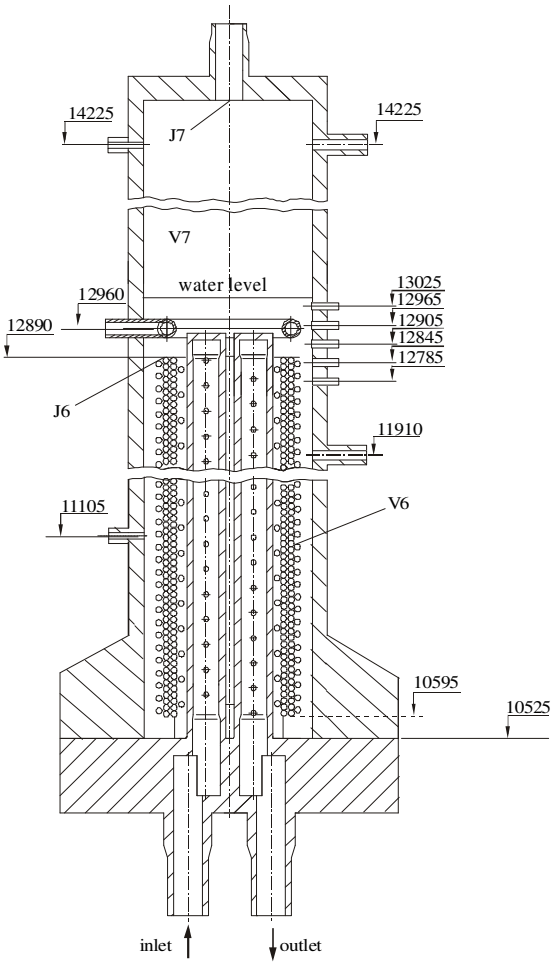

Fig. 48 Steam Generator

Heat is removed from primary circuit using steam generators (*Fig. 48*). Steam generator is a vertical vessel with two vertical headers inside, which are interconnected with horizontal helical heat exchanging tubes forming a heat-exchanging surface. The elevation marks, the headers and heat-exchanging surfaces are located in such a way to correspond to the ones in the prototype. The steam generator primary side consists of a hot and a cold collector and of 34 tubes coiled in 10 complete turns. The difference from inlet and outlet height is 51 mm. The length and the diameter of one tube is the same of the reference plant (10.656m and 13mm respectively). The total surface for heat exchanging is 18.4 m².

The main interfacing and safety systems have been also implemented in the PSB-VVER facility in order to simulate the corresponding systems necessary for the prototype NPP operation.

Below are reported the primary side and the secondary side safety systems available in the facility:

- ✓ Primary circuits: active ECCS (high pressure and low pressure), passive ECCS (hydro-accumulators), PRZ spray, emergency gas removal system (in the top of pressurizer and upper heat), make-up system, safety/relief valves in pressurizer.
- ✓ Secondary circuit: feed water pumps, emergency and/or auxiliary feed water pumps, ADS (BRU-A) valves, SG isolation valves, turbine valve, secondary side cooldown system.

All these equipments permit the modeling and representation of phenomena and physical phases that are relevant to VVER-1000 under transient and emergency conditions and to investigate the regimes with Accident Management. For investigation of DBA type accidents, in the rig systems for modeling a double ended break of cold and hot legs can also be installed

No	LIST OF EXPERIMENT	REMARK
1	Closing of all steam isolation valves due to false signal	Design basis accident
2	Instant stoppage of coolant flow rate in one of the loops	Design basis accident
3	Unexpected opening of pressurizer's pulse protective device with subsequent failure	Design basis accident
4	DBA, Main Coolant Pipe break	Design basis accident
5	Steam line break	Design basis accident
6	Shut down of 2 turbine driven Feed Water Pumps	Design basis accident
7	Sudden load change of turbine generator	Design basis accident. Decreasing o power and subsequent increasing
8	Leak from Primary System	Design basis accident. Flow rate <200t/h
9	Leak from Primary to Secondary Side without operation of BRU-A valves	Design basis accident
10	Break down of primary natural coolant circulation	Design basis accident
11	Leak of Primary System with High Pressure ECCS failure	Beyond-design basis accident. Flow rate <200 t/h
12	Leak of Primary System with High Pressure and Low pressure ECCS failure	Beyond-design basis accident. Flow rate <200 t/h

Tab. 24The test matrices: list of tests in the TOR

Finally, connections to different primary and secondary side components are envisaged for the break simulation in order to test and optimize different system operating regimes and operational procedures during the LBLOCA, the IBLOCA, the SBLOCA, the MSLB and the primary to secondary side leak events. Regarding the primary to secondary side leak events the PSB.VVER facility can simulate the SG tube rupture (one or more) and the rupture of the hot/cold SG header. Finally MCP shaft rupture can be simulated.
The ideal matrices: the first list of tests was proposed in the Terms of Reference (ToR) of the TACIS project (*Tab. 24*); this list had been changed: particularly the test n. 2 had been considered not relevant for the AM in the reference plant.

Starting from this test matrix, F.D'Auria and A.Suslov have derived the ideal test matrix.

No	ID	CHARACTERIZATION	MAIN TARGET
1	**SBLOCA**	Counterpart to experiments performed in LOBI, SPES, BETHSY and LSTF. No HPIS.	Scaling issue.
2	**LOOSP-1**	Equivalent (in terms of nomenclature) to LOFW-SBO. Unavailability of EFW and/or AFW. Recovery procedure based on fast depressurisation of all SG, following proper signal. SIT and LPIS assumed available. (*)	AM validation. Scaling issue.
3	**LOOSP-2**	Same as LOOSP-1. Recovery procedure based on fast depressurisation of all SG and 'controlled' PS depressurisation through PRZ PORV and gas removal system. (*)	AM validation
4	**SBLOCA**	PORV-stuck open. Simulation of the Zaporozhye NPP transient of 1995. RPV cooling with limited depressurisation	Scaling issue. PTS issue.
5	**PRISE-MSLB**	Largest assumed leakage (PS-SS) across one SG. The affected SG becomes "solid". Occurrence of the MSLB. Only BRU-A operable.	Radioactivity release to the environment.
6	**PRISE-MAX**	Largest assumed leakage from SS to PS checking whether amount of deborated water can be delivered to PS that are dangerous for the recriticality issue.	Boron dilution.
7	**MSLB-SBLOCA**	MSLB followed by PORV stuck open or by PS leakage.	PTS issue.
8	**NC-1**	Evaluation of the maximum power at which the loop can operate in 1F NC and in 2F NC. Core power and FW flow-rate are consistently increased, keeping constant PRZ and SG pressure.	Code and system design challenging
9	**NC-2**	Part 1: NC flow-rate and NC regimes established when draining PS coolant and keeping available the SG heat sink. Part 2: Following DNB/DO occurrence, start PS refilling and observing hysteresis.	Scaling issue for part 1. Phenomena investigation for part 2.
10	**LBLOCA**	Starting from full power. Delayed scram of electrical rods to account for the difference in thermal energy stored in electrical and nuclear pins.	Scaling issue. ECCS adequacy.
11	**SBLOCA-CBA**	No HPIS. 1) to show the need of optimising SIT initial pressure and coolant volume. 2) CBA such to cause PS pressure stabilisation at a value close to the LPIS pump shut-off head.	Code challenging.
12	**MSLB-4SL**	Simultaneous break of 4 SL. EFW only in one SG.	To address the '18.8' m issue. PTS relevant
13	**IBLOCA-MCP**	No HPIS. MCP restart following SIT injection. PRZ refilling	Code challenging.

Tab. 25 The test matrices: list of ideal tests proposed by F. D'Auria

The purpose of this matrix (*Tab. 25*) is the identification of experiments to connect the PSB tests matrix with experiments already performed or planned in other ITF simulator of PWR. The ideal TM accounts for the specificities of the PSB-VVER facility and for the current state of the art in the area of system thermal-hydraulics. Therefore, the final purpose of the this ideal TM is to connect the PSB-VVER to the context of international research programs in the area of system thermal-hydraulics. From this point of view D'Auria puts in evidence the following aspects considered relevant in the selection of his ideal TM:

- ✓ relevance of the scaling issue (counterpart experiment is part of the ideal TM).
- ✓ priority of transient scenarios with involved range parameters that have not been extensively investigated in previous experimental programs.
- ✓ tests are proposed in the ideal TM without considering the distinction between DBA and BDBA.

Another ideal TM had been proposed by A. Suslov (*Tab. 26*). The basis for the Suslov ideal TM are:

- ✓ Focus on AM (consideration of BDBA).
- ✓ AM strategies of Balakovo optimal recovery procedures.
- ✓ AM strategies of Balakovo CSF restoration procedures.
- ✓ Results of Balakovo EOP analytical justification.
- ✓ Intention to support development of missing EOP.

No	CHARACTERIZATION
1	PRISE leak with equivalent diameter of 100 mm with BRU-A stuck open in affected SG
2	PRISE leak with equivalent diameter of 100 mm with loss of primary pressure control
3	SBLOCA (break of letdown pipeline) outside containment with failure to close shut valves
4	PRISE leak (rupture of several SG tubes) with break of main steam line
5	SBLOCA (from cold leg or pressurizer relief valve stuck open) – analog of BETHSY 9.1b experiment with delayed accident management
6	SBLOCA (corresponding to 70 mm) from cold leg with HPIS failure, cooldown through secondary circuit and recovery of one HPIS train into broken leg
7	Station blackout (similar to LOOSP-1 from PSB ideal TM but more strong)
8	Station blackout (similar to LOOSP-2 from PSB ideal TM but more strong)
9	Total loss of feedwater, primary “feed and bleed” procedure, with use of one HPIS pump and opening of emergency gas removal system
10	Total loss of feedwater, primary “feed and bleed” procedure, with use of two HPIS pump and opening of emergency gas removal system
11	Total loss of feedwater, primary “feed and bleed” procedure, with use of one HPIS pump and opening of pressurizer relief valve
12	Loss of off-site power with one BRU-A stuck open and failure to switch off emergency feedwater supply into affected SG

Tab. 26 The test matrices: list of ideal tests proposed by A. Suslov

From the previous test matrix the final test matrix configuration is reported in the following. It includes the results from the discussion about the tests contained in the ideal TMs and takes into account the suggestions, among the others, from the Balakovo NPP and from EREC.
No large differences exist between the ideal and actual TM. Many of the experiments in the actual TM are conceptually the same experiments identified in the ideal TM.

However some details in the boundary and initial conditions had been changed or redefined to make possible the execution of the tests in the PSB-VVER facility. Different steps have been performed to identify the correct boundary and initial conditions of the experiments from the point of view of the PSB facility and of the relevance of the test for the AM in the reference NPP.

At the end of the design process of the Test Matrix had 12 tests with the detailed scenario, but during the tests execution further 4 tests have been added. These tests are:

No	Accident
1	Total loss of feedwater with failure of HPIS pumps and operator actions on secondary circuit depressurization
2	Total loss of feedwater with failure of HPIS pumps and operator actions on secondary circuit and primary circuit depressurization
3	Accident with opening and failure to close pressurizer safety valve
4	Leak from primary circuit with delayed accident management (analogous to BETHSY 9.1b)
5	Steam line break with simultaneous PRISE leak with equivalent diameter of 42 mm (to be scaled), with failure of HPIS pumps and possibility to use pressurizer relief valve for primary circuit depressurization
6	Total loss of feedwater, primary “feed and bleed” procedure (pressurizer relief valve and HPIS pumps are available)
7	Station blackout with operator actions on secondary circuit depressurization for passive feedwater supply from deaerator (to be confirmed by REA and EREC – alternative is use of mobile pumps)
8	Leak from primary circuit with failure of HPIS pumps: 1) to show the need of optimizing SIT initial pressure and coolant volume. 2) CBA such to cause PS pressure stabilization at a value close to the LPIS pump shut-off head.
9	PRISE leak with equivalent diameter of 100 mm (to be scaled) with failure to close BRU-A and accident management actions
10	Natural circulation: Part 1: NC flow-rate and NC regimes established when draining PS coolant and keeping available the SG heat sink. Part 2: Following DNB/DO occurrence, start PS refilling and observing hysteresis.
11	SBLOCA 70 mm (to be scaled) with failure of HPIS pumps, cooldown through secondary circuit, and recovery of one HPIS train in affected loop (to define time of HPIS recovery)
12	SBLOCA with failure of HPIS and LPIS pumps and use of normal operation systems for water supply to primary circuit

Tab. 27 The test matrices: actual TM

Nodalizations development and qualification

In this section the description and the qualification processes of the Cathare2 code VVER-1000 NPP and PSB-VVER nodalizations. The qualifying procedure set up at the DIMNP of Pisa University (UNIPI) has been applied in order to evaluate the nodalization performance. Two steps of the of the qualification process have been applied: ‘steady state’ level and an ‘on transient’ level.

VVER-1000

Four loops are modeled separately, each loop including hot legs, steam generators, main cooling pumps and cold legs. The pressurizer is connected with loop 4 via a surge-line joining the bottom part to the hot leg of the loop. The relief

valve is modeled on the top of the pressurizer. For a better understanding of the Cathare2 objects used in the nodalization, some definition will be provided in the following Tab. 48

MODULE	DEFINITION
AXIAL	1-dimensional 6 equations 2 fluids model
VOLUME	Punctual two nodes models. It's used to describe large volume where gravity effects are dominant, or to connect together several modules.
TEE	Point model used to connect a pipe to another pipe (for example to connect the surge line to the hot leg)
BCONDIT	Boundary condition element which can be put at the extremity of a pipe, of a volume or a tee and allows the imposition of one or more hydraulic conditions for each phase (pressure, enthalpies, velocities, mass flowrates..)

Tab. 28 VVER-1000 Cathare2 nodalization: definitions of main modules used by Cathare2.

RPV modeling

Two Axial components (DCA and DCB) are used to simulate the down-comer region that extends till the bottom of the RPV to avoid the presence of nodes with stagnant flow. This choice is made according to a Cathare2 VVER-440 nodalization already available at the DIMNP). Down-comer stacks are connected in the upper part with two volumes (DOWNA, DOWNB) for the connection of the four cold legs. The core model consists of an axial, CORECH, simulating just one fuel road and the surrounding water with WEIGHT 50856. The core bypass region is simulate by the axial COBY. For the active core region a neutron kinetics model of Cathare is used, with the FUEL object the main geometrical and physical property of the fuel elements has been given. With the FUELCHAR object other parameter are added in order to define the fuel property. At the end, the CORE object is required in order to define the main parameter of the core like power, decay constants, etc. For the decay power, the same 11 groups energy and the same decay constants have been used for the fissions products from the ANS79-3 implemented in Relap5 (see Tab. 50).

RESENER	**DEFINITION**	keyword to enter the value of the fraction of residual energy for the 11 decay groups.
	VALUES IMPLEMENTED	0.00299 0.00825 0.01550 0.01935 0.01165 0.00645 0.00231 0.00164 0.00085 0.000430 0.00057
RESDECAY	**DEFINITION**	keyword to enter that the decay constants for the 11 decay groups.
	VALUES IMPLEMENTED	1.772 0.5774 0.06743 6.214E-3 4.739E-4 4.810E-55.344E-6 5.726E-7 1.036E-7 2.959E-8 7.585E-10

Tab. 29– VVER-1000 Cathare2 nodalization: 11 groups of energy and decay constant for ANS79-3 curve

HYDR. COMPONENT/SYSTEM	HYDRAULIC ZONE	NODALIZ. ID.	ELEMENT TYPE
PRESSURE VESSEL	LOWER PLENUM	RPVBOT	VOLUME
		LPTOBOHC	VOLUME
	CORE REGION	CORECH	AXIAL
	UPPER PLENUM	COREUP	VOLUME
		UPHLR	VOLUME
		UPHT2	AXIAL
		UPHT1	AXIAL
	UPPER HEAD	RPVTOP	VOLUME
	UP-UH BYPASS	UPBYP	AXIAL
		UPBYP1	AXIAL
		UPBYP2	AXIAL
	DOWNCOMER	DOWNA	AXIAL
		DOWNB	AXIAL
		DCA	VOLUME
		DCB	VOLUME
	CORE BYPASS	COBY	AXIAL
	LP-UH BYPASS	CRGT	AXIAL
LOOP 1 PIPING	HOT LEG 1	HOTL1	AXIAL
	SG #1 PRIMARY SIDE	SG1CHE	VOLUME
		SG1BHT	AXIAL
		SG1MHT	AXIAL
		SG1THT	AXIAL
		SG1HHE	VOLUME
	CL 1	COLDL1	AXIAL
LOOP 2 PIPING	HOT LEG 2	HOTL2	AXIAL
	SG #2 PRIMARY SIDE	SG2CHE	VOLUME
		SG2BHT	AXIAL
		SG2MHT	AXIAL
		SG2THT	AXIAL
		SG2HHE	VOLUME
	CL 2	COLDL2	AXIAL
LOOP 3 PIPING	HOT LEG 3	HOTL3	AXIAL
	SG #3 PRIMARY SIDE	SG3CHE	VOLUME
		SG3BHT	AXIAL
		SG3MHT	AXIAL
		SG3THT	AXIAL
		SG3HHE	VOLUME
	CL 3	COLDL3	AXIAL
LOOP 4 PIPING	HOT LEG 4	HOTL4	AXIAL
	SG #4 PRIMARY SIDE	SG4CHE	VOLUME
		SG4BHT	AXIAL
		SG4MHT	AXIAL
		SG4THT	AXIAL
		SG4HHE	VOLUME
	CL 4	COLDL4	AXIAL

Tab. 30– VVER-1000 Cathare2 nodalization: correspondence between nodes and hydraulic zone.(1 of 2).

Control rods (actually control rods ‘equivalent’) guide tubes (CRGT) are modeled into UP. This characterizes a ‘tube–internal’ flow path separated from the main flow–path into the UP. Full mixing is assumed for the main flow path in the UP and the four hot legs are connected to a unique node UPHLR. Two parallel stacks of nodes have also been distinguished in the UH to separate the flows in the open region and inside the CRGT. This nodalization structure prevents dead zone and allows fluid from the top of the core to flow into the UH (through CRGT). The liquid temperature and the flow-rate directions during nominal operation are affected by

the selected nodalization structure that may be seen as typical user choices not supported by the available documentation.

The four loops have been modeled separately as already mentioned and by the same number of nodes and other modeling assumptions. The various bends (or 'loop seals') in the vertical plane present in the cold legs have been considered. The primary side of steam generators has been modeled by two vertical stacks of nodes simulating the hot and the cold header and by tree groups of horizontal tubes, as in the VVER-440 cathare2 nodalization developed at DIMNP.

HYDR. COMPONENT/SYSTEM	HYDRAULIC ZONE	NODALIZ ID	ELEMENT TYPE	NOTE
PRZ	SURGE LINE	TEEPRZ	TEE	
		SULI	AXIAL	
	PRZ	PRZ	VOLUME	

SG #i SS
i = 1, 2, 3, 4
	FW	FWi	BCONDIT	

	TUBE ZONE	SGiSSBOT	VOLUME	
		SGiSS	AXIAL	
	STEAM DOME	SGiDOM	VOLUME	
STEAM LINES	STEAM LINE 1	STEAML1	AXIAL	
	STEAM LINE 2	STEAML2	AXIAL	
	STEAM LINE 3	STEAML3	AXIAL	
	STEAM LINE 4	STEAML4	AXIAL	
	MAIN STEAM LINE CONNECTION	COLLECT	VOLUME	
	DISCHARGE TANK	EXTERN	BCONDIT	
ACC	ACC 1	ACCU1	0-dimensional	
	ACC 2	ACCU2	0-dimensional	
	ACC 3	ACCU3	0-dimensional	
	ACC 4	ACCU4	0-dimensional	
LPIS	TQ2	TQ12UP1		Injection in UP
		TQ12UP2		Injection in UP
		TQ12DC3		Injection in DOWNA
HHPIS	TQ14	TQ14CL1		Injection in Coldleg 1
		TQ14CL3		Injection in Coldleg 2
		TQ14CL4		Injection in Coldleg 3
HPIS	TQ13	TQ13CL1		Injection in Coldleg 1
		TQ13CL3		Injection in Coldleg 2
		TQ13CL4		Injection in Coldleg 3

Tab 30 VVER-1000 Cathare2 nodalization: correspondence between nodes and hydraulic zone.(2 of 2)

For the qualification, the test 11% equivalent break in UP comparing the results of the calculation with the data of the test carried out in PSB-VVER facility, 11% equivalent break in UP with the actuation of one high pressure injection system, connected to the hot leg of the loop #4, and 4 passive systems (ECCS, hydro-accumulators), connected to the outlet plenum and to the inlet chamber of the downcomer. The low-pressure injection system is not available in the test. The goal of this section is to demonstrate that the criteria foreseen in this methodology are fulfilled and that nodalization qualification adopted for the VVER1000 NPP test

analyses is achieved and the input deck is available and ready to use to analyze the real Plant behavior .

Four loops are modeled separately, each loop including hot legs, steam generators, main cooling pumps and cold legs. The pressurizer is connected with loop 4 via a surge-line joining the bottom part to the hot leg of the loop. The relief valve is modeled on the top of the pressurizer. For a better understanding of the Cathare2 objects used in the nodalization, some definition will be provided in the following *Tab. 30*

Secondary side modeling

According to previous work performed by Cathare team, and to the above mentioned VVER-440 cathare2 nodalization, the secondary side is simulated simply with tree node: a volume for the lower part in order to connect the feed water and auxiliary feed water, an axial for the of the thermal exchange region, and a volume to simulate the upper part of the SG. An axial simulating the steam line is connect to the upper part of the SG. On this axial the BRU-A valve is attached by mean of a pipe, with a time boundary condition component at the end. All the four steam lines are connected to a collector (COLLECT), and this is in connection with a boundary condition component simulating the rest of the line. The turbine is not simulated.

The three LPIS an the three HPIS are simulated by a SOURCE . The two lines of the TQ12 (LPIS) inject directly in the UPHLR and the third one in the upper plenum region DOWNA. The TQ13 (HPIS) and TQ14 (HHIS) are connected downstream the main coolant pump in the loop 1, 3 and 4. The ACC are schematized as 0-dimensional object by mean the ACCU element.

Material properties for both passive and active structures, including nuclear fuel, have been taken from the available databases at DIMNP and from ref. [15].

No	PARAMETER	VALUE
1	**Total number of hydraulic modules**	
2	primary side	52 (1745)
3	secondary side	34 (508)
4	total	86 (2153)
5	**Number of junctions**	
6	primary side	69
7	secondary side	33
8	total	102
9	**Number of thermal structures**	
10	primary side	41
11	secondary side	21
12	total	62
13	**Number of core active structures**	15

Tab. 31– VVER-1000 Cathare2 nodalization: adopted code resources for Cathare2 VVER1000 nodalization

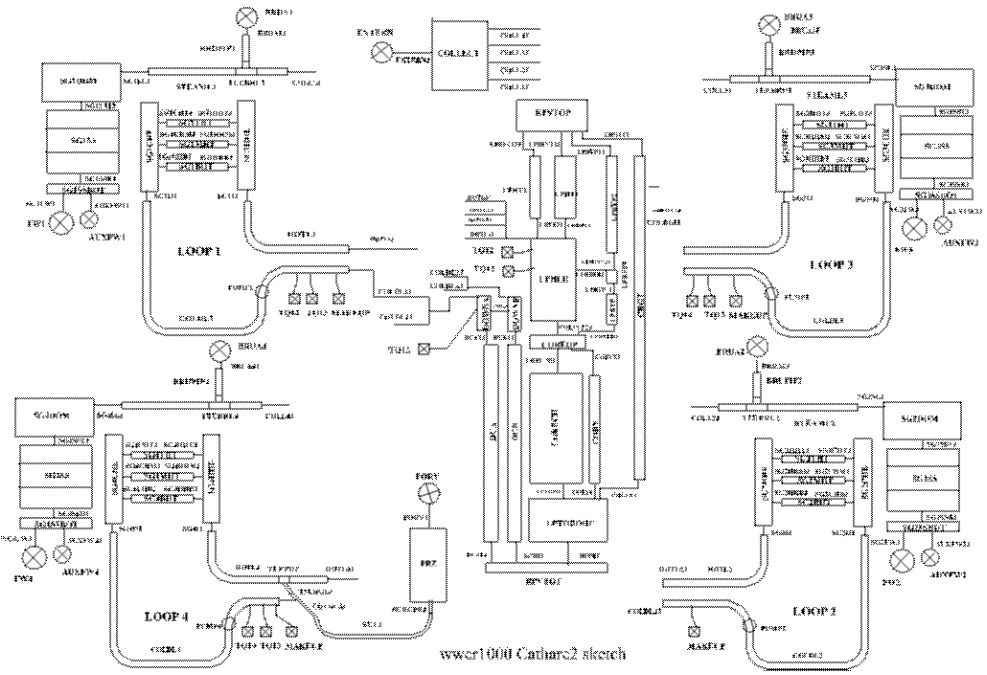

Fig. 49 VVER-1000 Cathare2: nodalization sketch

Tab. 31 summarizes the resources adopted in the VVER1000 Cathare2 nodalization. It should be noted that the number of meshes adopted in the nodalization is 2153 meshes but the main part (1745) is used to simulate the primary side, while just 508 meshes are used to simulate the secondary side of the SG.

Steady State

Following the rules of the methodology developed at UNIPI, the first step is to check the geometrical fidelity between the hydraulic nodes and the real plant. The second step is to check the pressure drop along the circuit and finally the run the calculation with no variation of the variables. The requirements of the methodology applied for the geometrical fidelity are reported in Tab. 59, in which the elevation of the various parts of the nodalization is compared with the elevation of the corresponding part in the real plant and with the Relap5 nodalization.

Fig. 50 compares the pressure drop distribution calculated by Cathare2 nodalization with the available data for the reference NPP and with the one calculated by Relap5. In the Balakovo unit N°3, the pressure drops are known only for the core region and for the primary side of the SG. The head of the MCP is also known. It can be seen that there is a very good agreement between experimental data and the values foreseen by Cathare2. In order to test the nodalization performances, a 'steady–state' level calculation has been performed by a transient calculation without imposing any variation to the input parameters. This is also

referred in the literature as null–transient. The suitable duration for the null–transient is 100 s or more. Results achieved have been compared with VVER-1000 thermal hydraulic design values, and the acceptability criteria foreseen in the Pisa methodology are summarized in *Tab. 31*.

Relevant results of the steady state calculation are given in *Tab. 31* and in *Fig. 51* and *Fig. 55*. In *Tab. 31* the calculated values for the steady state conditions are compared with the real data and with the acceptable errors. All the calculated parameters are inside the limits foreseen in the Pisa methodology, so that it's possible to conclude that the nodalization is qualified at steady state level.

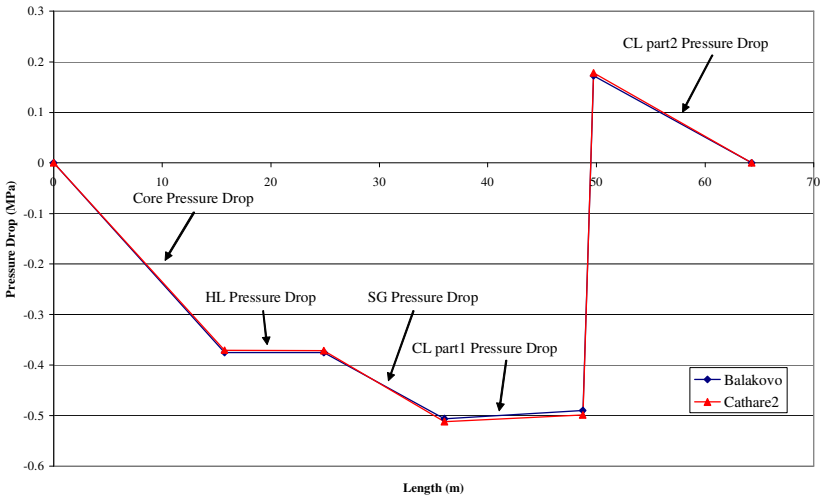

Fig. 50 VVER-1000 Cathare2: pressure drop along the circuit

"On Transient" qualification

The nodalization has been qualified at the"on transient" level by a LOCA transient already performed in PSB-VVER experimental facility. The same boundary and initial conditions foreseen for the PSB-VVER test "11% Upper Plenum LOCA" performed in the framework of OECD Joint Project 6 have been implemented and the obtained results compared with the experimental data from the test. The qualification process may be considered as achieved when the developed plant nodalization demonstrates the capability to foreseen the same phenomena, at about the same time, as in the analyzed test. This process is known as "Kv scaled" analysis and the right scaling factor must be used to adapt the NPP initial and boundary conditions to those of the facility. A calculation at the "nominal" NPP conditions has also been performed in order to evaluate the response of the plant (at the correct initial and boundary conditions and with all the emergency systems available) to the considered accident scenario.

No	LEVEL LOCATION	DESIGN (m)	CATHARE2 (m)	NOTES
1	RPV bottom	0.0	0.0	RPV inside bottom is considered as level zero
2	DC bottom	-	0.3	
3	BAF	1.82	1.82	
4	CL loop seal axis	3.71	3.71	
5	TAF	5.35	5.37	
6	HL axis	8.77	8.77	
7	CL axis	6.97	6.97	
8	DC top	8.17	8.18	Design value is extrapolated
9	UP-UH separation	10.71	-	
10	RPV top	12.43	12.439	Inside level
11	PRZ bottom	5.14	4.86	Beginning of nozzle (Cathare)
12	PRZ top	16.4	16.03	
13	PS inlet & outlet SG header	-	10.91	
14	SG H-tube top	13.53	12.525	
15	SG H-tube bottom	-	11.36	
16	SG vessel top	15.19	15.13	Inside vessel
17	SG vessel bottom	11.48	11.41	
18	ACC 1&2 top	19.73	n.a.	The Cathare “ACCU” module used
19	ACC 3&4 top	13.41	n.a.	as above
20	ACC 1&2 bottom	10.35	n.a.	as above
21	ACC 3&4 bottom	4.69	n.a.	as above

Tab. 32 VVER-1000 Cathare2 nodalization: comparison between design and Cathare2 nodalization values of the elevations of the main components of the Balakovo 3 NPP

No	QUANTITY	UNIT	DESIGN	RELAP5 (°)	CATHARE2	CATHARE2 ERRORS (%)
1	Core thermal power	MWth	3000.	3000.	3000.	0.
2	RPV pressure loss	bar	–	1.14		
3	Core inlet temperature	°C	289.	287.	289.	0.
4	Core outlet temperature	°C	320.	321.	320.	0.
5	Core bypass flow rate (LP–UP)	% Kg/s	– –	5.5 845.	3.5 581.	-
6	PS total mass inventory	ton	240.	240.	241.	0.4
7	PRZ pressure	bar	157.	157.	157.	0.
8	PS total loop coolant flow rate	Kg/s	16.800	15444.	16500.	1.7
9	PS total loop pressure loss	bar	–	–	-	
10	MCP head	bar	6.2	-	6.5	-
11	MCP speed	Rad/s	104.	-	103.	0.9
12	SG SS mass inventory	ton	200.	156.	208.	4.
13	SG thermal power	MWth	750.	750.	750.	0.
14	SG exit pressure	bar	62.7±1.9	62.43	63.0	0.4
15	SG feed–water temperature	°C	220.	220.	220.	0.
16	SG feed–water mass flow rate	Kg/s	1632.	1628.	1640.	0.4
17	SG steam mass flow rate	Kg/s	437.	439.	446.	2.
18	PRZ liquid level	M	8.77	8.46	8.7	0.78
19	SG pressure loss	bar	1.33	1.58	1.26	5.2

(°) the reported Relap5 data refer to the a generic VVER 1000

Tab. 33 VVER-1000 Cathare2 nodalization: comparisons between design and Cathare2 calculated values of some quantities of the Balakovo 3 NPP and the related percent errors

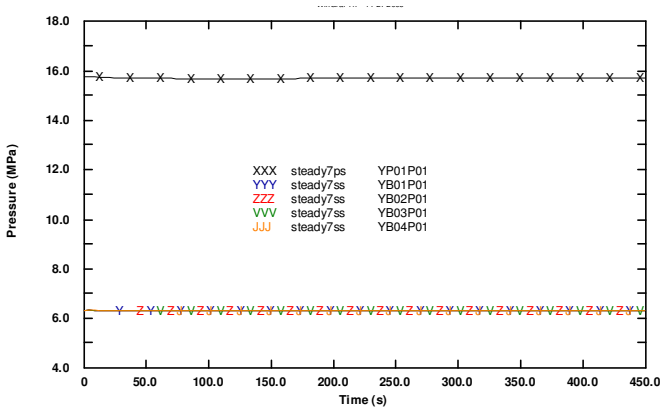

Fig. 51 VVER-1000 Cathare2: PRZ and SG pressure

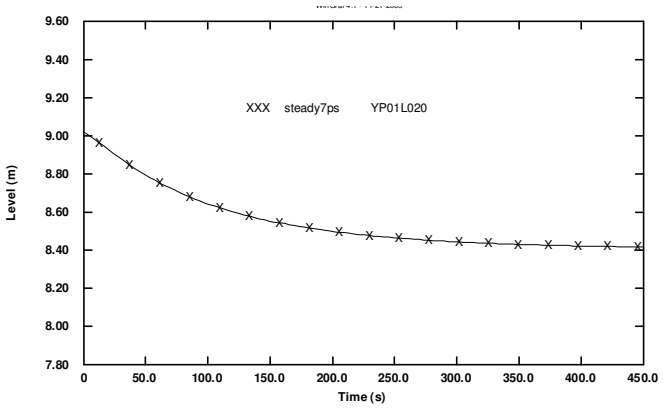

Fig. 52 VVER-1000 Cathare2: PRZ level

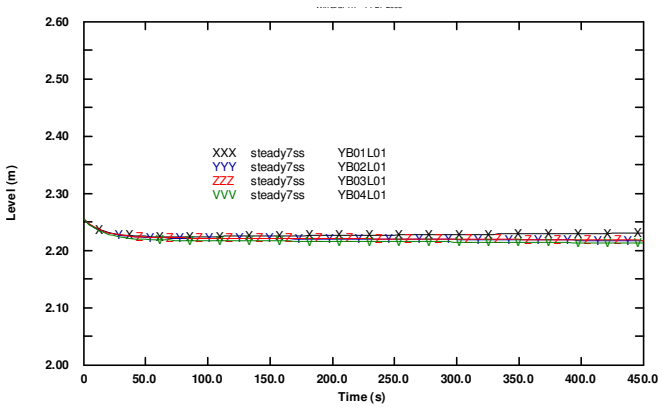

Fig. 53 VVER-1000 Cathare: SG level.

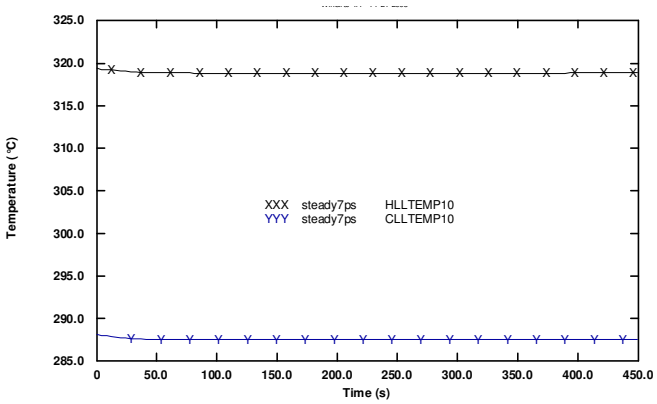

Fig. 54 VVER-1000 Cathare2: CL and HL fluid temperature.

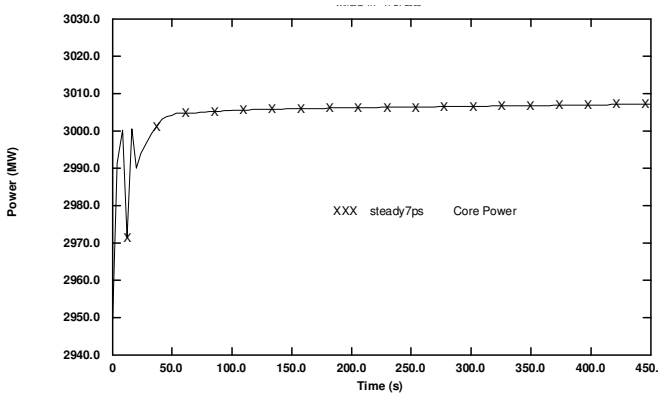

Fig. 55 VVER-1000 Cathare2: core power.

11% UP break test experiment description

The chosen PSB-VVER test simulates a LOCA due to the break of one of the injection line of the SIT located in the UP. The rupture area is equivalent to 11% of the area of the main pipe connected to the reactor pressure vessel. The test is the counterpart of a test previously performed in the ISB-VVER facility (an older small scale facility) and the initial and boundary conditions derive from that test and in some cases (like pressure, …), don't reflect the actual steady state values reported in the previous sections.
The test scenario can be subdivided into three main periods, in which the following main phenomena can be highlighted (see *Fig. 56*):

1. Sub-cooled blow down, first dry-out of the core, minimum mass inventory, emergency systems intervention (0-350 s);

2. Saturated blow-down and primary to secondary side pressure decoupling, (350 s - accumulators emptying);
3. Final dry-out of the core, maximum cladding temperature (accumulators emptying -1037. s).

The imposed sequence of main events in the test is summarized in *Tab. 34*. The test starts with the opening of the valve connected to the break system that simulates the rupture. After 5 seconds from the test initiation the SCRAM is actuated and the power of the FRSB (Fuel Road Simulator Bundle) and of the core

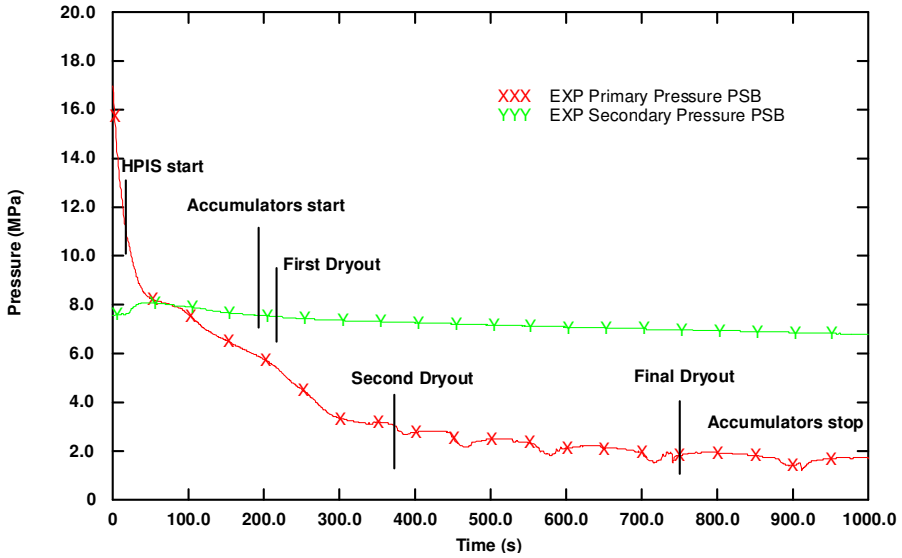

Fig. 56 VVER-1000 Cathare2: PSB-VVER OCD-CSNI Test #1 "11% UP break" PS and SS experimental pressures

bypass starts to decrease. At the same time the feed-water valves start to close: The isolation valves of the 4 steam generators are closed following the SCRAM signal. At 10 seconds the main coolant pumps are stopped; their coast down time is 4 seconds. The pressurizer level has a rapid decrease and after few seconds the pressurizer results empty. The active and passive ECCS systems start to inject when the corresponding pressure set points in the primary side are reached. The set points of the available ECCS are 10.5 MPa for the HPIS (only one train is foreseen that injects in the hot leg of loop no. 4) and 5.9 MPa for the hydro-accumulators (all available: 2 connected to the downcomer and 2 to the UP upstream the break). The pressure decreasing in the primary side and the pressure increasing in the secondary side due to the SG isolation cause at about 90 s an inversion of the heat exchange in the SG. The primary side depressurization goes on and not-withstanding also the injection of the passive system, the cladding heat up occurs in some zones of the FRSB. The temperature trends of the fuel rods show some dry out and rewet in particular in the middle and upper part. The experiment is terminated due to a high temperature of the bundle (more than 1000 K) at about 1000 s.

No	EVENT	TIME AND/OR SET POINT VALUES
1	Break opening	0 s
2	SCRAM signal	5 s
3	MCP coastdown initiation/full stop	10 s/14 s
4	SG SS isolated	5 s
5	Normal SG SS FW supply stopped	15 s
6	PRZ internal heaters stop	PRZ pressure = 13.73 Mpa
7	SG SS safety valves opening	Not operative
8	Safety injection signal (HPIS active)	PS pressure = 10.5 Mpa
9	ACC injection start	PS pressure = 5.89 MPa
10	ACC injection stop	About 900 s
11	End of transient	1037 s

Tab. 34 VVER-1000 Cathare2 nodalization: PSB-VVER OCD-CSNI Test #1 "11% UP break": imposed sequence of main events

Kv scaled calculation results

As a first step, starting from the Kv scaling factor based on the ratio between the primary system volumes of the concerned facility and of the reference NPP, the BIC (Boundary and Initial Conditions) of the test have been scaled to the one suitable for the NPP nodalization. This step is required in order to compare the results of the calculation with the experimental data, to prove that the system code (Cathare) is able to reproduce the same phenomena at different scale and to demonstrate that the NPP nodalization is able to reproduce the behavior of the plant. All these consequences are based on the hypothesis that the facility (PSB-VVER) is a suitable scaled simulator of the reference VVER1000 NPP.
The relevant results of the first step are given in *Tab. 35*. In this table the BIC of the 'nominal calculation' (the one with the nominal BIC of the reference NPP) are also reported. The main geometrical parameters are properly scaled, e.g.. the value of the break area, and the ratio AreaBreak/Volumesystem are properly scaled up as the loop mass flow rates in order to have the core inlet and outlet temperature in agreement with the experiment.

The Fuel Rod Simulator Bundle, available in the PSB-VVER facility, can supply 1.5 MW (low power) instead of 10 MW (full power) that is the value correctly scaled. Given this consideration the power used in the plant Kv calculation is obtained by multiplying the facility power (1.5 MW) for the volume scale factor (Kv=300). All the other parameters reported in the *Tab. 35* respect the similarity foreseen for this calculation.

No.	Parameter/System	Unit	PSB-VVER1000 '11%UP' SBLOCA	VVER1000 'Kv Calculation'	VVER1000 'Nominal Conditions'
1	**Primary system volume**	m^3	1.23	362.	362.
2	**Break:**				
	- area	m^2	2.03E-4	0.0611	0.0611
	- location	-	Upper Plenum	Upper Plenum	Upper Plenum
	- A_{fr}/V	m^{-1}	1.65E-4	1.68E-4	1.68E-4
3	**Primary system:**				
	- HL temperature	K	589.0	589.0	593.0
	- CL temperature	K	559.0	559.0	564.2
	- mass flow rate	kg/s	9.3	2864.0	16900.0
	- G_{loop}/Core power	kg/s/MW	6.12	6.28	5.63
4	**PRZ:**				
	- pressure	MPa	17.0	16.8	15.6
	- level	m	8.4	8.6	8.7
5	**Core:**				
	- initial power	MW	1.520	456.	3000.
	- decay power	-	-	-	-
	- ΔT	K	30.0	30.0	31.0
	- core power/volume	MW/m^3	1.23	1.25	8.28
6	**SG SS:**				
	- pressure	MPa	7.54	7.41	6.27
	- DC level	m	2.3	2.3	2.25
	- FW temperature	K	493.	493.	493.
7	**Accumulators:** **- water level**	MPa m	5.9 4.85	5.9 4.84	5.9 4.84
8	**HPIS and AFW:**				
	- HPIS set point	MPa	10.5	10.5.	15.6 MPa (TQ14); 10.88 MPa (TQ13)
	- HPIS trend	-	Time dependent law	Time dependent law	Pressure dependent law
	- HPIS temperature	K	298.	298.	298.
	- LPIS set point	MPa	-	-	2.5
	- LPIS temperature	K	-	-	298.
	- LPIS trend	-	-	-	Pressure dependent law
9	**Reactor Coolant Pump:**				
	- trip	s	10.	10.	10.
	- coast down duration	s	4	4	232.
	- seal flow rate trend	-	-	-	-
10	**Scram**	-	5.0s after transient start	5.0s after transient start	5.0s after transient start
11	**TEST END**	s	1037.	1037.	1037.

Tab. 35 VVER-1000 Cathare2 nodalization: BIC of PSB-VVER facility test scenario, VVER1000 'Kv-scaled' calculation and VVER1000 'nominal condition' calculations

		UNIT	EXP	VVER-1000 Kv CALCULATION	VVER-1000 CALCULATION NOMINAL CONDITIONS	Judg. C2
RTA: PRZ empting						
TSE	emptying time	s	19.0	30.	30	R
	SCRAM time	s	5.0	5.0	5.0	E
IPA	Integrated SL flow (from 0 to PRZ emptying)	kg	-	-	-	-
RTA: SG SS behavior						
TSE	main steam line valve closure	s	---	--	--	-
	difference between PS and SS, (100 s)	MPa	0.31	0.54	0.54	R
SVP	SG level: end of sub-cooled blow-down when PS pressure equals SS pressure when ACC starts when LPIS starts	m	2.29;2.25; 2.38;2.30 2.29;2.26; 2.39;2.31 2.27;2.22; 2.38;2.29 ----;----; ----;----	2.36;2.36; 2.35;2.27 2.36;2.36; 2.34;2.28 2.35;2.36; 2.34;2.24 ----;----; ----;----	2.28;2.26; 2.25;2.18 2.14;2.17; 2.12;2.03 2.15;2.18; 2.13;2.04 ----;----; ----;----	E.E E,E E,E E,E E,E E,E --
SVP	SG pressure: at the end of sub-cooled blow-down when PS pressure equals SS pressure when ACC starts when LPIS starts	MPa	7.67;7.58; 7.81;7.85 7.99;7.90; 8.06;8.21 7.50;7.36; 7.70;7.62 ----;----; ----;----	7.8;7.8; 7.8;7.8 7.5;7.5; 7.5;7.5 7.43;7.43; 7.43;7.43 ----;----; ----;----	7.00;7.00; 7.00;7.11 6.4;6.4; 6.4;6.4 6.44;6.44; 6.44;6.44 ----;----; ----;----	R,R E,E R,R R,R E,E R,R --
RTA: Sub-cooled blow-down						
TSE	upper plenum in saturation conditions	s	21.	17.	18.	E
	break two phase flow	s	55.	58.	58.	E
IPA	break flow up to 30 s	kg	244.	63400.	65400.	R
RTA: First dryout occurrence						
TSE	time of dry out	s	217	175	--	R
	range of dry out occurrence at various core levels	s	217 - 270	175 - 206	--	R
	peak cladding temperature	K	749	578	--	M
SVP	average linear power	kW/m	2.54	2.53	--	E
	maximum linear power	kW/m	2.54	2.53	0.5 (*)	E
	core power / primary mass	kW/kg	5.4	5.3	1.4(*)	E
IPA	integral of dry out at 2/3 of core height	K s	-	-	-	-
NDP	PS mass / initial mass	%	20.	23	27	E
	time of loop seal clearing	s	300 – 300 loop 1&4	500 – 500 Loop1&4	--- - --- loop 3&4	

Tab. 36 VVER-1000 Cathare nodalization: PSB-VVER experimental data, VVER1000 'Kv-scaled' and VVER1000 'nominal conditions' calculations: qualitative accuracy evaluation (based on RTA) (1 of 2).

RTA: Rewet by loop seal clearing						
TSE	range of rewet occurrence	s	241 - 320	200 – 229	-- - ---	R
	time when rewet is completed	s	350	250	--	R
TSE	PS pressure equal to SS pressure	s	75.	72.	--	E
SVP	break flow at 200 s break flow at 1000 s	kg/s	3.74 3.25	469. 187.	-- --	- -
IPA	integrated flow from 200 to 1000 s	kg	1379.	182415.		
RTA: Mass distribution in PS						
TSE	time of minimum mass occurrence	s	869. 1027.	187. 1037.	163. ---	M E
SVP	minimum primary side mass	kg	94. 94.3	55720. 48834.	63700. ---	M R
	av. linear power at min. mass	kW/m	2.54	2.53	0.5	E
RTA: Second dry-out occurrence						
TSE	time of dry out	s	373.	410.	-	R
	range of dry out occurrence at various core levels	s	373.-375.	410.-420.	-	R
	peak cladding temperature	K	573.	537.	-	R
SVP	average linear power	kW/m	2.54	2.53	-	E
	core power / primary mass	kW/kg	6.28	5.0	-	R
IPA	integral of dry out at 2/3 of core height		-	-	-	-
NDP	primary mass / initial mass	%	18.0	26.0	-	R
RTA: ACC behavior						
TSE	accumulators injection starts	s	161. – 193.	169.	100.	E
	accumulators injection stops	s	900 – 907	460.	320.	R
IPA	total mass delivered accumulators	kg	-	-	-	-
NDP	primary mass/initial mass, Acc. On	%	22.	25.	37.1	E
	primary mass/initial mass, Acc. Off	%	18.0	27.	49.8	M
RTA: Final dry-out occurrence						
TSE	time of dry out	s	750.	450.	---	M
	dry out occurrence at various core levels	s	750.-823.	450. – 1037.	---	M
	peak cladding temperature	K	1073.	577.	---	M
SVP	average linear power	kW/m	2.54	2.53	---	E
	rate of rod temperature increase	K/s	2.0	0.42	---	M
	core power / primary mass	kW/kg	6.73	4.61	---	R
IPA	integral of dry out at 2/3 of core height	°K s	-	-	-	-
NDP	primary mass / initial mass	%	17.0	27.	---	M

(*) value evaluated at the time of minimum mass inventory
E = Excellent – the calculation falls within experimental data uncertanty band
R = Reasonable – the calculation shows only correct behaviour and trends
M = Minimal – the calculation does not lie within experimental data and sometimes does not have correct trends
U = Unqualified – calculations does not show correct trend and behaviour, reasons are unknown and unpredictable

Tab. 37 VVER-1000 Cathare nodalization: PSB-VVER experimental data, VVER1000 'Kv-scaled' and VVER1000 'nominal conditions' calculations: qualitative accuracy evaluation (based on RTA) (2 of 2)

No	EVENT	EXPERIMENT	CALCULATION
1	Break opening	0 s	0 s
2	SCRAM signal	3.8 s	5 s
3	MCP coast-down initiation	10 s, full stop at 14 s	9 s, full stop at 16 s
4	SG SS isolated	5 s	5 s
5	Normal SG SS FW supply stopped	15 s	15 s
6	PRZ internal heaters stop	-7.75 s	- s
7	SG SS safety valves opening	-	-
8	Safety injection signal (HPIS active)	20.5 s	20.8 s
9	ACC injection start	193 s	164 s
10	ACC injection stop	About 900 s	About 400 s
11	End of transient	1037 s	1037 s

Tab. 38 VVER-1000 Cathare2 nodalization: resulting sequence of main events

The second step consists in the execution of the “Kv scaled” calculation and in the comparison of the predicted results with the available experimental data base derived from the considered PSB-VVER test.
The time sequence of calculated key events is reported in *Tab. 38* and compared with the experimental one.
Following the temporal subdivision made for the experimental data base, the same main three phases can be recognized also if characterized by different timing:

1. Sub-cooled blow-down and first core dry-out – rewet and primary to secondary side pressure decoupling (0 – 250 s),
2. Saturated blow-down and second dry-out - loop seal clearing (250 s – accumulators emptying, 450 s);
3. Mass depletion in primary loop (accumulators emptying – final dry-out).

In the first phase of the transient it is possible to observe the same phenomena as in the experiment, with some differences in timing. The first core dry-out occurs earlier (175 seconds) in the Kv calculation than in the experiment (217 seconds) and the predicted peak cladding (PCT) temperature is lower than the experimental one. The reason can be understood looking at *Fig. 57*, in which the comparisons of the mass inventory trend and of the core cladding temperatures at different levels in the core, are reported. The dry-out occurrence causes a rod surface temperature excursion when the mass inventory reaches the minimum value both in the experiment and in calculation, but at different times. The subsequent repeated oscillations in the core level due to start and stop of the injection of the accumulators, coupled to loop seal clearing and formation (see *Fig. 58*, where the differential pressure across the core is reported) causes in the experiment some sort of dry-out and rewet cycling not predicted in the calculation, where the residual mass from the accumulation intervention time is always increasing. The particular design features both of the discharge lines of the accumulators and of the upper core support plate in the facility may explain the above differences. On the other side the early intervention of the accumulators in the calculation with respect to the experiment may explain the underestimation in the predicted maximum cladding temperature excursion during this phase. In the experiment the temperature reaches 749 K while in the calculation the predicted maximum is 578 K.

In the second phase (from 250 s to about 450 s), the maximum cladding temperature (second dry-out) calculated by the code is 537 K and it is met at 410 s against 573 K and 373 s in the experiment. This dry-out is quenched by the loop seal clearing at about 500 seconds. Again the behavior of the accumulators injection may explain the difference. The larger effect of the heat released by the non-active structures to the coolant in the PSB facility may play a role in relation to this as can be seen from *Fig. 60*, where measured and calculated primary pressure trends are reported together with the secondary ones. The same scaling distortion effect is evident after 450 s, where the heat losses in primary and secondary side cause a decrease in pressure larger in the experiment than in the Kv scaled calculation.

After the loop seal clearing (500 seconds), the surface cladding temperatures at different heights start to increase, and continue until the end of the transient. The maximum temperature reached by the cladding surface in the calculation is about 720 K. In the experimental results the last dry-out starts at about 750 seconds and reaches the maximum cladding temperature of 1073. K before the test stop; at this value the experiment is terminated. The difference in the maximum peak cladding temperature reached is due to the ratio core power/primary mass of just 4.61 kW/Kg with respect to 6.73 kW/Kg from measured data in the test.

Tab. 35 and *Tab. 38* show the results of the qualitative accuracy evaluation of the Kv scaled calculation based on some RTA (Relevant Thermal-hydraulic Aspects). The table reports also the conclusions from the calculation at “nominal conditions” discussed in the following subsection. Only few “Minimal” (M) accuracy marks are evidenced in the table, that are related to the specific hardware features of the facilities as above discussed and no “Unqualified” (U) marks. Thus the transient may be considered predicted by the code with sufficient accuracy and the used nodalization qualified.

Results of the calculation at “nominal conditions”

As a last step in the on transient qualification process, a calculation has been runs at NPP nominal conditions (e.g. 100% nominal power, all ECCS available). The results of this calculation are analyzed from a qualitively point of view in *Tab. 36* and *Tab. 38*. The comparison with the experimental data and with the Kv calculation results shows a complete absence of dry-outs for the whole transient.

Three main reasons justify this difference:

1. Low linear power in the system at the time of minimum mass inventory.
2. “Big” amount of mass inventory in the system: all ECCS are available.
3. “Long” MCP coastdown.

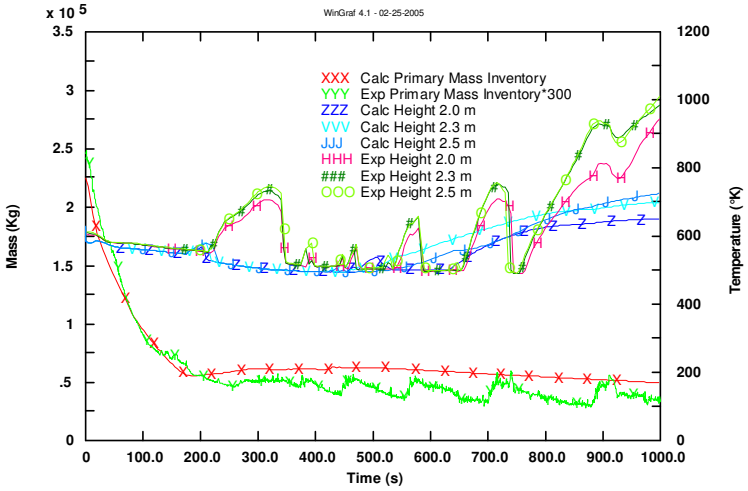

Fig. 57 VVER-1000 Cathare2 nodalization: Kv scaled calculation, comparison PS Mass Inventory and core cladding temperature at different levels calculated and experimental

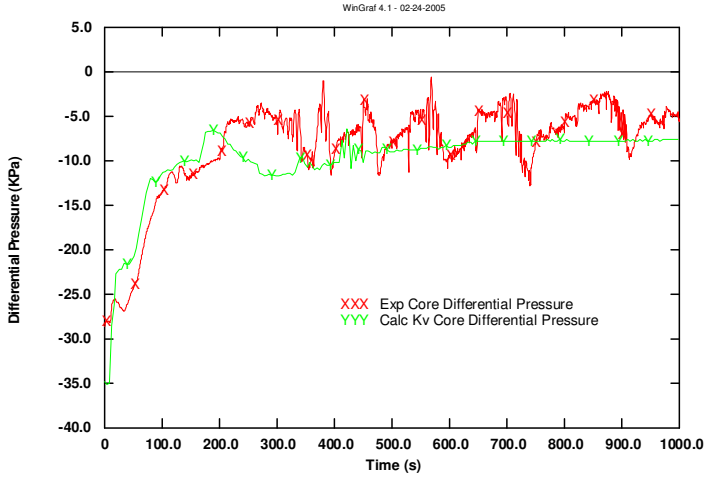

Fig. 58 VVER-1000 Cathare2 nodalization: Kv scaled calculation, comparison of core differential pressure calculated with the experimental data

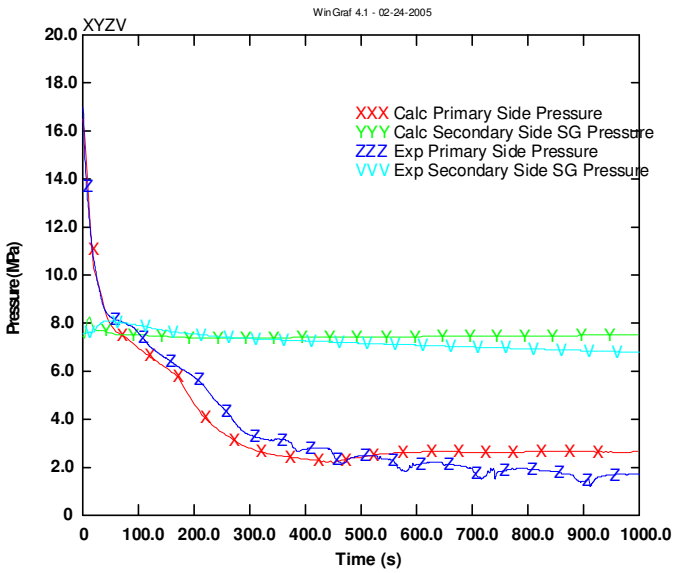

Fig. 59 VVER-1000 Cathare2 nodalization: Kv scaled calculation: comparison PS and SS pressure with the experimental data

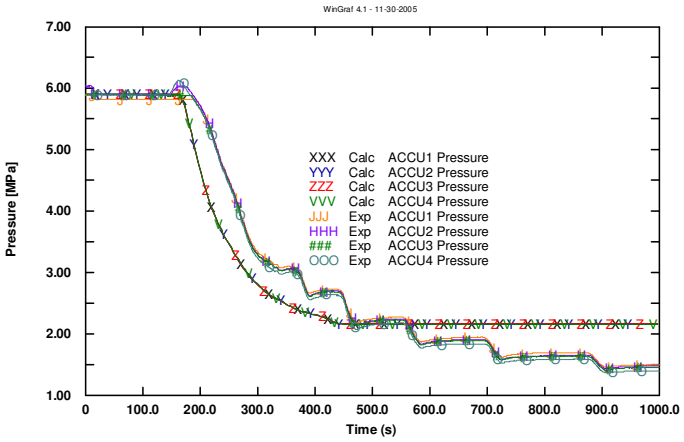

Fig. 60 VVER-1000 Cathare2 nodalization: Kv scaled calculation, comparison ACC pressure calculated with the experimental data

Looking at *Tab. 35*, the minimum mass inventory occurs in the primary side when the linear power is 0.5 kW/m and the amount of the mass is 63700 Kg. In the experiment the linear power at the time of minimum mass is 2.54 kW/m, and the equivalent mass inventory is 55720 Kg.

Fig. 61 shows the comparison between the cladding temperatures at different core levels and primary side mass inventory in the nominal conditions calculation and in the experiment. It is evident that the nominal conditions calculation is characterized by larger primary mass inventory than the experiment.

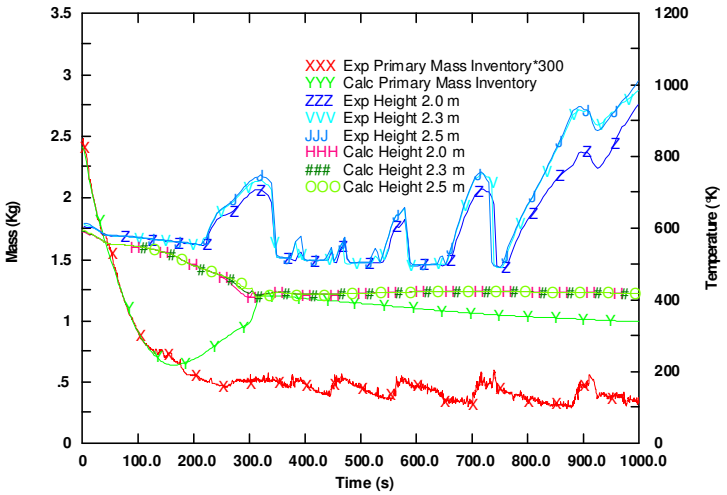

Fig. 61 VVER-1000 Cathare2 nodalization: nominal calculation, comparison between experimental and calculated PS mass inventory and core cladding temperatures at different levels.

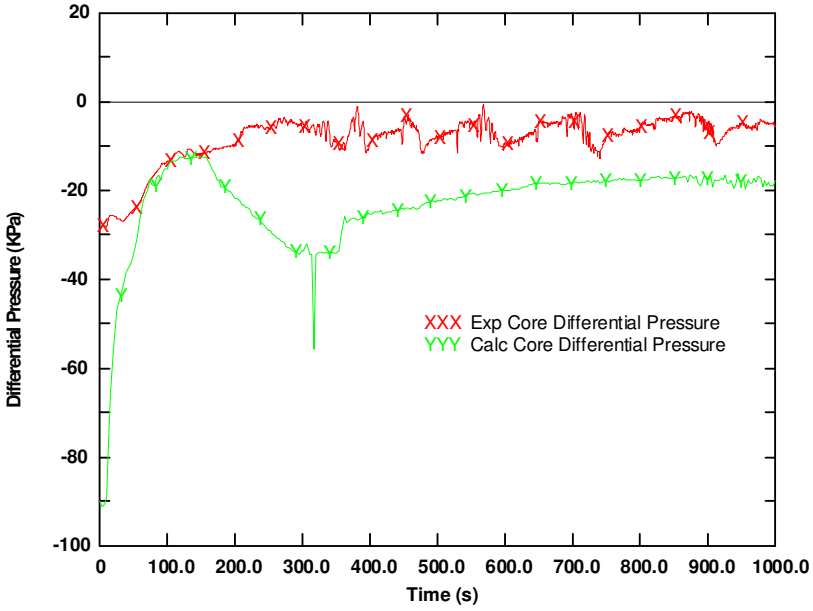

Fig. 62 – VVER-1000 Cathare2 nodalization: nominal calculation, comparison between calculated and experimental PS and SS pressure

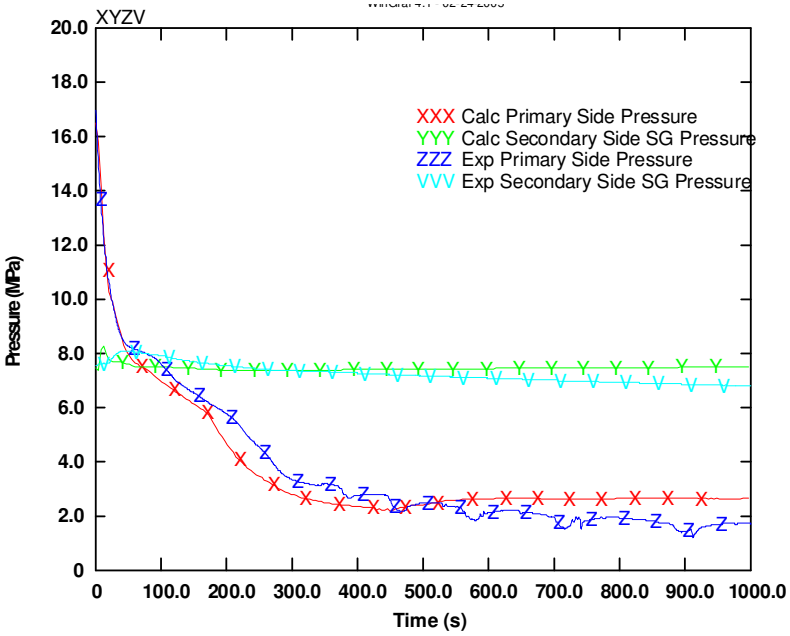

Fig. 63 VVER-1000 Cathare2 nodalization: nominal calculation, comparison between experimental and calculated core differential pressure.

In *Fig. 63* the comparison between differential pressure over the core in the experiment and in nominal conditions calculation is shown. The pressure over the core is higher than the experimental data during all the transient because the level in the core is higher than in the experiment. Relevant, for the core cooling is also the long MCP coast-down: in accordance with the data of Balakovo unit 3; the MCP require 232 seconds for complete stop. In this scenario the pump coast-down start 10 seconds later the beginning of the transients. This means that, when the minimum mass inventory in the primary side is met, the pumps are still coasting-down. In this conditions an improved heat exchange is expected then in the experiment, where the natural circulation is already established. In *Fig. 62* the comparison of the experimental and calculated pressure trends of the primary and secondary systems are shown. The calculated depressurization in the nominal conditions is faster; this allows the emergency systems to inject earlier and to supply more water. The calculation has been interrupted before reaching the set point for the intervention of the LPIS (TQ12).

The two steps of the qualification process foreseen in the methodology developed at UNIPI have been applied to qualify the Cathare2 v1.5/mod5.1 VVER1000 NPP nodalization at the “steady state” and the “on transient” levels. The first one, “steady state” level, has been fulfilled comparing the reference NPP main geometrical data with the one of the developed nodalization and running a calculation at steady state conditions (about 500 s to allow quite stable conditions in the calculations) to check the capability of the nodalization to reproduce in a stable way the nominal conditions of the real plant with errors in the limits foreseen by the methodology. For the second step, “on transient” level, a comparison has been done with the experimental data of the test no. 1 “11%UP break” carried out

in PSB-VVER facility. The NPP calculation, called “Kv scaled” calculation, starts from boundary and initial condition properly scaled from the ones measured in the experimental facility during the experiment. In addition, a calculation in nominal conditions of the real plant has been performed, in which all the systems in the real configuration have been used. The comparison of the “Kv scaled” calculation with the experimental data shows a quite good behavior of the nodalization in reproducing the main phenomena of the test performed in the facility. Difference in the timing of the phenomena may be connected to scaling distortion of the same phenomena due to specific features of the facility, e.g the mass to surface ratio of the heat structures. The nominal conditions calculation shows that the available ECCS are enough to keep the plant in safe conditions in the analyzed accident scenario.

Therefore it is possible to conclude that the VVER1000 Cathare2 nodalization is qualified at “steady state” level and “on transient” level. Following the criteria of the methodology developed at UNIPI an ASM (Analytical Simulation Model) is ready to be used to analyze the behavior of the real plant [21].

Cathare2 PSB-VVER nodalization

The PSB facility nodalization scheme is shown in *Fig. 64* (only the loop 4 is reported), and information about the code resources is given in *Tab. 39*.

The correspondence between the zones of the facility and the nodes of the code model are exposed in *Tab. 40* and *Tab. 41*. In these tables the facility is divided in main hydraulic components or systems, composed by single zones according to flow paths in nominal conditions. The name and the type of the hydraulic elements included in the nodalization and corresponding at each single component of the facility are indicated in the table itself.
This nodalization has been improved during the contract execution in order to have as much as possible fidelity between the real facility and the simulated one. The first step of this process is shown in *Fig. 65*), where all the loops are shown and it’s possible to observe the presence of the 4 steam line, the SS cooldown system and a refined mesh of all the pipes (“AXIAL” module in Cathare2). The fourth column of *Tab. 41* reports the adopted code resources.

Another improvement have been introduced in the nodalization showed in the *Fig. 66* where starting from the nodalization b), the only difference is a more detailed SG secondary side. The downcomer has been introduced in order to improve the simulation of the phenomena of steam fluid interaction in the SS of the SG. The fifth column of *Tab. 41* reports the adopted code resources

Primary system model

The vessel model is composed of 19 hydraulic components which are connected through 23 junctions. The steady state and the transient is performed without any boundary condition in order to stabilized pressures, levels or other nodalization parameter. The lower part of the down-comer is duplicated to simulate as well as

possible the inner and the outer part of the element. The components are subdivided into:

- ✓ 10 axial type elements;
- ✓ 9 volume type elements.

The heat structures utilized in the RPV scheme are represented by 30 wall type elements (excluding core heat structures) to simulate the heat release from structures during the transient; heat losses are foreseen. To take into account the heat losses in the facility a Heat Transfer Coefficient (HTC) based on the data provided by EREC is inserted in the Cathare2 nodalization.
A wall structure is provided to generate the electric thermal power to simulate power generation along the FRS with uniform power distribution. The heated zone of the core bypass is simulated by an equivalent heat flux imposed to the passive structure.
In the vessel model all the bypass flow paths, reported in the facility description, have been modeled:

- ✓ bypass from downcomer top to upper head via holes simulated by axial component 'A8DCUHBY' and it is a blind pipe;
- ✓ bypass from core bypass top to upper plenum simulated by junctions 'cobytopj".

Four loop represent with geometrical fidelity the real hydraulic configuration of the experimental facility. All four loops are modeled separately; each loop includes a hot leg, a steam generator, a pump, a loop seal and a cold leg. The primary side piping is composed of 40 components for the 4 loops which are connected through 60 junctions, plus 4 junctions for the vessel connection and 1 for the connection to the pressurizer.

The components of each loop are subdivided into:

- ✓ 8 axial type elements;
- ✓ 2 volume type elements;
- ✓ 1 tee type elements.

The heat structures in the primary side piping are represented by 8 wall type elements (excluding horizontal tubes connected heat structures) for each loop to simulate the heat release from structures during the transient.
At present the pumps are schematized with 'pumpchar' components and they are running with the LOBI facility homologous curve, given the actual lack of data. It must been stressed that anyway in near future detailed data on the pump characteristics will be provided by EREC.

The SG horizontal tubes are schematized by a 6 axial element representing all the 34 tubes of the PSB facility steam generator. The height and the length of the elements are the same of the tubes in the average position. The only exception is the first and the last tube in order to reproduce the same heated length in the secondary side of the steam generator. The axial element is constituted by a large

HYDR. COMP. / SYSTEM	HYDRAULIC ZONE	NODALIZ. ID	ELEMENT TYPE	NOTE
PRESSURE VESSEL	LOWER PLENUM	V1LP1	VOLUME	Cells from V1 to V4 (V4 from 0mm to 580mm of 987mm) it is included the volume V53 and v52 until 0.758
		V2LP2	VOLUME	Cells from V4 to V6 (V4 from 580mm to 987mm)
		A2LPPIPE	AXIAL	Cell V7
		V4COIN	VOLUME	Cells from V8 to V10
	CORE REGION	A3CORE	AXIAL	Cells from V11 to V13
	UPPER PLENUM	V5UP1	VOLUME	Cells from V14 to V18
		A6UP2	AXIAL	Cells from V19 to V22
		V6UP3	VOLUME	Cells from V23 to V25
		V8UHEAD	VOLUME	Cells from V26 to V28
		A7UHCRBY	AXIAL	Cell V29
	DC-UH BYPASS	A8DCUHBY	AXIAL	Cells from V30 to V38
	DOWNCOMER	A1DC3	AXIAL	Cells from V48 to V52 (from h=0.758 tp 0.996)
		V3DC1	VOLUME	Cells from V45 to V47
		A5DC2	AXIAL	Cell V44
		V7DC2T	VOLUME	Cells from V39 to V43
	CORE BYPASS	COBY1A	AXIAL	Cells from V54 to V60
		COBY1B	AXIAL	Cells from V54 to V60
		COBY2	VOLUME	Cell V61
		COBY3	AXIAL	Cells from V62 to V72
LOOP 1 PIPING	HOT LEG 1	AHL1	AXIAL	
	STEAM GENERATOR 1 PRIMARY SIDE	SG1HC	VOLUME	
		SG1A1	AXIAL	
		SG1A3	AXIAL	
		SG1A5	AXIAL	
		SG1A7	AXIAL	
		SG1A9	AXIAL	
		SG1A11	AXIAL	
		SG1CC	VOLUME	
	COLD LEG 1	LSCLA1	AXIAL	

Tab. 39 Cathare PSB-VVER: correspondence between code nodes and hydraulic zones (1 of 2)

number of nodes (45 nodes with an height of about 0.20m, for each loop) to better reproduce the heat exchange process between primary and secondary side.

The pressurizer is connected to the hot leg loop 4 via the surge-line.

HYDR. COMP / SYSTEM	HYDRAULIC ZONE	NODALIZ ID	ELEMENT TYPE	NOTE
LOOP 2 PIPING	HOT LEG 2	AHL2	AXIAL	
	STEAM GENERATOR 2 PRIMARY SIDE	SG2HC	VOLUME	
		SG2A1	AXIAL	
		SG2A3	AXIAL	
		SG2A5	AXIAL	
		SG2A7	AXIAL	
		SG2A9	AXIAL	
		SG2A11	AXIAL	
		SG2CC	VOLUME	
	COLD LEG 2	LSCLA2	AXIAL	
LOOP 3PIPING	HOT LEG 3	AHL3	AXIAL	
	STEAM GENERATOR 3 PRIMARY SIDE	SG3HC	VOLUME	
		SG3A1	AXIAL	
		SG3A3	AXIAL	
		SG3A5	AXIAL	
		SG3A7	AXIAL	
		SG3A9	AXIAL	
		SG3A11	AXIAL	
		SG3CC	VOLUME	
	COLD LEG 3	LSCLA3	AXIAL	
LOOP 4 PIPING	HOT LEG 4	AHL4	AXIAL	
	STEAM GENERATOR 4 PRIMARY SIDE	SG4HC	VOLUME	
		SG4A1	AXIAL	
		SG4A3	AXIAL	
		SG4A5	AXIAL	
		SG4A7	AXIAL	
		SG4A9	AXIAL	
		SG4A11	AXIAL	
		SG4CC	VOLUME	
	COLD LEG 4	LSCLA4	AXIAL	
PRESSURIZER	SURGE LINE	TEEPRZ	TEE	
		SLINE	AXIAL	
	PRESSURIZER	PRESSUR	VOLUME	
STEAM GENERATOR 1 SECONDARY SIDE	FEEDWATER	FW1	BCONDIT	
	TUBE ZONE	SSSG1VB	VOLUME	
		SSSG1AX	AXIAL	
	STEAM DOME	SSSG1VT	VOLUME	
	STEAM LINE	SL1	BCONDIT	
STEAM GENERATOR 2 SECONDARY SIDE	FEEDWATER	FW2	BCONDIT	
	TUBE ZONE	SSSG2VB	VOLUME	
		SSSG2AX	AXIAL	
	STEAM DOME	SSSG2VT	VOLUME	
	STEAM LINE	SL2	BCONDIT	
STEAM GENERATOR 3 SECONDARY SIDE	FEEDWATER	FW3	BCONDIT	
	TUBE ZONE	SSSG3VB	VOLUME	
		SSSG3AX	AXIAL	
	STEAM DOME	SSSG3VT	VOLUME	
	STEAM LINE	SL3	BCONDIT	
STEAM GENERATOR 4 SECONDARY SIDE	FEEDWATER	FW4	BCONDIT	
	TUBE ZONE	SSSG4VB	VOLUME	
		SSSG4AX	AXIAL	
	STEAM DOME	SSSG4VT	VOLUME	
	STEAM LINE	SL4	BCONDIT	
ECCS (HIGH PRESSURE INJECTION SYSTEM)	HPIS	IHPIP	SOURCE	

Tab. 40 Cathare PSB-VVER: correspondence between code nodes and hydraulic zones (2 of 2)

The pressurizer and surge line are composed of 2 components which are connected through 2 junctions. The components are subdivided into:

- ✓ 1 axial type element;
- ✓ 1 volume type elements;
- ✓ 1 tee type elements.

The heat structures in the pressurizer and surge line are represented by 3 wall type elements to simulate the heat release from structures during the transient and the heaters foreseen in the PRZ. The Emergency Core Cooling System (ECCS) is simulated by a source component connected to hot leg. It must been stressed that only one HPIS is assumed available and it is connected to the loop 4. The SIT are simulated by four accumulator components and they are connected in pairs to the down-comer and to the upper plenum. The line connecting the SIT and the DC or UP is implicit in the definition of the accumulator component.

Secondary system model

The secondary system model is composed by only 5 components. Two "bcondit" components represent the boundary conditions: one upstream the steam generator simulates the FW component, the second is downstream the steam generator and it is a boundary condition for the pressure simulating the SL.
The secondary side is very simple and straight forward. Each steam generator model is composed of 5 components which are connected through 4 junctions. The components are subdivided into:

- ✓ 1 'axial' type element;
- ✓ 2 'volume' type elements;
- ✓ 2 'bcondit' type elements.

The heat structures in the secondary side are represented by 6 wall type elements for each steam generator to simulate the heat release from structures during the transient. The heat exchange between primary and secondary circuits is provided by an exchanger operator. The geometrical features of the piping and system connected with SG are not simulated (e.g. feed water lines, pre-heaters, steam lines - including condenser - etc.), because this is not relevant for the prediction of the transients of interest.

No	PARAMETER	VALUE (2004)	VALUE (2005)	VALUE (2006)
1	**Total Number of Hydraulic Modules**			
2	PS	63 (1742)	66 (1919)	67 (1922)
3	SS	20 (64)	52 (729)	58 (706)
4	Total	83 (1806)	118 (2648)	125 (2628)
5	**Number of junctions**			
6	PS	92	92	92
7	SS	16	16	16
8	Total	108	108	108
9	**Number of thermal structures**			
10	PS	117	117	117
11	SS	24	24	24
12	Total	141	141	141
13	**Number of core active structures**	10	10	10
14	**Number of mesh points**			
15	Core slabs	120	120	120
16	SG slabs	392	392	392
17	**Overall volume (m^3)**	1.78927	1.78927	1.78927

Tab. 41 Cathare2 PSB-VVER: overview of the code resources

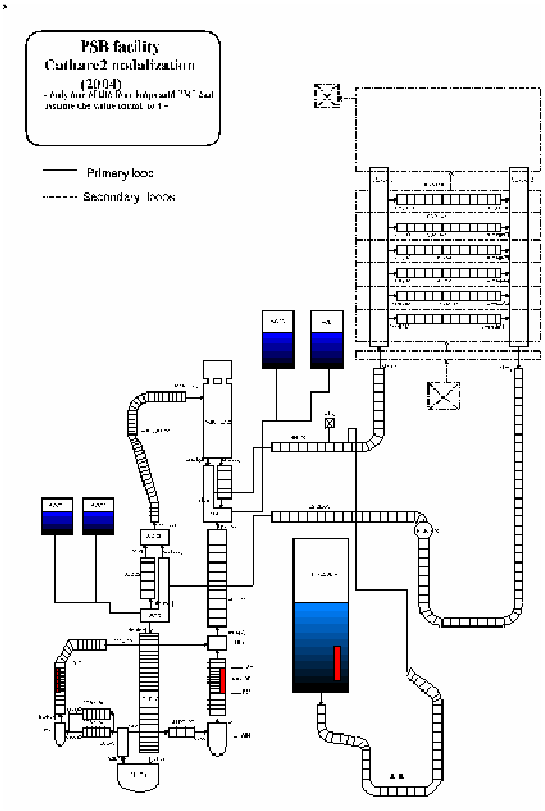

Fig. 64 Cathare2 PSB-VVER: nodalization schemes first (2004)

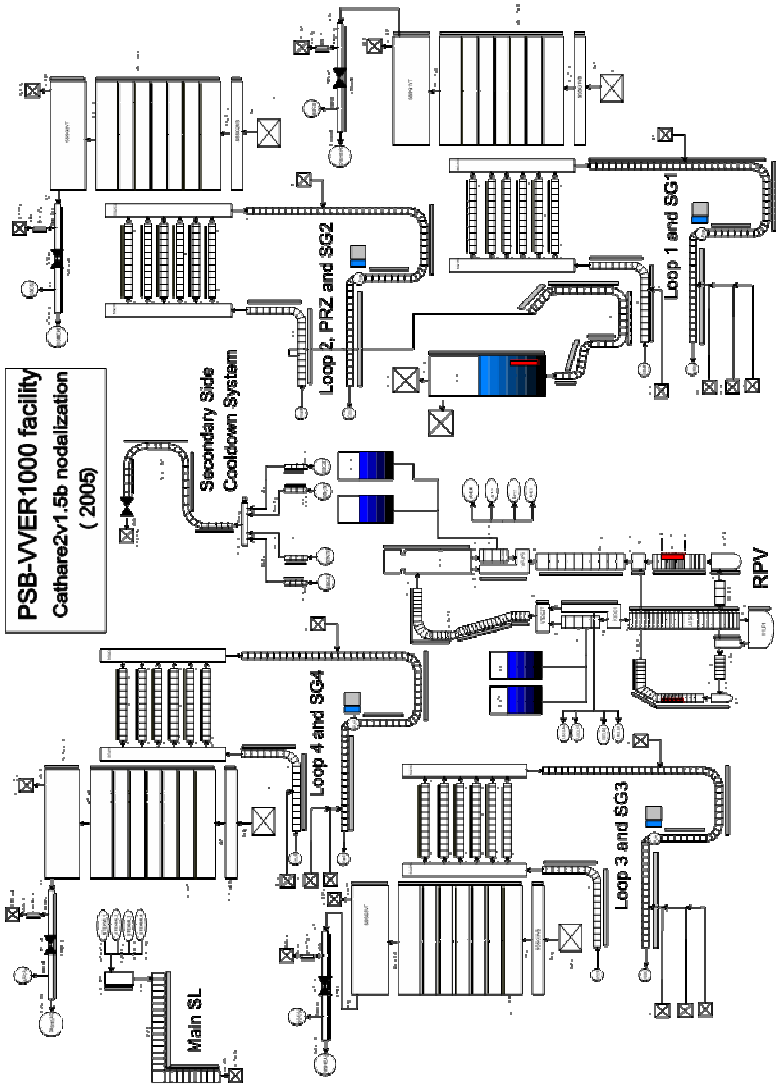

Fig. 65 Cathare PSB-VVER: nodalization schemes b) second (2005)

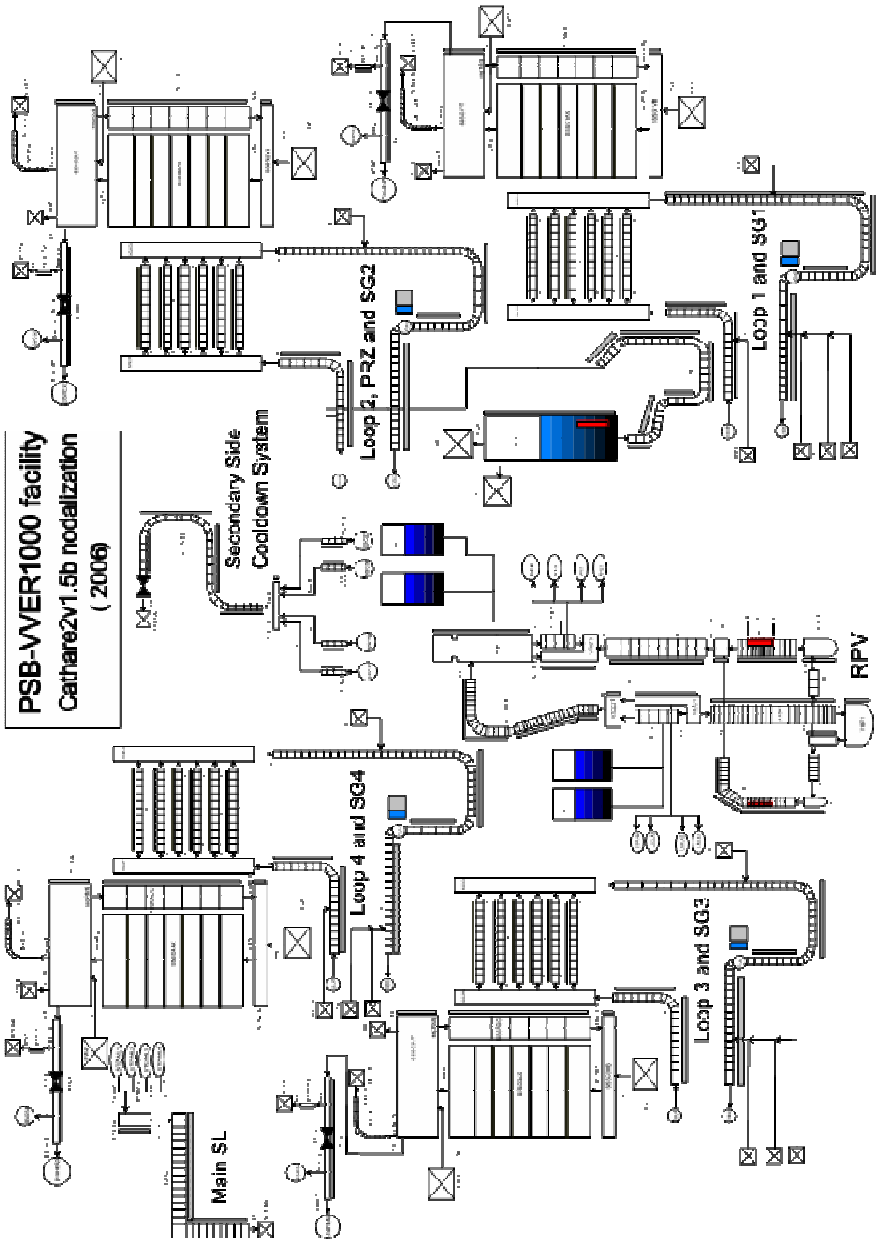

Fig. 66 Cathare2 PSB-VVER: nodalization schemes third (2006)

ID Cathare Volume	Element type	Abs height (m) lower part	Volume (m^3)	Volume PSB Facility (m^3)	Error
V3DC1	Volume	6.7	0.00664	0.00661	-0.50%
A5DC2	Axial	6.79	0.00486	0.00486	-0.04%
V7DC2T	Volume	7.25	0.01041	0.01084	3.95%
A8DCUHBY	Axial	7.25	0.00083	0.00084	1.24%
V8UHEAD	Volume	9.05	0.08920	0.09028	1.20%
A7UHCRBY	Axial	9.05	0.00486	0.00486	-0.05%
A1DC3	Axial		0.06465	0.06477	0.19%
V1LP1	Volume	0	0.01370	0.01371	0.06%
V2LP2	Volume	0.758	0.00732	0.00735	0.38%
COBY1A	Axial	1.34	0.00053	0.00052	-1.74%
COBY1B	Axial	1.34	0.00053	0.00052	-1.74%
COBY2	Volume	1.325	0.00056	0.00056	0.13%
COBY3	Axial	1.7475	0.00797	0.00811	1.69%
A2LPPIPE	Axial	1.34	0.00460	0.00460	-0.01%
V4COIN	Volume	1.234	0.01121	0.01100	-1.94%
A3CORE	Axial	1.574	0.05637	0.05616	-0.39%
V5UP1	Volume	5.73	0.02313	0.01992	-16.13%
A6UP2	Axial	6.43	0.06199	0.06198	-0.01%
V6UP3	Volume	8.5	0.00671	0.00670	-0.29%
PIPBRE	Axial	8.655	0.00136		
AHL1	Axial	8.855	0.01851	0.01851	-0.01%
SG1HC	Volume	10.325	0.01009	0.00999	-0.98%
SG1A1	Axial	10.68	0.00283	0.00283	0.00%
SG1A3	Axial	11.1152	0.00990	0.00990	0.00%
SG1A5	Axial	11.5504	0.01132	0.01132	0.00%
SG1A7	Axial	11.9856	0.01132	0.01132	0.00%
SG1A9	Axial	12.4208	0.00990	0.00990	0.00%
SG1A11	Axial	12.856	0.00283	0.00283	0.00%
SG1CC	Volume	10.325	0.01009	0.00999	-0.98%
LSCLA1	Axial		0.07909	0.07244	-9.18%
PUMP1				0.01000	
AHL2	Axial	8.855	0.01851	0.01851	-0.01%
SG2HC	Volume	10.325	0.01009	0.00999	-0.98%
SG2A1	Axial	10.68	0.00283	0.00283	0.00%
SG2A3	Axial	11.1152	0.00990	0.00990	0.00%
SG2A5	Axial	11.5504	0.01132	0.01132	0.00%
SG2A7	Axial	11.9856	0.01132	0.01132	0.00%
SG2A9	Axial	12.4208	0.00990	0.00990	0.00%
SG2A11	Axial	12.856	0.00283	0.00283	0.00%
SG2CC	Volume	10.325	0.01009	0.00999	-0.98%
PUMP2			0.00000	0.01000	
LSCLA2	Axial		0.08021	0.07258	-10.51%
AHL3	Axial	8.855	0.01851	0.01851	-0.01%
SG3HC	Volume	10.325	0.01009	0.00999	-0.98%
SG3A1	Axial	10.68	0.00283	0.00283	0.00%
SG3A3	Axial	11.1152	0.00990	0.00990	0.00%
SG3A5	Axial	11.5504	0.01132	0.01132	0.00%
SG3A7	Axial	11.9856	0.01132	0.01132	0.00%
SG3A9	Axial	12.4208	0.00990	0.00990	0.00%
SG3A11	Axial	12.856	0.00283	0.00283	0.00%
SG3CC	Volume	10.325	0.01009	0.00999	-0.98%
LSCLA3	Axial		0.08131	0.07273	-11.80%
PUMP3				0.01000	
AHL4	Axial	8.855	0.01851	0.01851	-0.01%
SLINE	Axial	4.892	0.01701	0.01632	-4.24%
PRESSUR	Volume	4.892	0.25100	0.25958	3.31%
SG4HC	Volume	10.325	0.01009	0.00999	-0.98%
SG4A1	Axial	10.68	0.00283	0.00283	0.00%
SG4A3	Axial	11.1152	0.00990	0.00990	0.00%
SG4A5	Axial	11.5504	0.01132	0.01132	0.00%
SG4A7	Axial	11.9856	0.01132	0.01132	0.00%
SG4A9	Axial	12.4208	0.00990	0.00990	0.00%
SG4A11	Axial	12.856	0.00283	0.00283	0.00%
SG4CC	Volume	10.325	0.01009	0.00999	-0.98%
PUMP4			0.00000	0.01000	
LSCLA4	Axial		0.07984	0.07254	-10.06%
Total data primary side			**1.31164**	**1.31667**	**0.38%**

Tab. 42 Cathare2 PSB-VVER: ccorrespondence between volume of the PS in PSB-VVER facility and PSB-VVER Cathare2 nodalization

11% UP break results

A meaningful nodalization assessment process has been provided by the following steps:

a) steady state results;
b) calculation results;

It may be noted that item a) may constitute a part of the nodalization qualification process, described in the previous section; however, the fulfillment of criteria foreseen in the methodology is necessary each time a new experiment is considered and before starting transient calculations by using the previously qualified nodalization. The attention is focused hereafter toward the analysis of the calculation results in order to qualify the nodalization, item b), considering that steady state calculation, item a), is part of the nodalization qualification. When calculating the quantitative accuracy, 18 time trends have been selected in relation to which experimental data exist: these are assumed to be the minimum number of measured quantities that fully describe the experimental scenario.

Steady state results

This constitutes the final step of the nodalization qualification process at steady state level. The related results are shown in *Tab. 43*. Resulting values are compared with experimental data. It may be noted that the data deal with most of the parameters imposed for the nodalization qualification process.
The analysis of data brings to the following conclusions:

- ✓ the criteria for nodalization qualification are generically fulfilled, though the complete comparison between data in *Tab. 43* with acceptability criteria has not been done owing to the lack of experimental data;
- ✓ The curve volume vs. height shows a good agreement between the implemented data and the experimental one *Fig. 67*;
- ✓ a good agreement in the case of pressure drops is observed (see *Fig. 68* and *Fig. 69*);
- ✓ the heat losses are not completely cover: In particular the heat losses of the MCP are not foreseen;

the tuning or adjustments of steady state code results was considered unnecessary owing to the low influence that the observed discrepancies has in the selected transient.

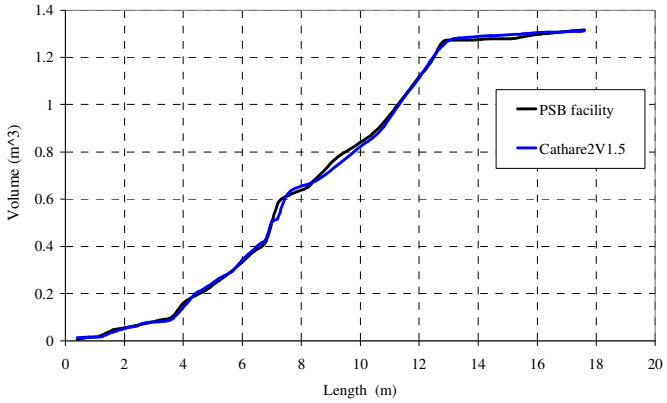

Fig. 67 Cathare2 PSB-VVER: volume vs. height curve.

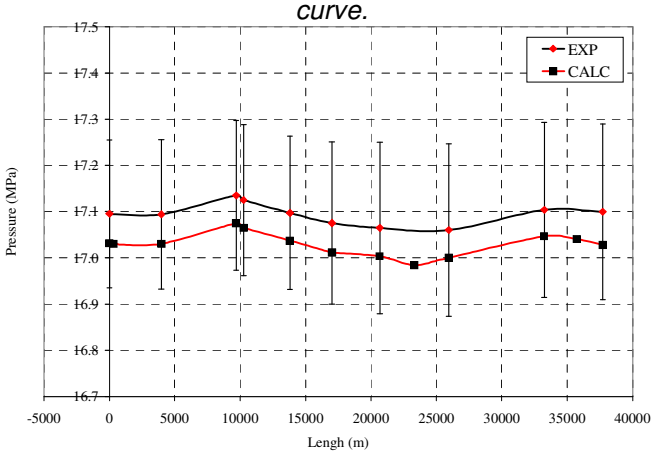

Fig. 68 Cathare2 PSB-VVER: comparison between measured and calculated DP vs. length curve for the PS.

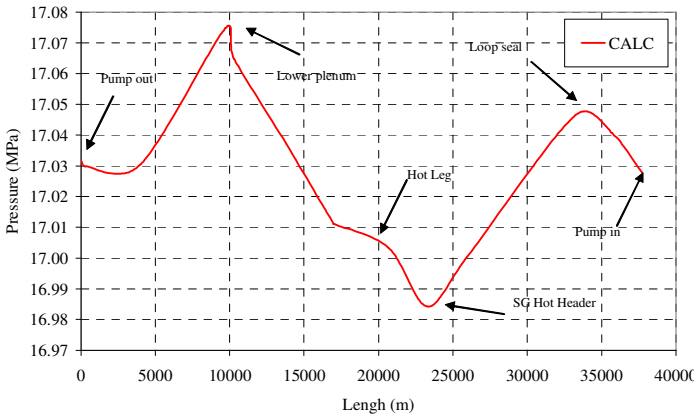

Fig. 69 Cathare2 PSB-VVER: calculated DP vs. length curve for the primary side (detailed image).

PARAMETER	UNIT	CODE MEASURE	ACTUAL VALUE	SET VALUE
				Cathare2V1.5b
Primary Side				
Pressure in UP	MPa	YC01P17	16.9±0.06	16.9
Coolant temperature at:				
DC inlet	K	YA01-04T02	559.7±3	560.6
UP outlet		YA01-04T03	589.7±3	589.8
Mass flow rate in loops:				
loop 1		YA01F01	2.3±0.05	2.29
loop 2	kg/s	YA02F01	2.3±0.05	2.29
loop 3		YA03F01	2.3±0.05	2.29
loop 4		YA04F01	2.4±0.05	2.27
Power of FRS bundle	kW	YC01N01	1520±15	1521
By-pass power	kW	YC01N02	17.4±0.7	17.4
Coolant level in PRZ	M	YP01L02	6.99±0.3	6.94 (8.83)
Secondary Side				
Pressure:				
SG1		YB01P01	7.43±0.05	7.42
SG2	MPa	YB02P01	7.47±0.05	7.40
SG3		YB03P01	7.33±0.05	7.40
SG4		YB04P01	7.43±0.05	7.40
Level:				
SG1		YB01L01	1.71±0.07	1.71
SG2	m	YB02L01	1.71±0.07	1.71
SG3		YB03L01	1.84±0.07	1.80
SG4		YB04L01	1.74±0.07	1.72
ACC				
Pressure:				
ACCU 1		TH01P01	5.8±0.03	5.9
ACCU 2	MPa	TH02P01	5.9±0.03	5.9
ACCU 3		TH03P01	5.9±0.03	5.9
ACCU 4		TH04P01	5.9±0.03	5.9
Level:				
ACCU 1		TH01L01	4.84±0.07	4.84
ACCU 2	m	TH02L01	4.84±0.07	4.84
ACCU 3		TH03L01	4.86±0.07	4.84
ACCU 4		TH04L01	4.85±0.07	4.84

Tab. 43 Cathare PSB-VVER: measured and calculated relevant BIC.

PSB 11% UP break test calculation results

The initial and boundary conditions see *Tab. 35*.

The test calculation is performed starting from the input deck suitable for Cathare2V1.5b code. The reference calculation for this study is labeled “PSB_04e10”; the related time trends and significant single valued parameters are reported, together with experimental data, respectively (in the figures the label “PSB_04e10” and “EX_11UP” identify calculated and experimental results trends respectively).

A comprehensive comparison between measured and calculated trends or values is performed, including the following steps:

a) comparison between experimental and calculated time.

b) quantitative evaluation of calculation accuracy, utilizing the FFTBM, (see paragraph 3.1), as given *Tab. 44*.

Comments related to items a) are given below, distinguishing groups of homogeneous variables, while the discussion about items b) is given in the section 'Quantitative accuracy evaluation' of this section.

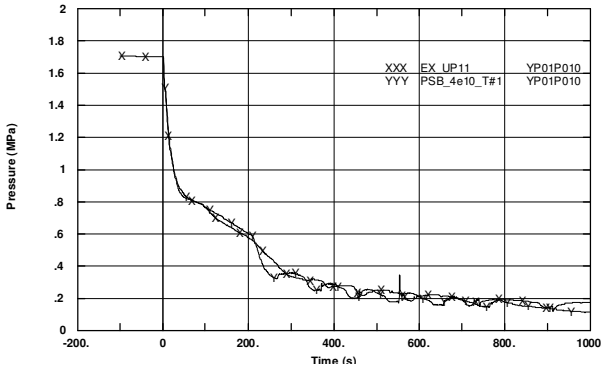

Fig. 70 Cathare2 PSB-VVER: PRZ pressure

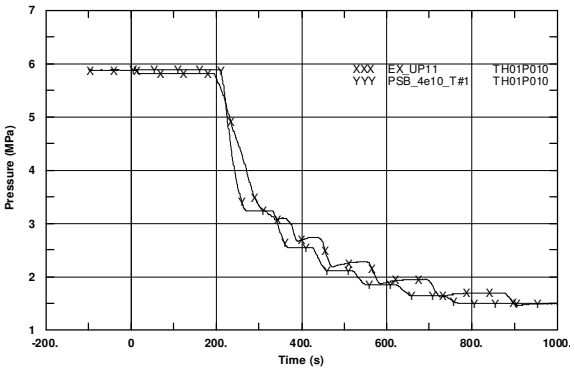

Fig. 71 Cathare2 PSB-VVER: ACC #1 pressure

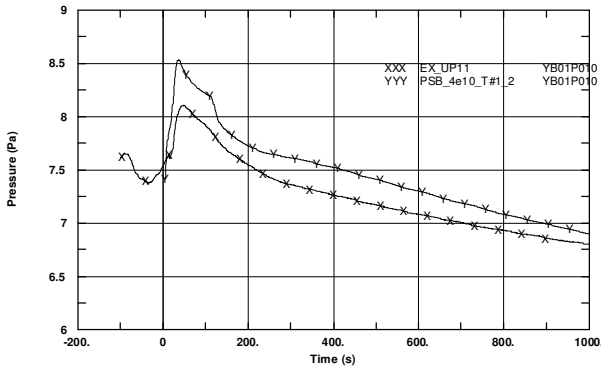

Fig. 72 Cathare2 PSB-VVER: SG#1 SS pressure

The primary system pressure is quite well predicted by the code. *Fig. 70 a*nd *Fig. 71* show the primary pressure and the accumulator pressure trends. A very good agreement can be observed in the first 200s of the transient, time when the pressure reaches 5.9 MPa and the accumulators start to inject water in the RPV (two trains in the downcomer and two train in the upper plenum). The following 80 seconds of the transient the calculated pressure trends in pressurizer differ from the experiment one. Consequence is the different intensity of the dry out in the core.

The accumulator pressure generally follows the primary pressure; time of accumulator actuation is consequence of the primary pressure and the value of the set point (5.9 MPa). The accumulator actuation is predicted about at the same time, showing the good agreement of the primary pressure in the first part of the transient, but the pressure trend is different in the following 80 seconds. This discrepancy is due to the different primary pressure trend during this phase.

The secondary pressures for SG #1 is reported in *Fig. 72.*

Core inlet and outlet fluid temperatures are qualitatively well predicted during all transient (*Fig. 73*).

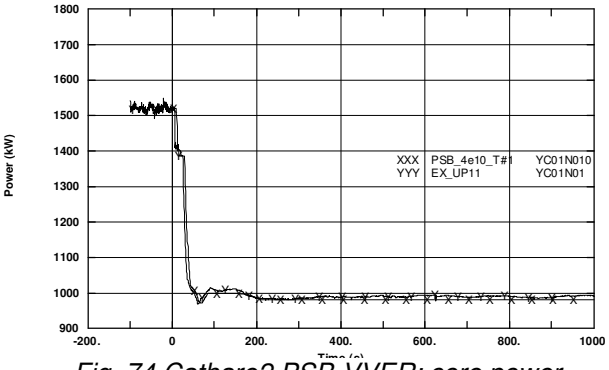

Fig. 74 Cathare2 PSB-VVER: core power

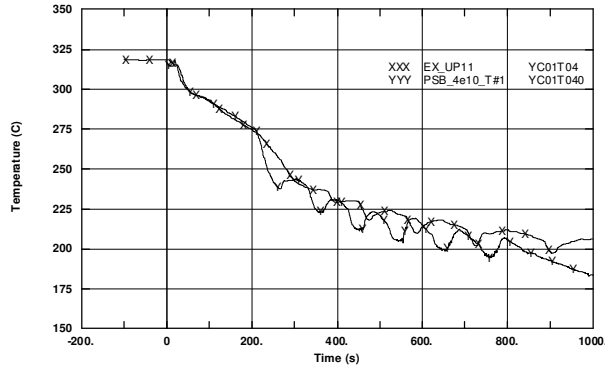

Fig. 73 Cathare2 PSB-VVER: core outlet fluid temperature

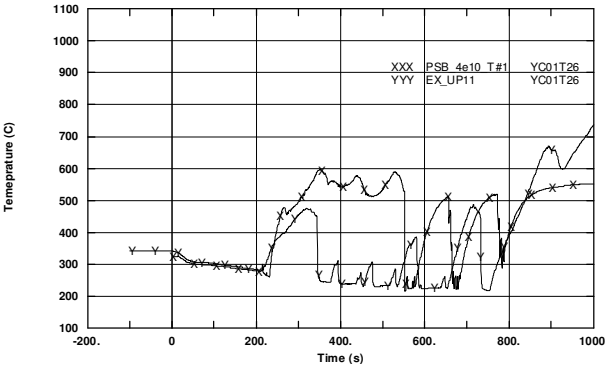

Fig. 75 Cathare2 PSB-VVER: rod temperature (h=3.20m)

When analyzing the rod surface temperature trends (*Fig. 75*), the three-dimensional situation in the core must be considered (as it is already mentioned above).

After deep and careful considerations of the experimental data, it has been observed at the same high of the core in the experimental facility PSB, there are zones in dry out with very high temperature of the fuel cladding and zones with very low temperature. A mono-dimensional TH code, such as Cathare2, represents the parameters only of the average channel, but in any case the qualitative behavior (i.e. the dry out and the reflood phases) is quite well observed. The main difference is showed by the intensity and the duration of the first dry out in the core.

Notwithstanding the experimental data do not result homogeneous at the same level of the core, regarding the fuel cladding temperature, any research has been performed in order to find suitable results for these parameter trends.

Predicted rod surface temperature trends show discrepancies in the higher part of the core, in particular the first dry-out is larger than the dryout highlighted by the experimental results.

It must be stressed that the 2D reflood (bottom-top and top- bottom) model is activate. This Reflood submodule has been implemented in Cathare2 code where

the heat exchanges are different from the standard low, and it allows to calculate in a rather accurate way the rewetting of a hot wall or rod or fuel.

Pressure drop between different point of the primary circuit are considered in the comparison, and they are shown from *Fig. 68*. These figures are focused on the differential pressure between BAF and TAF of the core simulator, and on the loop 2 of the nodalization. The pressure drops are reasonably well predict by the code.

Quantitative accuracy evaluation

The results of the 11%UP break test performed with Cathare2 code has been submitted to the accuracy evaluation in order to perform the on transient level quantitative qualification of the nodalization. To this aim a special methodology, developed at University of Pisa, and widely used has been adopted. The methodology is based upon the use of the FFT-BM and its main features are detailed in reference see paragraph 3.2.
The results of the application of the method are given in *Tab. 44*. The conclusions from the quantitative accuracy evaluation analysis are as follows:

- ✓ The achieved results are considered acceptable notwithstanding the overall accuracy is higher then the limit. In detail, as reported in *Tab. 44*, the primary system pressure accuracy limit is satisfied (AA = 0.1 compared with the acceptability limit of 0.1); whereas the overall accuracy is higher then the limit (AA = 0.36 compared with the acceptability limit of 0.4).

Definitely, the documented calculation is acceptable and the nodalization carried out may be considered suitable to be applied to the analyses of the PSB-VVER tests.

PARAMETERS			PSB_04e10_test#1	
No	**Measured parameter**	**Identifier**	**AA**	**WF**
1	PRZ pressure	YP01P01	0.10	0.062
2	SG2 pressure - secondary side	YB01P01	0.09	0.042
3	SG3 pressure - secondary side	YB02P01	0.24	0.058
4	ACC1 pressure	TH01P01	0.08	0.019
5	ACC2 pressure	TH02P01	0.08	0.025
6	Core inlet fluid temperature	YC01T06	0.32	0.052
7	Core outlet fluid temperature	YC01T04	0.10	0.034
8	Upper head fluid temperature	YC01T05	0.82	0.057
9	Heater rod temp. (bottom level)	YC01T113	0.24	0.069
10	Heater rod temp. (middle level)	YC01T82	0.99	0.068
11	Heater rod temp. (high level)	YC01T26	1.00	0.043
12	Integral break flow rate	MASSBR	0.06	0.055
13	Break flow rate	XL01F01	0.98	0.162
14	Primary side total mass	MASS1	0.18	0.065
15	Core power	YC01N01	0.13	0.068
16	DP inlet-outlet SG 2	YA02DP03	0.98	0.134
17	DP SG 2 inlet hot header top	YA02DP14	0.34	0.090
18	ECCS flow rate	TJ04F02	0.06	0.136
TOTAL			0.368	0.221

Tab. 44 Cathare2 PSB-VVER: summary of results obtained by application of FFT method

PSB-VVER Calculations

All the 12 transients of the TM have been reproduced with the Cathare2 PSB-VVER nodalization and compared with the experimental data. In the following the main parameters registered during the execution of the experiment in the PSB-VVER facility is reported in few tables and figures for test 1, the same procedure has been applied for all the others 11 transients of the TM.

Experimental database

Test 1

Test is a total loss of feed-water with failure of HPIS pumps and operator actions on secondary circuit depressurization. The AM actions are:

- ✓ closure of MSIV in SG #2 and SG #3 when after 1800 seconds the core exit coolant temperature reaches 350 °C;
- ✓ depressurization of two steam generators: full opening of BRU-A in SG-1 and SG-4, 15 seconds after the signal for MSIV closure in SG #2 and SG #3;
- ✓ water supply from external source into SG #1 and SG #4 with a mass flow rate of 0.033 Kg/s when the pressure in both SG decreases to 1 MPa.

The systems configuration in this test is summarized in *Tab. 45*. The PRZ is connected to the hot leg of loop #2, the core by-pass has 2 orifices of 7 mm of diameter installed, the ACC the same configuration the LPIS injecting in the HL and CL if loops #3 and #4. The BIC are summarized in the *Tab. 46* with the related error in the measurement. In the *Tab. 47* the imposed sequence of main events is reported together with the delay of the occurrence. The test has been subdivided in 7 phenomenological windows (Ph.W.) summarized in following together with the AM actions. Hereafter the test results (see *Fig. 76*, *Fig. 77*) are discussed.

- ✓ Ph. W. 1: soon after the closure of the FW and the steam dump valve, the SG pressures start to increase and the first opening of the BRU-A valves occur. The PS pressure remains under 16 MPa because of the energy lost from the system by the SS of the SG and the injection of the spray in the PRZ.
- ✓ Ph. W. 2: the SG levels decrease because of the cycling of the BRU-A valves. The pumps start to coast down when the level in all SG decreases of 50 cm. Following the low SG level signal, the third pump start to coast down and the scram occurs. The decreasing of the level in the SG reduces the heat exchange between PS and SS and as consequence, the capability to remove energy from the PS decreases. The temperature in the PS starts to increase. As consequence the volume of water in the PS increases, because the density decreases, and the PRZ level increases. These phenomena continue also in the Ph.W 3.

- ✓ Ph. W. 3: the PS pressure slightly increases because of the reduced capability of the SG to remove heat from the PS. The PRZ level continues to increase and at the end of this phase the PRZ is full of water. It's important to note that during this phase, the power applied to the PRZ heaters has a peak, while the pressure in PS has very small variation.
- ✓ Ph. W. 4: PS pressure starts to increases faster (because the PRZ is full) and the set point for the PORV opening is reached. Then PORV the valve starts to cycle. Since this, the SG pressure has a small variation inside the range of BRU-A but not further opening of the valves is observed. The core outlet continues to increase during this phase.
- ✓ Ph. W. 5: This phase starts when set point of the AM procedure is met. The BRU-A valves of the SG #1 and #4 are completely opened and the MSIV of SG #2 and #3 are completely close and insulated. The pressure in SG #1 and #4 decreases very fast. The other two SG insulated keep the pressure almost constant. The PS pressure starts to increases but it does not reach the set point of the PORV opening.
- ✓ Ph. W. 6: the pressure in SG #1 and #4 equal to 1 MPa is the set point of the simulation of the fire brigade intervention. It consists in the injection in SG #1 and #4 of a mass flow rate of 0.035 Kg/s. The PS pressure and temperature decrease and the level in PRZ decreases too.
- ✓ Ph. W. 7: at the beginning of this phase, the low level in PRZ is the signal of the heaters switched off. The PS depressurization increases, but the primary side temperature decrease rate does not change

No	EQUIPMENT	CONNECTION STATUS
1	PRZ	connected to loop #2
2	Core by-pass*	2 diaphragms with 2 orifices D= 7 mm installed at inlet and outlet of core by-pass.
3	ACC	ACC #1 and ACC #3 connected to UP, ACC #2 and ACC #4 connected to DC.
4	LPIS	two lines of LPIS are connected to the HL and CL of loops #3 and #4 .
5	ADS (BRU-A) simulation system	each ADS line has throttle nozzle (L/D=10) with D=12.1 mm Opening/closure set points are 7.16/6.28 MPa
6	Warming-up line for UP	during steady state the line is open. It is stopped about 2 min before the test starts
7	Warming-up line of break line	open during steady state. It is stopped about 1 min before the test starts.
8	Spray line	located on the PRZ. Actuation set points are 18.14/16.67 MPa. Throttle nozzle: D=3 mm, 20 mm of length.

*** Present in all tests the same configuration**

Tab. 45 PSB-VVER experimental data base, Test 01: systems configuration

In this experiment a number of thermal-hydraulic phenomena were observed, which are recorded in the system code verification matrices developed by an international group of experts under the auspices of OECD-CSNI.

No	PARAMETER	MEASUREMENT	UNIT	VALUE	ERROR
	Primary System				
1	UP pressure	YC01P17	MPa	15.8	±0.05
2	UP outlet fluid temperature	YA01T03 YA02T03 YA03T03 YA04T03	℃	310. 308. 307. 310.	±3. ±3. ±3. ±3.
3	DC inlet fluid temperature	YA01T02 YA02T02 YA03T02 YA04T02	℃	277. 277. 276. 275.	±3. ±3. ±3. ±3.
4	Core power	YC01N01	kW	1519.	±15.
5	Core by-pass power	YC01N02	kW	15.1	±0.4
6	PRZ level	YP01L02	m	6.67*	±0.3
7	Level: ACC-1 ACC-2 ACC-3 ACC-4	TH01L01 TH02L01 TH03L01 TH04L01	m	4.86* 4.85* 4.85* 4.88*	±0.07 ±0.07 ±0.07 ±0.07
8	Pressure: ACC-1 ACC-2 ACC-3 ACC-4	TH01P01 TH02P01 TH03P01 TH04P01	MPa	5.9 5.9 5.9 5.9	±0.03 ±0.03 ±0.03 ±0.03
	Secondary System				
9	Pressure: SG 1 SG 2 SG 3 SG 4	YB01P01 YB02P01 YB03P01 YB04P01	MPa	6.29 6.29 6.32 6.28	±0.05 ±0.05 ±0.05 ±0.05
10	Level: SG 1 SG 2 SG 3 SG 4	YB01L01 YB02L01 YB03L01 YB04L01	m	1.70* 1.68* 1.70* 1.69*	±0.08 ±0.08 ±0.08 ±0.08
11	FW: SG 1 SG 2 SG 3 SG 4	RL01T02 RL02T02 RL03T02 RL04T02	℃	216. 216. 216. 216.	±3. ±3. ±3. ±3.
12	AFW: SG 1 SG 4	RL01T02 RL04T02	℃	20. 20.	±3. ±3.

The levels marked with (*) are measured at: 1.89m for the PRZ, 0.58m for the SG, 0.75m for the ACC from the bottom of the vessel

Tab. 46 PSB-VVER experimental data base, Test 01: boundary and initial conditions

No	EVENT	SET POINT			
		QUANTITY	UNIT	VALUE	DELAY
1	FW SG and turbine valve simulation start to close	operator action	s	0.	-
2	MCP coast down start	SG level: YB01L01 YB02L01 YB03L01 YB04L01	m	1.21 1.19 1.20 1.19	-
3	SCRAM	third pump coast down starts	-	-	-
4	PRZ heaters switched off	PRZ level	m	4.31	-
5	MSIV of SG #2 and #3 closure begin	core outlet fluid temperature	℃	350.	-
6	BRU-A of SG #1 and #4 start to close	core outlet fluid temperature	℃	350.	+ 10.
7	AFW injection start	pressure: SG #1 SG #4	MPa	1. 0.96	- -

Tab. 47 PSB-VVER experimental data base, Test 01: imposed sequence of main events

The PSB-VVER capabilities to induce and to measure a phenomenon were evaluated separately on the basis of the following grade terms:

PSB-VVER capabilities to induce phenomenon:
S the phenomenon was replicated in the experiment;
R limited replication of the phenomenon in the experiment.
PSB-VVER capabilities to detect phenomenon:
S the phenomenon was recorded in the experiment;
R insufficient recording of the phenomenon by instrumentation.
The general grade term for PSB-VVER capabilities (bold letters in the column):
S the phenomenon is suitable for code assessment
R the phenomenon is restricted suitable for code assessment

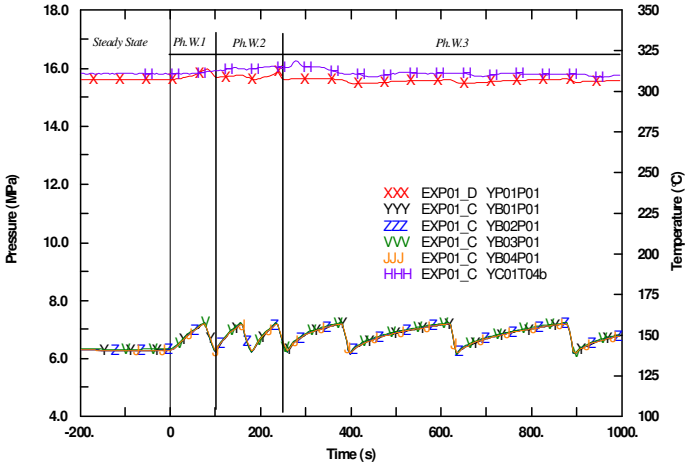

a) short term

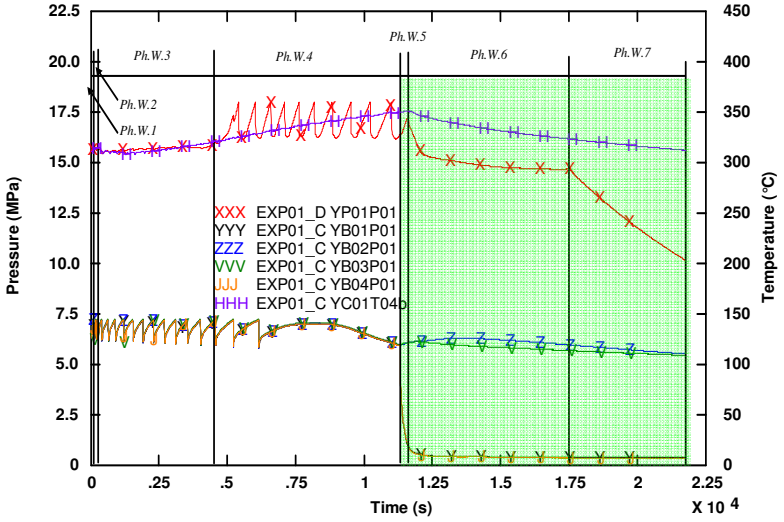

b) long term

Fig. 76 PSB-VVER experimental data base, Test 01: PS and SS pressures and fluid temperature at core outlet

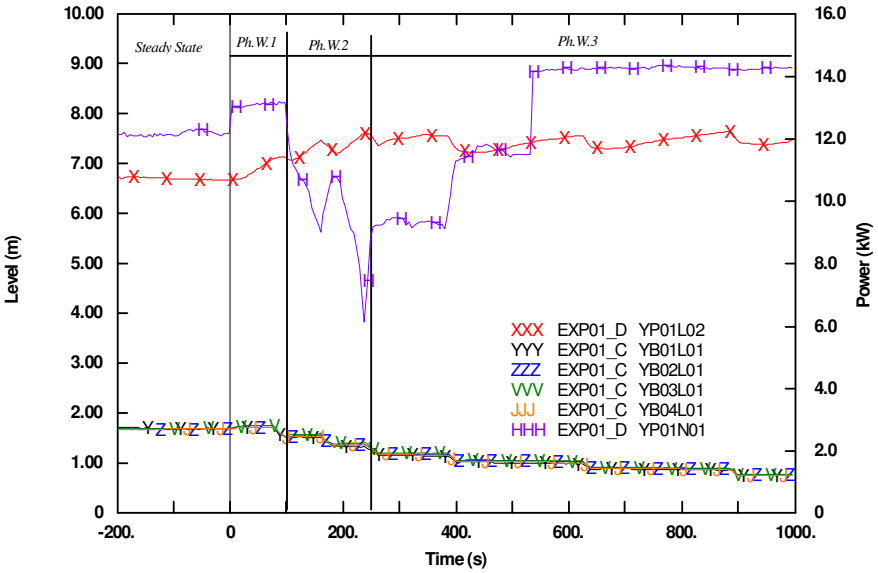

a) short term

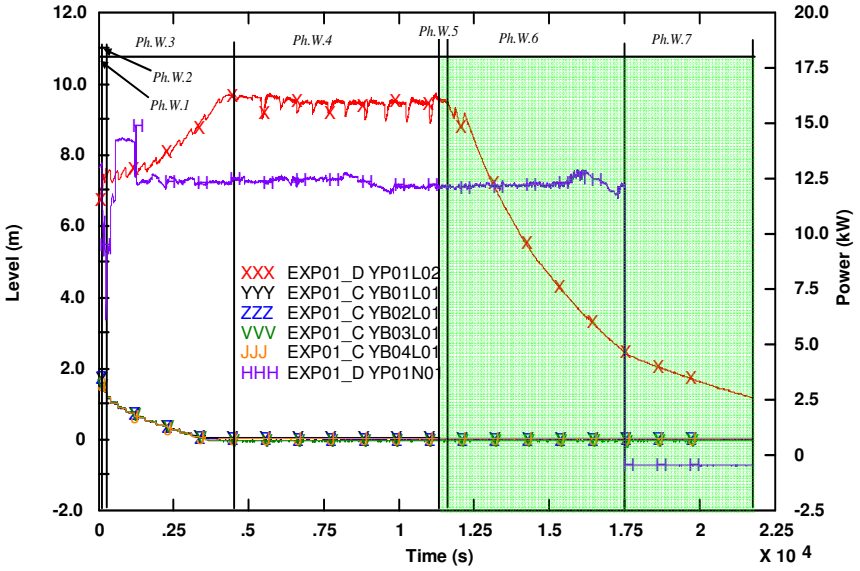

b) long term

Fig. 77 PSB-VVER experimental data base, Test 01: PRZ, SG levels and PRZ heaters power

Comparison Exp/calc

Steady state results
The steady state conditions are achieved running the code for 500 s. This constitutes the final step of the nodalization qualification process at steady state level. The values of the main parameters at the end of the stationary phase are summarized in *Tab. 48*, where the related values of Cathare2 codes are compared with the experimental data. It should be noted that the error has been calculated between the value calculated by the code and the measured parameters including the measurement error.

The analysis of data brings to the conclusions itemized below.

- ✓ The relevant initial and boundary conditions of the test are generically acceptable (see *Tab. 48*).
- ✓ The calculated values checked in the last 100s of the steady state calculation, are stable.
- ✓ The difference related to the primary pressure in steady state calculation is accepted because it should not affect the general behavior of the transient. It should be noted that the higher value of the pressure in stationary conditions causes the activation of the PRZ spray system as demonstrated in the sensitivity analysis.
- ✓ Finally, notwithstanding the mass flow rate in the loops (item 13) does not fulfill the acceptable limits in all loops (Cathare2), this has been accepted. The difference is because the MCPs in the experiment have different rotation velocities during the steady state, while in the calculations it has been set equal in all loops.

Reference calculation results
The test calculations ware performed starting from the last input deck developed for Cathare2 (see *Fig. 66*). The related time trends and the resulting sequence of the events are reported, together with experimental data and compared with the relap5 calculations performed in *Fig. 78*, *Fig. 78 Fig. 80* and *Tab. 49*.

In the figures the labels “T#1_EXPx”, “T#1_R5” and “T#1_C2” identify experimental and calculated result trends. In particular T#1 identifies the test, in this case the number 1 in the TM of the Project; the extensions EXPx, C2, the experiment, the Cathare2 time trends (where “x”, attached to the EXP extension is an alphanumeric added to the label because the experimental data are constituted by more than one file).

In the following discussion the calculations performed by application of Cathare2 are presented. In the discussion the two calculations are also indicated as C2 for Cathare2.

Absolute pressures
The primary side pressure is generally in agreement with the experimental results: the PORV cycling period is well evident; the decrease of the pressure depends by

secondary side depressurization actuation. However a better result is obtained in the C2 calculation. Formally the FFTBM application to the two codes calculations produces a result, for the primary side pressure, that is out of the range of acceptability. That result is mainly related to the pressure oscillations during the PORV actuation: the fast oscillation trend largely affects the FFTBM obtained result.

What is considered relevant in the primary side pressure time trend is the actuation of the PORV and the effect of the secondary side depressurization. The two aspects are well evident in both the calculation results. As a consequence the results are assumed as acceptable. The secondary side pressure time trends show that the secondary side depressurization is actuated early in both calculations following the core rods temperature different excursion in comparison with the experimental trend.

Fluid temperatures

The trends of the fluids temperatures are generally reproduced in a good way. The discrepancies between the two calculations and the experimental results are related to different timing of the secondary side depressurization (and as a consequence of the primary side temperature). A remarkable difference about the fluid temperatures in UH for the two calculations and the experiment results is evidenced. The main cause of these discrepancies is related to the nodalization of the UH adopted in the C2 calculation that emphasize the heat losses and in particular the not correct simulation of the circulation occurring in the facility.

Levels

The isolation and the actuation of the SG safety valves decrease the secondary side level in the SG up to zero. The R5 calculation shows a faster decrease of the SG level in comparison with the experimental result while the C2 has a time trend in good agreement with the experiment. In the depressurization phase the PRZ level is well predicted by the C2 calculation while an anticipated trend is obtained in the R5 calculation. Particularly the PRZ level in the R5 calculation starts to increase at about 15000s; this increase of the PRZ level is not observed in the experiment and is observed at the end of the C2 calculation only.

Pressure drops

The differential pressure results show a generally good agreement between the results obtained by the application of the codes and the experimental results. This is true for the DP measured over the core section, over the HL and loop seal. Some discrepancies are evidenced in the DP over the UP and hot and cold collectors of the SG 2 (the pressurizer is connected with the loop 2) that show a decrease of the differential pressure for the R5 calculation results (after about 16000s) in comparison with the experimental results.

#	Parameter	Exp. Code	Exp. Data		CALC. C2	ERR. C2	ACCEPT. ERR
			YE	Error			
1.	**Pres. in UP, MPa**	YC01P17	15.73	±0.08	15.76	0.0 %	0.1 %
2.	**Coolant T at UP out., °C**	YA01T03	310	±3	311	0.0 %	0.5 %
		YA02T03	308	±3	311	0.0 %	
		YA03T03	307	±3	311	0.3 %	
		YA04T03	310	±3	311	0.0 %	
3.	**Coolant T at DC in., °C**	YA01T02	277	±3	277	0.0 %	0.5 %
		YA02T02	277	±3	277	0.0 %	
		YA03T02	276	±3	277	0.0 %	
		YA04T02	275	±3	277	0.0 %	
4.	**Core pow., kW**	YC01N01	1519	±15	1520	0.0 %	2 %
5.	**Bypass pow., kW**	YC01N02	15.1	±0.4	15	0.0 %	2 %
6.	**Lev. in PRZ, m**	YP01L02 *	6.67	±0.3	6.54	0.0	0.05 m
7.	**Pressure, MPa**						
	- SG 1	YB01P01	6.29	±0.05	6.26	0.0 %	0.1 %
	- SG 2	YB02P01	6.29	±0.05	6.26	0.0 %	0.1 %
	- SG 3	YB03P01	6.32	±0.05	6.25	0.3 %	0.1 %
	- SG 4	YB04P01	6.28	±0.05	6.26	0.0 %	0.1 %
8.	**Level, m**						
	- SG 1	YB01L01 *	1.70	±0.08	1.68	0.0	0.1 m
	- SG 2	YB02L01 *	1.68	±0.08	1.68	0.0	0.1 m
	- SG 3	YB03L01 *	1.70	±0.08	1.68	0.0	0.1 m
	- SG 4	YB04L01 *	1.69	±0.08	1.68	0.0	0.1 m
9.	**Pressure, MPa**						
	- HA-1,	TH01P01	5.9	±0.03	5.9	1.0 %	0.1 %
	- HA-2,	TH02P01	5.9	±0.03	5.9	1.0 %	0.1 %
	- HA-3,	TH03P10	5.9	±0.03	5.9	1.0 %	0.1 %
	- HA-4,	TH04P01	5.9	±0.03	5.9	1.0 %	0.1 %
10.	**Level, m**						
	- HA-1,	TH01L01 *	4.86	±0.07	4.85	0.0	0.1 m
	- HA-2,	TH02L01 *	4.85	±0.07	4.85	0.0	0.1 m
	- HA-3,	TH03L01 *	4.85	±0.07	4.85	0.0	0.1 m
	- HA-4,	TH04L01 *	4.86	±0.07	4.85	0.0	0.1 m
11.	**Core mass flow rate, kg/s**	-	-	-	-	-	2 %
12.	**Core bypass mass flow, kg/s**	-	-	-	-	-	10 %
13.	**Loop #1 mass flow rate, kg/s**	YA01F01	2.24	±0.2	2.00	1.7 %	2 %
	Loop #2 mass flow rate, kg/s	YA02F01	2.24	±0.2	2.00	1.7 %	2 %
	Loop #3 mass flow rate, kg/s	YA03F01	2.24	±0.2	2.00	1.7 %	2 %
	Loop #4 mass flow rate, kg/s	YA04F01	2.26	±0.2	2.00	2.6 %	2 %
14.	**Core ΔT, °C**	-	35	-	35	0.0 %	0.5 %
15.	**Primary mass, kg**	Mass1	-	±30	886	-	2 %
16.	**Feed water temperature, °C**	RL01T02	216	±3	217	0.0 %	0.5 %
17.	**Feed water flow rate, kg/s**	RL01F02	0.189	±0.004	0.190 §	0.0 %	2 %
		RL02F02	0.171	±0.004	0.190 §	11.0 %	2 %
		RL03F02	0.175	±0.004	0.190 §	8.5 %	2 %
		RL04F02	0.175	±0.004	0.190 §	8.5 %	2 %
18.	**Primary side heat losses (no PRZ and MCP), kW**	-	60 **	-	65	8 %	10 %
19.	**MCP heat losses during normal operation (after coast-down), kW**	-	18 (6) §§	-	16 (-)	11 (-) %	-
20.	**Total primary side heat losses (no MCP), kW**	-	72 **	-	77	6.9 %	10 %
21	**Total secondary side heat losses, kW**	-	65**	-	67	3 %	10 %

* The levels are not the water levels from bottom. They are readings of transducer that do not sense the vessel lower parts. The PRZ lower part that is not sensed in level measurement is 1.89 m, whereas the SG and ACC un-sensed lower parts are 0.58 and 0.75 m, respectively.

** These data have been taken in reference I.V. Elkin, et al. "Report about PSB-VVER Heat Losses" PSB-VVER Report, PSB-04, EREC, Electrogorsk, Russia, 2003

§ The FW mass flow rate is regulated during the steady state in order to keep the SG level

§§ This datum has been assumed. The analysis of the MCP data show a large variation of heat losses due to the MCP depending upon the transient and the boundary conditions

Tab. 48 Comparison exp/calc for Cathare2 calculation

Mass flow rates and residual mass

The calculated mass flow rates in the loops are in good agreement with the experimental results. The PORV mass flow rate results put in evidence the differences between the two calculated results; this affects the primary side pressure and inventory mass; particularly it is sensible the difference between the two codes about the total mass discharged by the PORV. About the primary side mass inventory, it is relevant to note the difference at the end of the calculation related to the primary side inventory mass for the R5 and the C2 results (about 50 kg).

Rod surface temperatures

The calculated rods surface temperatures at the three levels (bottom, middle and top) and at the level where maximum temperature takes place are close the experimental results. The discrepancies are related to the timing of the temperature evolution that are anticipated in both the calculations.

Synthesis of codes results

The calculated results are both anticipated in comparison with the experimental results, especially the simulation performed with R5 code. The behavior of the PORV discharge affects the mass inventory and as a consequence the timing of the increase of core rod temperature. The calculated result for the PORV discharged mass should be improved to improve the timing of the calculations. The trend of the pressurizer level in R5 calculation and the trend of the temperature in UH for C2 calculation are other two aspects to be improved. As a global comment the calculation results, R5 and C2, are considered acceptable.

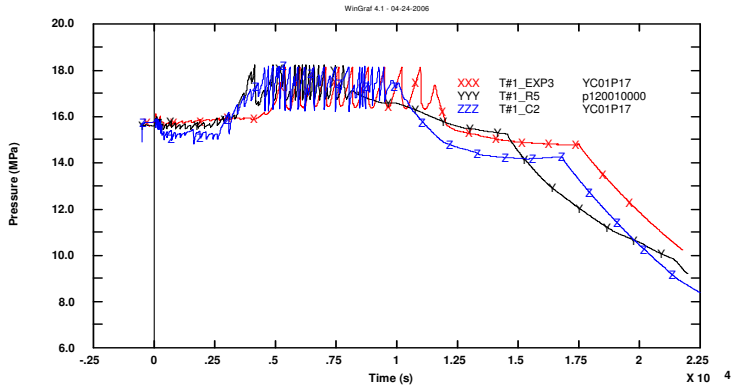

Fig. 78 PSB-VVER experiment LFW-25, Cathare2 and Relap5/Mod3.3. UP pressure (MPa) – Exp, C2.

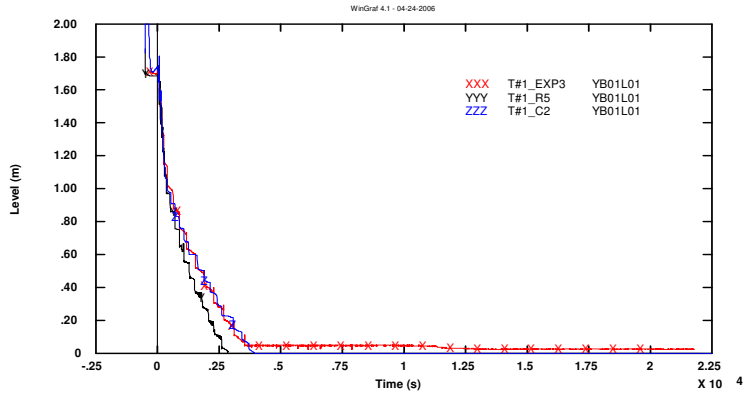

Fig. 79 PSB-VVER experiment LFW-25, Cathare2 and Relap5/Mod3.3. SG#1 level (m) – Exp, C2

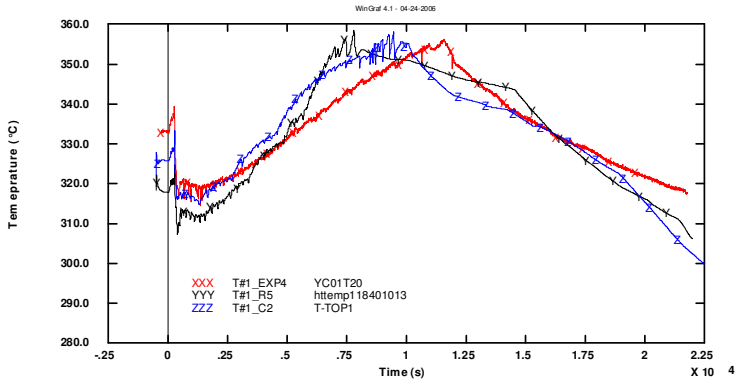

Fig. 80 PSB-VVER experiment LFW-25, Cathare2 and Relap5/Mod3.3. Maximum cladding temperature (°C) – Exp, C2.

Qualitative accuracy

The qualitative accuracy evaluation here discussed is based upon a systematic procedure consisting in the identification of phenomena and of the RTA. It essentially derives from a visual observation of the experimental and predicted trends. The following judgments are envisaged for the RTA analysis.

a) the code predicts qualitatively and quantitatively the parameter (Excellent – the calculation result is within experimental data uncertainty band);
b) the code predicts qualitatively, but not quantitatively the parameter (Reasonable – the calculation result shows only correct behavior and trends);
c) the code does not predict the parameter, but the reason is understood and predictable (Minimal – the calculation result is not within experimental data uncertainty band and sometimes does not have a correct trend);

d) the code does not predict the parameter and the reason is not understood (Unqualified - calculation result does not show correct trend and behavior, reasons are unknown and unpredictable).

		UNIT	EXP	CALC C2	Judg. C2
RTA: Pressurizer behavior					
TSE	emptying time*	s	--	--	--
	scram time	s	265.5	271	E
	heaters switched off	s	17524	16820	E
	time of first automatic PORV opening	s	5396.5	4550	M
NDP	N. of PORV automatic opening and closure	--	10	18	M
RTA: Steam generators secondary side behavior					
TSE	time of actuation of AFW/EFW	s	11569-11601	8880	M
	main steam line valve closure	s	15	24	M
	time of first automatic BRU-A opening	s	71	61	R
	SG level below 0.1 m	S	3100-3230	3420	E
SVP	difference between PS and SS pressure at 100 s	MPa	9.63	8.81	R
	SG level	m			
	- after 100 s		1.50-1.52	1.53	E
	- after 250 s		1.24-1.30	1.21	E
	- after 500 s		1.00-1.04	0.97	E
	- after 1000 s		0.75-0.77	0.75	E
	- after 2000 s		0.40-0.41	0.43	E
	- after 3000 s		0.15-0.17	0.22	E
	- end of the transient		0.00-0.02	0.00	E
	SG pressure	MPa			
	- end of the transient		0.37-5.53 5.45-0.37	0.37-5.97 5.97-0.37	E-R R-E
NDP	N. of BRU-A automatic opening and closure	--	17	28	M
RTA: Mass distribution in primary side					
TSE	time of minimum mass occurrence	s	--	9495 (#)	--
SVP	minimum primary side mass	kg	--	790	--
	loop seal differential pressure at time of minimum mass for each loop	kPa	--	36.6-35.8 35.8-36.8	--
	residual mass in primary system	kg			
	- when PS pressure/initial pressure =0.7		--	790	--
	- when PS pressure/initial pressure =0.5		--	--	--
	av. linear power at min. mass	kW/m	--	0.52	--
	minimum mass/ITF volume	kg/m3	--	603	--

(*) Empty time means PRZ level lower than 0.1m
(**) Experiment: the total height of the PRZ is 12.563m, but the maximum measured level (YP01L02) 9.975m. Relap5: the maximum calculated collapsed level in the component PRZ is 9.55m, as defined in the control variable. Catahre2: the maximum calculated collapsed level in the component is (12.563-1.89)=10.673m
(#) This value is referred to the time when the last PORV valve closure occurs

Tab. 49 PSB-VVER experiment LFW-25, Cathare2. Judgment of code calculations on the basis of RTA

#	PARAMETER	CATHARE2 (0-21700)		FFTBM weighting factor*		
		AA	WF	W_{exp}	$W_{s_{af}}$	W_{norm}
1	YC01P17 - UP pressure	0.403	0.011	1.0	1.0	1.0
2	YB01P01 - SG 1 pressure	0.787	0.008	1.0	0.6	1.1
3	YB04P01 - SG 4 pressure	0.785	0.008	1.0	0.6	1.1
4	TH01P01- ACC 1 Pressure	--	--	1.0	0.6	1.1
5	TH01L01 - ACC 1 level	--	--	0.8	0.9	0.6
6	YB01L01 - SG 1 level	0.141	0.019	0.8	0.9	0.6
7	YB04L01 - SG 4 level	0.139	0.019	0.8	0.9	0.6
8	YP01L02 - PRZ level	0.190	0.010	0.8	0.9	0.6
9	Lrm - RPV level	--	--	0.8	0.9	0.6
10	YC01DP11+12+13+14+15 - DPup	0.318	0.009	0.7	0.7	0.5
11	YC01DP07+08+09+10 - DPcore	0.133	0.010	0.7	0.7	0.5
12	YA01DP04+05 - DP loop seal #1 - descending side	0.182	0.005	0.7	0.7	0.5
13	YA02DP04+05 - DP loop seal #2 - descending side	0.149	0.005	0.7	0.7	0.5
14	YA04DP04+05 - DP loop seal #4 - descending side	0.182	0.005	0.7	0.7	0.5
15	YA01DP13 - DP SG 1 inlet and top	0.649	0.008	0.7	0.7	0.5
16	YA01DP14 - DP SG 1 inlet and top	0.294	0.005	0.7	0.7	0.5
17	YC01T20 - Heater temperature top level	0.119	0.014	0.9	1.0	1.2
18	YC01T120 - Cladding temperature lower level	0.097	0.009	0.9	1.0	1.2
19	YC01T85 - Cladding temperature middle level	0.108	0.011	0.9	1.0	1.2
20	YC01T04b - Core outlet fluid temperature	0.111	0.011	0.8	0.8	2.4
21	YC01T06- Core inlet fluid temperature	0.105	0.007	0.8	0.8	2.4
22	YC01T05 - UH coolant temperature	0.908	0.010	0.8	0.8	2.4
23	XL01F01 - Break mass flow rate	--	--	0.5	0.8	0.5
24	*Mass1 - Primary side total mass	--	--	0.8	0.9	0.9
25	*MassBr - Integral break flow rate	--	--	0.8	0.9	0.9
26	YC01N01 - Core power	0.167	0.026	0.8	0.8	0.5
27	Integral ECCS (active)	--	--	0.8	0.9	0.9
Total		0.314	0.0103	--	--	--
* These weights are used by the FFTBM to derive the Total values from the single parameter values						

Tab. 50 PSB-VVER experiment LFW-25, Cathare2. Summary of results obtained by application of FFT method for the reference calculations

The conclusions of the quantitative accuracy evaluation are as follows:

1. the achieved results are well below the acceptability threshold in relation to the overall accuracy (AA=0.314 and AA=0.291 for Cathare2 and Relap5 respectively compared with the acceptability limit of 0.4);
2. the primary pressure results are AA=0.403 (Cathare2) and AA=0.356 (Relap5). Notwithstanding the acceptability threshold is fixed to 0.1 the Cathare2 and Relap5 posttest analysis were accepted. This is because the results of the accuracy are affected mainly by the following reason:
    a. the length of the transient;

b. the frequency and the number of the PORV cycling;
c. the signal of the AM procedure on high temperature in primary coolant (350°C) that is affected by errors for several reasons such as heat losses in primary side (in particular the MCP and PRZ), heat losses in secondary side, primary to secondary heat exchange, PRZ behavior, etc...

3. In general it can be concluded that the application of the FFTBM highlights the general agreement between experimental measurements and the calculated results.
4. Finally, the discrepancy between the acceptability threshold of the FFTBM for primary pressure and the results derived by the application of the Cathare2 and Relap5 codes can be explained mainly by the imperfect knowledge of boundary conditions.

VVER-1000 Calculations

All the 12 transients of the TM have been reproduced with the Cathare2 VVER-1000 nodalization and the comparison with the experimental data registered during the execution of the experiments in the PSB-VVER facility have been executed. Hereafter the results of the calculation of the Test 1 are reported.

Test 1

Test No 1 is a simulation of a total loss of feed water accident in which the operator action aims at the SS depressurization fully opening the BRU-A valves of SG # 1 and 4, to make possible a water injection from an external source.

Fig. 81 reports the comparison between PS pressure, SG 1 and 2 pressure related to the NPP pre-test calculation, the PSB-VVER pre-test calculation and the experimental data. In all the pictures below it can be seen the PORV and the BRU-A cycling as dominant phenomena in the first part of the experiment interrupted when the operator starts the AM procedure depressurizing two SG (only the SG 1 is reported in the figure) to permit their feeding from external source. Such procedure is able to control the plant even though the experiment is terminated before the reaching of a low PS pressure condition. Nevertheless a (low) level formation in the two feeded SG is showed in *Fig. 82* in all the three sets. In the same figure the PRZ level is plotted too showing a qualitative common trend: it is completely full in the initial part of the test and after the PS cooling it starts to decrease.

It should be noted that the experimental data related to the PRZ and SG level do not take into account the distance between the sensor and the bottom of the corresponding vessel, 0.58 m for the SG and 1.89 m for the PRZ.

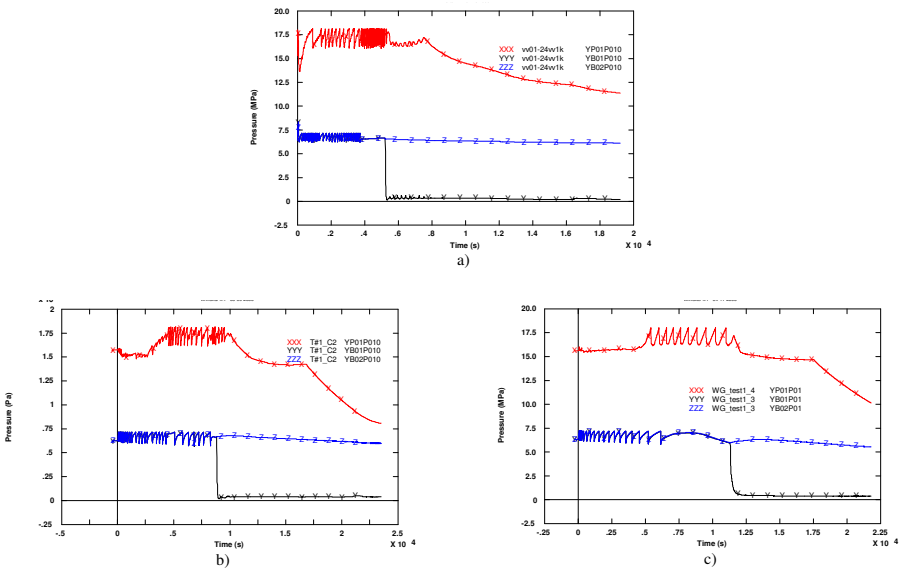

Fig. 81 Addressing the scaling issue: test 1 PS pressure, SG 1 and 2 pressure, comparison between NPP post-test C2 calculation (a), PSB-VVER post-test C2 calculation (b) and PSB-VVER experimental data (c).

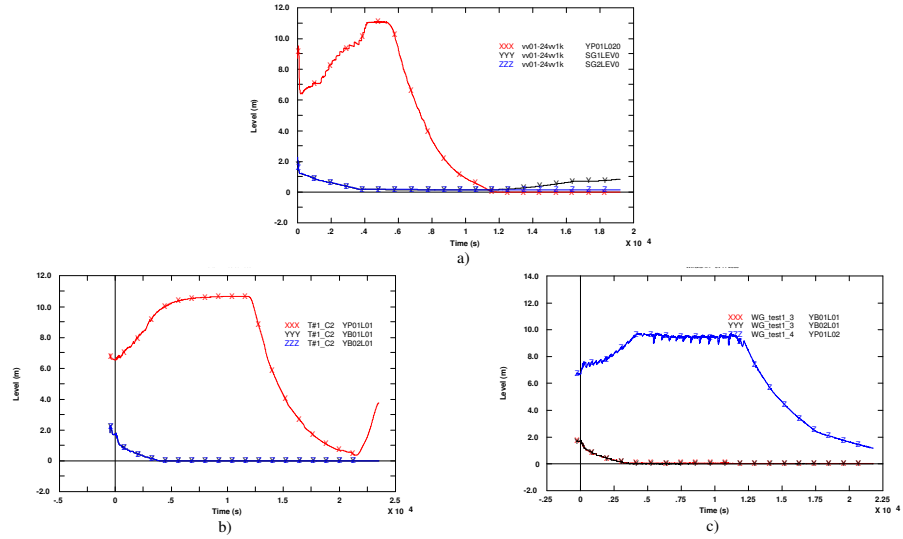

Fig. 82 Addressing the scaling issue: test 1 PRZ level, SG 1 and 2 level, comparison between NPP post-test C2 calculation (a), PSB-VVER post-test C2 calculation (b) and PSB-VVER experimental data (c).

4.2 Assessment of the Cathare2 code against Boron transport phenomena

Within the frame of the PWR safety analysis, the investigation on boron dilution events which could potentially lead to reactivity transient has been investigated intensively in the recent past. Different points (simultaneity of NC restart, minimum boron concentration at RPV inlet, mixing process in SG and RCL, size of the slugs) are relevant and can be investigated following different initiating events and different NPP configurations. Many experimental and analytical investigations have been performed by different organizations and joint international programs (OECD/CSNI EURATOM) in order to address these issues.

In the framework of the code assessment and boron dilution investigation, the present document is related to the application and the validation process of the Cathare2 code. The selected tests are 3 boron dilution experiments carried out in PKL III facility . The aims of the tests are:

- F1.2 has been specifically designed to investigate the relationship between primary coolant inventory (affecting the coolant circulation conditions) and boron concentration in the condensate at the outlet of the SG;
- E2.2 has been designed to investigate the boron distribution inside the facility during the asymmetrically injection of the HPIS and LPIS (loop1 and 2) and the following filling up of the facility;
- F1.1 has been designed to investigate the boron distribution inside the facility during the injection of the HPIS (all loops) and the following filling up of the facility.

The validation process of the code involved the performances of the code, as a system of mathematic and physical models to reproduce thermal hydraulic phenomena, but it also concerns nodalization and user qualification. The user qualification is related to code validation because the user choices affect the code response adopting nodalization solutions and selecting the several available options. The user choices include the 'tuning' of the nodalization in order to obtain a better response of the code (both in terms of results and resources for the calculation).

The purpose of this report is to document the performance of the Cathare2 code. In order to achieve this, a systematic qualitative and quantitative accuracy evaluation has been performed. The quantitative analysis has been performed adopting a method developed at DIMNP, which has capabilities in quantifying the errors in code predictions related to the measured experimental signal; the Fast Fourier Transform (FFT) is used aiming to have an integral representation of the code calculation discrepancies (i.e. error between measured and calculated time trends) in the frequency domain.

PKL III Facility

The PKL facility is full high ITF (elevations scaled 1:1), shown in *Fig. 83* that models the entire primary system and most of the secondary system (except turbine and condenser) of a 1300-MW PWR NPP. It has been used for extensive

experimental investigations on the study of the integral behavior of PWR NPP accident conditions (PKL is a German acronym for "Primary System"). Different test programs have been carried out with the PKL facility: PKL I and II test programs (1977 - 1986) focused on LBLOCA and SBLOCA and the PKL III test program (starting from 1986) addressed on the simulation of accident sequences, mainly on the BDBA and the issues related to the day-to-day operation of Siemens-built PWR.

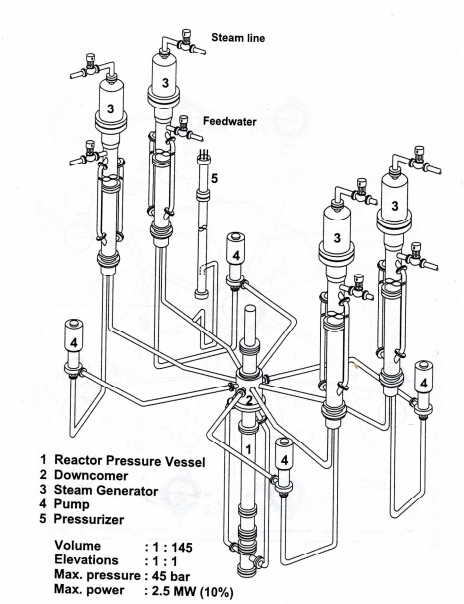

Fig. 83 PKL: general view of the facility

The PKL facility has been designed using the specific data of Philipsburg NPP unit 2, and the scaling concepts to simulate overall thermal hydraulic behavior of the full-scale power plant.
The following features can be highlighted:

- full-scale hydrostatic head;
- power, volume, and cross-sectional area scaling factor of 1:145;
- full-scale frictional pressure loss for single-phase flow;
- simulation of all four loops;
- core and SG have full-scale rod and U-tube dimensions, spacers, heat storage capacity but the numbers of rods and tubes are scaled down;
- the simulation of phenomena are priority objective compared with the consistent simulation of the geometry, (e.g., in order to account for important phenomena in the hot legs such as flow separation and countercurrent flow limitation – CCFL -, the geometry of the hot legs is based on conservation of the Froude number and was finally designed on the basis of experiments at the full scale UPTF);
- the configuration of the RPV DC, modeled as two stand pipes connected to the lower plenum and as an annulus in the upper region, allows the

frictional pressure losses preservation and a reasonable volume/surface ratio distortion;

- the operating pressure of the PKL facility is limited to 45 bar on the primary side and to 56 bar on the secondary side. This allows simulation over a wide temperature range (250°C to 50°C) that is particularly applicable to the cool-down procedures investigated.

The PKL test facility is subdivided into RCS, SG SS, the interfacing systems on the primary and secondary side and the break.
RCS comprises the vessel, the four loops (pipes, pumps and steam generators), and the pressurizer (PRZ) connected via the surge line to the loop #2.
The vessel models the following:

- ✓ the upper head plenum is a cylinder, full scale in height and 1:145 in volume. It contains the shaft of the RPV liquid level detector and in the bottom houses the top plate, the upper core support and the control rod guide assemblies.
- ✓ The upper plenum is full scale in height and scaled down in volume. The internals are simulated by means of seal-welded tube.
- ✓ The upper head bypass is modeled by four lines associated with the respective loops to enable detection of asymmetric flow phenomena in the RCS (e.g., single-loop operation).
- ✓ The reactor core model consists of 314 electrically heated fuel rods (diameter 10.75 mm and pitch 14.3 mm) and 26 control rod guide thimbles (diameter 13.6 mm). Three concentric zones can be heated independently and simulate a radially variable power profile. The maximum electrical power of the test bundle is 2512 kW distributed as follows: 504 kW in the inner zone (63 rods with 8 kW each one); 944 kW in the central zone (118 rods with 8 kW each one) and 1064 in the outer zone (133 rods with 8 kW each one). Thermocouples are located in the rod bundle for measuring the rod temperatures.
- ✓ The reflector gap is between the rod bundle vessel and the bundle wrapper (the barrel in the real plant). Following the reference plant, the flow resistance has been designed in order to have 1% of the total primary side mass flow (with MCP in operation) across the reflector gap. In this zone are also located 2 concentric 1.5 mm thick nickel sheets with the function to protect the rod bundle vessel against overheating (max allowable temperature is 300°C).
- ✓ The lower plenum contains the 314 extension tubes connected with the heated rods. The down-comer pipes are welded on the lower plenum bottom in diametrically opposite position. Two plates are located in this zone: the Fuel Assembly Bottom Fitting and the Flow Distribution Plate.
- ✓ The down-comer is modeled as an annulus in the upper region and continues as two stand pipes connected to the lower plenum. This configuration, as already mentioned above, permits symmetrical connection of the 4 CL to the RPV, preserves the frictional pressure losses and does not unacceptably distort the volume/surface ratio. The hydraulic diameter of the down-comer vessel is equal to that of the reactor down-comer. The down-comer pipes simulate the lower portion of the reactor

down-comer and the diameter is equal to the hydraulic diameter of the annular down-comer in the prototype reactor.

The facility has four loops; each one is constituted by a hot leg, a U-tube SG (primary side), a loop seal, a main circulation pump and a cold leg. The hot legs have been designed taking into account the relevance of an accurate simulation of the two phase flow phenomena, in particular CCFL, in the hot leg piping as in the reactor. For these reason the hot leg has the scaled diameter in the part flanged to the upper plenum and then a concentric increase from 80.8 mm to 154 mm upstream the connection to the SG inlet plenum. The cold legs connect the SG to the MCP through the loop seal and the MCP to the DC vessel. The hydrostatic elevations of the loop seals are 1:1 compared with the prototype NPP. The cold legs have also nozzles located between thee MCP and the DC vessel for the ECCS injection and two seats in CL 1 and 2 for the break simulation.

The PKL MCP are vertical single-stage centrifugal pumps, driven by variable-speed motors provided with anti-reverse rotation devices.

The PKL PRZ has full height and it is connected through the surge line to the hot leg #2. The electrical heaters and the water spray have been modeled in the water and steam plenum respectively.

The four SG (primary side) of the PKL Test Facility are vertical U-tube bundle heat exchangers like in the prototype NPP. The scaling factor has been preserved by reducing the number of tubes: 28 tubes with outside diameter of 22 mm and wall thickness of 1.2 mm. Seven different lengths are modeled with the shortest and the longest tubes that have the same height of the reactor SG.

The SG (secondary side) is constituted by the tube bundle zone where the interface between the RCS and secondary side occurs. Below the shortest tubes, seal welded hollow fillers allow to achieve the correct volumetric scaling of the SG secondary side. The DC model can be divided into three parts: the upper, located above the U-tube zone, is annular and contains the FW ring; the central, in the tube bundle zone, is modeled by two tubes outside of the SG housing; the lower has annular shape formed by a cylindrical shroud within the vessel. The flow distribution plate has been attached to the bottom of the shroud.

The uppermost part of the SG, the larger part of the SG vessel, models the steam plenum. The SG outlet nozzle has a restriction, like the prototype system, in order to reduce the blow-down rate in the MSLB events. Finally the moisture separator, the dryer and the perforate plate of the reactor SG have been simulated with a perforate plate, with appropriate flow resistance, located below the SG outlet nozzle. The condensate, formed in this plate, returns to the SG DC through a funnel place in the uppermost part of the SG below the perforate plate.

The main interfacing systems have been also implemented in the PKL test facility in order to simulate the corresponding system necessary for the prototype NPP operation.Finally, connections to different primary and secondary side components are envisaged for the break simulation in order to test and optimize different system operating regimens and operational procedures during the SBLOCA events. Also the SGTR events are simulated by means of pipes with isolation valves connecting the SG primary side (tube bundle) to the SG secondary side at different elevations.

In *Fig. 84* the sketch of the PKL III facility is shown.

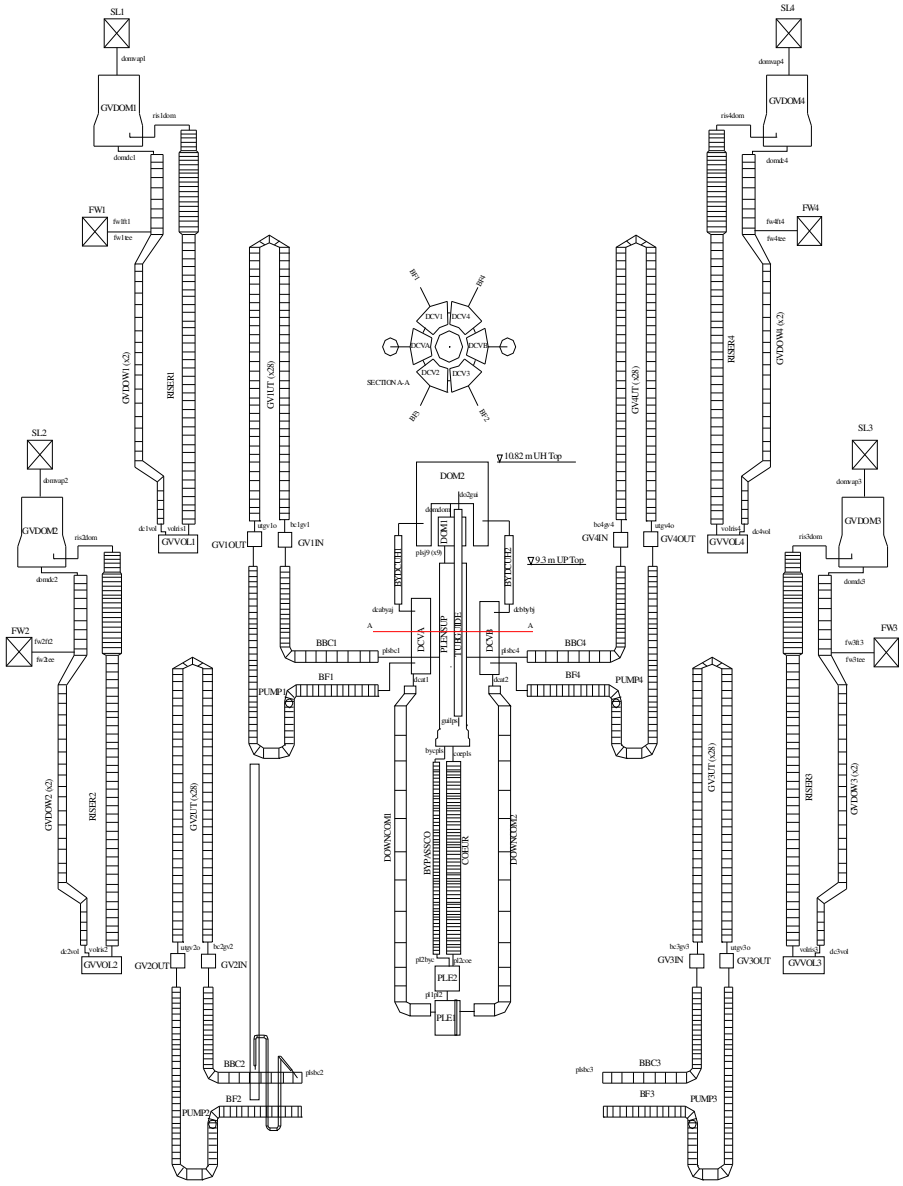

Fig. 84 Sketch of Cathare2 of PKL III facility input deck: all system

#	Parameter	Unit	Design Value
1	Delivery	[m3/h]	120
2	Total delivery head	[m]	90
3	NPSH reqd.	[m]	3
4	Design pressure	[bar gauge]	50
5	Design temperature:	[°C]	250
6	Operating pressure	[bar gauge]	45
7	Speed	[rpm]	2950
8	Required drive power	[kW]	42
9	Motor rating	[kW]	55
10	Nominal speed	[rpm]	2950
11	Min. speed	[rpm]	60

Tab. 51 PKL MCP data

Symbol	Interfacing System	P/S	System/Main components	Features	Functions	Note
KBA	Volume Control System	P	- Volume control tank - HP charging pump - Recuperative heat exchanger - Cooler - 5 valves	V = 1.5 m^3 T = 50 °C P = 1 bar G = 0.41 kg/s H = 560 m W = 275 kW W = 275 kW D = 15 mm	Compensating for changes in the volume in the RCS on the PRZ level signal Auxiliary spray injection in PRZ with MCP switched off and supporting the normal spray operation for the purpose of coolant pressure limitation	
JN(A)	Residual Heat Removal System:	P	- 1 RHR pump - 1 RHR heat exchanger - 2 valves	G = 9.66 kg/s H = 75 m W = 1500 kW D = 80 mm	Decay heat removal from the core and stored heat removal during shutdown and cool-down to 50 °C Post LOCA residual heat removal from the core	4 trains with suction line in HL and injection line in CL
JND	Emergency Core Cooling System:	P	High Pressure Safety Injection System: - 1 Safety Injection pump - 1 Borated water storage tank - 8 valves	G = 1.72 kg/s H = 500 m V = 10 m^3 T = 30-80 °C P = 1 bar D = 15 mm	Inject emergency coolant into the core when the primary pressure is < 45 bar	4 trains connected to each HL and CL in the suction line and injection nozzle of the RHRS
JNG			Accumulator Injection System (8 systems)	P = 50 bar Gas Nitrogen	Inject automatically emergency coolant when the primary pressure is < 26 bar	8 systems connected to each CL and HL
JNA			Low Pressure Safety Injection System: - 1 LP pump - 1 Borated water storage tank - 8 valves	G = 9.66 kg/s H = 94 m V = 10 m^3 T = 30-80 °C P = 1 bar D = 25 mm	Inject emergency coolant into the core when the primary pressure is < 10 bar	4 trains connected to each HL and CL in the suction line and injection nozzle of the RHRS
-	PRZ Control System	P	Operational spray		To reduce the PRZ pressure during operation	Connected to CL 2 - 3
-			2 Auxiliary spray from VCS		To reduce the PRZ pressure during the MCP breakdown or after the MCP shutdown	HP pump connected to the VCS
-			PRZ relief valve			
LBA	Main Steam Piping System	S	MS isolation valve			
			MS isolation valve			
			MS safety valve			
			MS relief control valve		50 or 100 K/h cool-down procedure	
			MS warm-up control valve			
LAB	Feed-Water System	S	- 1 FW pump - 1 FW tank	G = 7.1 kg/s H = 890 m V = 20 m^3 P = 9 bar		
LAR	Emergency Feed-Water System	S	- 1 EFW pump - 1 EFW tank	G = 2.1 kg/s H = 890 m V = 10 m^3 P = 1 bar	FW malfunctions 100 K/h cool-down procedure during LOCA	
LCQ	Steam Generator Blowdown System	S			It is manly a line connecting two SG on the water side	
P Primary Side Interfacing Systems S Secondary Side Interfacing Systems						

Tab. 52 Interfacing systems

The transients: Test F1.2, Test E2.2, Test F1.1

Test F1.2

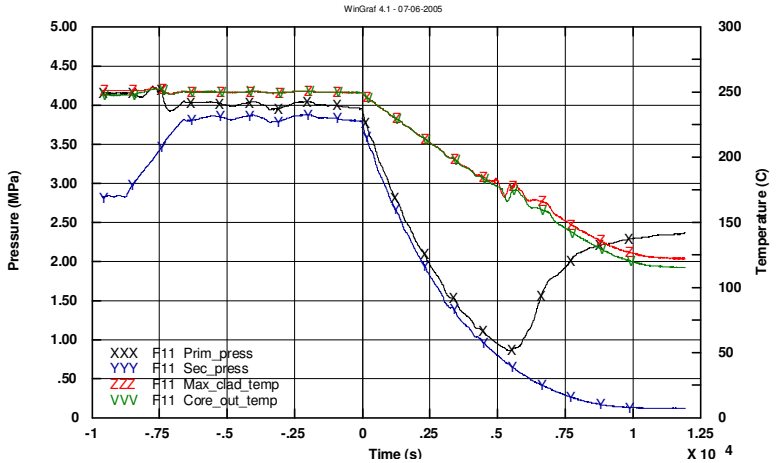

Fig. 86 PKL III experiment F1.1: measured trends of primary pressure, secondary side pressure, maximum rod surface temperature and core outlet fluid temperature

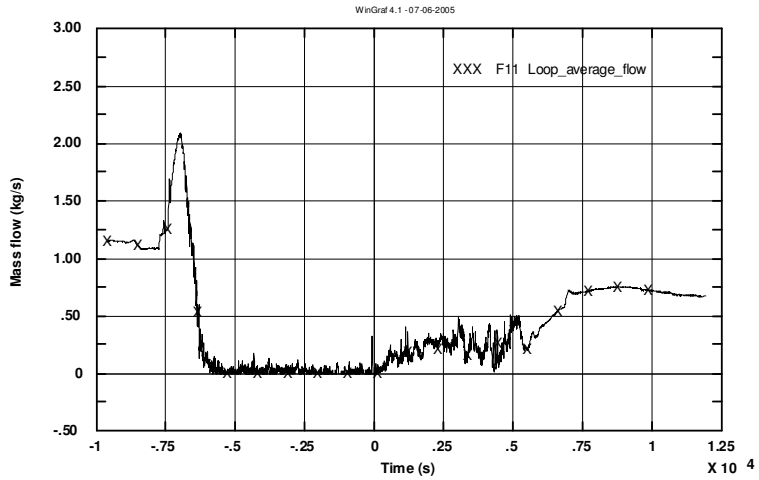

Fig. 85 PKL III experiment F1.1: measured trends of loop average mass flow rate and mass inventory (this data is not available in the preliminary data issued)

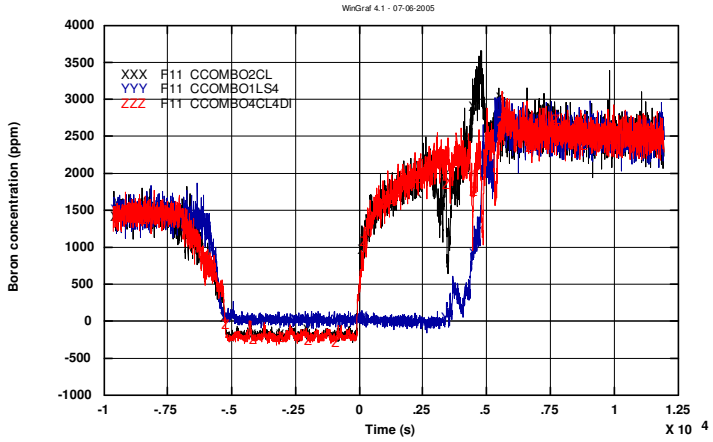

Fig. 87 PKL III experiment F1.1: measured trends of boron concentration in loop seal #1 and cold leg #2 and #4

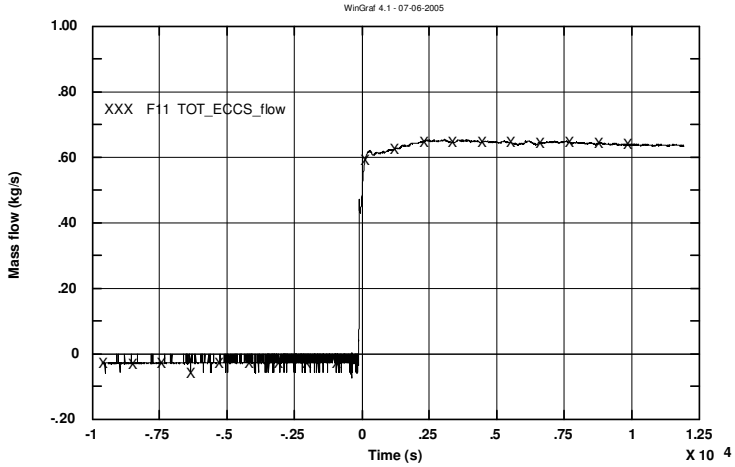

Fig. 88 PKL III experiment F1.1: measured trends of ECCS total mass flow rate

The performed test investigates the boron dilution distribution in condition of reduced mass inventory (e.g. SB-LOCA event). From *Fig. 86* to *Fig. 88* have been presented the main parameter trends that characterize the experiment. The boron dilution takes place when conditions for reflux-condenser phenomenon are established in the plant. This phenomenon produces de-borated water plug in the primary circuit namely in the loop seals.

The test OECD-PKL F1.1 has been designed to investigate the boron distribution in the facility during the symmetric ECCS injection (HPIS) and the following filling up of the facility.

The main relevant aspect of the test is constituted by boron distribution in the facility during the transition between the reflux condenser to natural circulation conditions particularly paying attention to the low borated slug of water accumulated in the loop seals.

For sake of completeness the results carried out in the experiments F1.1 have been reported in the NCFM, *Fig. 89* shows that the results are coherent and consistent with the limits established, based on calculated transients in ITF.

Boundary conditions are reported in the *Tab. 53*. The initial conditions of the test are summarized in the *Tab. 54*.

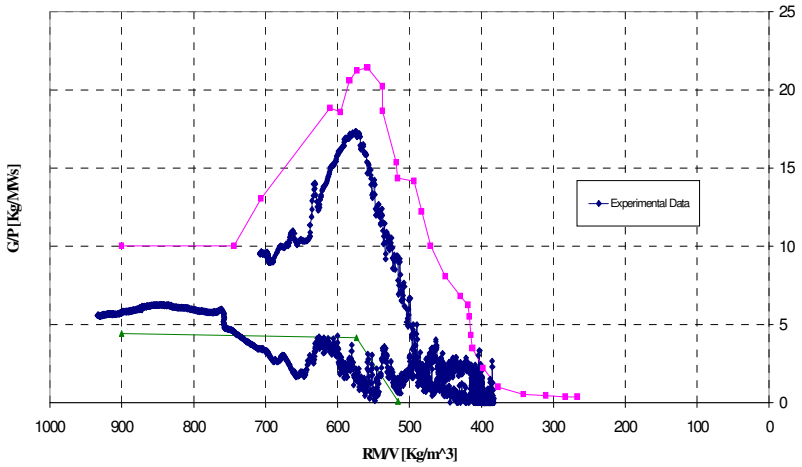

Fig. 89 PKL III experiment F1.1: natural circulation maps

#	System/component	Characteristics	Definition/value
1	SBLOCA event	-	Simulation is from reflux condenser conditions occurrence in the facility
2	Break in CL 1 between MCP and RPV	21 cm^2 (equivalent)	
3	Cool-down of all SG	56 K/h	
4	HPIS available	-	Only 1 out 2 pumps are actuated Injection symmetrically in all CL Boron concentration 2500 ppm
5	LPIS and Accumulators not available	-	
6	Heat losses	RPV upper head 1 kW PRZ heaters 3 kW PRZ additional heaters 3kW RCP1 cooling 4.5 kW RCP2 cooling 5.5 kW RCP3cooling 3.9 kW RCP4cooling 4.6 kW SG 1-4 bypass 15 kW	
7	Butterfly valve	Closed	Simulation of MCP hydraulic resistance

Tab. 53 PKL III experiment F11: boundary conditions

#	Conditions	Value	Note
1	U-Tubes filled with steam		reflux condenser conditions
2	Coolant inventory	1280 kg (57%)	
3	Boron concentration	< 50 ppm in LS and DC > 4000 ppm in core	
4	Core power (decay heat)	482 kW	1.48% +86kW for heat losses
5	Primary side pressure	39 bar	
6	Coolant temperature a t core outlet	249 °C	
7	Sub-cooling at core inlet	0. °C	
8	Pressurizer fluid temperature	249 °C	
9	Pressurizer level	0.9 m	
10	Flow rate in loops	-	No circulation in all the loops RCP stopped
11	Main steam pressure in SG secondary side	37.3 bar	
12	Main steam temperature in SG secondary side	246 °C	
13	Collapsed level in SG secondary side	12.2 m	
14	Feedwater temperature	110-120 °C	

Tab. 54 PKL III experiment F11: initial conditions

#	Phase	Duration of the phase	Note
1	Conditioning Phase	-6925.0 – 0.0	Conditioning phase to reach reflux condenser condition
2	Start of the test	0.0	Opening of the break, HPIS injection, core power reduction
3	Boron concentration change in loop seal	0.0 – 3600.0	
4	Filling up of loops	3600.0 – 5000.	
5	Natural circulation establishment	5000. – 12000.0	12000.0s is the end of test

Tab. 55 PKL III experiment F11: phenomenological analysis

The test can be considered subdivided in main phases as listed in *Tab. 55* and are hereafter described.

It should be noticed that the available data from the experiment are in the preliminary form and not all the relevant data are included in the available documentation (i.e. primary side mass and break flow rate). Some of the parameter time trends are in a raft format making difficult the correct interpretation. Some other data are not clearly identified (the reported measures of the instruments are sometime not clear). The interpretation of the test results must be considered as preliminary and it is not possible to clarify all the phenomena for the same reasons. As a consequence the following analysis of the experimental tests results is mainly a description of the event recorded during the test

Analysis of post-test calculation results: test F1.2 (nodalization qualification)

This section has been reported the standard procedure to obtain a "qualified nodalization" foreseen in the UNIPI methodology. Three main calculation types, performed with Cathare2 code, can be distinguished:

a) steady state results (500 s),;
b) reference calculation results, (including the evaluation of the RTA and the application of the FFTBM procedure) ;

Qualification of the nodalization at steady state level

#	QUANTITY	UNIT	DESIGN	Cathare	ERROR	ACCEPTABLE ERROR
1	Primary circuit volume	m^3	3.282	3.254	0.8%	1 %
2	Secondary circuit volume	m^3	5.824	5.5275	5 %	2 %
3	Non-active structures heat transfer area (overall)	m^2	-	-	-	10 %
4	Active structures heat transfer area (overall)					
4-1	Core heat transfer surface (active)	m^2	41.7421	41.7421	0%	0.1 %
4.2	SG UT heat transfer surface (active)	m^2	143.175	143.175	0%	0.1 %
5	Non-active structures heat transfer volume (overall)	m^3	-	-	-	14 %
6	Active structures heat transfer volume (overall)	m^3	-	-	-	0.2 %
7	Volume vs. height curve (i.e. "local" primary and secondary circuit volume)	-			-	10 %
8	Component relative elevation	m			-	0.01 m
9	Axial and radial power distribution (°°)	-	-	-	-	1 %
10	Flow area of components like valves, pumps orifices	m^2	-	-	-	1 %
11	Generic flow area	m^2	-	-	-	10 %
(*)						
12	Primary circuit power balance					
12-1	Core thermal power	MWth	0.6	0.6	0%	2 %
13	Secondary circuit power balance	MWth	-	-	-	2 %
14	Absolute pressure (PRZ, SG, ACC)					
14-1	Primary pressure	bar	12.0	12.1	0.8 %	0.1 %
14-2	SG exit pressure	bar	5.9	5.89	0.1 %	0.1 %
15	Fluid temperature (**)					
15-1	Core inlet temperature	°C	158	158.5	0.3 %	0.5 %
15-2	Core outlet temperature	°C	184	185	0.5 %	0.5 %
15-3	SG feed–water temperature	°C	120	120	0 %	0.5 %
16	Rod surface temperature	°C	181	186	5K	10 K
17	Pump velocity	-	-	-	-	1 %
18	Heat losses (^^^)	kW	~ 70	~ 65	~ 7%	10 %
19	Local pressure drops	bar				10 % (^)
20	Mass inventory in primary circuit	Kg	2500	2557	0.4 %	2 % (^^)
21	Mass inventory in secondary circuit	Kg	-	-	-	5 % (^^)
22	Flow rates (PS and SS)					
22-1	PS total loop coolant flow rate	Kg/s	4.8	4.7	2 %	2 %
22-2	SG feed–water mass flow rate	Kg/s	0.05	0.05	0 %	2 %
22						
23	Bypass mass flow rates					
23-1	Core bypass flow rate (UH–DC) (+)	%	0.5	0.5	0.0 %	10 %
24	Pressurizer level (collapsed)	m	1.3	1.95	0.65	0.05 m
25	Secondary side or downcomer level	m	-	-		0.1 m (^^)

$$\frac{|\text{reference or measured value} - \text{calculated value}|}{|\text{reference or measured value}|}$$

(°) The % error is defined as the ratio
The "dimensional error" is the numerator of the above expression
(°°) Additional consideration needed
(*) With reference to each of the quantities below, following a one hundred s "transient-steady-state" calculation, the solution must be stable with an inherent drift < 1% / 100 s.
(**) And consistent with power error
(^) Of the difference between maximum and minimum pressure in the loop.
(^^) And consistent with other errors.
(^^^) The heat losses calculated by the code are affected by oscillation due to the SG secondary side behavior. This is a middle value
(+) This is a design data of the PKL III facility

Tab. 56 PKL III experiment F12, Cathare2: comparison between measured and calculated relevant initial and boundary conditions

A nodalization representing an actual system (ITF or NPP) can be considered qualified when:

- ✓ it has a geometrical fidelity with the involved system;
- ✓ it reproduces the measured nominal steady state conditions of the system;
- ✓ it shows a satisfactory behavior in time dependent condition.

As concerns the steady state acceptability criteria have been verified. In particular the comparison between the calculated and the measured volume vs. height curve and the distribution of the pressure drops along the length (for different values of the mass flow) are reported (*Fig. 92*).
Other results related to the TH parameters are shown in *Tab. 58* where are reported the steady state conditions carried out after 500 seconds with Cathare2 code.

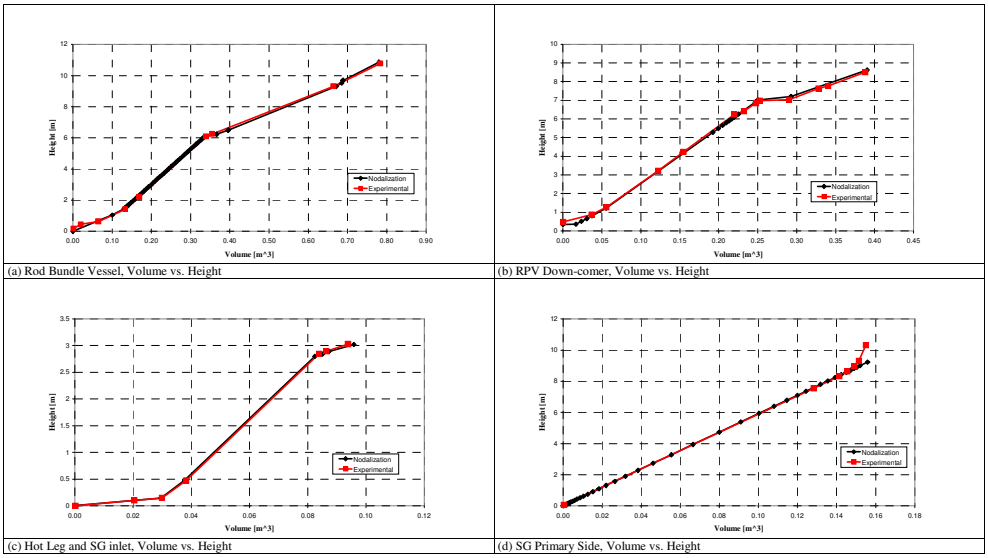

(a) Rod Bundle Vessel, Volume vs. Height

(b) RPV Down-comer, Volume vs. Height

(c) Hot Leg and SG inlet, Volume vs. Height

(d) SG Primary Side, Volume vs. Height

Fig. 90. PKL III facility nodalization qualification (part 1 of 4). Comparison between the calculated and the measured volume vs. height curves

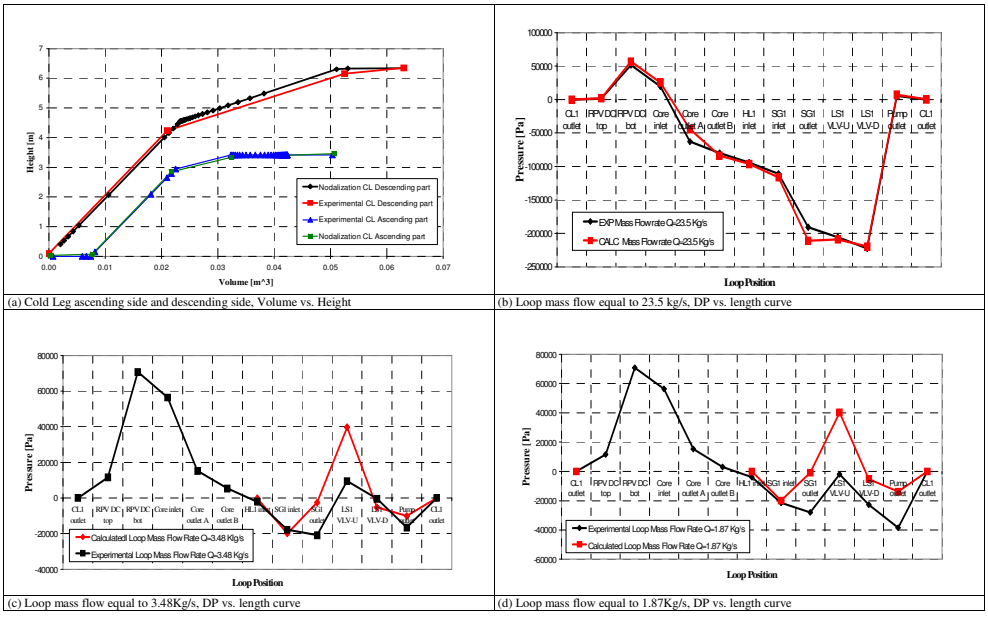

(a) Cold Leg ascending side and descending side, Volume vs. Height

(b) Loop mass flow equal to 23.5 kg/s, DP vs. length curve

(c) Loop mass flow equal to 3.48Kg/s, DP vs. length curve

(d) Loop mass flow equal to 1.87Kg/s, DP vs. length curve

Fig. 91 PKL III facility nodalization qualification (part 2 of 4). Comparison between the calculated and the measured: (a) volume vs. height curves; (b, c, and d) DP vs. length curve

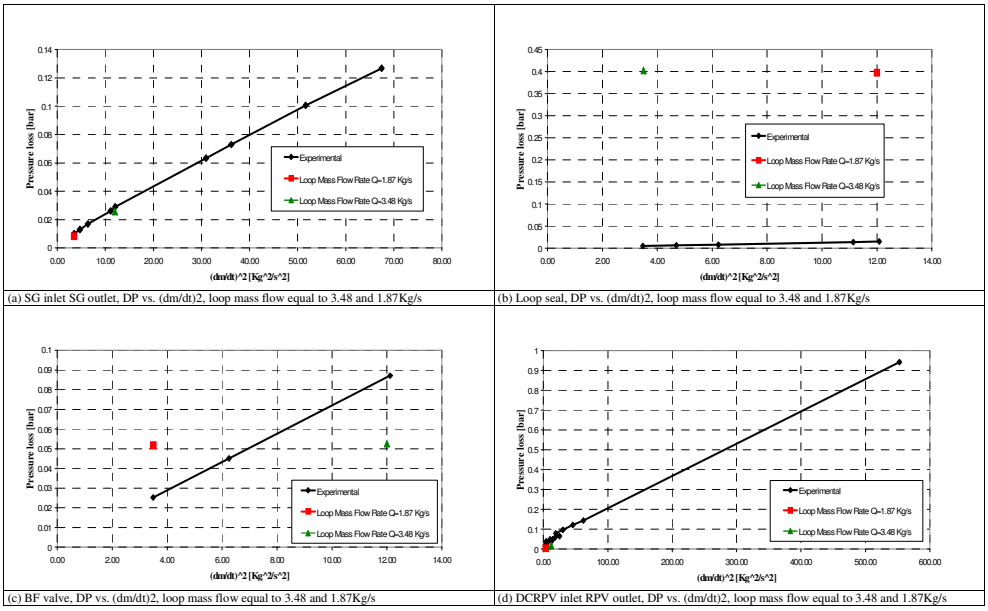

(a) SG inlet SG outlet, DP vs. (dm/dt)2, loop mass flow equal to 3.48 and 1.87Kg/s

(b) Loop seal, DP vs. (dm/dt)2, loop mass flow equal to 3.48 and 1.87Kg/s

(c) BF valve, DP vs. (dm/dt)2, loop mass flow equal to 3.48 and 1.87Kg/s

(d) DCRPV inlet RPV outlet, DP vs. (dm/dt)2, loop mass flow equal to 3.48 and 1.87Kg/s

Fig. 92 PKL III facility nodalization qualification (part 3 of 4). Comparison between the calculated and the measured DP vs. (dm/dt)2

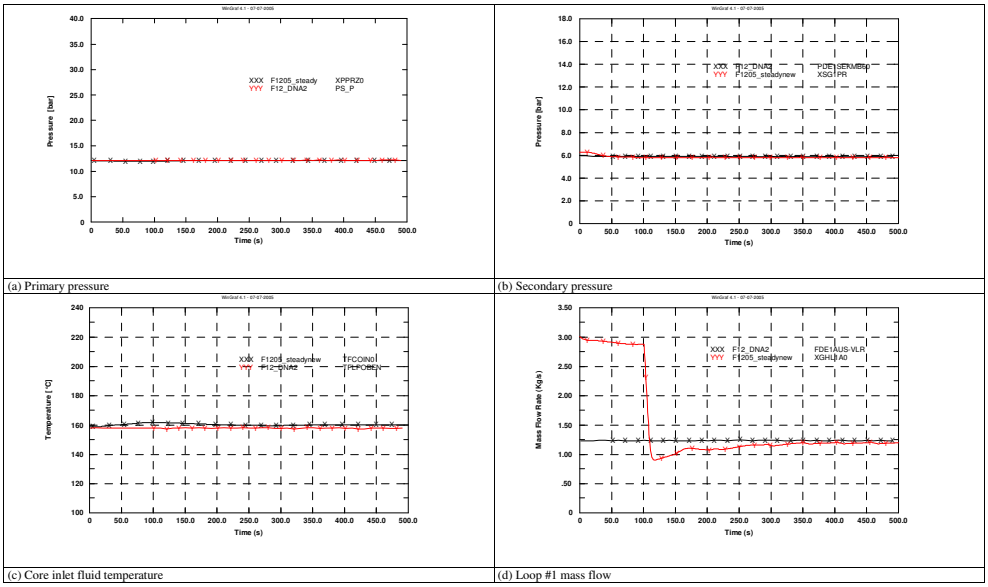

(a) Primary pressure

(b) Secondary pressure

(c) Core inlet fluid temperature

(d) Loop #1 mass flow

Fig. 93 PKL III facility nodalization qualification (part 4 of 4). Comparison between the calculated and the measured parameters during steady state

Nodalization qualification at "on transient" level

A comprehensive comparison between measured and calculated trends or values was performed, including the following steps:

a) comparison between experimental and calculated time trends on the basis of the selected variables;
b) comparison between values of quantities characterizing the sequence of resulting events and the qualitative evaluation of calculation accuracy on the basis of the Relevant Thermal-hydraulic Aspects (RTA, also used for code uncertainty derivation);
c) quantitative evaluation of calculation accuracy, utilizing the FFT based method *Tab. 57*.

From a phenomenology point of view the code results are in agreement with the experiment results. The main phenomena occurring in the test are predicted. The discrepancy about the pressurized level does not affect the evolution of the transient (*Fig. 94* to *Fig. 96*): the conditioning phase, the increase of the mass flow rate due to the occurrence of the two phases mass flow condition is reproduced in the calculation, but calculated value is larger; the boron concentration time trend is quite well reproduced in the period of two phases flow and reflux condensation when drainage is performed. The boron concentration in the refilling phase is qualitatively comparable with the experiment results, but calculated results show some discrepancies (*Fig. 94*).

The post test analysis of the test F1.2 can be summarized as following:

1. the code show generally good behavior with regard to the single phase natural circulation, the two phase natural circulation (qualitatively) and the reflux condensation mode;
2. the range of the mass inventory for the single phase natural circulation, the two phase natural circulation and the reflux condensation has been predicted properly;
3. the different maximum mass flow rate observed during the two phase flow has been highlighted and it confirms the post test analyses already performed in other facilities;
4. the calculation tends to result in a simultaneous restart of natural circulation in the individual loops and it is in contrast with the experiment in which a delay in loop #3 has been detected;
5. the differential pressure between inlet and outlet chambers of the steam generators have been discussed and the more negative prediction of the code has been related to the larger amount of liquid in the descending side of the U-tubes than in the experiment. This may be also caused by the same factors already mentioned in item 3, in particular the interfacial drag;
6. discrepancies between the code prediction and the experimental measurement have been discussed also considering the evolution of local boron concentration in particular during the refilling phase. They may be related to the above mentioned (item 4) problems in reproducing the natural circulation but also to the implemented boron transport model.

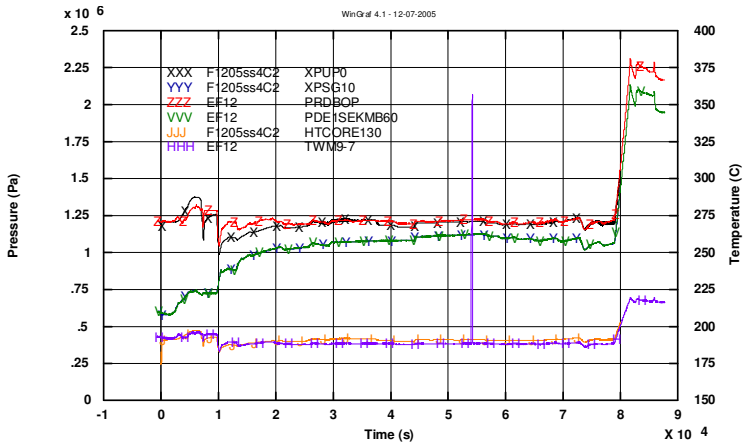

Fig. 94 PKL III experiment F1.2, primary and secondary pressure and maximum cladding temperature

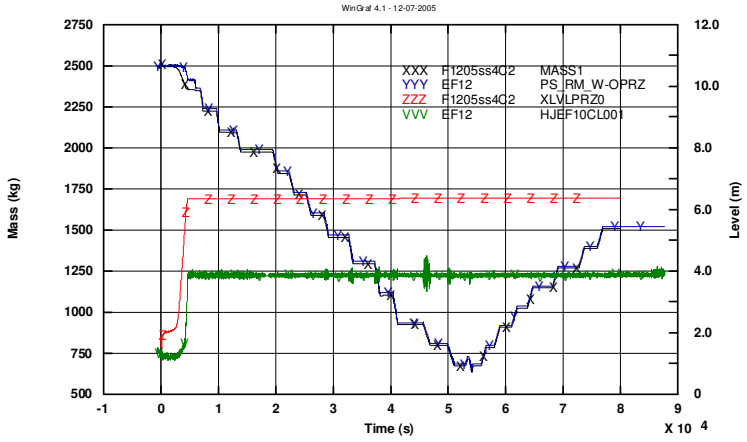

Fig. 95 PKL III experiment E2.2, Cathare2: primary mass, and PRZ level

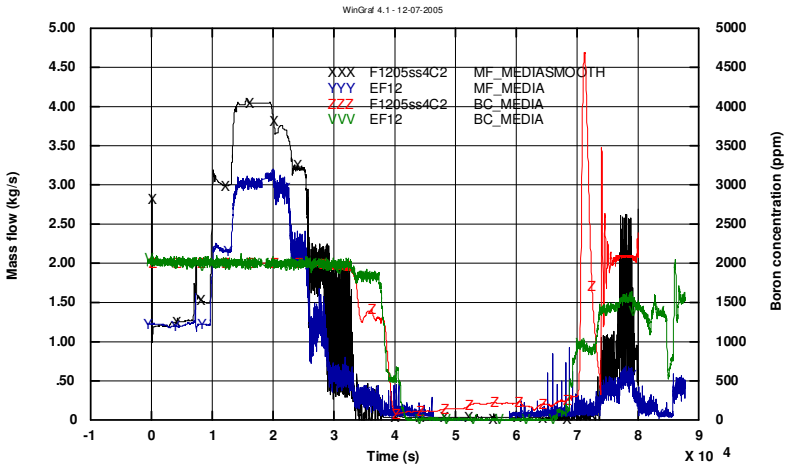

Fig. 96 PKL III experiment E2.2, Cathare2: media of the mass flow rate and boron concentration in loops

#	PARAMETER	AA	WF
1	**UP pressure**	**0.2175**	**0.003**
2	**SG 1 pressure - secondary side**	**1.0000**	**0.009**
3	**Core inlet fluid temperature**	**0.5155**	**0.005**
4	**Core outlet fluid temperature**	**0.1096**	**0.003**
5	**Upper head fluid temperature**	**0.2458**	**0.005**
6	Integral break flow rate	n.c.	n.c.
7	**SG DC bottom fluid temperature**	**0.0868**	**0.008**
8	Break flow rate	n.c.	n.c.
9	ECCS integral flow rate	n.c.	n.c.
10	Heater rod temp. (bottom level)	n.c.	n.c.
11	**Heater rod temp. (middle level)**	**0.1179**	**0.007**
12	**Heater rod temp. (high level)**	**0.3567**	**0.008**
13	**Primary side mass**	**0.0387**	**0.004**
14	Core level	**0.3257**	**0.009**
15	SG DC level	**0.7556**	**0.004**
16	**PRZ level**	**0.5914**	**0.009**
17	Loop seal 1 ascending side level	**0.6022**	**0.005**
18	Loop seal 1 descending side level	**0.0576**	**0.007**
19	**Core power**	**0.7556**	**0.004**
20	**Boron concentration in loop seal #1**	**1.2583**	**.004**
21	**Boron concentration in loop seal #2**	**1.3314**	**.004**
22	**Boron concentration in loop seal #3**	**1.4246**	**.003**
23	**Boron concentration in loop seal #4**	**1.4252**	**.004**
24	Boron concentration core inlet	**1.2583**	**.004**
Average calculation results w/wo boron related parameters		**0.403/0.312**	**0.005/0.005**

Tab. 57 PKL III experiment F1.2, Cathare2: summary of results obtained by application of FFT method for the reference calculation

#	PHASE	TIME (s)	AAp
1	Conditioning up to draining	0 – 30000	0.236
2	Boron dilution (draining period)	30000 – 45000	0.077
3	Loop refilling	45000 – 75000	0.086
4	Overall transient	0 – 75000	0.217

Tab. 58 PKL III experiment F1.2, Cathare2: summary of results obtained by application of FFT method for the reference calculation

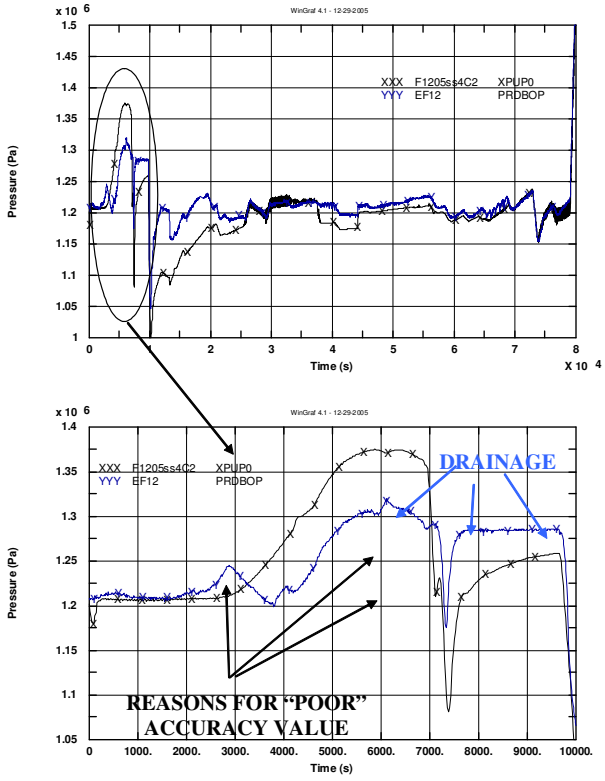

Fig. 97 PKL III experiment F1.2, Cathare2: FFT application

Test E2.2

The test is constituted by the filling up phase by injection of HPIS and LPIS during a SBLOCA event. The test start from the time when reflux condenser conditions occurs up to natural circulation is established. HPIS and LPIS injection occurs asymmetrically (loop 1 and 2)
The initial conditions of the test are summarized in the are reported in the *Tab. 60*.
The test can be subdivided in main phases and sub phases as listed in *Tab. 63* and are hereafter described.

#	System/component	Characteristics	Definition/value
1	SBLOCA event	-	Simulation is from reflux condenser conditions occurrence in the facility
2	Break in CL 1 between MCP and RPV	32 cm^2 (equivalent)	
3	Cool-down of all SG	100 K/h	
4	HPIS	-	Only 1 out 2 pumps are actuated Injection in CL 1 and 2 Boron concentration 2200 ppm
5	LPIS	-	Only 1 out 2 pumps are actuated Injection in CL 1 and 2 Boron concentration 2200 ppm Injection when primary pressure < 10 bar
6	Accumulators not available		
7	Heat losses	RPV upper head 1 kW PRZ heaters 4 kW PRZ additional heaters 3kW RCP1 cooling 4.6 kW RCP2 cooling 4.6 kW RCP3cooling 4.6 kW RCP4cooling 4.6 kW SG 1-4 bypass 15.8 kW	
8	Butterfly valve	Closed	Simulation of MCP hydraulic resistance

Tab. 59 PKL III experiment E22: system configuration

#	Conditions	Value	Note
1	U-Tubes filled with steam		reflux condenser conditions
2	Coolant inventory	1440 kg (64%)	40 kg in PRZ
3	Boron concentration	< 50 ppm in LS > 4000 ppm in core outlet <1000 ppm in SG inlet	
4	Core power (decay heat)	530 kW	1.8% +60kW for heat losses
5	Primary side pressure	40.5 bar	
6	Coolant temperature a t core outlet	251 °C	
7	Subcooling at core inlet	0. °C	
8	Pressurizer fluid temperature	251 °C	
9	Pressurizer level	1.1 m	
10	Flow rate in loops	-	No circulation in all the loops RCP stopped
11	Break flow rate	1.1 kg/s	At time 0.s
11	Main steam pressure in SG secondary side	39.0 bar	
12	Main steam temperature in SG secondary side	249 °C	
13	Collapsed level in SG secondary side	12.2 m	
14	Feedwater temperature	110-120 °C	

Tab. 60 PKL III experiment E22: initial conditions

#	Phase	Sub-Phase	Note
1	Conditioning phase	Secondary-side pressure build-up	
2		Establishing reflux-condenser conditions	
3		Condensate build-up	
4		Transition to start of test	
5	Test execution	Start of the Test	
6		Draining and Refill Process	
7		Onset of Natural Circulation in the Unfed Loop 4	
8		Onset of Natural Circulation in the Unfed Loop 3	
9		Refill in the Fed Loops1 and 2	
10		Onset of Natural Circulation in the Fed Loops	
11	Test end	-	

Tab. 61 PKL III experiment E22: phenomenological analysis

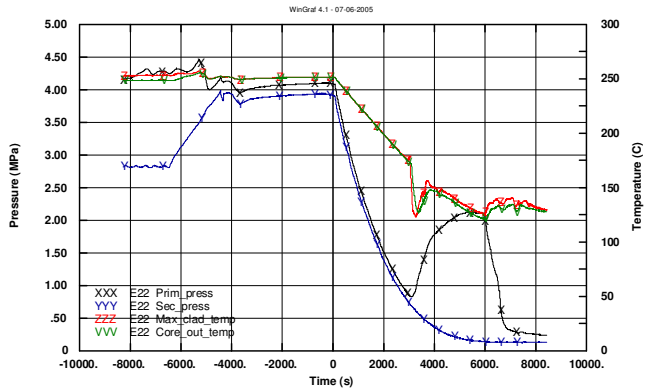

Fig. 98 PKL III experiment E2.2: measured trends of primary pressure, secondary side pressure, maximum rod surface temperature and core outlet fluid temperature

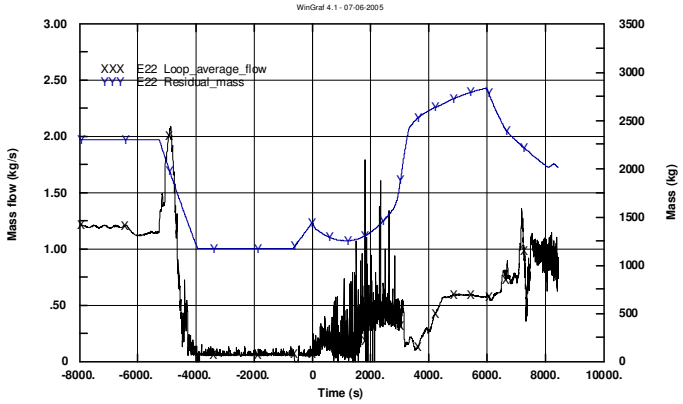

Fig. 99 PKL III experiment E2.2: measured trends of loop average mass flow rate and mass inventory

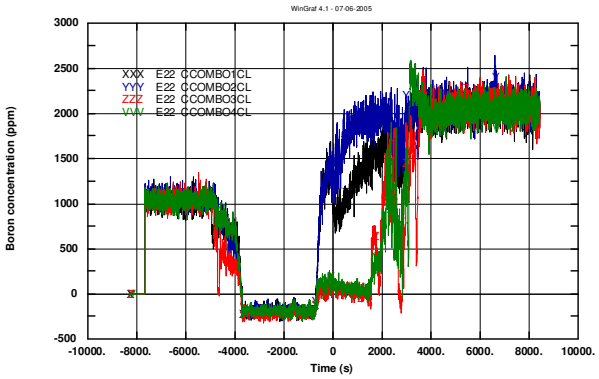

Fig. 100 PKL III experiment E2.2: measured trends of boron concentration in cold leg 1 to 4

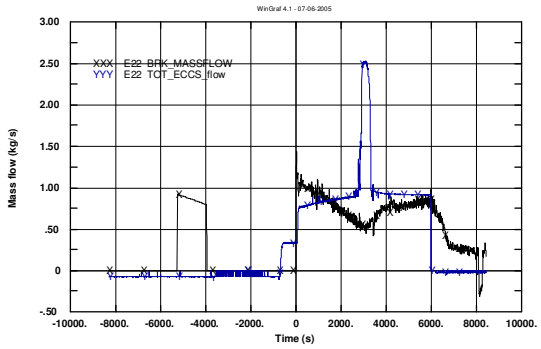

Fig. 101 PKL III experiment E2.2: measured trends of break and ECCS total mass flow rate

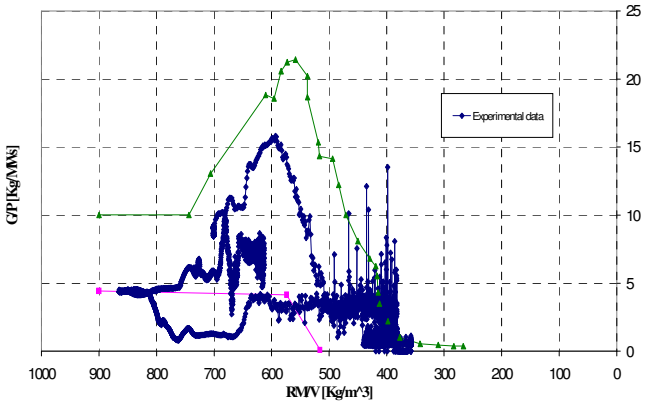

Fig. 102 PKL III experiment E2.2: natural circulation maps

The pictures from *Fig. 103* to *Fig. 105*in the following show the comparison exp/calc for some variables registered during the experiment and calculated by the Cathare2 code

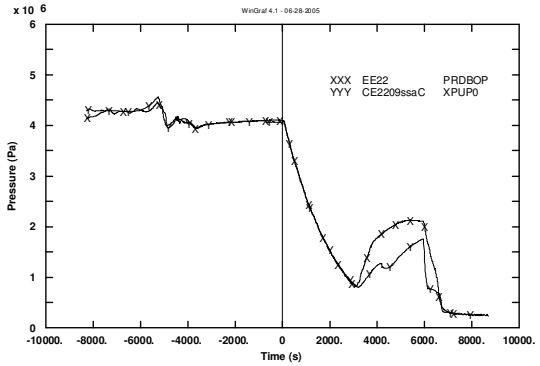

Fig. 103 PKL III experiment E2.2, Cathare2V2.5rev6.1: UP pressure

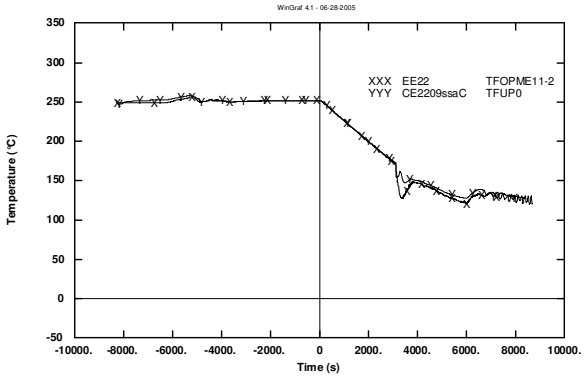

Fig. 104 PKL III experiment E2.2, Cathare2: UP pressure – conditioning phase

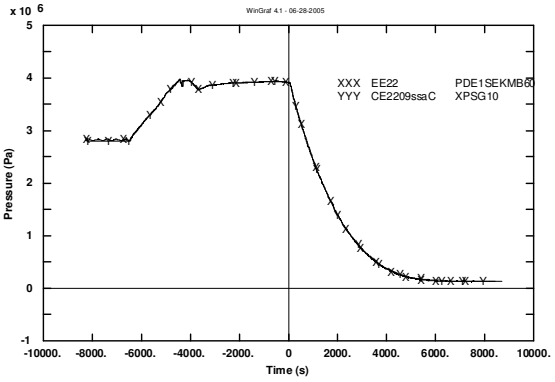

Fig. 105 PKL III experiment E2.2, Cathare2: SG 1 pressure

Here after the *Tab. 62* summarizes the results of the application of the FFTBM to the results of the calculation for the E2.2 transients. As can be observed, the values resulting from the comparison exp/calc, are in the limits of acceptability foreseen by the methodology.

#	PARAMETER	AA	WF
1	**UP pressure**	**.10**	**.005**
2	**SG 1 pressure - secondary side**	**.01**	**.023**
3	**Core inlet fluid temperature**	**.30**	**.014**
4	**Core outlet fluid temperature**	**.10**	**.010**
5	**Upper head fluid temperature**	**.48**	**.010**
6	**Integral break flow rate**	**.18**	**.015**
7	**SG DC bottom fluid temperature**	**.09**	**.014**
8	**Break flow rate**	**.77**	**.015**
9	**ECCS integral flow rate**	**.002**	**.014**
10	Heater rod temp. (bottom level)	n.c.	n.c.
11	**Heater rod temp. (middle level)**	**.20**	**.010**
12	**Heater rod temp. (high level)**	**.15**	**.012**
13	**Primary side mass**	**.91**	**.002**
14	**Core level**	**.39**	**.030**
15	**SG DC level**	**.42**	**.028**
16	**PRZ level**	**1.01**	**.013**
17	**Loop seal 1 ascending side level**	**.66**	**.045**
18	**Loop seal 1 descending side level**	**.58**	**.033**
19	**Core power**	**.03**	**.032**
20	**DP inlet-outlet SG 2 (IL)**	**1.64**	**.026**
21	**Boron concentration in loop seal #1**	**.76**	**.034**
22	**Boron concentration in loop seal #2**	**.81**	**.032**
23	**Boron concentration in loop seal #3**	**.88**	**.025**
24	**Boron concentration in loop seal #4**	**.80**	**.028**
25	Boron concentration core inlet	n.c.	n.c.
Average calculation results w/wo boron related parameters		**0.38/0.31**	**0.017/0.015**

Tab. 62 .PKL III experiment E2.2, Cathare2: summary of results obtained by application of FFT method for the reference calculation

Test F1.1

The performed test investigates the boron dilution distribution in condition of reduced mass inventory (e.g. SB-LOCA event). From *Fig. 106* to Fig. *108* have been presented the main parameter trends that characterize the experiment. The boron dilution takes place when conditions for reflux-condenser phenomenon are established in the plant. This phenomenon produces de-borated water plug in the primary circuit namely in the loop seals.
The test OECD-PKL F1.1 has been designed to investigate the boron distribution inside the facility during the ECCS injection and the following filling up of the facility.
The main relevant aspect of the test is constituted by boron distribution in the facility during the transition between the reflux condenser conditions to natural circulation conditions particularly paying attention to the low borated slug of water accumulated in the Loop seals.

#	System/component	Characteristics	Definition/value
1	SBLOCA event	-	Simulation is from reflux condenser conditions occurrence in the facility
2	Break in CL 1 between MCP and RPV	21 cm^2 (equivalent)	
3	Cool-down of all SG	56 K/h	
4	HPIS available	-	Only 1 out 2 pumps are actuated Injection symmetrically in all CL Boron concentration 2500 ppm
5	LPIS and Accumulators not available	-	
6	Heat losses	RPV upper head 1 kW PRZ heaters 3 kW PRZ additional heaters 3kW RCP1 cooling 4.5 kW RCP2 cooling 5.5 kW RCP3cooling 3.9 kW RCP4cooling 4.6 kW SG 1-4 bypass 15 kW	
7	Butterfly valve	Closed	Simulation of MCP hydraulic resistance

Tab. 63 PKL III experiment F11: boundary conditions

#	Phase	Duration of the phase	Note
1	Conditioning Phase	-6925.0 – 0.0	Conditioning phase to reach reflux condenser condition
2	Start of the test	0.0	Opening of the break, Hpis injection, core power reduction
3	Boron concentration change in loop seal	0.0 – 3600.0	
4	Filling up of loops	3600.0 – 5000.	
5	Natural circulation establishment	5000. – 12000.0	12000.0s is the end of test

Tab. 64 PKL III experiment F11: phenomenological analysis

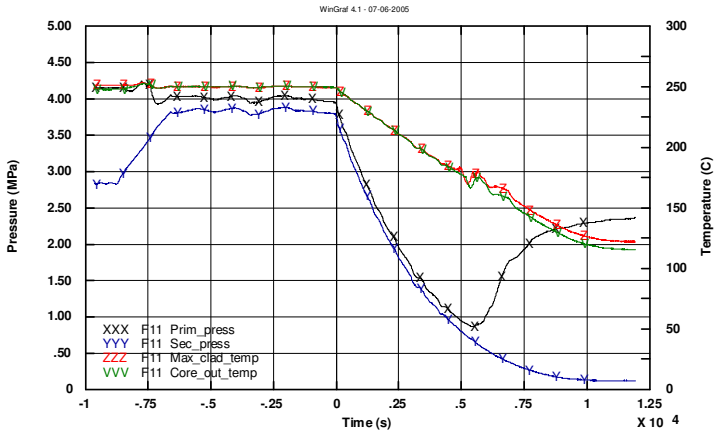

Fig. 106 PKL III experiment F1.1: measured trends of primary pressure, secondary side pressure, maximum rod surface temperature and core outlet fluid temperature

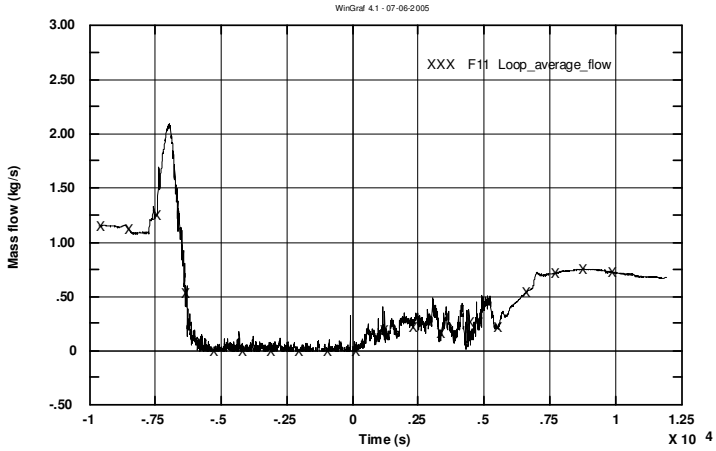

Fig. 107 PKL III experiment F1.1: measured trends of loop average mass flow rate and mass inventory (this data is not available in the preliminary data issued).

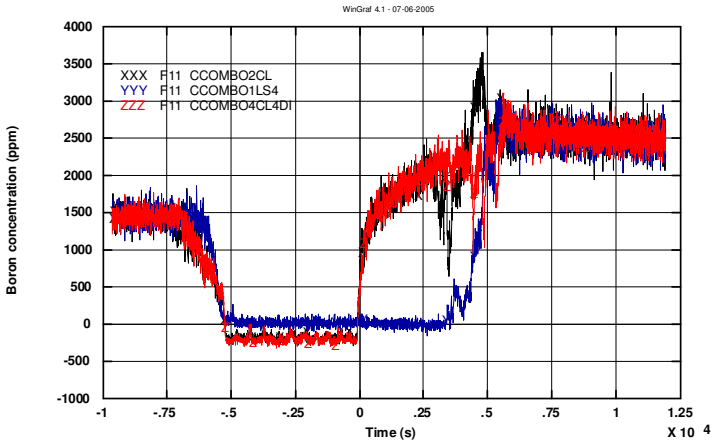

Fig. 108 PKL III experiment F1.1: measured trends of boron concentration in loop seal #1 and cold leg #2 and #4

The pictures in the following show the comparison exp/calc for some variables registered during the experiment and calculated by the Cathare2 code.

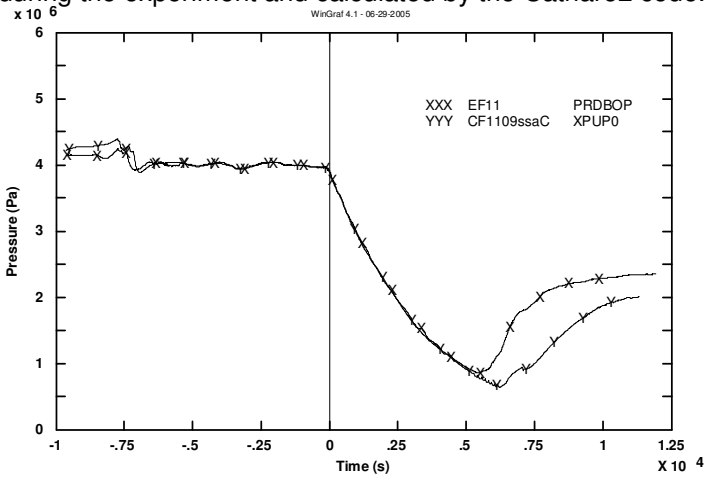

Fig. 109 PKL III experiment F1.1, Cathare2: UP pressure

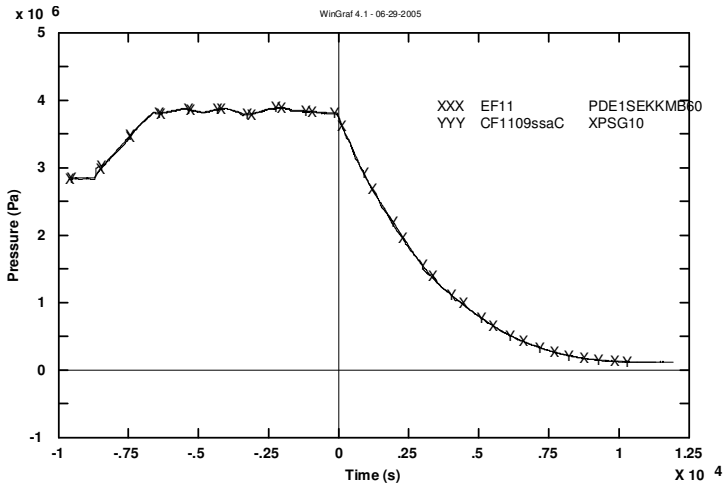

Fig. 110 .PKL III experiment F1.1, Cathare2: SG 1 pressure

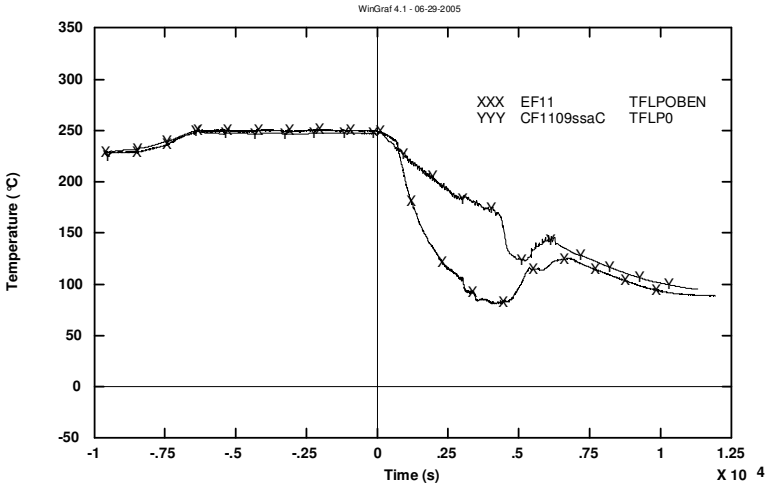

Fig. 111 PKL III experiment F1.1, Cathare2: core inlet fluid temperature

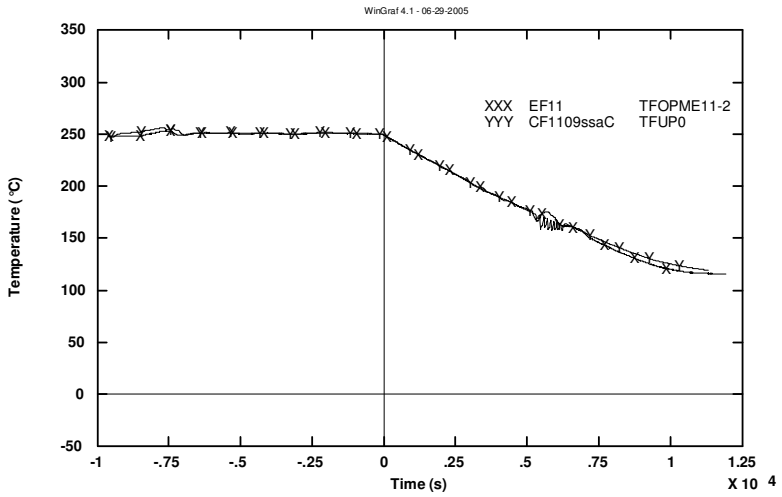

Fig. 112 PKL III experiment F1.1, Cathare2: core outlet coolant temperature

Here after the *Tab. 65* summarizes the results of the application of the FFTBM to the results of the calculation for the F1.1 transients. As can be observed, the values resulting from the comparison exp/calc, are in the limits of acceptability foreseen by the methodology.

#	PARAMETER	AA	WF
1	**UP pressure**	**.09**	**.008**
2	**SG 1 pressure - secondary side**	**.02**	**.013**
3	**Core inlet fluid temperature**	**.26**	**.006**
4	**Core outlet fluid temperature**	**.07**	**.009**
5	**Upper head fluid temperature**	**.43**	**.010**
6	Integral break flow rate ^	n.c.	n.c.
7	**SG DC bottom fluid temperature**	**.08**	**.013**
8	Break flow rate	n.c.	n.c.
9	**ECCS integral flow rate**	**.001**	**.002**
10	Heater rod temp. (bottom level)	n.c.	n.c.
11	**Heater rod temp. (middle level)**	**.21**	**.009**
12	**Heater rod temp. (high level)**	**.10**	**.013**
13	Primary side mass	n.c.	n.c.
14	**Core level**	**.42**	**.015**
15	**SG DC level**	**.29**	**.023**
16	**PRZ level**	**.46**	**.009**
17	**Loop seal 1 ascending side level**	**.62**	**.025**
18	**Loop seal 1 descending side level**	**.55**	**.015**
19	**Core power**	**.04**	**.020**
20	**DP inlet-outlet SG 2 (IL)**	**1.79**	**.019**
21	**Boron concentration in loop seal #1**	**.95**	**.024**
22	**Boron concentration in loop seal #2**	**.97**	**.024**
23	**Boron concentration in loop seal #3**	**.89**	**.025**
24	Boron concentration in loop seal #4	n.c.	n.c.
25	Boron concentration core inlet	n.c.	n.c.
Average calculation results w/wo boron related parameters		**0.34/0.25**	**0.012/0.011**

Tab. 65 PKL III experiment F1.1, Cathare2: summary of results obtained by application of FFT method for the reference calculation

Io this paragraph, few examples of the application of the methodology developed at DIMNP in the framework of the two contracts TACIS and EDF have been shown.
With regard to the TACIS contract, the Cathare2 nodalization of the PSB-VVER facility has been developed and qualified. The 12 tests foreseen in the test matrix have been simulated and the comparison of the calculations results with the experimental data registered during the experiment performed in the PSB-VVER facility has shown that all the requirements foreseen by the methodology developed at DIMNP are fulfilled from a qualitative and quantitative point of view.
Moreover, the Cathare2 nodalization of the Balakovo unit 3 reference VVER1000 NPP has been realized and qualified. The 12 tests of the test matrix have been executed with the Cathare2 NPP nodalization. The results of the calculations performed with the Cathare2 nodalization of the VVER1000 have shown that all the phenomena observed in the experiments executed in the PSB-VVER facility are observed in the calculations, so that, the VVER1000 Cathare2 nodalization and the Cathare2 code are simulate the reference NPP behaviour and is qualified with regard to the requirement of the UNIPI methodology.
For the EDF contract, the PKL III facility Cathare2 nodalization has been developed and qualified with the experimental data coming from the F1.2 experiment executed in the PKL III facility. Three experimental data sets for the experiments F1.2, E2.2, F1.1 available have been used for the comparison with the results coming from the execution of the calculations with the Cathare2 nodalization. The results of the application of the UNIPI methodology have shown that all the requirements foreseen in the methodology are fulfilled.
At the end it is possible to state that the Cathare2 is qualified respect to the requirement of the methodology developed at DIMNP.

CONCLUSIONS

Thermal hydraulic system codes play an important role for the safety of the nuclear power plants. The assessment of the uncertainty of the results of TH-SYS codes is one of the key aspects of nuclear technology.

This is the framework in which the work described in the present thesis is placed. The revision of the methodology developed in the years at Department of Mechanical Nuclear and Production Engineering of the University of Pisa regarding the assessment of the results of the BE codes is the main objective of the present thesis.

The procedure above is called: Uncertainty Methodology based on Accuracy Evaluation (UMAE).

The Cathare2 code, developed at the CEA in France, has been considered as reference code among other codes in the support applications of the presented analyses.

The work starts with a preliminary analysis of the needs of the Nuclear Technology and in particular, focuses the attention on the relevance of the system thermal hydraulic code.

The code development covers a key role because it involves code-developers, the independent assessment process performed in the common practice by group of users different from the developers and the experimental data used for the comparison with the code results and a robust and systematic procedure for the use of the code. In the present work: the UMAE based method.

The UMAE provides a path for the code user assessment and the code user qualification. It is relevant to note that one of the results of this thesis represents the qualification of the Cathare2 code following the requirements foreseen in the UMAE. This thesis is to be considered among the work performed by the external code users for the assessment.

The second relevant point analyzed in the thesis, strictly connected to the previous one, is the nodalization set up. The system code requires as input the geometrical and thermal hydraulic data concerning the studied system collected in the nodalization. The difficulty to simulate a real three dimensional systems with a one-dimensional model, the difficulty to simulate part of the system, the translation of the data about the BIC to be implemented are evidenced and discussed as some of the possible source of error. Assuming a qualified code and a qualified user, it is necessary to define a qualification procedure for the nodalization. In addition the quality and the correctness of the data used for the nodalization realization is stressed. The quality of the data used for the nodalization realization, in general for all the data coming from the experiment performed in the facilities (ITF, SEF) is of fundamental relevance. QA programs have to be followed during the experiments execution and for the data collections.

Once the nodalization is realized, a control activity has to be performed in order to check the geometrical fidelity between the model and the system studied. As a way to perform the correct simulation of the volume versus height curve is outlined. Another control involves the verification if all the significant thermal-hydraulic parameters necessary to identify the plant status are correctly selected and evaluated. The steady state conditions are related to the plant conditions before the accident or transient occurrence and generally correspond to the nominal conditions of the plant. The steady state level check is completed with the verification of the capacity of the nodalization to reproduce the pressure drop curve measured in the experiment.

The next step is the qualification of the nodalization “on transient” dealing with the verification if the nodalization is able to reproduce the main time dependent data registered in the experiment. The comparison is made from a qualitative but even quantitative point of view.

The role of the user on the code results is relevant because he is involved in every phase from the nodalization realization, the selection of the data, and the choice of the computer used for the execution of the calculations. The user effects can be defined as: any differences in calculations that use the same code version and the same specifications (e.g., initial and boundary conditions) for a given plant or facility.

The “user effect” can be reduced, following the indication coming from the IAEA guidelines thanks to the adoption of user training and qualification programs. The aim of the training is to give to the user a systematic approach for a best use of the BE code capabilities. Regarding the computer and compiler effect, the dependence of the result from the machine can be reduced adopting an adequate code validation method and a correct and structured programming strategy.

The basis and the main features of the procedure for qualification of the results of the BE codes developed at University of Pisa (UMAE based method) have been presented. The flexibility of the method and its possible use for different scopes have been highlighted. Namely, among the steps of the method, different paths can be followed for the qualification of the facility nodalization, the qualification of the NPP nodalization, the code-user qualification. One of the main objectives of the UMAE method is the possibility to derive the uncertainty from the accuracy.

The FFTBM for quantifying the accuracy between calculated and experimental measured data is also presented. The need of such tool comes from the possibility to have a rigorous method for the quantitative accuracy evaluation of the code results independent from the judgment of the user.

A relevant role in the UMAE is covered by the “Scaling Issue”. The impossibility to perform experiment at full scale of the NPP lead to the unavoidable use of the TH codes and ITF The ITF normally designed to preserve geometrical similarity with the reference reactor system are used to investigate, by direct simulation, the behavior of a NPP in case of off-normal or accident conditions. Three main objectives can be associated to the scaling analysis: the design of a test facility, the

code validation, i.e. the demonstration that the code accuracy is scale independent, the extrapolation of experimental data (obtained into an ITF) to predict the NPP behavior.

In the UMAE methodology the scaling issue has a relevant role because the uncertainty related to the NPP code prediction is extrapolated from the database built considering Integral Test Facility (ITF) calculations accuracy. This aspect represents the connection between the scaling issue and the code uncertainty evaluation, a needed step within the Best Estimate (BE) approach. The scaling approach proposed by University of Pisa is substantiated by the use of experimental data and by the results of supporting analyses.

As highlighted, the quality of data used during the nodalization realization referring to the studied system has a primary role. Sometimes the data are incorrect or missing because of errors of the experimentalist or because a certain parameter could not be measured. In order to provide to the user a tool able to calculate the pressure drop along the circuit of the studied system (facility of NPP), the use of a CFD code for the calculation of missing or uncertain data as been suggested as an improvement of the methodology. An application of the proposed tool has been described. The Ansys-CFX has been used for the calculation of the pressure drop coefficients distribution in the four CLs of the PSB-VVER facility and the implementation of these calculated coefficients in an already qualified Cathare2 nodalization of the facility. The results of the calculations for one selected transient (test 11 of the PSB-VVER test matrix) obtained with the new pressure drop coefficients calculate with Ansys-CFX and the results obtained with the already qualified nodalization have been compared with the experimental one. A better accuracy has been observed for the results with the nodalization updated with the new pressure drop coefficients and the obtained improvement quantified by the application of FFTBM.

Furthermore, another activity inside this thesis has been the investigation by mean of Ansys-CFX code of the main geometric and thermalhydraulic parameters affecting the energy loss coefficient K. In order to reach this goal a simple geometry has been taken into account, the injection region between the CL and the DC of the Lobi facility. The tube fitting radius at the intersection CL-DC, the fluid velocity and direction, the turbulence model, the mesh etc. have been varied and their effect on the calculated value of K have been observed. The results of the analysis have shown that the tube fitting radius is the main parameter influencing the K value. For this analysis, the Best Practice Guidelines for the use of the CFD code have been taken into account, even if, not all the requirements have been considered as for example the convergence of the results with the mesh size. But this deep investigation is out of the scope of the present thesis and can constitute an interesting follow up with the additional comparison with experimental data.

Finally, the results of the application of the UMAE based method in the assessment of the Cathare2 code for the set up of an AM procedures suitable in case of Station Black Out with Loss of OFF Site Power transient in VVER-1000 NPP and the assessment of the Cathare2 code for the evaluation of Boron transport phenomena in PWR reactors primary loop in accident conditions, have been shown. In both the

two mentioned activities, the results of the Cathare2 code calculations have been performed fulfilling all the requirements of the methodology developed at UNIPI.

BIBLIOGRAPHY

1. IAEA “Accident Analysis for Nuclear Power Plants” Safety Report Series No.23 IAEA, Vienna, November 2002.
2. M. Bonuccelli, F. D’’Auria, N. Debrecin, and G. M. Galassi “A Methodology for the Qualification of Thermalhydraulic Codes Nodalizations” Proc. 5th Int. Mtg. Nuclear Reactor Thermal Hydraulics, NURETH-5, Grenoble, France, October 5-8, 1993.
3. F. D’Auria, O. Melikhov, V. Melikhov, I. Elkin, A. Suslov, M. Bykov A. Del Nevo, D. Araneo, N. Muellner, M. Cherubini, W. Giannotti; “Accident management in VVER-1000 technology” Industrie grafiche Pacini Editore – Pisa ISBN 88-902189-1-6. (Final Report Tacis project R2.03/97 in form of a textbook).
4. European Utility Requirements for LWR Nuclear Power Plants, Volume 1 & 2, Rev. C, April 2001 – Volume 4 revision B (March 2000).
5. OECD NEA/CSNI/R(98)22, “Good Practices for User Effect Reduction”, 27th January 1999 Satus Report.
6. S.N. Aksan, F. D’Auria, H. Staedtke, “User Effect on the Transient System Codes Calculations”, OECD/CSNI Report, NEA/CSNI/R(94)35, Paris, 1995.
7. E. O. Brigham “The Fast Fourier Transform” Prentice Hall, Englewood Cliffs (NJ), 1974.
8. R. Bovalini, F. D’Auria, M. Leonardi “Qualification of the Fast Fourier Transform based methodology for the quantification of thermal-hydraulic system code accuracy” University of Pisa, DCMN NT 194(92), Pisa (I), 1992.
9. F. D’Auria, “Proposal for Training of Thermal-hydraulic System Code Users”, Presented at IAEA Specialist Meeting on User Qualification for and User Effect on Accident Analysis for Nuclear Power Plants, IAEA Vienna, 31 August - 2 September, 1998.
10. R. Ashley, M. El-Shanawany, F. Eltawila, F. D’Auria, “Good Practices for User Effect Reduction”, OECD/CSNI Report, OCDE/R(98) 22 Paris, 1998.
11. F. D’Auria, M. Leonardi, R. Pochard “Methodology for the evaluation of thermahydraulic codes accuracy” Int. Conf. on 'New Trends in Nuclear System Thermohydraulics', Pisa (I), May 30 - June 2, 1994.
12. D’Auria, G.M. Galassi, “Code Validation and Uncertainties in System Thermalhydraulics”, J. Progress in Nuclear Engineering, Vol 31 1/2, pp 175-216, 1998.
13. S.N. Aksan, F. D’Auria, H. Glaeser, R. Pochard, C. Richards, A. Sjoberg, “Separate Effects Test Matrix for Thermalhydraulic Code Validation: Phenomena characterisation and selection of facilities and tests”, OECD/CSNI Report OCDE/GD(94) 82, Paris, 1993.
14. F. D’Auria, G.M. Galassi, P. Gatta “Scaling in nuclear system thermal hydraulics: a way to utilise the available database” ASME - 32nd National Heat Transfer Conference, vol. 350, pp. 35-, Baltimore (Md) - US 1997.
15. R. Bovalini, F. D’Auria, A. De Varti, P. Maugeri, M. Mazzini “Analysis of counterpart tests performed in boiling water reactor experimental simulators” Nuclear Technology Vol. 97 January 1992.

16. F. D'Auria, W.Giannotti "Development of code with capability of Internal Assessment of Uncertainty" Journal Nuclear Technology, 131, 1, 159 2000.
17. F. D'Auria, N. Debrecin, G.M. Galassi, "Outline of the Uncertainty Methodology based on Accuracy Extrapolation", J. Nuclear Technology, Vol. 109 No. 1, 1995, pages 21-38.
18. Francesco D'Auria, Dino Araneo, Anis Bousbia Salah, Nikolaus Muellner: *Safety of Nuclear Power Plants*; Bulatom conference 6-8 June 2007 Varna, Bulgaria.
19. A. Petruzzi, F. D'Auria, W. Giannotti, K. Ivanov, "Methodology of Internal Assessment of Uncertainty and Extension to Neutron-Kinetics/Thermal-Hydraulics Coupled Codes", Nuclear Science and Engineering, 149, 1-26, 2005.
20. F. D'Auria, G.M. Galassi, P. Vigni, A. Calastri "Scaling of natural circulation in PWR systems" Nuclear Engineering and Design, Volume 132, 1991, Pages 187-205.
21. Dino Araneo, Alessandro Del Nevo, Francesco D'Auria, Giorgio Galassi: Addressing the scaling issue with Cathare2 simulation of VVER1000 transient scenario Nureth11 "11th International Topical Meeting on Nuclear Reactor Thermal Hydraulic", Avignone, France, 2-6 Ottobre 2005.
22. R. Bovalini, F. D'Auria "Scaling of the accuracy of the Relap5/mod2 code" Nuclear Engineering and Design, Volume 139, Issue 2 , February 1993, Pages 187-203.
23. A. Spadoni, A. Del Nevo, D. Araneo, F.Moretti, , F. D'Auria: Assessment of TH Codes Against Boron Transport Phenomenon at System Level; Proceedings of the 6th International Conference on Nuclear Option in Countries with Small and Medium Electricity Grids Dubrovnik, Croatia, 21-25 May 2006.
24. "Use of the natural circulation flow map for natural circulation systems evaluation," Marco Cherubini, Walter Giannotti, Dino Araneo and Francesco D' Auria. Science and Technology of Nuclear Installations November 2007.
25. Dino Araneo, Alessandro Del Nevo, Francesco D'Auria, Giorgio Galassi: Scaling of small break LOCA in VVER1000 system International Conference New Energy for New Europe 2005, Bled, Slovenia September 5-8, 2005.
26. D. Araneo, G. Galassi, W. Giannotti Cathare2v1.5b and Relap5/Mod3.3 Post Test Analyses and Accuracy Quantification of PSB Test 3, WD A 2.2.-PTA/4, Pisa, 30 November 2005.
27. D. Araneo: Post-Test Analysis of the 12 PSB VVER Test Scenarios with the Nodalization of Balakovo 3 VVER 1000 NPP Set-up for CATHARE2 V1.5B/MOD5.1 Code; WD Pisa, 30 Gennaio 2006.
28. N. Muellner, D. Araneo Cathare2v1.5b and Relap5/Mod3.3 Post Test Analyses and Accuracy Quantification of PSB Test 12, WD A 2.2.-PTA/2, Pisa, 16 September 2005.
29. D. Araneo, N. Muellner Cathare2v1.5b and Relap5/Mod3.3 Post Test Analyses and Accuracy Quantification of PSB Test 11, Pisa, 16 September 2005.

30. D. Araneo: Nodalization of Balakovo 3 VVER 1000 NPP For The Cathare2 V1.5b/Mod5.1 Code: Qualification Report; WD A 2.2.1-PTA/2 Pisa, 15 November 2005.
31. Terms Of Reference “Safety Analysis Report of Kozloduy NPP Units 5 and 6 Review and Assessment in Compliance with International Requirements, PHARE PROJECT: 2004/016-815.01.02 - Delivered By European Commission.
32. NEA/CSNI/R(2007)5 Best Practice Guidelines for the use of CFD in Nuclear Reactor Safety Applications 15-May-2007.
33. ECORA: “CFD Best Practice Guidelines for CFD Code Validation for Reactor-Safety Applications” EC 5th Euratom FP 1998-2002.
34. Ansys-CFX v.10: “User Manual” 1997-2003 Oracle Corporation.
35. F. D’Auria, G.M. Galassi, W. Giannotti, D. Araneo, A. Del Nevo: “Assessment of Cathare2V2.5 code against boron transport experiment” Pisa, July 4, 2005. Contract N. CQN01690 EDF-DIMNP.
36. Foreign Trade Organization “Safety Ltd.” “Input Data Base for Analyses on VVER-1000 type NPP (Balakovo)” Final Report, Riskaudit Report No 87, February 1997.
37. J. Misak “AMP & AMG in VVER 1000” Tacis 30303 project internal document – restricted, 2004.
38. V. Denisov, G. Dragunov “WWER Reactor Units for Nuclear Power Plants” Moskva, IzdAT, 2002.